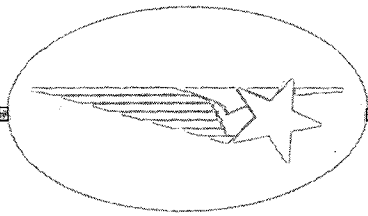


2(mix)



(NASA-CR-123921)	FEASIBILITY OF WAKE	N73-11229
	VORTEX MONITORING SYSTEMS FOR AIR TERMINALS	
	Final Report, Jan. 1971 - Jul. 1972 D.J.	
Wilson, et al (Lockheed Missiles and Space		Unclas
Co.) Aug. 1972 234 p	CSSL 01E G3/11	16398

*Lockheed*

Reproduced by  
 NATIONAL ARCHIVAL  
 INFORMATION SERVICE  
 U.S. Department of Commerce  
 Springfield, VA 22151

**HUNTSVILLE RESEARCH & ENGINEERING CENTER**

**LOCKHEED MISSILES & SPACE COMPANY, INC.**  
 A SUBSIDIARY OF LOCKHEED AIRCRAFT CORPORATION

**HUNTSVILLE, ALABAMA**

234

LOCKHEED MISSILES & SPACE COMPANY  
HUNTSVILLE RESEARCH & ENGINEERING CENTER  
HUNTSVILLE RESEARCH PARK  
4800 BRADFORD DRIVE, HUNTSVILLE, ALABAMA

FEASIBILITY OF WAKE VORTEX  
MONITORING SYSTEMS  
FOR AIR TERMINALS  
FINAL REPORT  
August 1972

Contract NAS8-26668

Conceptual Design of Laser Doppler Systems for Monitoring  
Aircraft Trailing Vortices in the Terminal Area

Prepared for National Aeronautics and Space Administration  
Marshall Space Flight Center, Alabama 35812

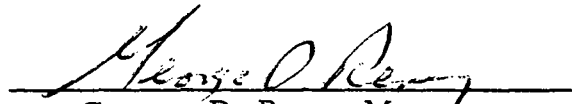
by

D. J. Wilson  
K. R. Shrider  
T. R. Lawrence

APPROVED:



T. R. Lawrence, Supervisor  
Laser Systems



George D. Reny, Manager  
Aeromechanics Dept.



J. S. Farrior  
Resident Director

## FOREWORD

This document presents results of an investigation by Lockheed Missiles & Space Company, Inc., Huntsville Research & Engineering Center under Contract NAS8-26668 for the National Aeronautics and Space Administration, George C. Marshall Space Flight Center. The work was undertaken to perform feasibility studies of wake vortex monitoring systems for air terminals.

The work was performed during the period January 1971 through July 1972. The NASA Contracting Officer's Representatives (COR) for this contract are Mr. Edwin A. Weaver and Mr. R. M. Huffaker of S&E-AERO-AF.

## ABSTRACT

Wake vortex monitoring systems, especially those using laser Doppler sensors, were investigated under this contract. The initial phases of the effort involved talking with potential users (air traffic controllers, pilots, etc.) of a wake vortex monitoring system to determine system requirements from the user's viewpoint. These discussions involved the volumes of airspace to be monitored for vortices, and potential methods of using the monitored vortex data once the data are available. A subsequent task led to determining a suitable mathematical model of the vortex phenomena and developing a mathematical model of the laser Doppler sensor for monitoring the vortex flow field. The mathematical models were used in combination to help evaluate the capability of laser Doppler instrumentation in monitoring vortex flow fields both in the near vicinity of the sensor (within 1 kilometer and at long ranges (10 kilometers). A number of computer simulations were made which scanned the modeled laser Doppler sensor through the modeled flow field and plotted the sensor output along with the actual (simulated) flowfield velocity as a function of position with respect to the vortex core. These plots indicated that a one-dimensional laser Doppler sensor will be satisfactory for viewing a vortex at large angles to the vortex axis. The plots also indicated that a two-dimensional sensor having relatively coarse resolution along each sensor optic axis will provide satisfactory vortex data to a range of 10 kilometers.

## CONTENTS

Section		Page
	FOREWORD	ii
	ABSTRACT	iii
1	INTRODUCTION AND SUMMARY	1-1
	1.1 The Wake Vortex Problem	1-1
	1.2 Wake Monitoring System Economics	1-3
	1.3 What is a Wake Turbulence Monitoring System?	1-8
	1.4 User Requirements for a Wake Turbulence Monitoring System	1-10
	1.5 System Categories	1-12
2	PREDICTIVE WAKE VORTEX MONITORING SYSTEM	2-1
	2.1 Introduction and Summary	2-1
	2.2 The Trailing Vortex Phenomenon and Behavior	2-2
	2.3 Design of a Wake Turbulence Predictive System	2-21
	2.4 Information Acquisition, Storage and Processing	2-29
	2.5 Communications and Action Command Processes	2-31
3	DETECTIVE WAKE VORTEX MONITORING SYSTEM	3-1
	3.1 Introduction and Summary	3-1
	3.2 Typical Wake Vortex Detective System	3-2
	3.3 Considerations of Multi-Component (Multi-Dimensional) and Single-Component (One-Dimensional) Systems	3-17
	3.4 Simulation Program: Vortex Flow Field and Flowfield Monitoring with Laser Doppler Sensor	3-42
	3.5 Additional Effort Required Before the Long Range Wake Turbulence Monitoring System is Implemented	3-49
4	HYBRID WAKE WORTEX MONITORING SYSTEM	4-1
	4.1 Introduction	4-1
	4.2 Typical Hybrid Wake Turbulence Monitoring System	4-1
	4.3 Hybrid System Simulation	4-11
	4.4 Implementation of a Hybrid System	4-15
	4.5 Wind Shear and Turbulence Monitoring as a Bi-Product of Hybrid (and Probably Detective) Systems	4-17

CONTENTS (Continued)

Section		Page
5	CONCLUSIONS	5-1
	5.1 Is a Wake Turbulence Monitoring System Feasible ?	5-1
	5.2 Would a Wake Turbulence System be Cost Effective ?	5-2
	5.3 What Type System Should be Developed ?	5-4
	5.4 What are the Logical Steps to Develop the System ?	5-4
6	REFERENCES	6-1
Appendixes		
A	Numerical Vortex Model	A-1
B	Laser Velocimeter Volume Scan Simulation Program	B-1
C	Laser Velocity Line Scan Simulation Program	C-1

Section 1  
INTRODUCTION AND SUMMARY

1.1 THE WAKE VORTEX PROBLEM

Accidents associated with wake turbulence have become a significant reported proportion of the total aviation accident profile within the last fifteen years. In fact, within the 1960 to 1970 period, 128 general aviation and one air carrier accidents were attributed to wake turbulence.\* Approximately one-half of these accidents resulted in fatalities.

On 1 March 1970 the Federal Aviation Administration (FAA) implemented separation criteria for the express purpose of separating aircraft from wake turbulence.\*\* These criteria categorized as "heavy jets" those aircraft whose takeoff weights are greater than 300,000 pounds. Aircraft not in this category and which are radar vectored are required to follow the "heavies" by a minimum separation of five miles instead of the previous minimum of three miles. This introduction of another set of separation standards has a direct effect on terminal traffic in the arrival, departure and ground phases of operations (Fig. 1-1).

The above paragraphs mention two aspects of the wake turbulence problem:

- Safety — loss of life and equipment, and
- Terminal capacity — delays in handling aircraft due to imposed separation requirements.

The safety aspect of the wake turbulence problem has been improved significantly with the new (1970) separation standards. However, potentially

---

\* Thomas, David D., President, Flight Safety Foundation, Inc., Presented at FAA Turbulence Symposium, Washington, D. C., March 1971.

\*\* Krupinsky, E., FAA Air Traffic Service, Presented at FAA Turbulence Symposium, Washington, D. C., March 1971.

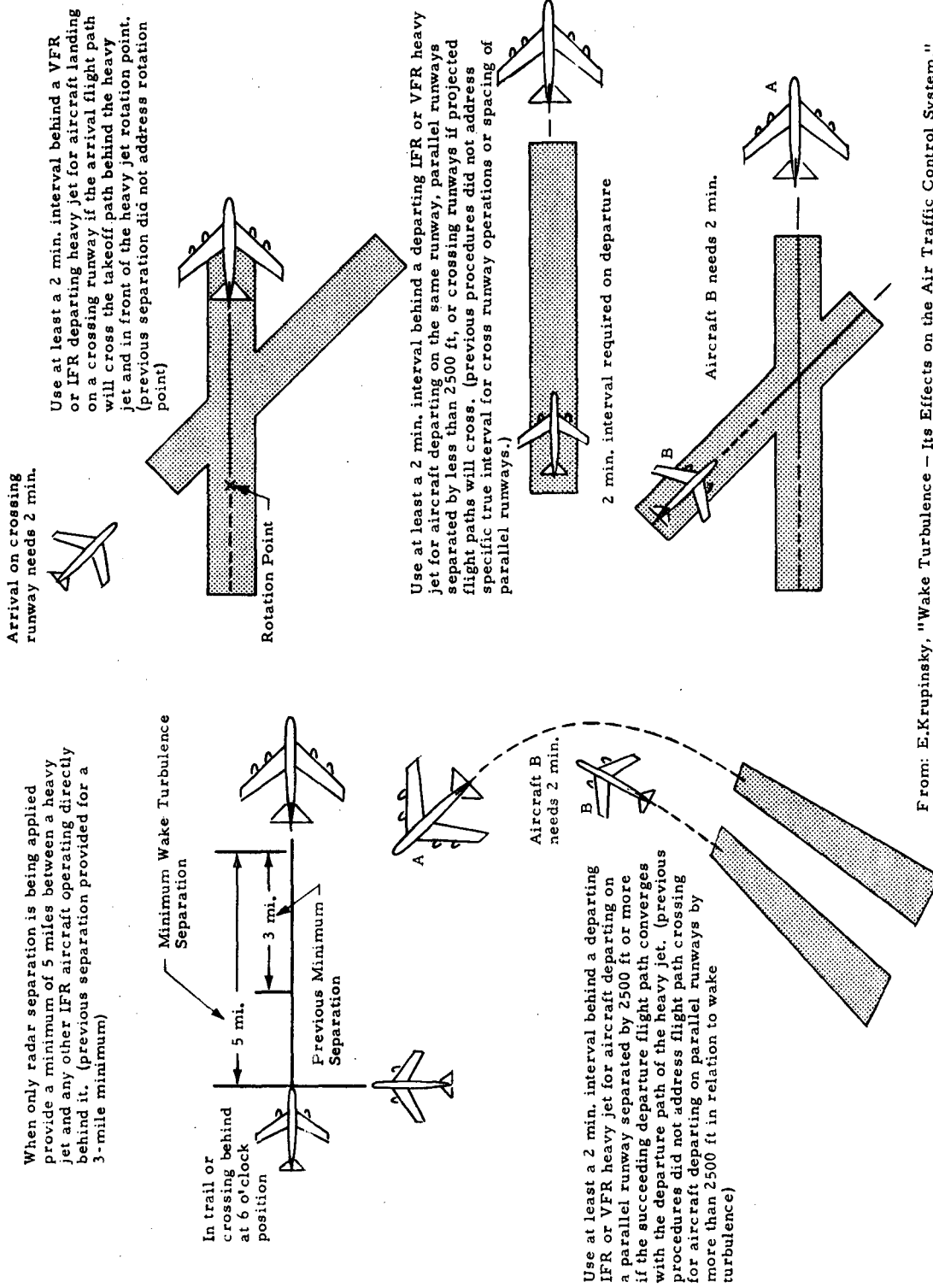


Fig. 1-1 - Aircraft Minimum Separation Requirements Influenced by Wake Turbulence

damaging vortices can be generated from moderately sized aircraft (Ref. 1-1) not explicitly covered by the new separation standards. Also, the imposed increased separation definitely decreases the traffic capacities of busy terminals during peak traffic periods.

A goal of the authorities during the decade of the 1970s is to:

- Increase air terminal capacities,
- Maintain or improve terminal safety.

An effective wake turbulence monitoring system would provide a means to achieve this goal without purchasing new real estate and building new runways. A prior knowledge of wake vortex conditions in the terminal area would allow aircraft to be spaced according to the prevailing vortex conditions. Thus, separation minimums would be increased during atmospheric conditions when vortices remain in the corridor and would be decreased when the vortices rapidly dissipate within or depart from the corridor. Air terminal capacities would be increased during all periods except when vortices remain in the corridors as a hazard to arriving or departing aircraft. Safety could be improved by regulating spacing according to the vortex transport and decay conditions instead of relying on the standard separations of today which are independent of meteorological conditions affecting the vortex hazard.

## 1.2 WAKE MONITORING SYSTEM ECONOMICS

The fact that major air terminals are built near major population centers dictates that major air terminals be constructed on very expensive real estate. The locations of John F. Kennedy International, O'Hare, Los Angeles International, Atlanta, etc., exemplify this. Major air terminals will continue to be located on very expensive real estate until ground transportation improves by several factors, since air terminals are located for the convenience of the populace.

As air traffic increases in the coming years, improving the utilization of these major air terminals becomes increasingly important. One means of increasing the capacities of major air terminals without purchasing additional real estate for more runways is to decrease the separation minimums for landing and departing aircraft. These decreased separation standards must be accomplished without simultaneously degrading safety. A logical first separation standard to attempt to decrease is the last significant separation standard imposed (1970) - the minimum IFR separation for "non-heavies" following "heavies."

Figure 1-2 depicts the projected increases in landing fees which could be collected at major air terminals through the use of effective wake turbulence monitoring systems. The effective wake turbulence monitoring system would allow the separations behind the "heavies" to be safely decreased in specific air corridors when the wake turbulence hazard was minimal. Backup data which were used to derive the increased-landing-fee data of Fig. 1-2 are depicted in Fig. 1-3. The number of hourly operations (landings or departures) during peak traffic hours and the approximate percentages of "heavies" using these terminals were obtained from discussions with air traffic control (ATC) tower personnel at these facilities. From these data the increase in airport capacities resulting from reducing separations behind "heavies" from five miles to three miles was projected. The capacity increase was multiplied by the typical landing fee to determine the increase in landing fees per hour at each terminal. The hourly increase in landing fees was multiplied by four hours per day and 250 days per year to project the annual landing fee collection increase through utilization of an effective wake turbulence monitoring system.

Another economic boost from an effective wake turbulence monitoring system is the savings to airlines from the reduction in holding delays at air terminals (Fig. 1-2). Backup data for these statistics are presented in Fig. 1-4 which were projected from surveys made from the operations of three major air carriers.

 Savings to airlines from reduction in delays  
 Additional landing fees from increased capacity

Note: In addition to these depicted benefits, the Government is involved in litigations of \$36,000,000 from dependents of possible victims of wake turbulence accidents. Many of these accidents could have been avoided with an effective wake turbulence monitoring system.

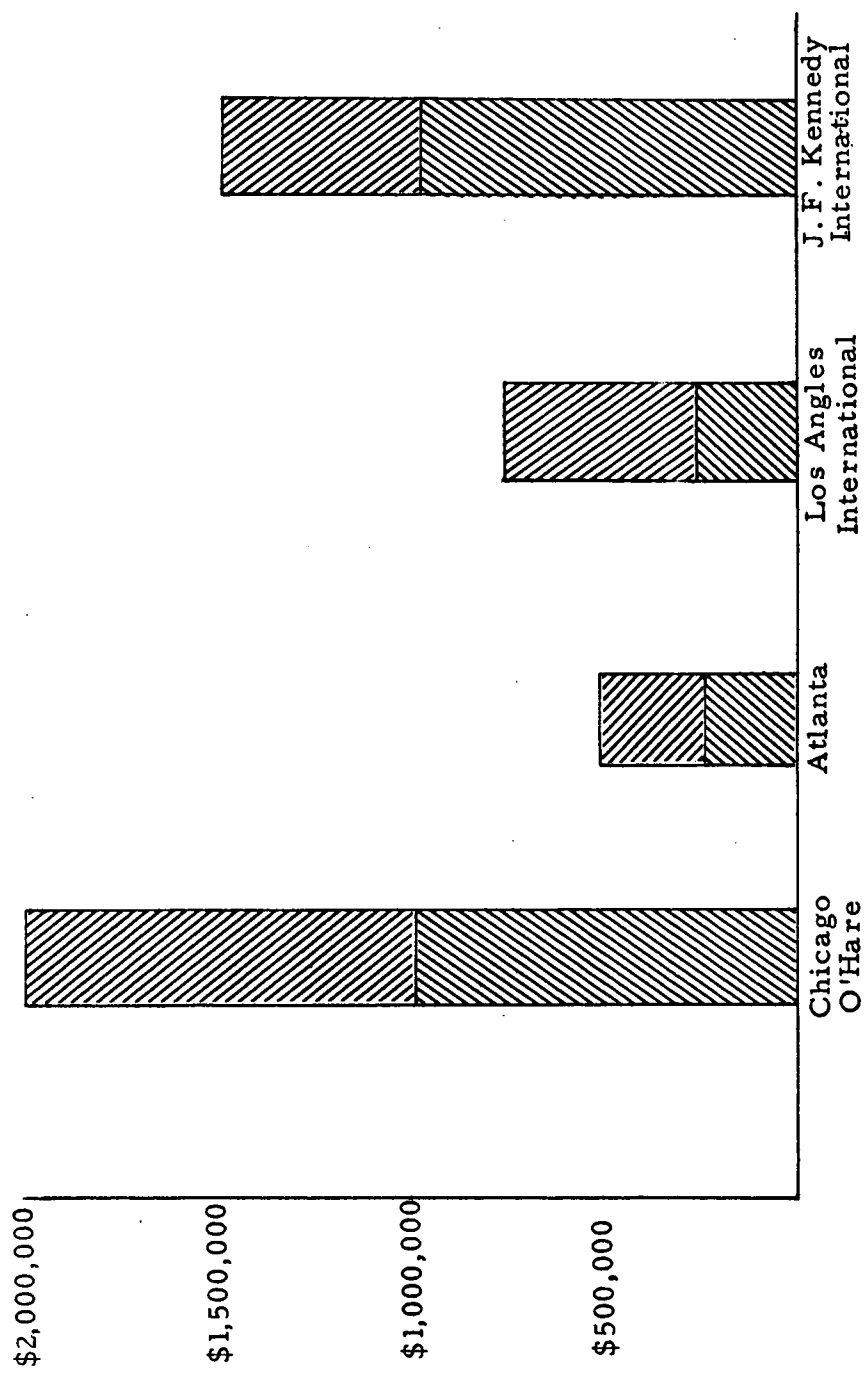


Fig. 1-2 - Economic Benefits from Wake Turbulence Monitoring Systems at Major Air Terminals

Combined Annual Savings to Airlines and Increased Revenues to Terminals

Air Terminal Data Description	Date of Data	Air Terminal			
		Chicago O'Hare	Atlanta	Los Angeles Intl.	John F. Kennedy
Peak Period Hourly Operations*	CY 71	~159/hr	~107/hr	~140/hr	~101/hr
Percent Heavy Aircraft (> 300,000 lb)**	CY 71 CY 76	~ 15 ~ 25	~ 5 ~10	~20 ~30	~65 ~75
Hourly Operations Affected by Wake Turbulence Separation Criteria	CY 71 CY 76	~ 15 ~ 25	~ 4 ~ 8	~15 ~25	~20 ~20
Projected Improvement in Operations with Effective Wake Turbulence Monitoring System	CY 76	+15	+6	+15	+15
Landing Fee (per 1000 lb) for Typical 200,000 lb Aircraft	CY 71 CY 71	0.72 \$150	0.54 \$100	0.38½ \$77	0.35 \$70
Increased Landing Fee Revenue During One Peak Hour***	CY 76	\$1000	\$300	\$500	\$500
<u>Annual Revenue Increase Assuming 4 peak hours/day and 250 days/year</u>	CY 76	\$1M	\$300K	\$500K	\$500K

\* Data from "Terminal Area Air Traffic Relationships," DOT/FAA, December 1971

\*\* Data from tower operations at air terminals depicted

\*\*\* Two operations (one landing and one departure) required to collect one landing fee.

Fig. 1-3 - Projected Increased Air Terminal Landing Fees with Effective Wake Turbulence Monitoring Systems

Air Terminal Data Description	Date of Data	Air Terminal					All Air Terminals
		Chicago O'Hare	Atlanta	Los Angeles Intl.	John F. Kennedy		
Air Carrier Operations Rankings	CY 71	Y	Z	Z	4		
Air Carrier Operations	CY 71	565,626	367,475	773,870	433,559		9,791,525
Projected Delays to All Carriers (min)	CY 69	3,286,688	1,315,180	1,008,108	2,537,080		23,908,080
Projected Delay Costs★	CY 69	\$21,871,500	\$9,363,500	\$5,885,780	\$18,812,700		\$157,880,800
Delays to Three Surveyed Carriers* Delay Costs★	CY 69	1,379,310	96,492	312,269	584,417		5,768,960
Delays to Three Carriers Attributed to Air Traffic Control (ATC)** Delay Costs★	CY 69	\$9,182,130	\$686,550	\$1,826,080	\$3,582,950		\$7,809,970
Projected Delays to All Carriers Attributed to ATC** Delay Costs★	CY 69	525,530	~40,000	~130,000	234,190		
Percentage of Heavy Aircraft Using Terminal	CY 69	\$4,256,240	~\$290,000	\$770,000	\$1,957,780		
Assumed Percentage of ATC Delays Due to Wake Turbulence***	CY 69	1,251,000	~550,000	~420,000	1,177,000		
Projected Annual Savings to Airlines from Effective Wake Turbulence Monitoring System	CY 69	\$10,134,000	~\$3,900,000	~\$2,400,000	\$9,838,000		
	CY 71	15	5	20	65		
	CY 76	25	10	30	75		
	CY 76	10	5	10	10		
	CY 76	~\$1M	~\$200K	~\$240K	~\$1M		

//// Data from "FAA Air Traffic Activity, CY 1971," DOT/FAA/Info. & Statistics Div., February 1972.  
 //// Data from "Terminal Area Airline Delay Data, 1964-69," DOT/FAA/Air Traffic Service, September 1970.  
 ★Average cost per delay → \$6.55/min; ATC attributed delay → \$7.68/min (\$8.00/min → arrival and \$6.54/min → departure).

\* UA, AA, NW  
 \*\* ATC attributed delays include awaiting ARTC clearance, holding and rerouting (weather delays excluded).  
 \*\*\* Projected from wake turbulence separation criteria (5 mi. for "non-heavy" following "heavy" instead of normal 3 mi.).

Fig. 1-4 - Projected Annual Airline Savings with Effective Wake Turbulence Monitoring Systems

1.3 WHAT IS A WAKE TURBULENCE MONITORING SYSTEM?

A wake turbulence monitoring system performs the following three functions:

- Detects and/or predicts current locus of aircraft trailing vortices in the air corridors of an airport, and
- Forecasts the future hazard to aircraft trailing (arriving or departing) the generator aircraft, and
- Interfaces with traffic controllers and/or pilots to prevent a hazardous vortex encounter.

The first of the above functions deals with locating vortices in the air corridors leading to and from an air terminal. This might be done with an active device that transmits radiation which is reflected or altered by the vortex presence, by a passive device which detects radiation emitted by the vortex itself, or by a predictive system which predicts the vortex locus from current meteorological data. Active and passive techniques which might be considered for a wake turbulence detector along with some of their characteristics are listed below:

TECHNIQUES FOR PERFORMING FIRST FUNCTION:

"Detect and/or Predict Current Vortex Locus"

<u>Radiation Frequency</u>	<u>Passive Technique</u>	<u>Active Technique</u>
0 to 100 Hz	Detection of pressure wave generated by vortex. <u>Characteristic:</u> Low amplitude signal. Detects vortices in ground effect.	
100 Hz to 20 kHz	Detection of audible sound generated by vortex. <u>Characteristic:</u> Low amplitude signal compared to background noise.	Detection of sound back-scattered by vortex. <u>Characteristic:</u> Affected by noisy acoustical environment. Is being tested at air terminal.

<u>Radiation Frequency</u>	<u>Passive Technique</u>	<u>Active Technique</u>
Microwave	Measure incoherent radiation associated with elevated vortex temperatures. <u>Characteristic: Low energy emission at RF wavelengths.</u>	Detection of RF energy scattered by vortex turbulence of similar wave length. <u>Characteristic: Vortex is poor RF reflector. Much transmitted energy required.</u>
Infrared, Visible and Ultraviolet	Measure radiation associated with elevated vortex temperature. <u>Characteristic: Background radiation and atmospheric effects upon transmission.</u>	Detection of backscattered energy by aerosol particles. <u>Characteristic: Fundamental questions are answered for IR frequencies. Method should be evaluated in air terminal environment.</u>

While the above chart depicts active and passive vortex detection devices, the totally predictive system would rely on none of the above devices but would utilize local meteorological data and aircraft coordinates to predict the presence of the vortices. The major portion of this report is devoted to wake turbulence monitoring systems which use active vortex detectors operating at infrared frequencies.

The second of the above functions — "Forecasts the future hazard to aircraft. . ." involves predicting vortex movements and their decay and forecasting the hazard to trailing aircraft. This forecasting function would be performed either by a minicomputer or a module of the existing computer system at the air terminal and would depend upon inputs from the detector sensors and/or meteorological inputs of the above paragraph. Air traffic controllers might also supply inputs to the forecasting subsystem of the turbulence monitoring system. The forecasting portion of the wake turbulence monitoring system would initially rely upon a very simple vortex model, but would likely become more sophisticated as more knowledge is gained about the vortex decay and transport phenomenon.

The third function of the monitoring system — "Interface with traffic controllers, pilots, etc. . ." is equally as important as the first two. For a

wake monitoring system to be effective, there must be a means of effectively communicating with the personnel involved. Communication with what personnel, and regarding what information should be relayed is yet unresolved. The air traffic controllers (ATC) prefer that the system communicate directly with the pilots and leave ATC out of the loop. However, if the system is to increase terminal capacities, aircraft separations must be decreased, and the controller becomes involved since he directs minimum spacing. The controller also becomes involved if a pilot decides to abort a landing, since not only the aborting aircraft is affected, but also the whole landing sequence.

#### 1.4 USER REQUIREMENTS FOR A WAKE TURBULENCE MONITORING SYSTEM

Lockheed interviewed potential users of a wake turbulence monitoring system in the early phases of the subject contract. These potential users included local and departure/arrival air traffic controllers at Atlanta Municipal and John F. Kennedy International airports, Delta Airline pilots in Atlanta, and district FAA officials in Atlanta. Lockheed felt that inputs from potential users in the early phases of system concept were essential for the development of an effective wake turbulence monitoring system. All of these persons recognized the need for a wake turbulence monitoring system and were most cooperative in helping to develop criteria for such a system. Figure 1-5 is a summary of user requirements developed from interviews with the above personnel.

The requirements developed from interviewing the potential system users included the "volume of interest" and the "communications/command process" of Fig. 1-5. The volume of interest includes the air corridor to the altitude above which an aircraft encountering a vortex would have a high probability of safe recovery. Other factors affecting this recovery altitude include the different aircraft configurations for arrival and departure and the configuration effect upon the likelihood of the aircraft stalling or becoming uncontrollable upon encountering a vortex. Since the aircraft is in an accelerating mode and is normally climbing rapidly, less range is probably required for a system

Volume of Interest

Range (beyond end of runway)

Two miles - Departure

Five miles - Arrival

Horizontal (Azimuth) Angle -

2.5 degrees to either side of runway centerline plus area to accommodate vortex drift between scans

Vertical (Elevation) Angle -

2 degrees to 15 degrees\* - Departure

2 degrees to 3 degrees\*\* - Arrival

Communications/Command Process

Traffic Controller's Viewpoint - Controllers are very busy; system should communicate directly with pilots.

Pilot's Viewpoint - Pilots are busy in terminal area; let controllers direct spacing interval.

Compromise - Controllers would be involved anyway if pilots perform evasive maneuver; therefore, controllers should probably control spacing interval according to prevailing vortex conditions and pilots take only evasive action when required.

\* 6 to 11 degrees would cover approximately 90% of cases

\*\* ILS and VASI glide paths nominally 2.0 ±0.5 degrees

Fig. 1-5 - User (Pilots, ATC, etc.) Requirements

monitoring departure corridors than is required for monitoring arrival corridors where aircraft are in near stall configurations coming in at a very shallow ( $\sim 2\frac{1}{2}$  deg) angle. The horizontal width of these volumes was projected from the instrument landing system (ILS) beam width. Some additional width should be included in the volume to prevent vortices from drifting into the flight corridor between successive sensor scans of the volume.

The communications/command process as discussed in Section 1.2 involves relaying the information obtained by the system to the user in an effective manner. The differences in the two depicted viewpoints must be resolved for the development of an effective system.

## 1.5 SYSTEM CATEGORIES

Wake turbulence monitoring systems are divided into three basic categories to facilitate discussion in this report. They are:

- Predictive
- Hybrid
- Detective

Each of the categories of wake turbulence monitoring systems performs the three functions described in Section 1.4: (1) detects and/or predicts current vortex locus; (2) forecasts future hazard; and (3) interfaces with ATC and/or pilots to prevent hazardous encounter.

The basic similarities and differences in the three types of systems involve the first two functions. They are depicted in the table on the following page. As seen in the table, all three types of systems perform measurements and forecast predictions. The different nomenclature for the three categories is derived from the relative degrees of prediction and measurement (detection) performed by the three basic systems:

System Function	Method of Performing System Function		
	Predictive System	Hybrid System	Detective System
1. Determine Current Vortex Locus	Predict	Measure and Predict	Measure
2. Forecast Future Hazard			
a. Determine meteorological conditions	Measure and Predict	Measure	Measure
b. Determine future vortex locus	Predict	Predict	Predict

- Predictive: Measures meteorological data with presently available instrumentation; forecasts additional meteorological data; forecast future vortex hazard.
- Hybrid: Measures vortex movement in several vertical planes; forecasts vortex movement between planes; forecasts vortex future hazard.
- Detective: Measures vortex movement throughout the air corridor of interest; forecasts future hazard.

All three systems both measure and forecast. The detective systems have more sophisticated instrumentation and therefore provide higher quality data to the forecasting computer. Therefore, the detective systems are likely to be more expensive to develop; yet they provide a more accurate forecast of the future vortex hazard. The predictive system relies upon presently available, limited meteorological data and therefore would provide a less accurate forecast. The hybrid system relies upon viewing the vortex at a limited number of loci and therefore would provide data to the computer of a higher quality than that of the predictive system but of lower quality than that of the detective system.

Since the detective system was said to provide the most accurate hazard forecast of the three system configurations discussed, the installation of a detective system would allow air terminal capacity to be increased to its maximum. The predictive system, which would provide a less accurate forecast, would require a greater safety margin than would the more accurate forecast. The greater safety margin requirements of the predictive system would decrease the effectiveness of the system in increasing air terminal capacities. The effectiveness of the hybrid system will likely lie between that of the predictive and detective systems. These facts are illustrated in the following table.

	Predictive	Hybrid	Detective
Sensor Sophistication (Therefore Expense)	Least	Median	Most
Hazard Forecast Reliability	Least	Median	Most
Required Safety Margin	Most	Median	Least
Increase in Terminal Capacity	Least	Median	Most
Complexity of Integration into Existing System	Least	Median	Most
Application to Other Air- Terminal Problems		Wind Shear Monitor	Wind Shear Monitor
Development Time	Least	Median	Most

A suggested path of development of the wake turbulence monitoring system is to field the predictive system first, while simultaneously developing techniques for the hybrid and/or detective systems. Next, additional sensors are incorporated into the predictive system, which evolves into a hybrid or detective system. This results in immediate improvement in air terminal capabilities with further improvements forthcoming as the systems become more sophisticated.

Figure 1-6 depicts an illustrator's concept of each of the three systems to be discussed. The left-hand system is a detective system, the right-hand system is a predictive system and the middle system is a hybrid system which uses some of the components of both the detective and predictive systems.

- Predictive System

The predictive system conceptually illustrated in Fig. 1-6 utilizes available meteorological data as input to a minicomputer which predicts lengths of time vortex elements will remain in the pertinent air corridors. The available meteorological data are used to calculate wind conditions aloft which are in turn used to calculate displacements of vortex elements in the air corridors. The computer output — a prediction of how long vortex elements will remain as hazards in the pertinent air corridors — is displayed to local controllers who in turn either increase or decrease minimum separation requirements according to the prevailing vortex conditions. The controller action is taken before aircraft enter the final approach corridors or, in the case of departing aircraft, before the aircraft enter the runway. This is the least expensive of the three systems. It requires only a minicomputer, display, and existing meteorological measurement facilities. The predictive system is discussed in Section 2 of this document.

- Detective System

The detective system briefly illustrated in Fig. 1-6 consists of, for example, a pair of laser Doppler velocimeters (LDV) for the runway with a range of 8 to 10 kilometers. These LDVs are tied together through a computer which directs their scanning and processes their outputs. Formatted data from the computer are transmitted directly to the cockpit and displayed to the pilot as well as to the controllers in real time. The velocimeters provide a real-time two-dimensional picture of the vortex condition in the air corridor directly to the aircraft pilot. The pilot can then take appropriate action to avoid vortex hazards. Similar displays would be provided to air traffic controllers to coordinate the actions of the pilots. This is the most expensive of the three illustrated systems, but it provides the highest resolution, longest-range data. The detective system is discussed in Section 3.

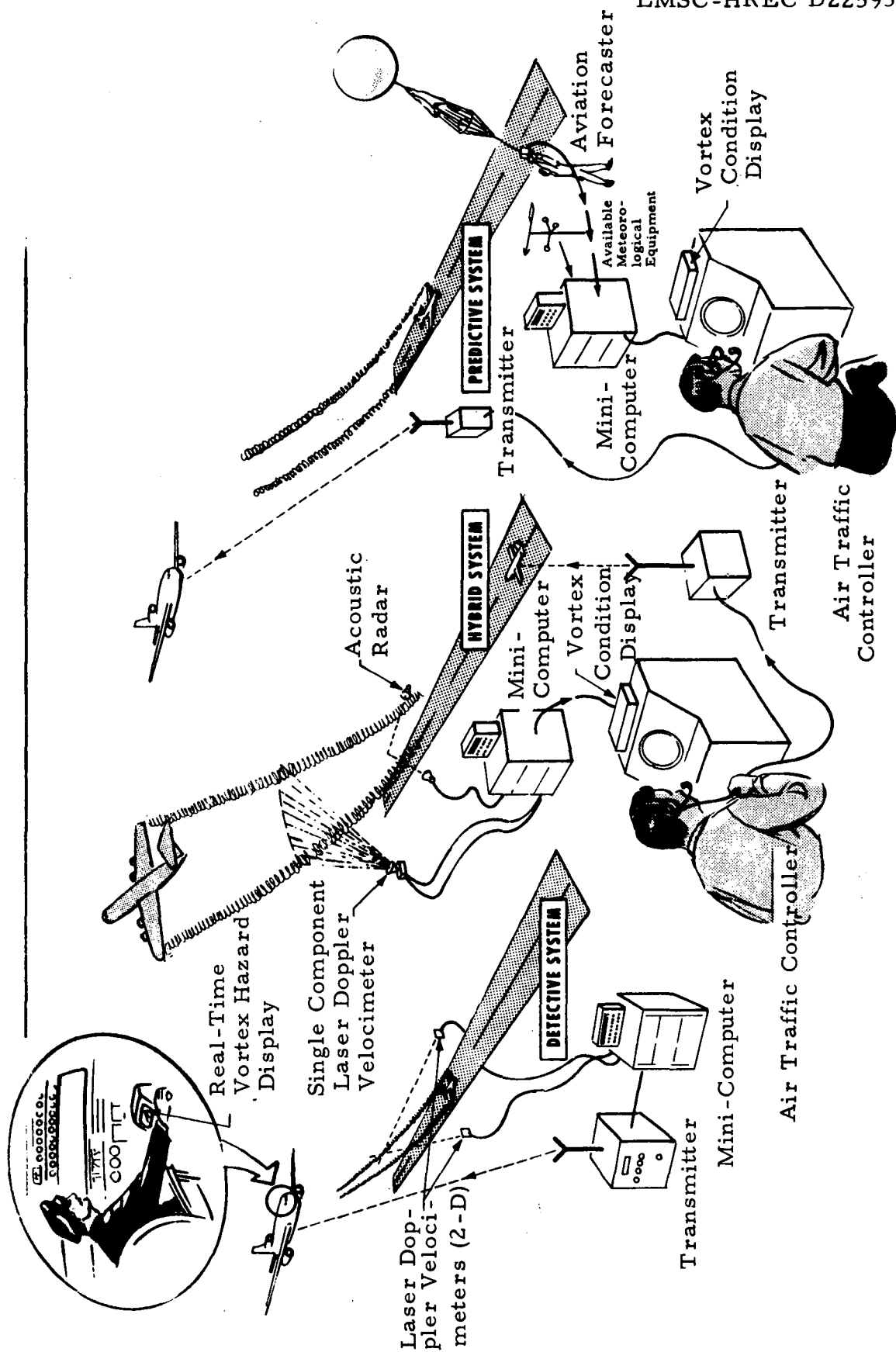


Fig. 1-6 - Concepts for Wake Turbulence Monitoring System

- Hybrid System

The hybrid system depicted conceptually in Fig. 1-6 is composed of certain elements of both the predictive and detective systems. Development time and implementation costs of the hybrid system will be less than for the detective system, yet longer and more costly than for the predictive system. The hybrid system utilizes for example, a single component LDV which scans the surface of a cone overhead to provide wind profiles for the prediction of vortex element movements. A single-component LDV located several kilometers beyond the end of the runway is also used to scan a vertical plane normal to the runway axis to locate vortices above the velocimeter and to determine the sizes and transport velocities of the vortices as they pass through this plane. Acoustic sensors may be feasible for locating vortices at lower altitudes. Section 4 of this document presents a detailed discussion of the hybrid system. A typical hybrid system will interface Doppler sensor outputs into a minicomputer which will predict the movements of the vortices in the air corridors from the available data. The computer output will be displayed to the air traffic controllers who in turn control the traffic spacing. The prediction of the vortex movement by the hybrid system is of finer resolution than the prediction by the predictive system since more pertinent input data are supplied to the computer. Thus air traffic spacing can be controlled to a finer tolerance (i.e., smaller minimum separations) than with the purely predictive system. Section 4 presents a detailed discussion of the hybrid approach to the wake turbulence monitoring problem.

Section 5 of this document, the conclusion, presents an attempt to answer four basic questions about the wake turbulence monitoring system. The four questions are:

- Is a wake turbulence monitoring system feasible or within the near state of the art?
- Would a wake turbulence system be cost-effective to develop, operate, and maintain?
- What type system should be developed?
- What are the logical steps to develop the system?

The primary sections of the report are followed by three appendixes. Appendix A describes the vortex models chosen by Lockheed to be used in system simulation studies. Development of the programs used for these simulation studies is outlined in Appendixes B and C.

## Section 2

## PREDICTIVE WAKE VORTEX MONITORING SYSTEM

## 2.1 INTRODUCTION AND SUMMARY

The five-mile minimum spacing regulation for an aircraft lighter than 300,000 pounds following a "heavy" (> 300,000 pounds) is presently enforced for all flying conditions, regardless of weather phenomena. However, our present knowledge of the vortex phenomenon indicates that for certain meteorological conditions the aircraft wake is either swept out of the flight path or breaks up internally in less time than that imposed by five-mile minimum spacing. If these conditions could be accurately predicted from measurements of local meteorological phenomena, spacing could be decreased during appropriate meteorological conditions. A predictive system based on considerations of local meteorological conditions, air terminal layout, aircraft involved, etc., could be beneficial to major air terminals. The initial wake turbulence prediction system which could be operational within a year or two could reduce spacing requirements from five miles to four miles or three miles for, perhaps, 50% of the operational conditions. As the state-of-knowledge of the vortex phenomenon improves, the spacing reduction might be extended to 60 or 70% of the operational conditions.

As previously discussed in Section 1, potentially damaging vortices can be generated from moderately sized as well as "heavy" aircraft. With a turbulence prediction system, more adequate warning of wake turbulence conditions could be given to small aircraft operators following a moderately sized aircraft in both approach and departure configurations.

A wake turbulence predictive system using existing instrumentation at the air terminal coupled with computer capability for predicting the vortex hazard (or lack of hazard) and a simple communications system could thus

provide an increased capability for handling more traffic without degradation of safety.

A typical wake turbulence predictive system is depicted in block diagram form in Fig. 2-1. The wake turbulence predictive system consists of several subsystems which are discussed below. Section 2.2 discusses the vortex phenomenon and its behavior. This will include definition of all parameters which enter into forecasting and displaying aircraft wake vortex strength, persistence and transport in terminal area operations. The acquisition of some of these parameters such as wind speed and direction at various altitudes and temperatures is illustrated in Fig. 2-1. Design of a wake turbulence predictive system is outlined in Section 2.3. This system will be the software utilized by the computer illustrated in Fig. 2-1. Section 2.4 discusses the information acquisition, storage and processing subsystem that will execute the decision-making process. The subsystems (as illustrated in Fig. 2-1) will likely consist of:

1. The sensors together with a means for entering their data into the computer;
2. Data from the aviation (weather) forecaster together with a means for entering this data into the computer, and
3. The computer itself.

The communications and action command process is discussed in Section 2.5. This process is illustrated typically as an air traffic controller display which forecasts local vortex conditions. The controller uses this display and knowledge of aircraft in the vicinity to project spacing requirements for departing and arriving aircraft. He can also enter data into the computer such as runways which are closed to heavy aircraft, aircraft departure angles, etc.

## 2.2 THE TRAILING VORTEX PHENOMENON AND BEHAVIOR

This subsection discusses pertinent properties of the trailing vortex system, including its generation, structure dissipation and transport.

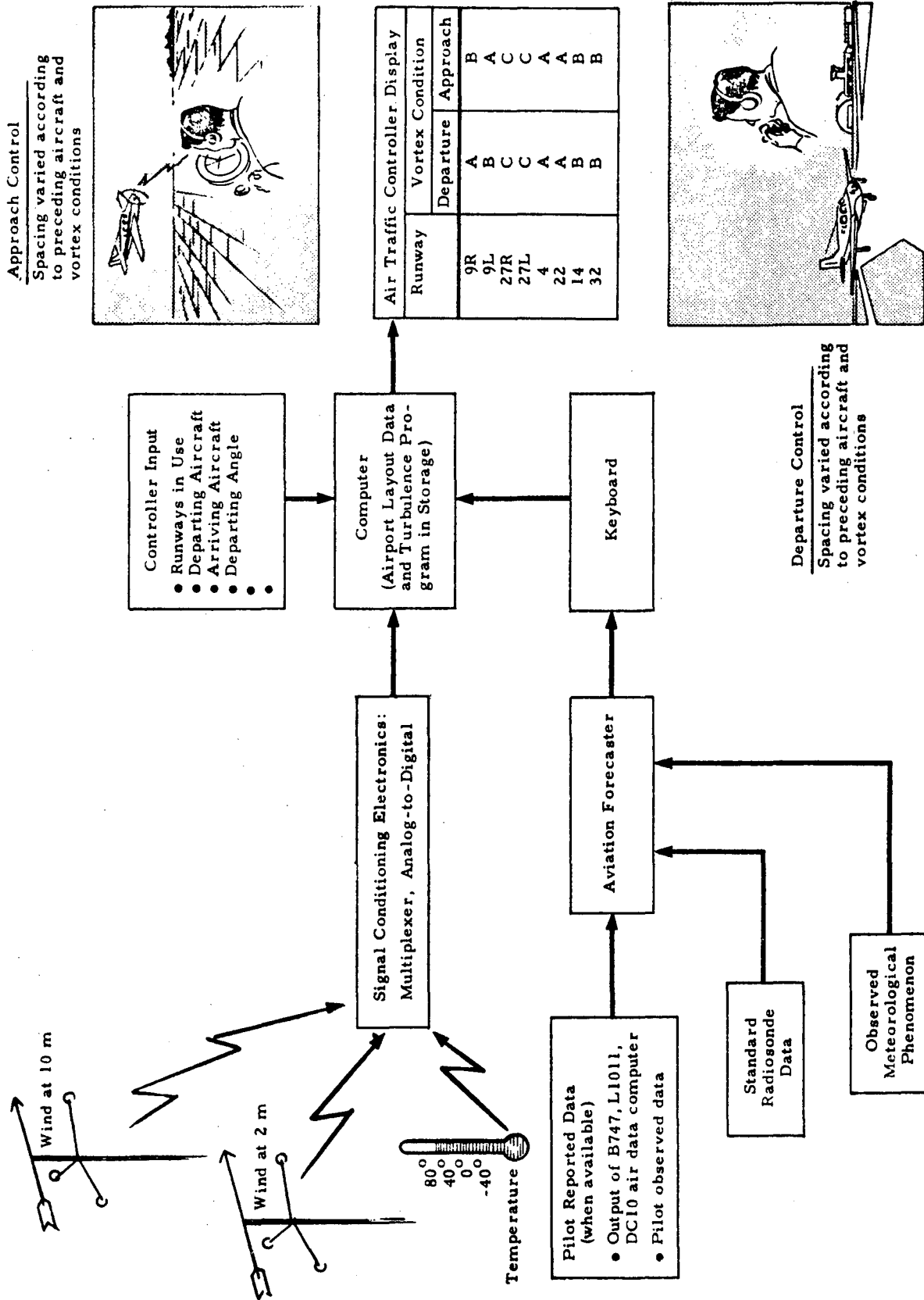


Fig. 2-1 - Typical Wake Turbulence Predictive System Block Diagram

● Mechanisms of Formation of Aircraft Trailing Vortices

The general principle by which an aircraft generates lift is directly related to Newton's Second Law ( $F = d(mV)/dt$ ), where the lifting force is a result of a downward acceleration of air. The process is usually described in theoretical analyses as producing circulation about the wing. This produces a continuous vortex sheet which is shed from the trailing edge of the wing. Because the wing is of finite span length, the high pressure air of the lower surface flows around the wing tip into the region of low pressure on the top of the wing; thus, a vortex core is created with its center near the trailing edge of the wing tip. The strength of these tip vortices is directly related to the lift produced by the aircraft wing.

The existence of these trailing vortices has been known for many years. Two decades ago Spreiter and Sacks (Ref. 1) presented what is still probably the most significant analysis of trailing vortices. Their approach, which was based upon a solution of the linearized potential equation, revealed that the distance required for the trailing vortex sheet to become established is

$$\frac{e}{c} = 0.28 \frac{A}{C_L} \frac{b}{c} \quad (2.1)$$

where

$e/c$  = roll up distance in chord lengths

$c$  = wing chord

$A$  = wing aspect ratio

$b$  = wing span

$C_L$  = aircraft lift coefficient

For a typical takeoff of a C-5A, this means that the trailing vortices will be completely formed approximately 300 feet behind the wing.

● Vortex Structure

A vortex consists of a rotating region of irrotational flow and a smaller central core of rotational flow. The core may be thought of as rotating as if it were a solid cylinder. Spreiter and Sacks (Ref. 1) estimated the diameter of this core by equating the total kinetic energy of the fluid inside the vortex core to the induced drag of the wing. This resulted in a core diameter of approximately 16% of the wing span for an elliptic wing load distribution. Although the assumptions involved in this computation are rather dubious and believed to be invalid during the decay phase of the vortex, it does provide an indication of initial core size. Core sizes are discussed further in Appendix A, where recent vortex models are considered.

Just as lift of a wing is generated by creating downwash, the drag of a wing results in a change of momentum of the air in the axial direction. Experimental data (Refs. 2 and 3) indicate that relatively high axial velocities exist in the center of the vortex. Quite possibly, most of the axial momentum of the vortex is restricted to this vortex core. However, the nature and origin of this axial component of velocity in the core of the vortex is apparently an area requiring additional investigation and comprehension. One explanation (Ref. 4) is that it is due to the pressure buildup along the vortex core due to vortex decay because of the coupling between core pressure and tangential momentum.

Outside the core the tangential (transverse) velocity, at a radial distance (r) from the center of the vortex, is estimated from simple theory as

$$v_{\theta} = \frac{\Gamma_o}{2\pi r}, \text{ where } \Gamma_o = \text{magnitude of circulation around the wing (Eq. 2.5)} \quad (2.2)$$

or in terms of aircraft weight (W), velocity (V), and wing span (b), and density ( $\rho$ )

$$v_{\theta} = \frac{2}{\pi} \frac{W}{\rho V b r} \quad (2.3)$$

By assuming the maximum velocity occurs at the radius of the core which is taken as 8% of the wing span, tangential velocities of up to 65 ft/sec might be expected to exist in a fully rolled-up vortex generated by a C-5A aircraft during takeoff. Recent flight measurements (Ref. 5) however, have indicated smaller cores and peak velocities considerably in excess of this figure, suggesting the simple model described above is inadequate for practical purposes. Recent models are discussed further in Appendix A.

Because of the rotational nature of the flow, the tangential velocity in the vortex core is more difficult to describe. Lamb (Ref. 6) presented the following approximate relation for computing the tangential velocity throughout the vortex:

$$v_{\theta} = \frac{\Gamma_0}{2\pi r} \left[ 1 - \exp\left(-\frac{r^2}{4\nu t}\right) \right] \quad (2.4)$$

where  $\nu$  = kinematic viscosity,  $t$  = time.

This expression not only includes the viscosity effect in the core, but allows this region to increase with time. For large values of  $r$ , the viscous contribution to this expression becomes negligible; hence the irrotational velocity is retained. For practical purposes it has been found necessary to define an eddy viscosity rather than the kinematic viscosity since the vortices are probably invariably turbulent. Such an approach is due to Squire (Ref. 7).

#### ● Vortex Strength

Spreiter and Sacks explain that "the strength of one of the trailing vortices is equal to the sum of the strengths of all the vortices shed from one-half of the

wing; hence it is equal to the magnitude of the circulation  $\Gamma_o$  around the wing in the plane of symmetry." By assuming an elliptic lift distribution over the wing (an idealized distribution of high lift devices), this circulation is

$$\Gamma_o = 2b V \frac{C_L}{\pi A} \quad (2.5)$$

The circulation (i.e., vortex strength) may also be written in a slightly different form by assuming that the lift generated by the wing is approximately the same as the aircraft weight,  $W$  and thus

$$\Gamma_o = \frac{4W}{\pi \rho V b} \quad (2.6)$$

where  $\rho$  and  $V$  are the ambient density and aircraft velocity, respectively.

#### ● Vortex Drift

The vortex cores are established slightly inboard of the wing tips at a position which is stabilized by their mutual interaction. The stable position of the two vortex cores is a function of the lift distribution over the wing, but a typical stabilized position, for the case of elliptical lift distribution, is at a distance  $b'$ , as given in Ref. 1 as

$$b' = (\pi/4)b \quad (2.7)$$

which is approximately 80% of the wing span.

The vortex system also drifts downward relative to the aircraft flight path at a vertical velocity,  $Z$ , determined as follows:

$$Z = \frac{\Gamma_o}{2\pi b'} \quad (2.8)$$

Assuming an elliptic lift distribution and that the wing lift equals the aircraft

weight, the formula for the settle rate of the vortex system is restated in aircraft terms as follows:

$$Z = \frac{8}{\pi^3} \frac{W}{\rho V b^2} . \quad (2.9)$$

For a typical C-5A takeoff, this vertical velocity will be approximately 7 ft/sec.

By neglecting any buoyancy effects due to density gradients in the atmosphere, these vortices are expected to continue this downward drift at essentially a constant rate until they either decay or approach the ground. As the vortices approach the ground the vertical velocity is reduced and the system starts to spread horizontally. This ground effect may be computed by considering the "mirror image" concept which is commonly used in potential solutions. In this approach the ground plane may be thought of as a plane of symmetry with two image vortices of equal strength drifting upward at identical velocities toward the ground plane. The real vortices will continue to drift downward until the influence of the image vortices slows and eventually stops their descent. The downward momentum of these vortices is conserved and serves to spread the vortices horizontally at approximately the speed of their original descent. The stabilized height of these vortices is established at  $b'/2$  above the ground. Vortices generated closer to the ground will rise to this height while spreading horizontally.

Ambient winds also significantly influence vortex drift. A uniform crosswind forces the vortices in the direction of the wind. For a crosswind from right to left, the system of vortices could be thought of as stationary relative to the crosswind and moving to the left relative to a fixed point on the ground. If the magnitude of the drift velocity of the vortices is equal to the wind speed, then the right vortex will become stationary relative to the ground. This vortex would remain stationary until it has lost its effect through normal decay. Should this stationary point be over a runway, the hazard to other aircraft attempting to take off or land is obvious.

A more general treatment of vortex motions is now given, considering the behavior of one vortex pair (Ref. 8).

In the analysis that follows, the vortex-induced velocities are assumed not to vary with time; i.e., the effects of eddy viscosity on the circumferential velocity distribution in the vortex have been neglected, as these effects are considerable only in the region adjacent to the vortex core and the mutually induced vortex motions are dictated by the velocities prevailing several core diameters away from the vortex center. This can of course be easily modified to the decaying vortex case. For typical aircraft under approach conditions Fig. 2-5 suggests that it will be several minutes before the relevant velocities decay to a harmless state.

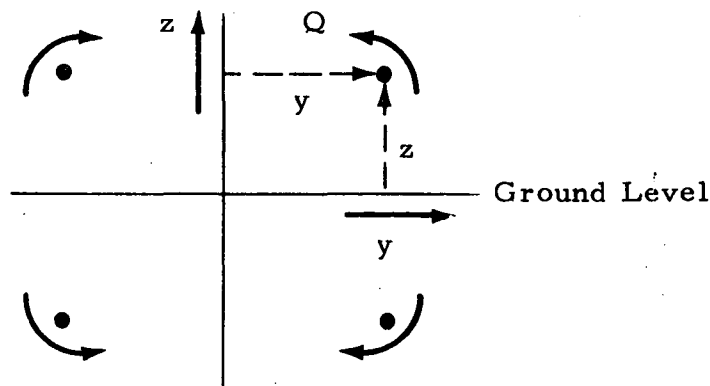


Fig. 2-2 - Vortex Drift Near the Ground

The analysis follows the methods of classical hydrodynamics. Let the trailing vortex pair be located a distance  $2y$  apart, and at height  $z$  above the ground, then the vortex system with its image may be represented as stated in Fig. 2-2.

Now the circumferential velocity,  $v$ , due to a single vortex of strength,  $K$ , is

$$v = K/2\pi r \quad (2.10)$$

where  $r$  is the distance from the vortex axis.

If we consider the velocities induced at  $Q$  by the remaining vortex and the two image vortices, and resolve velocities (i) horizontally and (ii) vertically we have

$$(i) \quad \dot{y} = \frac{K}{4\pi} \left[ \frac{1}{z} - \frac{z}{y^2 + z^2} \right],$$

and

$$(ii) \quad \dot{z} = \frac{-K}{4\pi} \left[ \frac{1}{y} - \frac{y}{y^2 + z^2} \right]$$

therefore,

$$\dot{y} = \frac{K}{4\pi z} \left( \frac{y^2}{y^2 + z^2} \right) \quad (2.11)$$

and

$$\dot{z} = \frac{-K}{4\pi y} \left( \frac{z^2}{y^2 + z^2} \right). \quad (2.12)$$

Combining Eqs. (2.11) and (2.12)

$$\frac{\dot{y}}{\dot{z}} = \frac{dy}{dz} = -\frac{y^3}{z^3}$$

or,

$$\frac{dz}{z^3} = -\frac{dy}{y^3}$$

and hence,

$$\frac{1}{y^2} + \frac{1}{z^2} = A. \quad (2.13)$$

The term  $A$  may be found by substituting  $y_0$  and  $z_0$  for  $y$  and  $z$ , respectively.

Equations (2.11) and (2.12) may now be rewritten as

$$\dot{y} = \frac{K}{4\pi Az^3} \quad (2.14)$$

$$\dot{z} = \frac{-K}{4\pi Ay^3} \quad (2.15)$$

By eliminating  $z$  from Eq. (2.11) and rearranging:

$$\dot{y} = \frac{K}{4\pi A} \left[ \frac{Ay^2 - 1}{y^2} \right]^{3/2}$$

or,

$$\frac{4\pi}{K} \left[ \frac{y^2}{Ay^2 - 1} \right]^{3/2} dy = \frac{dt}{A}$$

Hence, it can be shown that,

$$\frac{4\pi}{AK} \left[ \frac{Ay^2 - 2}{(Ay^2 - 1)^{1/2}} \right] = t + B$$

$B$  may be found by substituting  $y_0$  for  $y$  at  $t = 0$ .

Rearranging,

$$y^2 = \frac{2[64\pi^2/AK^2 + A(t+B)^2]}{64\pi^2/K^2} \left\{ 1 \mp \left( \frac{64\pi^2}{A^2K^2} (t+B)^2 + 1 \right)^{-1/2} \right\}$$

and, by symmetry,  $z$  is given by:

$$z^2 = \frac{2[64\pi^2/AK^2 + A(t+B)^2]}{64\pi^2/K^2} \left\{ 1 \pm \left( \frac{64\pi^2}{A^2K^2} (t+B)^2 + 1 \right)^{-1/2} \right\}$$

In each of these expressions, the upper alternative sign applies when  $t < B$ , and the lower alternative sign applies when  $t > B$ .

Hence, the vertical and horizontal displacements of the vortex cores can be calculated as a function of time to give the theoretical vortex positions.

The effect of wind on these results can be obtained by simply superimposing the wind velocity components on the above velocity components.

As an illustration of the application of the foregoing, it is interesting to recall test results obtained on the behavior of trailing vortices near the ground (Ref. 8). The test configuration is as shown in Fig. 2-3. Behavior of the two smoke-filled vortices generated by a Hunter aircraft were monitored over a measurement plane by both ground and airborne stations. The motions of these vortices were mapped and compared with the results of the previous theory after a measured wind velocity was incorporated. Typical examples of data obtained are shown in Fig. 2-4. From the good agreement between theory and practice, one must deduce that knowledge of the wind velocity is sufficient to determine the path of the vortex to good accuracy. The basis of an approach would therefore be to map the wind field in the pertinent regions either by multiple wind sensors or by a limited number of wind sensors plus inference (e.g., a 1/7 power law for the variation of wind strength with height was found to be satisfactory in the aforementioned study). A model for the spatial turbulence pattern might also be incorporated to yield more dependable predictions.

#### ● Vortex Decay and Breakdown

The process by which vortices decay and eventually break down is the least understood phenomenon associated with vortices. Under certain conditions a vortex will completely disintegrate a few seconds behind the aircraft; whereas under different conditions a vortex might persist for more than five minutes after generation by the same aircraft.

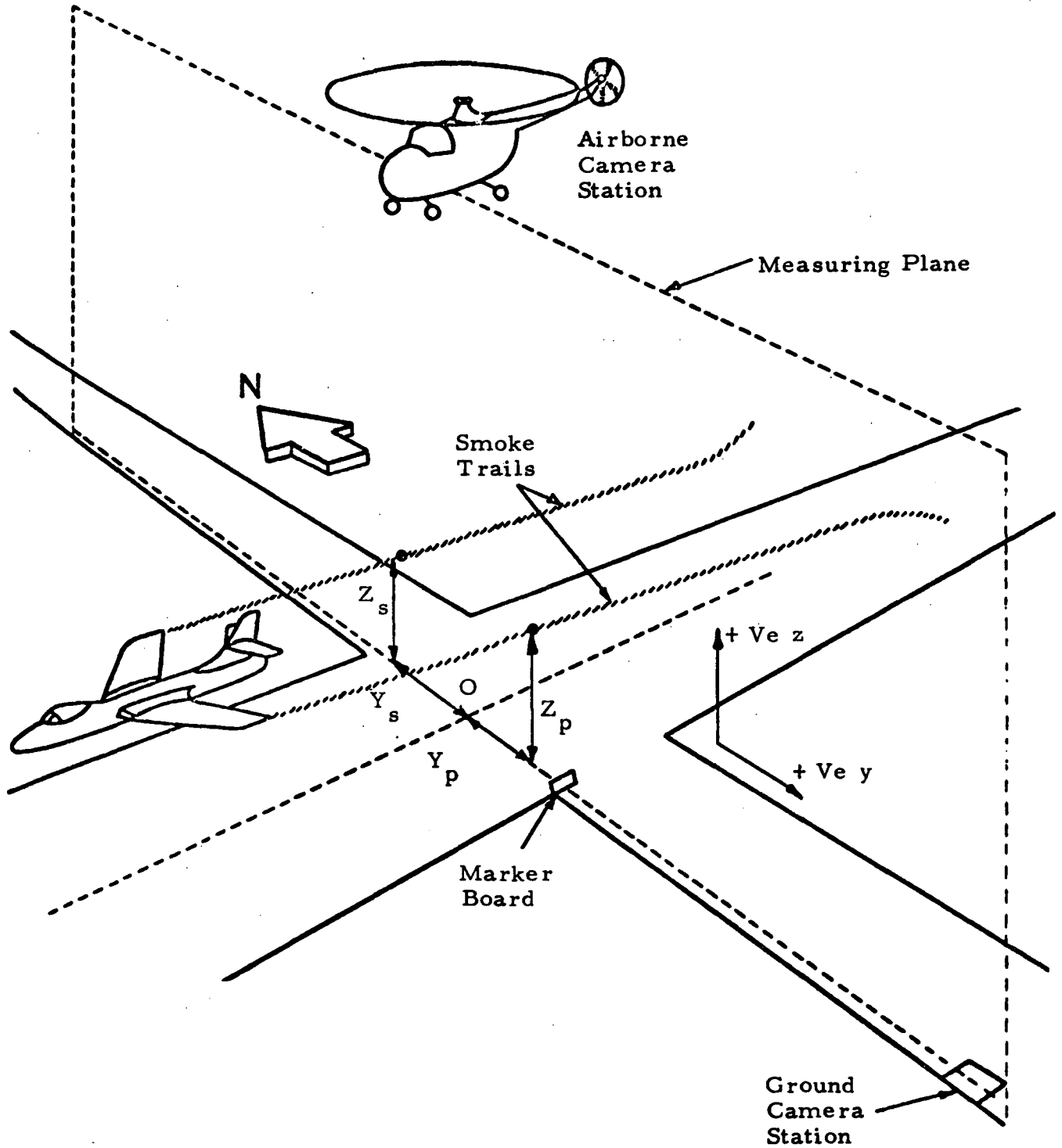
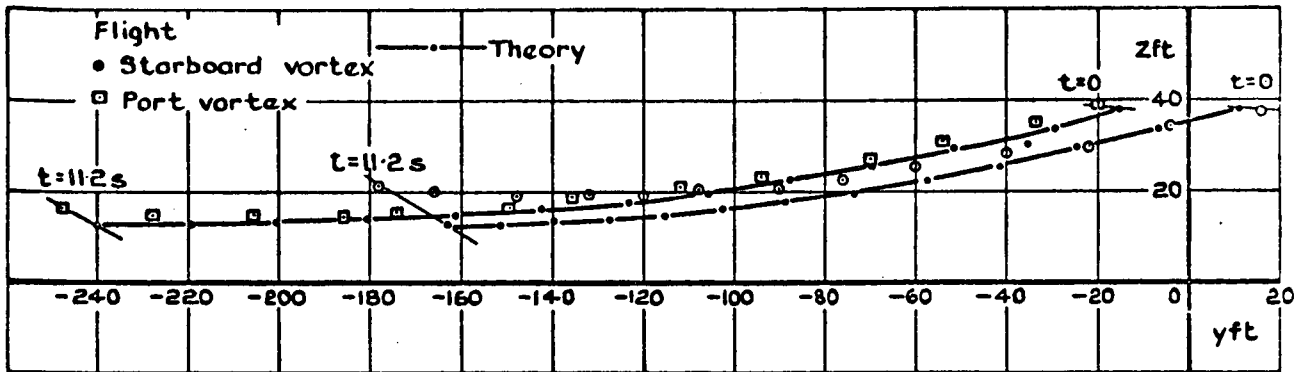
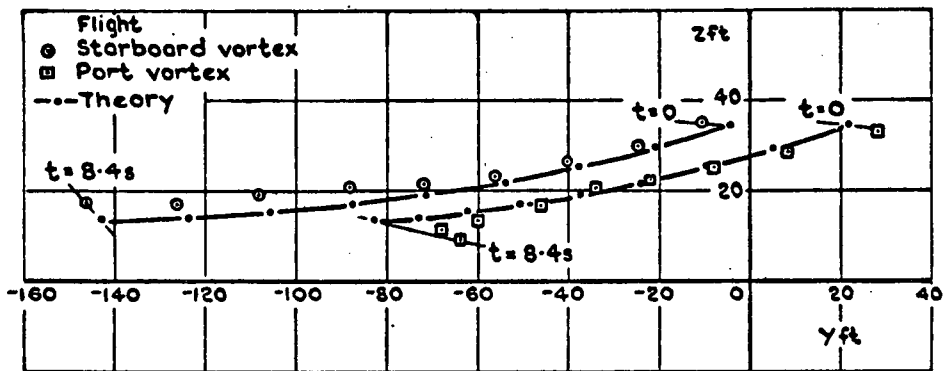


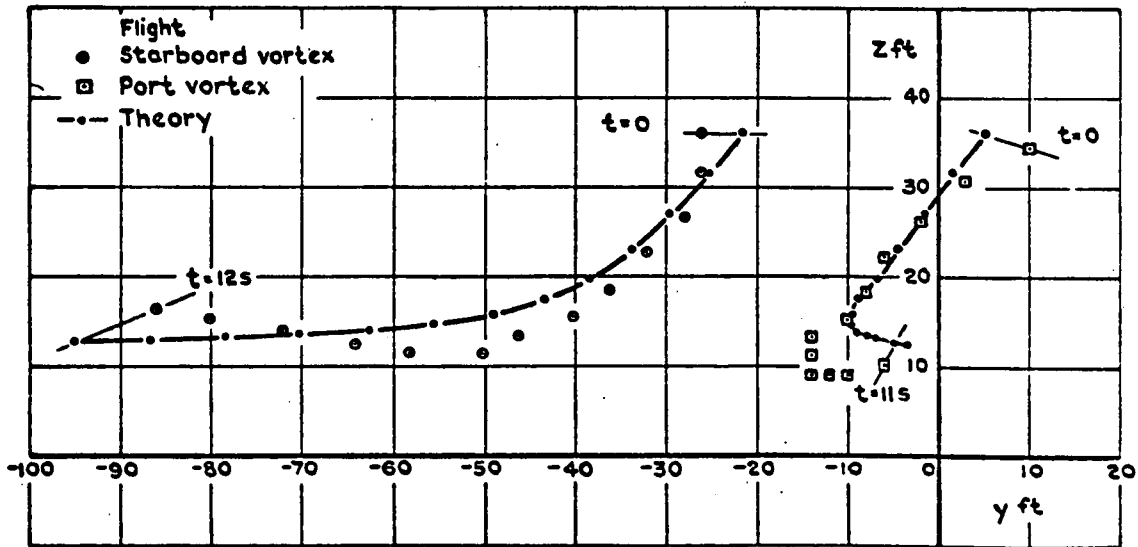
Fig. 2-3 - Diagrammatic View of Test Area



Crosswind = -14 ft/s



Crosswind = -11 ft/s



Crosswind = -3.5 ft/s (Ref. 8)

Fig. 2-4 - Comparison of Measured and Theoretical Vortex Positions

There are several theories which attempt to isolate the mechanisms which cause decay. The previously presented time-dependent expression  $v_{\theta}$  represents the original approach. This method assumes that the viscous core grows in size and the core velocities decrease with time. However, this expression predicts a growth of the core which is much slower than that which has been observed for trailing vortices. The explanation of this core growth was that turbulence existed in the core in addition to viscous effects. This would result in much higher shear forces than those of the expression for  $v_{\theta}$ . This turbulence could easily arise from atmospheric turbulence and from the turbulent wake of the airplane. A viscosity term known as "eddy viscosity" was derived empirically in an attempt to account for the turbulence effect on core growth. Wetmore and Reeder (Ref. 9) present an alternate expression for  $v_{\theta}$  which is based on such an eddy viscosity in calm air;

$$v_{\theta} = \frac{\Gamma_o}{2\pi r} \left\{ 1 - \exp - \left[ \frac{r^2}{(42 b^2 + 1.2 \bar{c} \Gamma_o t) (10^{-4})} \right] \right\} \quad (2.16)$$

where  $\bar{c}$  is the mean aerodynamic chord of the aircraft wing. This expression represents a maximum condition for vortex persistence. More rapid vortex decay would be expected if additional turbulence levels were created by such factors as:

- Cross winds
- Convection currents
- Friction resulting from vortex-ground interaction
- Irregular span-load distributions
- Jet exhaust entrainment.

One obvious disadvantage of this method of predicting vortex decay stems from its empirical nature and the neglect of the effect of the items listed above. A case when none of these items would be expected to influence the turbulence level would rarely occur. On the other hand, this method is easy to compute. If additional tests or more thorough analysis of existing test data can provide empirical constants to include the effect of the above listed items on the vortex decay, then this method can provide a practical engineering approach toward predicting vortex decay and breakdown.

Several theories have been proposed for providing a quantitative analytical description of, and isolating the mechanisms leading to vortex decay and eventual breakdown. Squire (Ref. 10) has suggested that breakdown will occur when long axisymmetric standing waves are sustained in the vortex. Another approach, suggested by Ludwig (Ref. 11) and Jones (Ref. 12), suggests that breakdown is a result of a hydrodynamic instability with respect to spiral disturbances. Still another idea proposed by Crow (Ref. 13) says that vortex decay and breakdown result from vortices undergoing a symmetric and nearly sinusoidal instability. Vortex breakdown is assumed when the vortices eventually join at intervals to form a train of vortex rings which quickly disintegrates into a harmless turbulent state.

Another entirely different approach to describing vortex breakdown was proposed by Benjamin (Ref. 14). This theory, which appears quite popular with British researchers (i.e., Hall in Ref. 15 and Harvey in Ref. 16), states that vortex breakdown does not result from an instability or any other infinitesimal disturbance alone. Instead, he describes two basically different types of axisymmetric flow which are analogous to subcritical and supercritical flow in hydraulic open-channel flow. The transition from the supercritical form of the axisymmetric flow to the conjugate subcritical flow results in phenomena analogous to the hydraulic jump in an open channel flow. This transition requires an energy loss which means that in practice a region of vigorous turbulence is generated; hence, vortex breakdown occurs.

Which, if any, of these theories correctly describes the conditions which determine the mechanism by which vortices decay and break down is not now known. Those derived analytically from such ideas as unstable disturbance propagation or the hydraulic jump analogy and sinusoidal instability certainly provide the most logical and scientific approach. However, the empirical technique using eddy viscosity probably provides the best engineering tool for predicting vortex decay. This approach, with perhaps a slight modification to include improved empirical constants obtained from recent flight tests, could easily be computerized and combined with a digital computer program for tracking aircraft trailing vortices.

The vortex lifetime data which should probably be utilized for immediate development of a predictive system is that presented by McGowan (Ref. 17). The curve of that reference is presented in Fig. 2-5 on which is also superimposed data on vortex lifetimes obtained from recent FAA/NAFEC tests on the vortices generated by a Convair 880. McGowan's curve conveniently yields an envelope to the experimental data and is probably a satisfactory state of the art curve. These vortex lifetimes can be considered as the time taken by the vortex to dissipate below some threshold peak velocity condition, the decay being due either to viscous effects or to vortex bursting, etc. The final model would probably allow for an eddy viscous decay up to the time limit given by the above curve at which time it will be assumed that the vortex no longer presents any danger.

- Previous Efforts to Define the Vortex Hazard in the Airport Environment

Previous efforts (Refs. 17 and 18) have mapped vortex motion in various wind fields to determine hazardous areas in airports for normal terminal operations. These efforts have resulted in plots like those shown in Figs. 2-6 and 2-7.

In this way caution areas surrounding a particular aircraft rotation point have been defined as being the envelope of such a system of curves. A similar system of curves exists for each touchdown and rotation point and each point on the flight path. The hazard area then becomes the envelope of the system of curves in Fig. 2-6 for each point of the flight path for a given wind velocity history. Such hazard areas may well include a parallel runway or taxi strips as indicated in the example of Fig. 2-7.

Similar considerations have been applied to the landing approach and climbout phases of flight. Figure 2-8 shows how a crosswind component of various magnitudes can modify and shift the vortex velocity pattern. From this, the importance of considering the possibility of the vortex drifting into the glide or takeoff path of a parallel runway is demonstrated.

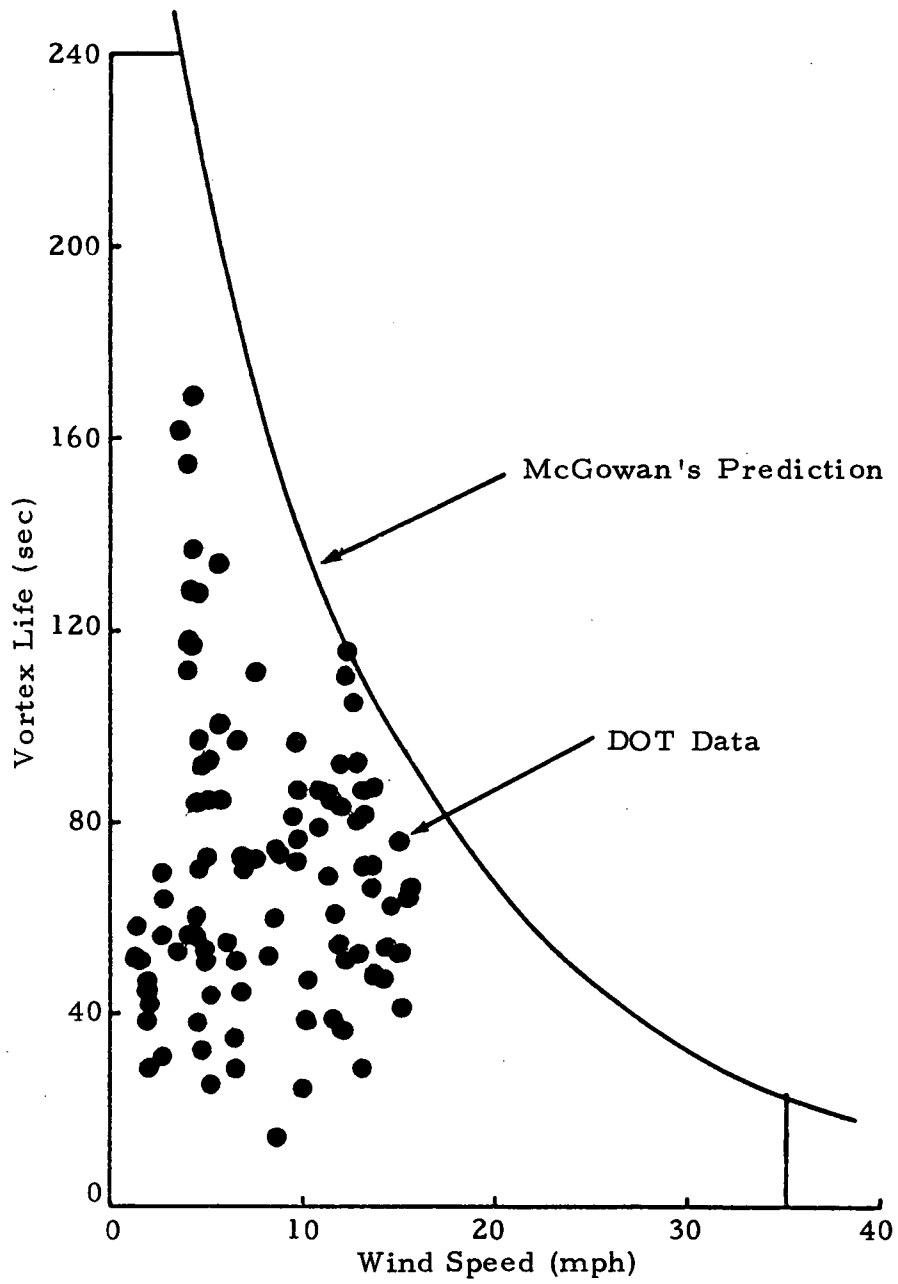


Fig. 2-5 - Vortex Lifetime Near Ground for CV 880 Aircraft

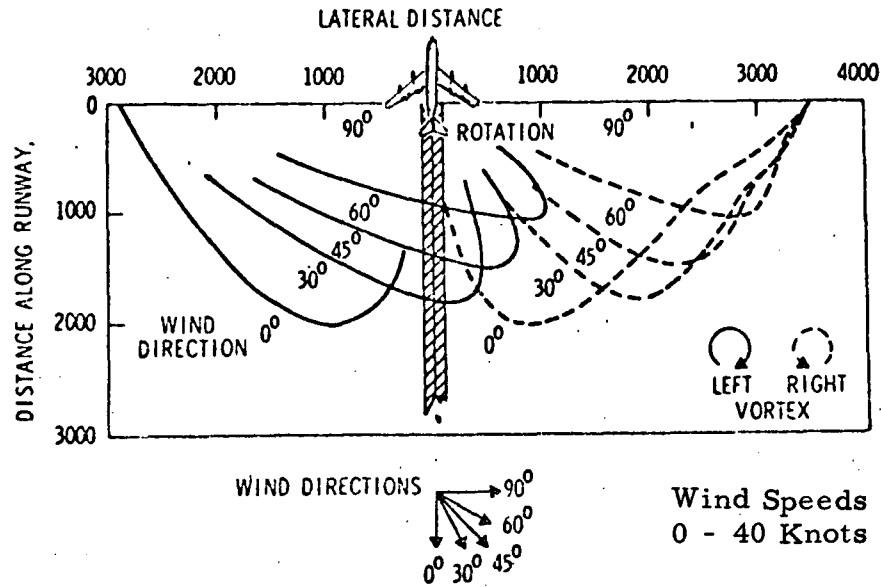


Fig. 2-6 - Vortex Movement Near Ground with Wind (Ref. 17)

Federal Aviation Administration separation regulations and Air Traffic Control operations have been established using curves and plots such as these for guidelines. The purpose of a wake turbulence predictive system development would be to develop a near real-time capability — a software accentuated predictive system — for establishing accurate separation requirements to allow increased utilization of air terminals without degradation of safety.

#### ● Recent Vortex Models

Prediction of vortex transport requires only a simplified model of vortex structure since one vortex moves in the field of another at relatively large separations, the inverse radius approximation being satisfactory under such circumstances. However, for aircraft-vortex interaction estimation, a more

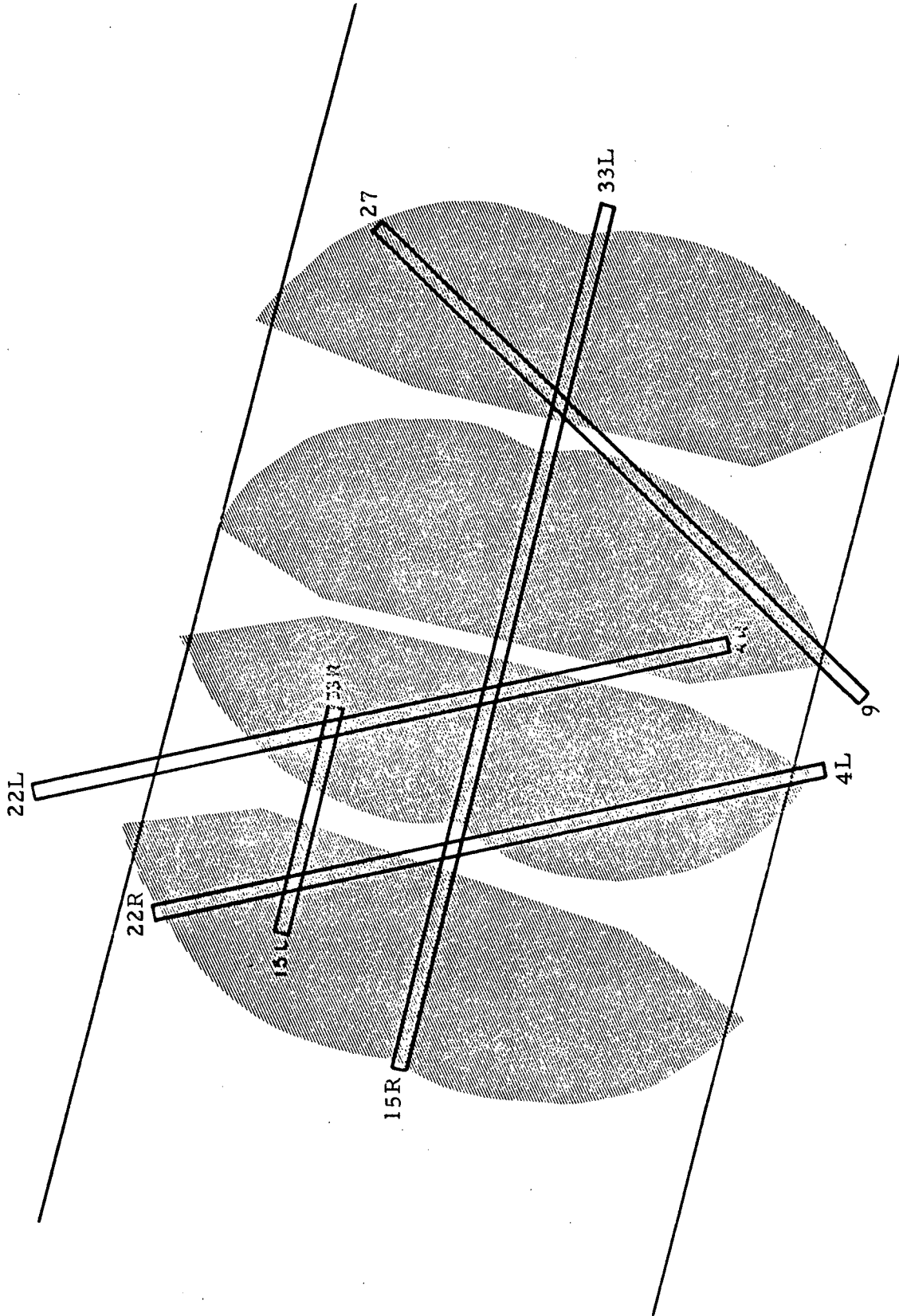


Fig. 2-7 - Vortex Drift Envelopes for Operation on 15L-33L at Logan (Ref. 18)

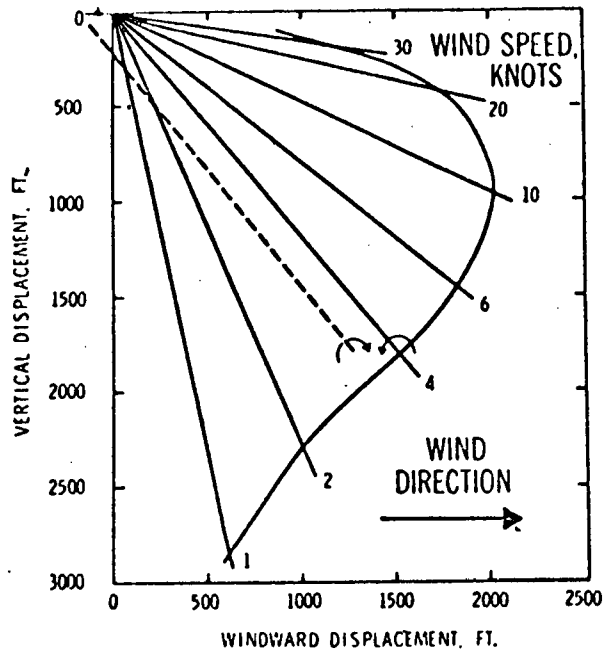


Fig. 2-8 - Envelope of Vortex System Displacement with Wind (No Ground Effect) (Ref. 17)

realistic vortex model is required — one that yields predictions of peak velocities and core diameters more in line with recent FAA data (Ref. 5). Lockheed, during this investigation, has surveyed current vortex models both empirical and theoretical. These current models are discussed in Appendix A.

### 2.3 DESIGN OF A WAKE TURBULENCE PREDICTIVE SYSTEM

This section discusses the design of a wake turbulence predictive system. The aim of this design was the simplest system capable of performing a useful role in vortex prediction. Also, flexibility was sought, so that sophistication could be added after the initial systems are operational. For the proposed design, the vortex pairs are divided into vortex elements, each of which consists of a cross sectional slice of the vortex. A segment of the vortex pair is treated as a single element when out of "ground effect." Once in "ground effect," the

pair is considered as two elements — one port element and one starboard element. A number of such elements are used to represent vortex pairs corresponding to vortices over each runway and in each air corridor leading to the airport.

The discussed system design assumes that at time  $t = 0$  the vortex system is frozen along the path of the generating aircraft (see Fig. 2-9). The vortex elements are then allowed to settle, move in the windfield and undergo ground effect. Equations in the computer provide vortex element positions as a function of time ( $t = 10, 20, 30$  sec, etc.) for the input wind field.

Volumes of the air space where presence of an active vortex would constitute a hazard; i.e., the active air corridors leading to and from the airport and the near vicinity of the runways themselves are specified in the same coordinate system as the vortex elements. These areas are entered into the computer as simple line equation coordinates. For the example illustrated, and probably the first system design, these danger areas are not extended beyond the middle marker; however, for operational type systems these would probably be extended at least to the outer marker. Initially, the danger zones are also considered to be two-dimensional. For an operational system this space might be reduced by including a "z" coordinate in the danger zone specifications.

After the vortex element initial conditions, meteorological conditions and danger areas are entered into the computer, the vortex elements are programmed to move according to the conditions for a specified time increment. After this displacement, the individual vortex elements are tested to determine if any elements are still in danger areas. The time increment and danger area identification are stored and the vortex elements are displaced via computer to their loci corresponding to the second time increment. Again, the time and danger areas are stored. This process is continued until all vortex elements have moved for time increments corresponding to their calculated lifetimes (Section 2.2).

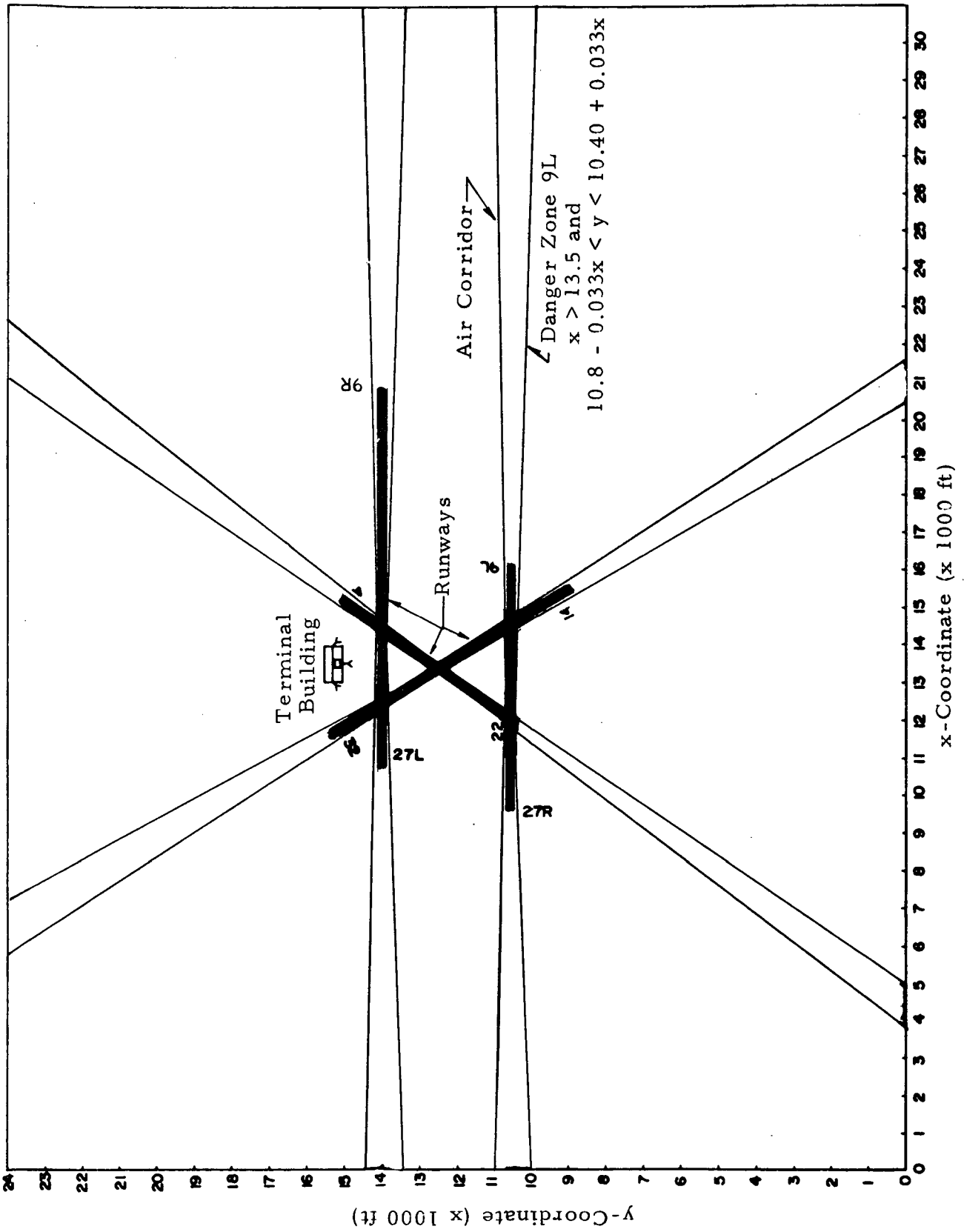


Fig. 2-9 - Danger Areas for Vortex Hazard Example: Atlanta Airport

Next, the stored time/danger-area data are examined to determine the length of time taken to clear all vortex elements from each danger area. This time to clear all elements should correspond to the time required for separation between aircraft using the corridor.

To repeat, the basic assumption of this proposed system software is that vortex elements at time  $t = 0$  are spatially at the points where they were generated. They are then allowed to drift in space for given time increments. Their positions at the end of each time increment are noted and compared to danger zones in air space which have been entered into the computer. The computer notes when elements are in specific danger zones and stores these data. After the elements have been processed for time increments equaling their lifetimes, the computer scans the data to determine when it would be safe for an aircraft to follow the wake-generating aircraft. Thus, a safe but not excessive separation distance is established.

Departing and arriving aircraft rotate and touch down in various segments of the airport and depart and arrive at different angles with respect to the vertical. (Departing aircraft rotate over the upwind two-thirds of the runway and climb out at 2 to 15 degrees, depending upon aircraft, load, atmosphere density, etc. Arriving aircraft usually aim for the 1000-foot marker and a  $2\frac{1}{2} \pm \frac{1}{2}$  degree glide slope but may land over the first third of the runway.) The proposed system could have feedback from the controller concerning the following:

- runways closed to heavy traffic (this would likely reduce vortex element drift to adjacent corridors),
- whether aircraft are arriving or departing (this would vary the calculated initial altitude of the vortex elements),
- the weight of the generating aircraft; etc.

The refinement of this controller input into the computer would come with use of a prototype system.

● Simplified Flow Chart

Figure 2-10 is a simplified flow chart of the computer operation for predicting the turbulence conditions. The initial inputs into the computer are the vortex element coordinates and danger area coordinates. The element pairs are spaced longitudinally approximately 1000 feet apart along the runways and with increasing separation along the approach and departure corridors. The total number of elements is approximately 80 in the example or 20 per runway. To extend the elements to the outer marker, either more elements or wider spacing could be used. The danger areas are entered as coefficients for the line equations which form boundaries of the danger zones. For runway 9L in the example, the danger zone would be defined in two dimensions as the following:

$$x > 13.5, \quad \text{and}$$

$$10.8 - 0.033x < y < 10.40 + 0.033x$$

As the model is extended, this two-dimensional representation of danger zones would be extended into three dimensions.

Meteorological data, next input into the computer model, will include whatever real time data are available as well as upper air windfield data when they are available. The upper air windfield data can be supplied by the Aviation Forecaster who supplies local forecasts to the field. The local forecaster in turn will receive his data from available instrumentation (radiosonde, etc) plus data supplied by pilots using the terminal. (The air data systems of the wide-bodied aircraft (i.e., inertial platform, airspeed and temperature sensors) could supply valuable, near real-time data to the forecaster.)

The wind field is next calculated. For the purpose of predicting the movement of the trailing vortices, the assumption will be made that the wind field in

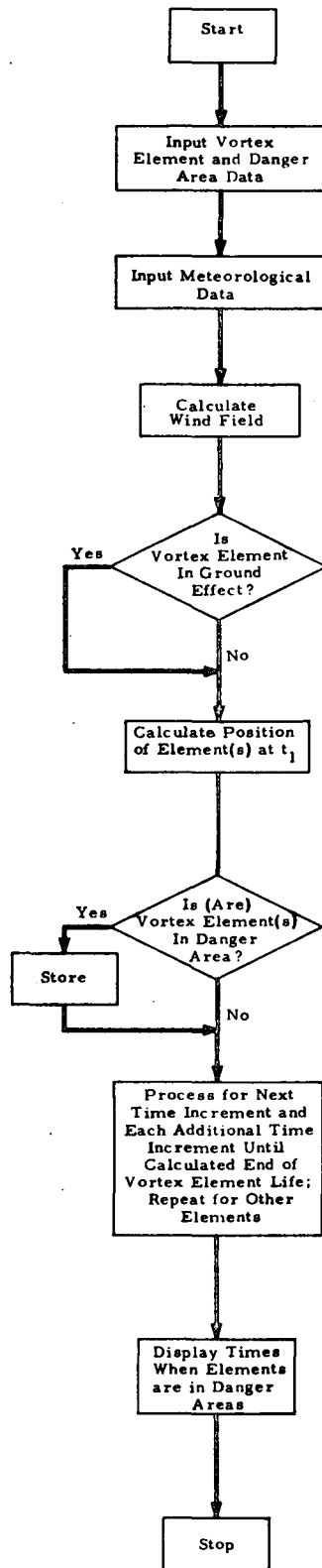


Fig. 2-10 - Flow Chart of Computer Software for Wake Turbulence Predictive System

the vicinity of an airport can be represented by a deterministic steady-state mean wind. The mean wind will be assumed to be a function of height only (i.e., variations in the horizontal plane and over time intervals less than one hour are assumed to be negligible). First, the wind near the ground will be averaged over a 10- to 20-minute period. Then the winds at altitude will be provided by the forecaster as indicated in the previous paragraph.

Wind speed and direction from near the surface to several hundred feet altitude will be fed into the computer on a periodic (likely hourly) basis. The computer will then generate least-squares polynomials (probably second- or third-degree) to fit the wind component data. The polynomials can then be used in the vortex transport prediction model to estimate the steady-state wind vector at any desired altitude.

There are, of course, many approaches which may be taken in estimating the wind profile in the lowest several hundred feet of the atmosphere. The approach taken here, however, eliminates the need for any elaborate and expensive wind measuring systems such as instrumented towers, frequent releases of pilot balloons, and so on. An experienced forecaster, using the information available to him, should be able to produce reasonably accurate estimates of the winds up to 2000 feet — even when conditions are changing rapidly as with a frontal passage. The prediction model will be set up to handle more precise wind inputs, if they become available through improved instrumentation or extrapolation techniques.

After the wind field is calculated, each vortex element is individually operated upon by the computer for a sequence of time increments equal to its calculated lifetime. These operations are represented in abbreviated form in the remainder of Fig. 2-10. The computer determines if the element is in ground effect; if it is not in ground effect, the computer treats the vortex pair segment as a single element. If it is in ground effect, the computer handles the individual (port and starboard) elements independently. The computer next determines the element positions at each time increment and checks to see if the element is in the danger zone. The process is repeated for each

time increment and each vortex element until all vortex elements are observed throughout their active lifetimes.

In particular, two areas deserve further study:

1. The relationship between observed decay rates and the spectrum of the winds near the level of the vortex; and
2. The relationship between decay and the Richardson number which is a nondimensional number containing the vertical shear of the mean wind and thermal stability, both of which are important in determining atmospheric turbulence.

● Confidence (Safety) Time Interval

Since many of the variables used in the computations are subject to varying degrees of accuracy, a safety factor will be built into the model to avoid prediction of safe conditions when hazardous conditions actually exist. This factor, in the form of a confidence interval in time, will be determined from estimated inaccuracies in aircraft trajectories, meteorological parameters, etc. (Note: The confidence time interval will be less for the hybrid system of Section 3.3 than for the predictive system due to the added input data of the hybrid system.)

● Use of the System

From the data of the persistence of vortex elements in the individual corridors, the Air Traffic Controller can mentally or from tables determine the spacing that is required between various classes of aircraft for a safe landing or departure. The controller would see how long is required for all vortex elements to clear each of the aircraft corridors for a specified generating aircraft type, departure, arrival, departure angle, etc. He would then know the conditions of wake turbulence persistence and judge the separation requirements following an aircraft of the indicated type. Use of the system is further discussed in Section 2.5. Communications and Action Command Processes.

## 2.4 INFORMATION ACQUISITION, STORAGE AND PROCESSING

The information acquisition, storage and processing subsystem should be compatible with the field meteorological instrumentation, system software design and display/command process, and yet will be as inexpensive and simple to interface with existing air terminal facilities as is possible.

### ● Information Acquisition

The information acquisition subsystem should gather the data required to forecast the wake turbulence and enter these data into the wake turbulence predictive computer (Section 2.3). The information to be entered into the computer may be of the following forms:

- Meteorological data from sensors presently installed at the airport
- Meteorological data from sensors to be installed at the airport
- Meteorological data from observers
- Aircraft operations data (aircraft type, departure or landing, departure angle, etc.).

Meteorological data from sensors presently installed at the facility must be formatted to be compatible with the wake turbulence predictive system computer. This formatting may require analog-to-digital converters, digital-to-digital converters, multiplexers, etc. However, for an interim system, input of these data into the computer should probably be via computer console and operator to read the indicated values and enter the data. Sensors presently available at air terminals are located near or on the control tower and at remote locations around the terminal. Consideration must be given to cabling lengths, cable routes, remote analog-to-digital converters, reliability, maintenance, etc., if present instrumentation is used with an operational prediction system.

Economic factors should be considered in deciding whether to use existing meteorological sensors and converting their outputs to be compatible with the data processing subsystem or purchasing new sensors to be compatible. In addition, new sensors might be required to provide additional meteorological data to these data already available at air terminals.

In addition to sensor-provided data, the system should be capable of receiving data through the forecaster for the local meteorological conditions. An experienced forecaster will filter information from pilots, radiosondes, etc., to provide the required input into the model. Wind shear data from the air data systems of the 747s, L1011s, and DC-10s would constitute a valuable input into the system which could come through the local forecaster. The trained forecaster should be a valuable system link for providing forecasts of wind profiles to several hundred or even several thousand feet.

It is envisioned that in an operational system, the air traffic controller will have a limited capability for communicating with the computer. He might supply the computer (Section 2.3) with the following data from a single console with a half-a-dozen push buttons:

- Runways closed to heavy aircraft
  - Type aircraft generating vortices
  - Landing configuration
  - Departing configuration
  - Departing angle with respect to horizon
- 
- Information Storage and Processing

Information storage and processing will be performed via digital computer for the wake turbulence predictive system. After the computer memory size and speed are defined, existing and planned computer facilities at the air terminals should be surveyed to determine if it is practical to add this burden to existing facilities or to determine if a "minicomputer" should be used for the predictive system which is independent of existing facilities.

The computer operation will be divided into three operations:

- Collect meteorological and other pertinent data
- Calculate wake turbulence conditions
- Provide data for display in proper format.

The computer size can be determined from summing the following storage requirements:

- (A) Pertinent Input Data Storage
- (B) Program Format
- (C) Arithmetic Functions
- (D) Display Data
- (E) Housekeeping

Initial estimates indicate 8 to 16K of memory should be sufficient for storage and performing the desired calculations.

Once computer storage, word length and computation time are specified from knowledge of the wake turbulence prediction system software design, a survey of existing and planned airport computer facilities would indicate the feasibility of integrating these data processing operations into existing or proposed (ARTS II) air terminal computational facilities. If existing or planned facilities are not compatible with requirements, a "mini-computer" will most probably perform the computational requirement at a cost of \$25,000 to \$50,000 per unit.

## 2.5 COMMUNICATIONS AND ACTION COMMAND PROCESSES

The communications and action command process for the wake prediction system should be compatible with the present National Aerospace System (NAS). The primary difference between the communication/command-action systems for detective and predictive systems is that detective systems

may provide short time-period data for possible aircraft wave-offs while the outputs of a predictive system should provide sufficient warnings of hazardous conditions to allow spacing procedures to provide a mechanism of hazard avoidance. The following paragraphs will discuss several methods of communications and action command processes which have been or should be considered for integration into the NAS. These methods include the following:

- Cockpit Display: Pilot takes precautionary action
  - Runway Display: Pilot takes precautionary action
  - Controller Display: ATC relays turbulence data; pilot takes precautionary action
  - Controller Display: ATC regulates traffic spacing according to turbulence forecast
- 
- Cockpit Display with Pilot Reaction

"A cockpit display would remove the overburdened controllers from the loop" is a view advanced initially by some air traffic controllers when discussing the subject of wake turbulence avoidance. However, ATC is not really removed from the loop in landing operations because any turbulence avoidance action taken by a pilot in the terminal area affects other aircraft in the area; therefore, ATC is automatically involved. In addition the pilot, who is very busy when landing an aircraft, must decide what kind of action to take. For a small aircraft he could possibly land over the turbulence; but for larger aircraft, unless the runway is very long, he can only abort the landing thus affecting the whole traffic pattern. In addition, pilot prejudice would enter into the picture with some pilots aborting landings and others continuing their landings under the same turbulence conditions. From the equipment standpoint, a turbulence indicator in a larger aircraft equipped with sophisticated landing equipment might be a minor additional expense; however, for a smaller aircraft which is affected more by turbulence than the larger aircraft, the additional expense of the warning device would likely pose an economic burden upon the owner of the craft.

The runway lighting display eliminates the purchase of equipment burden upon the individual aircraft owner. A system similar to VASI (Visual Approach Slope Indicator) has been recommended as a possible turbulence warning mechanism. Different colors could represent various degrees of turbulences. For departure this might work quite well. However, for approaches this system suffers from the same deficiencies as the cockpit display in that the pilot has to make a sudden decision at a time when he is already overburdened, and his decision likely affects the remainder of the airport traffic. ATC becomes involved if hazard avoidance maneuvers are necessary.

● Display for Air Traffic Controller

Today air traffic controllers are required to maintain a five-mile separation behind a "heavy" (>300,000 pounds) jet when the heavy aircraft is followed by a lighter aircraft. The controllers are also required to provide a turbulence warning if, in their judgment, wake turbulence constitutes a hazard. A typical tower message for landing behind a heavy jet on the same runway is "Number two to land, following Lockheed C-5A on final. Caution wake turbulence." For landing behind a heavy jet on a parallel runway closer than 2500 feet the message is similar, "Cleared to land runway 9-R - Caution wake turbulence -747 on final 9-L."\* The courts have declared the tower responsible for providing judgment decisions of when it is safe to depart or land under turbulence conditions.\*\* Lockheed-Huntsville personnel, after consulting with numerous pilots and controllers have concluded that a system which would provide meaningful turbulence prediction data to the controllers would be most beneficial in helping the controllers to make more accurate decisions about hazardous conditions. These data would allow the controllers

\* FAA Wake Turbulence Advisory Circular, AL No. 90-23B, 19 February 1971.

\*\* "How the Courts Look at Wake Turbulence," R. H. Jones, FAA Turbulence Symposium, Washington, D.C., 22-24 March 1971.

to provide adequate spacing between the aircraft — both arriving and departing — to minimize turbulence hazard risks and maximum utilization of the air terminal. A number of pilots and controllers alike have agreed that adequate but not excessive spacing, even without a turbulence message to the pilot, would be the best method of controlling wake turbulence hazard avoidance for the immediate future.

For a wake turbulence predictive system using state-of-the-art hardware and vortex theory, predictions of conditions conducive to vortex dissipation should be valid for several minutes at least. The data into the model will, for most cases (i.e., except in frontal conditions), not vary excessively over a period of several minutes. Therefore, a forecast of the conditions should be valid for the same period of time. Control of aircraft final landing spacing begins several minutes prior to aircraft touchdown. The controllers, given a vortex condition forecast, should be able to vary spacing intervals according to the hazard condition. No sudden wave-off should occur unless some unforeseen phenomenon occurs. In this case, the wave-off would be handled in the conventional manner.

A more advanced prediction system might provide the controller with additional data. Instead of forecasting meteorological conditions conducive to turbulence dissipation from meteorological data, the more advanced system might also take inputs of aircraft type, velocity and location and predict the hazard from and to other aircraft in the system. This type system would semi-automate the controller's judgment decision.

## Section 3

## DETECTIVE WAKE VORTEX MONITORING SYSTEM

## 3.1 INTRODUCTION AND SUMMARY

The detective wake vortex monitoring system is very likely the ultimate wake vortex warning system. The detective system will aim at providing a long range (10 km from runway threshold) warning of actual measured vortex conditions in a real time manner. To be most effective, the status of the detected vortex is to be displayed simultaneously in an easily interpreted format to both the pilot and to the departure-arrival and local air traffic controllers. The air traffic controllers are to maintain aircraft spacing according to vortex movement and decay trends and the pilot, in coordination with the controllers, would make real time decisions from his cockpit monitor if action were required to avoid hazardous contact with vortices which were determined to be in his projected flight path. While the predictive or hybrid system might increase maximum traffic handling rates in say 50 to 70% of the operational conditions, the detective system should increase maximum traffic handling capacities in a higher percentage (say 80 to 90%) of the operational conditions because of the increased knowledge of vortex conditions and less margins for error in predicting the hazard.

Although the detective wake vortex monitoring system is the most effective type of vortex monitoring system from the standpoint of increasing air terminal capacities, it is the most expensive system to both develop and install in the field. In order to build a system which will provide effective real-time, long-range vortex data, a research program must be planned to develop more basic knowledge about the vortex characteristics and presently available hardware (lasers, detectors, etc.) must be "Mil-spec'ed" for long life operation with minimum maintenance. The state-of-the-art of data transmission from the controller to the pilot should evolve from the present verbal communication system to a digital-data link system or equivalent with a simply

formatted (possibly CRT) cockpit display of data communicated from the ground. Considerable experimentation should be performed in probing vortices at long ranges with laser Doppler instrumentation. In addition to development costs, the detective system – although probably much more effective than the predictive or hybrid systems – will cost more than the other systems to install because of the additional hardware components.

A considerable amount of this contractual effort (NAS8-26668) has been expended in the investigation of detective vortex monitoring systems. This chapter of the report will first briefly describe a typical detective system (3.2) and then discuss studies which led to the selection of this typical system. Section 3.3 discusses the advantages and disadvantages of one-component (one-dimensional) and two-component (two-dimensional) detective systems. The program used to develop these data is discussed in Section 3.4. Conclusions and recommendations for additional effort toward predevelopment of the detective system are covered in Section 3.5.

### 3.2 TYPICAL WAKE VORTEX DETECTIVE SYSTEM

Figure 3-1 illustrates a typical system for monitoring wake vortices with a detective laser Doppler sensor. Figure 3-1, a two-component laser Doppler sensor – actually two each of single-component Doppler sensors scanning synchronously – provide data which are computer-processed to output two-dimensional visualizations of the vortex flow fields. The outputs of these sensors are processed either by a mini-computer or by a module of the Automated Radar Terminal System (ARTS III) which also performs a decision process in determining which vortices may be hazardous to oncoming aircraft. These vortices are displayed to the departure/arrival and local air traffic controllers via the plan position indicator (PPI) displays. Data are also relayed to the aircraft via the proposed digital data link and displayed in the cockpit by the multi-function display (MFD). These various functions are discussed in the following paragraphs. The subsystem subsections of Section 3 present the reasoning which led to the choice of the depicted system.

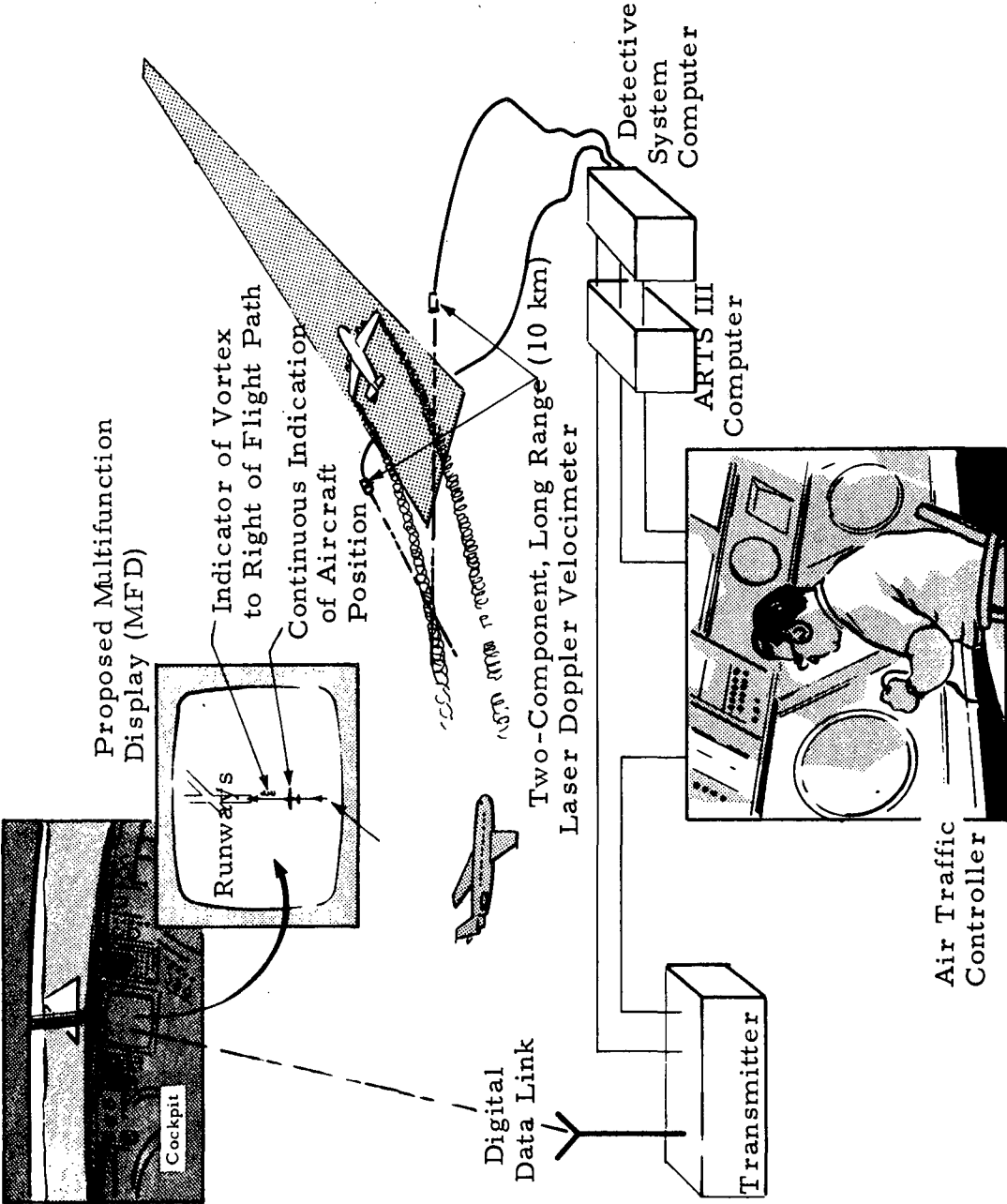


Fig. 3-1 - Typical Detective Wake Vortex Monitoring System

### 3.2.1 Sensor Subsystem

The sensor for the long range wake turbulence monitoring system is the laser Doppler velocimeter (LDV). This subsection will first describe the basic principle of the LDV; next a typical system layout at an air terminal will be described; and finally a number of alternate optical configurations for the LDV will be described.

The basic principle of the LDV is described below:

"An electromagnetic wave having an angular frequency,  $\omega_i$ , propagating in the direction  $\bar{k}_i$  ( $|\bar{k}_i| = \omega_i/C = 2\pi/\lambda_i$ ,  $C$  and  $\lambda_i$  being the velocity of light and the incident wavelength, respectively) and scattered by a particle moving with a velocity,  $V$ , into a direction  $\bar{k}_{sc}$  ( $|\bar{k}_{sc}| = 2\pi/\lambda_i$ ) experiences an angular frequency shift  $\Delta\omega$  which for nonrelativistic velocities is given by

$$\Delta\omega = (\bar{k}_{sc} - \bar{k}_i) \cdot \bar{V}.$$

The detected frequency shift is due, therefore, to the velocity component of  $V$  in the direction  $(\bar{k}_{sc} - \bar{k}_i)$ . Confining considerations to a backscatter system, the Doppler shift  $\Delta f$  ( $=\Delta\omega/2\pi$ ) is given by

$$\Delta f = 2|V|\cos\theta/\lambda,$$

where  $V$  is the target velocity,  $\lambda$  the wavelength, and  $\theta$  the angle subtended by the wind direction and the optical system line of sight" (Ref. 19).

Figure 3-2a depicts a typical (Atlanta) airport layout and the arrangement of laser Doppler velocimeter (LDV) sensors to provide measured vortex status data for the air corridors entering and departing the air terminal. In this illustration, one of the parallel runways is the primary approach

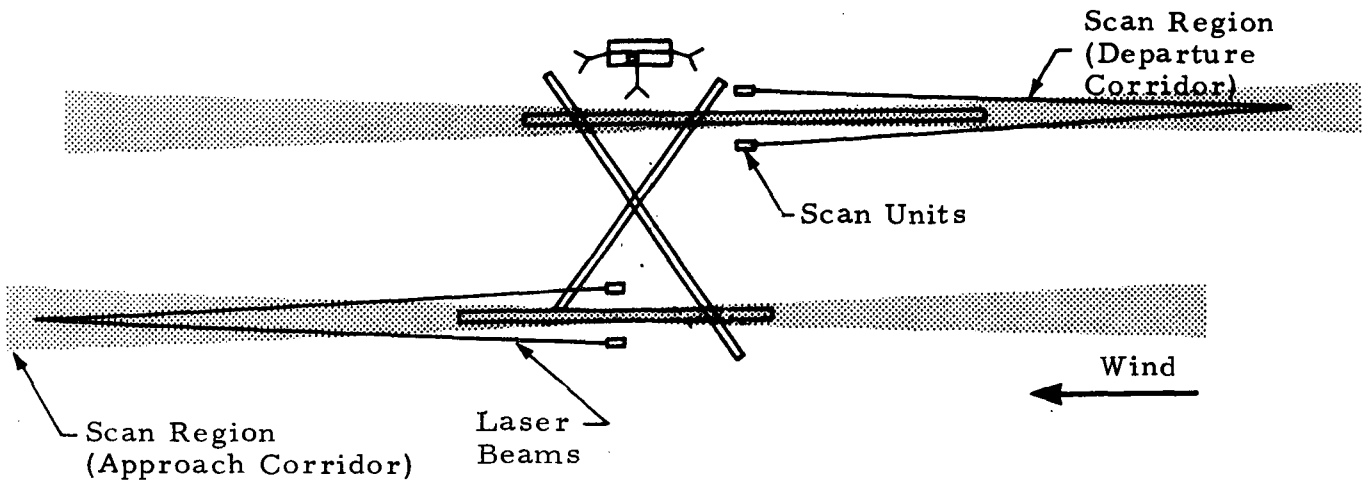


Fig. 3-2a - Typical Airport Layout of Detective, Long-Range, Laser Doppler Wake Monitoring System

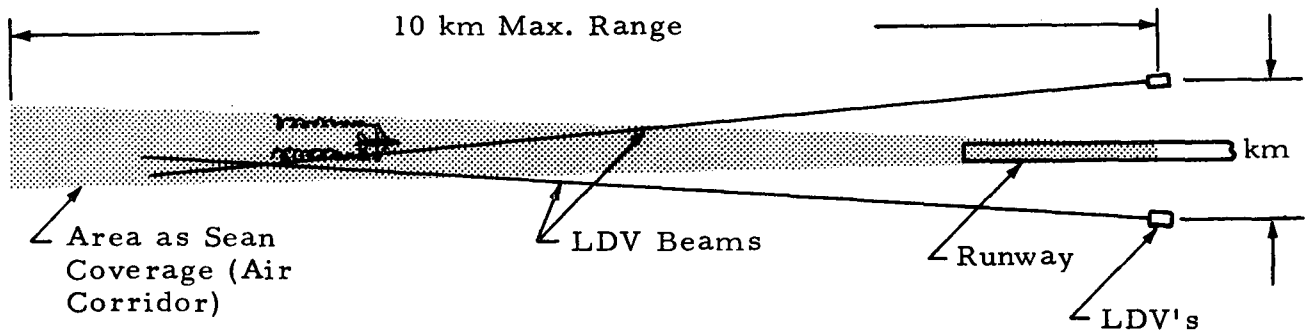


Fig. 3-2b - Typical Layout and Range of Two Component Laser Doppler Velocimeter for Specific Runway

runway and the other is the primary departure runway. LDV sensors are oriented to scan the appropriate corridors. Vortices are to be tracked within these corridors; therefore, flight within the corridors would not be considered safe in the presence of the vortex hazard. Aircraft entering or departing the terminal outside these corridors would do so at their own risk. The LDV sensors would be capable of scanning either end of the runway or both ends alternately depending upon the requirement.

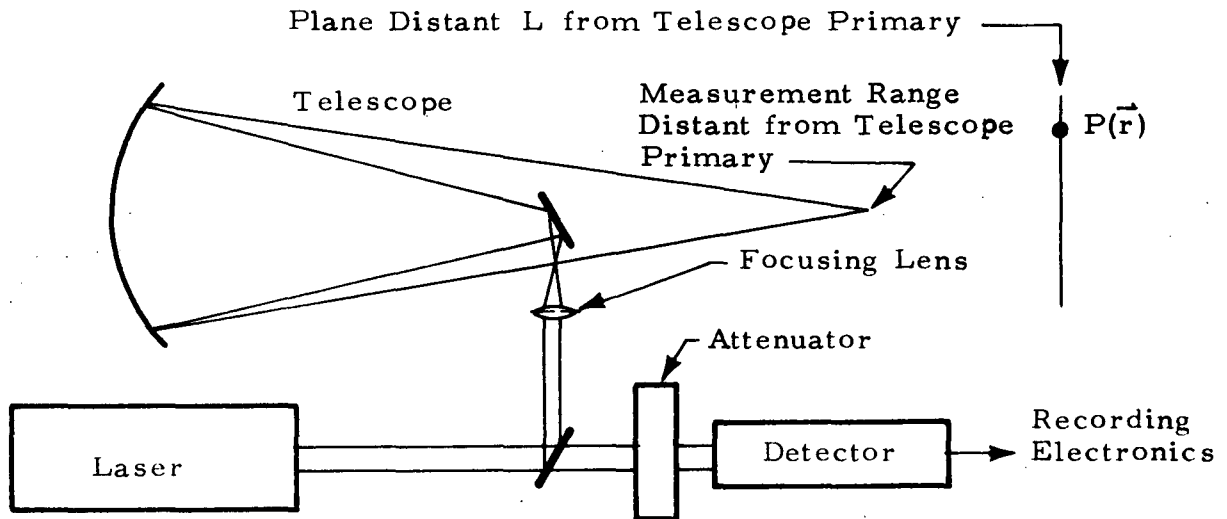
A typical range and dimension of an LDV sensor system is illustrated in Fig. 3-2b. The sensors are typically separated by approximately one kilometer. Separation requirements and range requirements are discussed in Sections 1.4 and 3.3 respectively. The requirement for two sensors to provide a two-dimensional picture of the vortex and the minimum separation between the sensors are discussed in Section 3.2. Basically, the two sensors are required to obtain a clear picture of the vortex flow field under all ambient wind conditions and maximum practical angular separation is required between the sensors and the data point being examined. Sensor separation is determined by airport real estate limitations, in the figure to approximately 1 km separation between the sensors and 6 deg angular separation between the sensors at the most distant data point (10 km).

#### ● Typical Detective System Optical Configuration

Selection of a specific optical configuration for a detective wake turbulence monitoring system sensor is probably premature at this point; however, several options are presented which might fulfill system sensor requirements. Basic optical configuration options are the following:

- Coaxial (monostatic), focused, continuous wave
- Coaxial (monostatic), pulsed
- Coaxial (monostatic), frequency modulated, continuous wave
- Bistatic focused, continuous wave
- Bistatic pulsed

Of the five configurations mentioned on the previous page, the coaxial focused laser Doppler velocimeter depicted schematically below is the optical configuration which has been most used to date.



"Radiation from the laser is focused at the required range via a Newtonian or Cassegrain telescope. Target range variation is provided by varying the position of the focusing lens which also serves to expand the small diameter laser beam to fill the primary telescope objective. The laser beam is divided by a beam splitter before it enters the telescope. A small portion of the laser energy is split off toward the detector. The Doppler shifted radiation scattered from the focal region of the telescope is collected by the telescope and allowed to reenter the laser cavity where it is amplified. Upon reemerging from the laser, a fraction of the frequency shifted component takes the path to the detector where it is photomixed with the original laser oscillation. The output of the detector is thus modulated at the frequency of the Doppler shift introduced by the motion of the particulate matter in the atmosphere at the telescope focus. For a  $10.6\mu$  wavelength (carbon dioxide laser wavelength) the Doppler shift  $\Delta f$  is given by

$$\Delta f = 188.5 v' \text{ kHz}$$

where  $v'$  is the velocity component along the optic axis in m/sec (Ref. 19).

"Spatial resolution from such a system is obtained by the requirement that wave fronts must match at the detector surface to be efficiently photomixed. Since the original laser radiation emerges from the laser as a plane wave front, only the scattered radiation collected by the telescope that emerges from it as a collimated beam is heterodyned efficiently. Essentially this means that only radiation scattered from the region near the focus of the telescope contributes to the Doppler signal" (Ref. 19).

Figure 3-3 indicates the spatial resolution of this optical configuration as a function of range. This figure indicates that the spatial resolution of the coaxial configuration is probably too poor at long ranges for this system to be considered as a candidate for the long range wake monitor.

The signal-to-noise ratio (SNR) for the coaxial system in the near field appears (Ref. 20) as:

$$\text{SNR} = \frac{1}{4} \eta \frac{n \sigma \lambda N}{B}$$

where

$\eta$  = efficiency of the optical system

$n\sigma$  = scattering cross section of the medium per unit volume

$\lambda$  = laser wavelength

$N$  = number of photons per second emitted by laser

$B$  = electronic bandwidth

This equation appears independent of range and optic diameter. However, as the range to the focal volume increases with a given coaxial optical configuration, the focal volume size increases and the velocity distribution within the focal volume spreads, requiring the bandwidth of the electronics to be increased. Thus, from the above equation the resultant SNR is decreased proportionately to the increased bandwidth requirement.

Signal-to-noise is affected by scan rate since scan rate and range determine time-on-target which in turn contributes to the signal bandwidth. This is depicted in Fig. 3-4.

The coaxial pulsed system depends upon pulse length for spatial resolution. However, as pulse lengths are shortened to improve spatial resolution, velocity resolution decreases proportionately (see Fig. 3-5). Interpulse

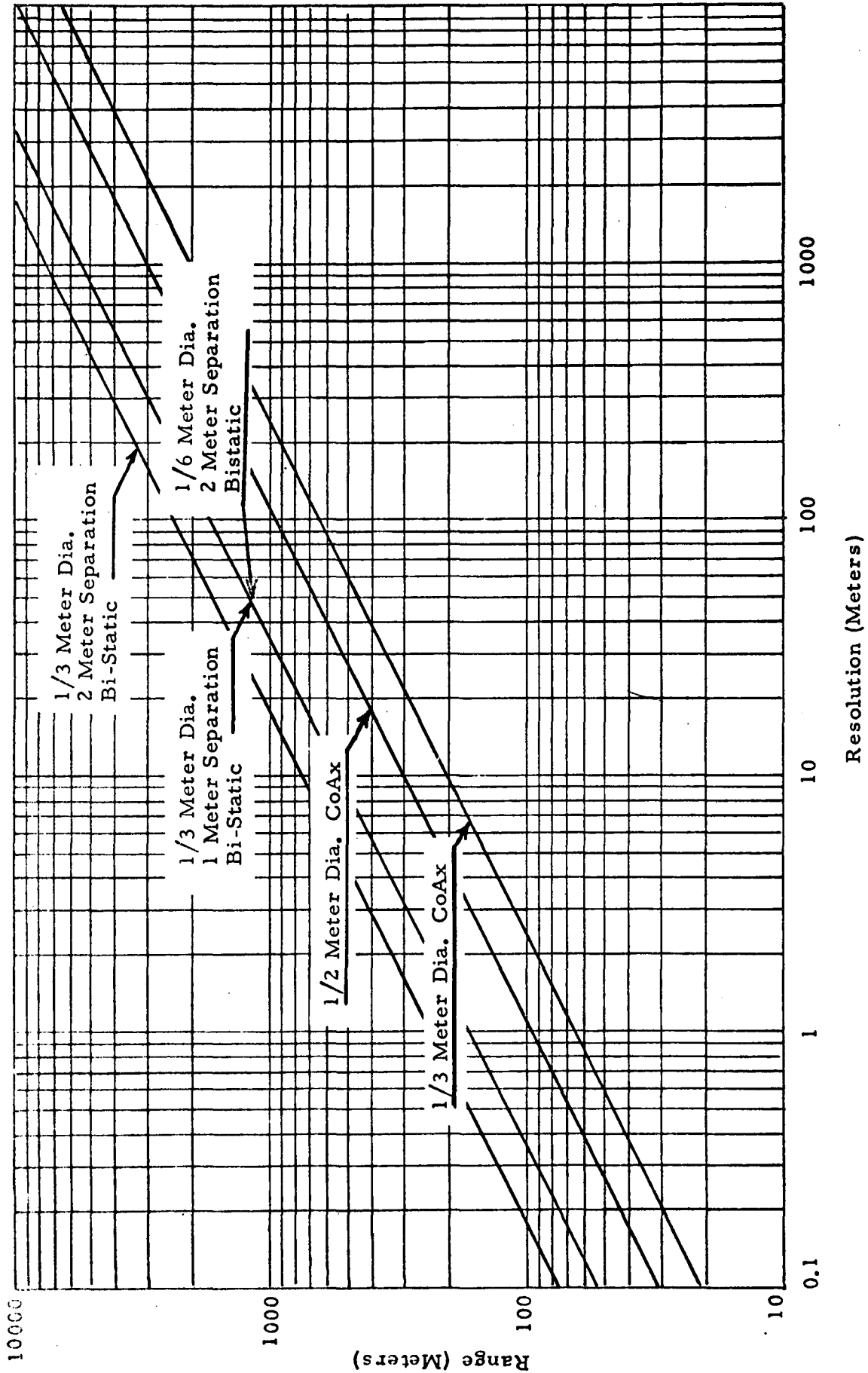


Fig. 3-3 - Range Resolutions (50% Return) at 10.6 Micron Wavelength

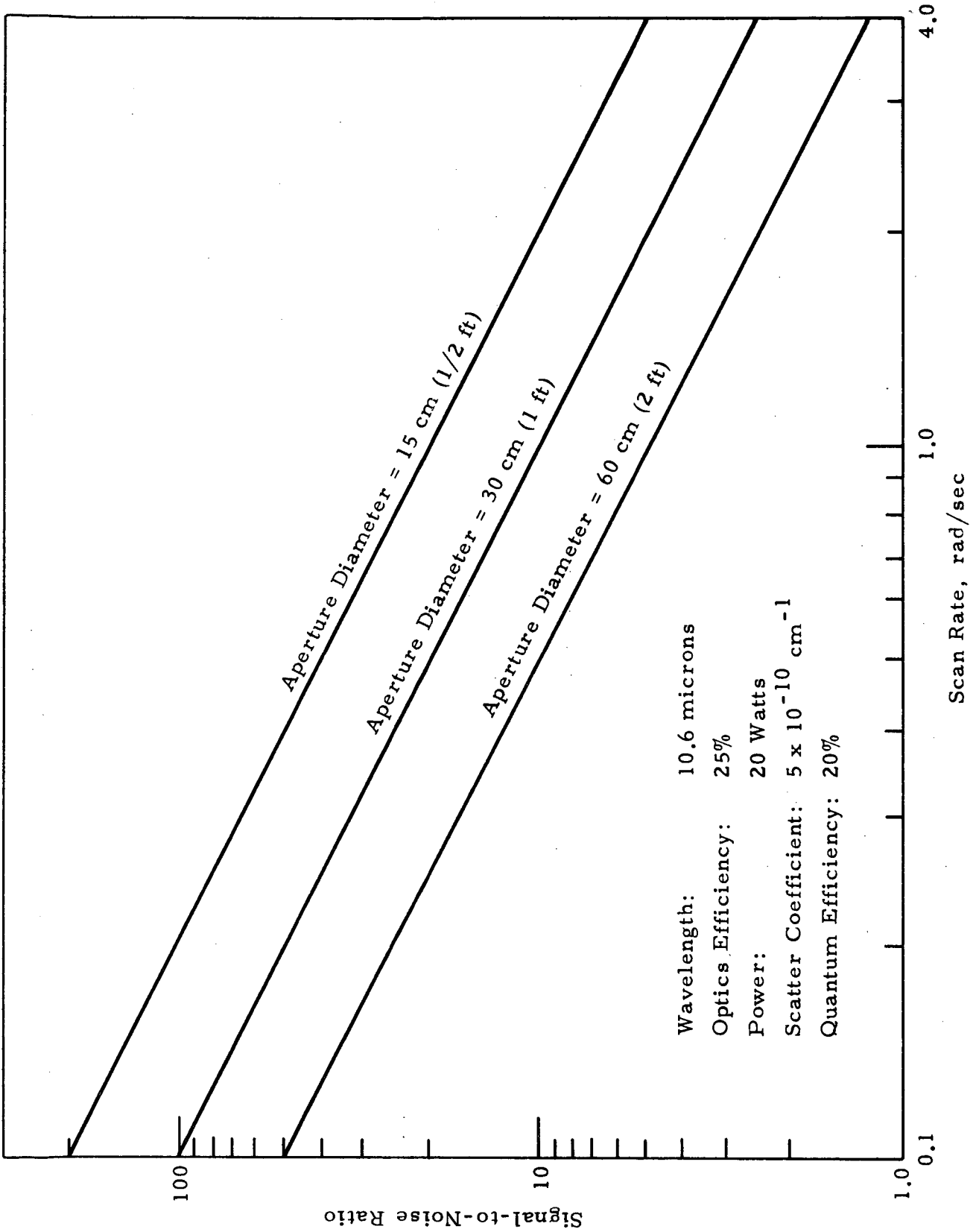


Fig. 3-4 - Signal-to-Noise Ratio for Coherent, Continuous-Wave Coaxial Configuration as a Function of Scan Rate

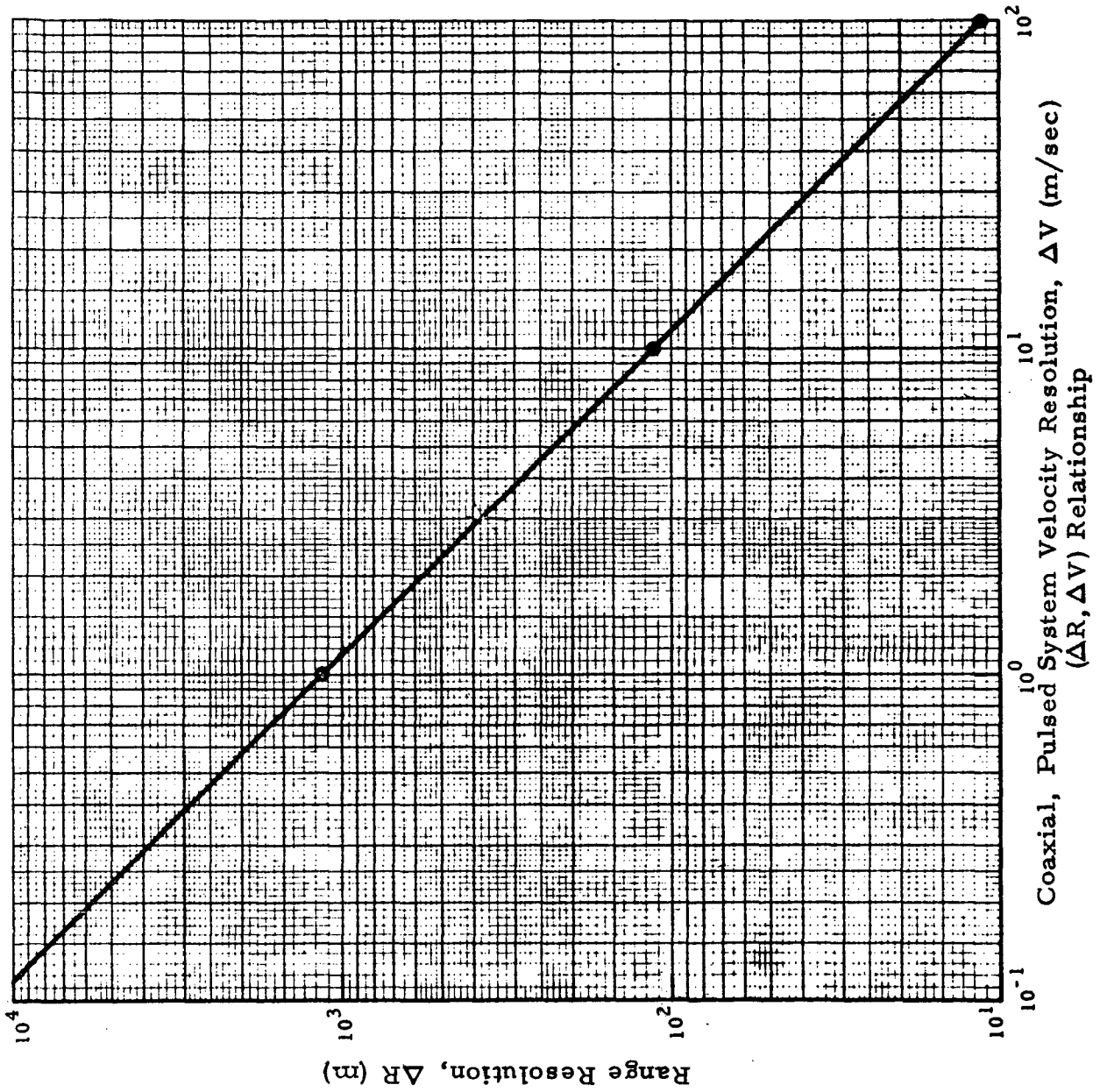


Fig. 3-5 - Coaxial, Pulsed System Range and Velocity Resolutions

modulation is used in microwave radar systems (Ref. 21) to improve spatial resolution. However, interpulse modulation with a CO<sub>2</sub> laser system would add sophistication to the overall system design and likely increase costs and reduce reliability.

Signal-to-noise per pulse for the coaxial pulsed configuration can be given by the same equation as for the standard coaxial system when the data point of interest lies in near field ( $R < D^2/\lambda$ ) with N redefined as the number of photons per pulse. However, when the data point lies in the far field ( $R > D^2/\lambda$ ), the following equation holds for SNR (Ref. 22)

$$\text{SNR} = \eta(J/h\nu)n\sigma c \tau D^2/R^2$$

where

$\lambda$ ,  $\eta$  and  $n\sigma$  are, as previously defined

J = net output energy in observation time

c = speed of light

$\tau$  = pulse duration

$h\nu$  = laser photon energy

D = optic operative diameter

R = range to data point

In both near and far field the SNR is proportional to the average energy illuminating the volume of interest. To obtain sufficient average energy to provide adequate SNR at long ranges with present technology requires sophisticated laser amplifiers or a high power laser operating in a Q-switched or mode-locked configuration. The power efficiencies of these types of laser configurations are nominally much lower than for continuous wave configurations. Since S/N depends upon the energy illuminating the target, S/N is also dependent upon scan rate as depicted in Fig. 3-6.

The frequency modulated coaxial system depends upon linearly varying

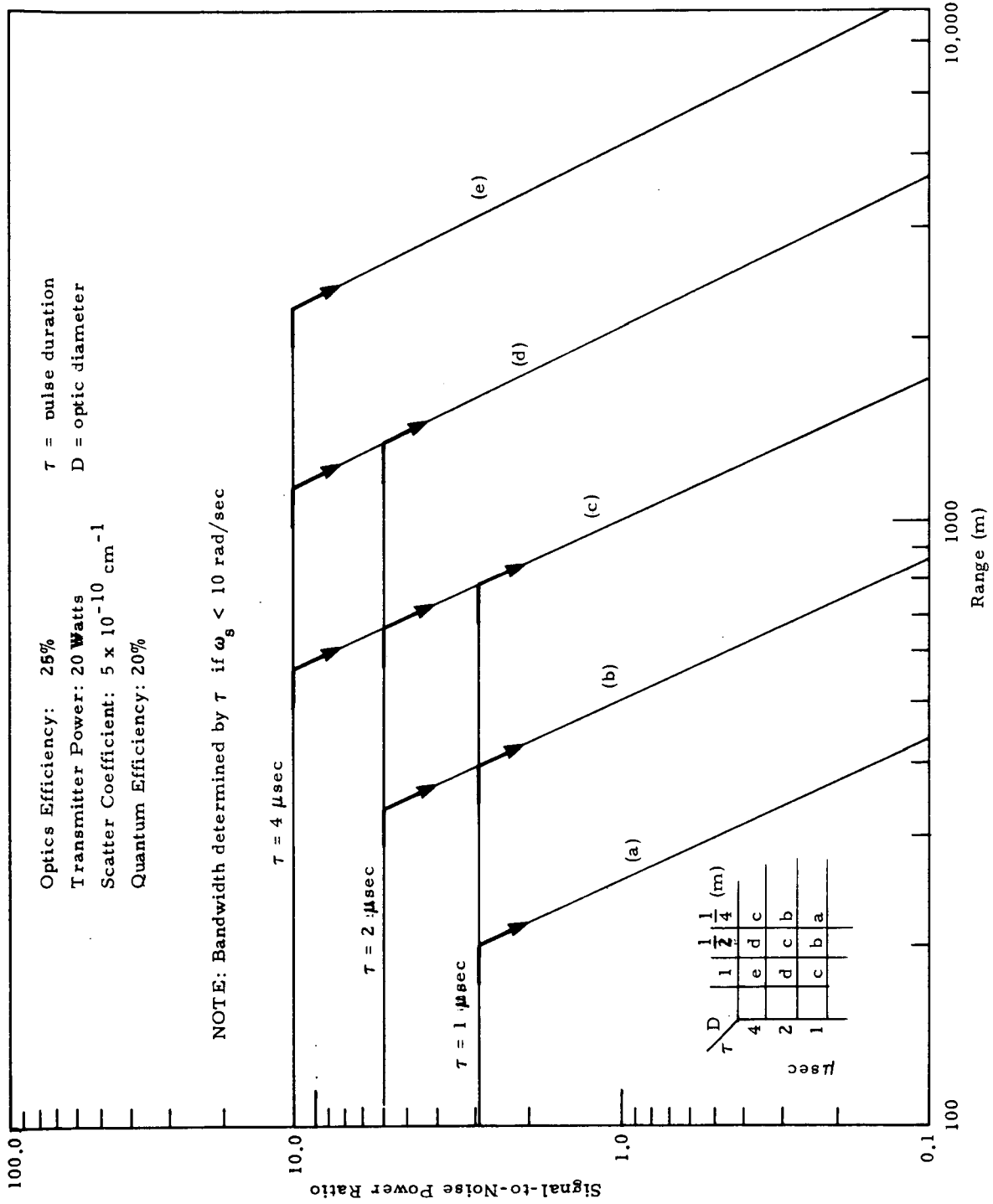


Fig. 3-6 - Signal-to-Noise Ratio for Coherent, Pulsed, Coaxial Configuration as a Function of Scan Rate

the frequency of the laser transmitter with time so as to oscillate above and below the mean frequency. The distance to the target is determined by comparing the phases of the received signal and local oscillator. The Doppler shift also translates the phase of the returned signal with respect to the transmitted signal; so that the difference in frequency in the two halves of the modulation period is a measure of the Doppler shift, which can be incorporated into the range calculation to determine Doppler shift (velocity) as well as range. Range error for this type system can be shown to be  $c \div \Delta f$ , where  $c$  is the speed of light, and  $\Delta f$  is the frequency excursion of the modulation. For  $\Delta f = 5$  MHz, the range error is 50 feet. This type system is again more sophisticated than the coaxial system and is in its infancy with regard to application at infrared frequencies.

The bistatic focused laser Doppler velocimeter, being developed for NASA by Lockheed (Ref. 23) offers hope of providing good spatial resolution at long ranges (Fig. 3-3) without sophisticated pulsing or modulation techniques. The bistatic laser Doppler velocimeter consists of a separate transmitting and receiving set of optics designed to intersect the transmitted beam's focal volume and receiver telescope's field of view (Fig. 3-7). The primary sophistication of the bistatic system involves the mechanical/optical difficulties of maintaining this intersection. If the bistatic system is constructed with a fixed mirror surface as indicated in Fig. 3-7, this mechanical alignment problem is lessened. The signal-to-noise ratio for the scanning bistatic system is depicted in Fig. 3-8. The scanning of the rather large mechanism presents interesting mechanical problems which, along with other aspects of the bistatic system, are discussed in detail in the recent Lockheed report of Ref. 24.

Bistatic pulsed systems offer the resolution of the bistatic configuration at short ranges and the resolution of the pulsed configuration at the longer ranges. This type system would require the combined complexities of the bistatic system and the pulsed system, which does not appear practical at the present time.

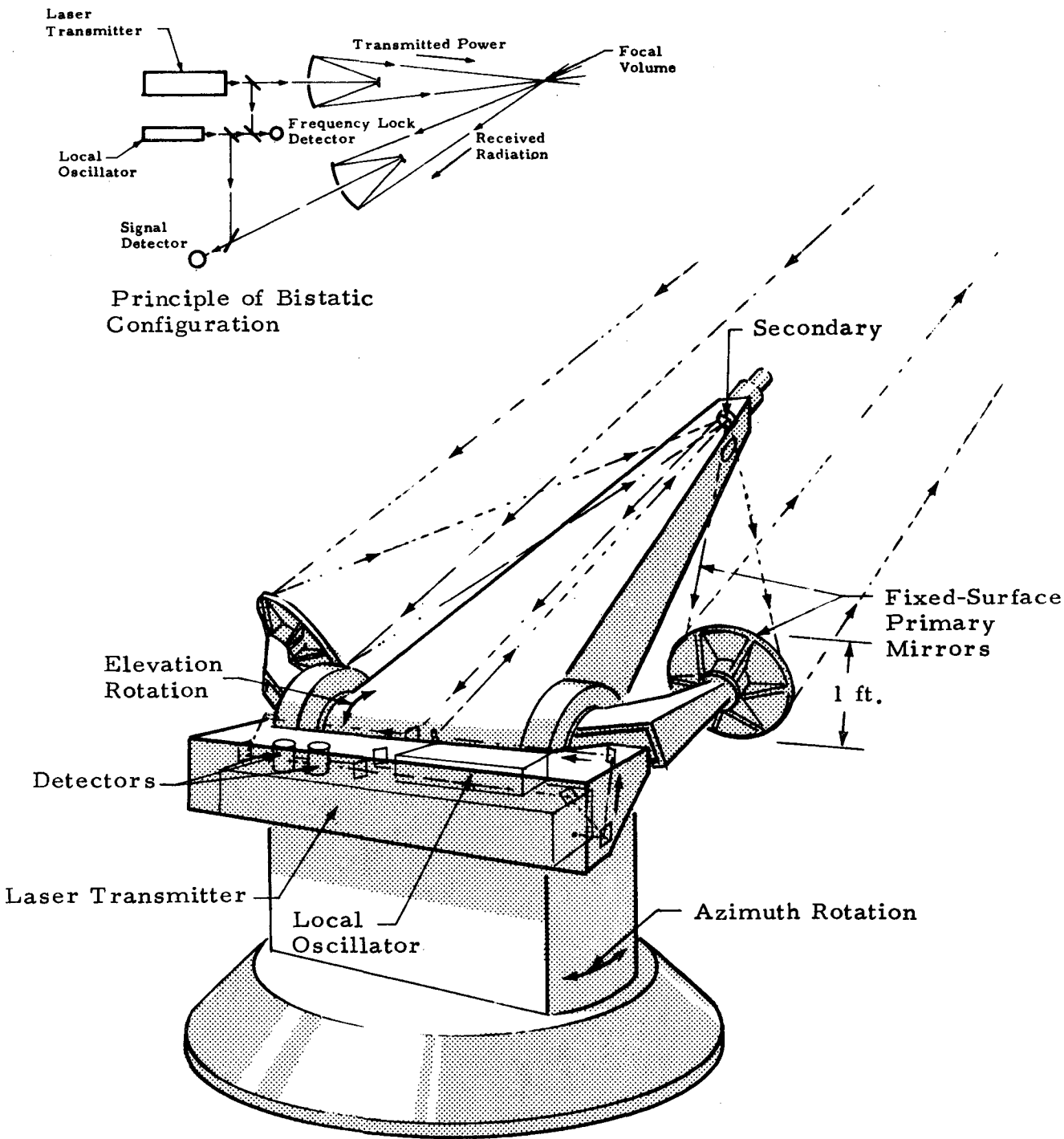


Fig. 3-7 - Fixed-Surface Bistatic Configuration

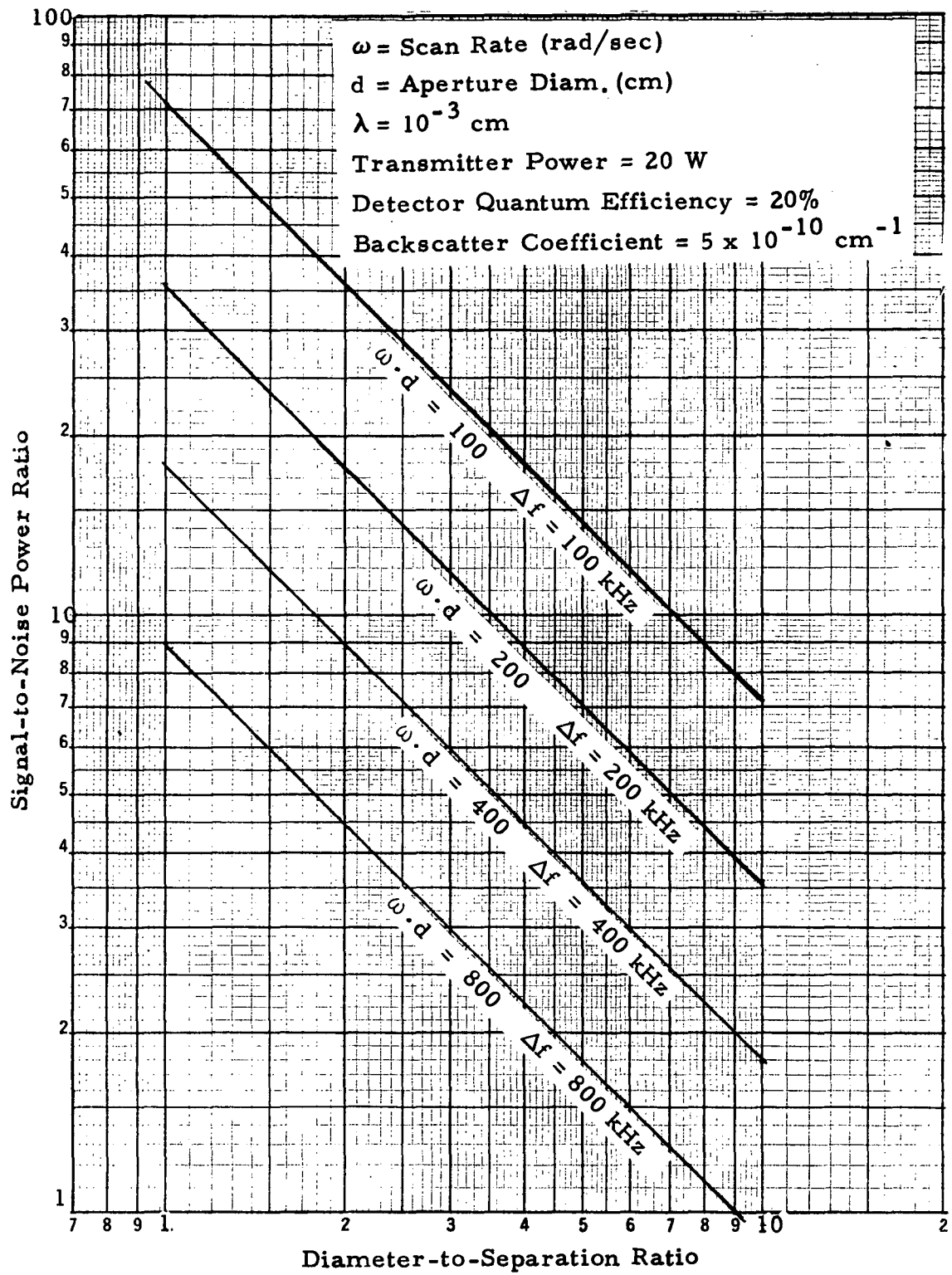


Fig. 3-8 - Signal-to-Noise Ratio for Coherent, Continuous-Wave, Bistatic Configuration as a Function of Scan Rate

### 3.2.3 Computer Subsystem

The computer subsystem for the typical detective wake monitoring system will consist of a mini-computer interfaced with the sensor pre-processor outputs and the automated air traffic control system. The mini-computer performs two functions:

- Control of the scanning process
- Processing of sensor output data

In performing the control function, the mini-computer forces the individual sensors to scan a preprogrammed pattern. A coarse scan is performed first at predetermined ranges to locate any irregularities in the normal wind patterns. Once an anomaly is discovered, the computer forces the scanners into a detailed scan routine to further determine if the anomaly is a vortex, and if it is a vortex, determine the vortex characteristics. Once a vortex is located, the sensors will likely be controlled to scan rapidly along the vortex to determine its position within the air corridor.

The data processing function of the mini-computer receives the pre-processed outputs of the individual (one-dimensional) sensors and records them in storage. After sufficient data are in storage, the computer combines the one-dimensional data to form a two-dimensional picture of the coarse scan area. The computer looks for anomalies (mentioned in the above paragraph) to determine if a vortex exists in the corridor. The outputs from the detail scan are processed to provide a two-dimensional picture of the vortex and to calculate circulation, position, movement and other pertinent parameters.

The mini-computer of the detective system, in conjunction with the local automated air traffic control system, integrates vortex data with traffic data to determine if a hazard exists to aircraft in the area. The computer performs this operation with stored vortex data and inputs of projected aircraft flight profiles. If the computer determines that a vortex of hazardous strength

lies in the projected path of an oncoming aircraft, a warning is displayed via the display subsystem to the controllers and pilot involved.

#### 3.2.4 Data Display/Communication Subsystem

The method of performing a real time display of wake vortex hazard data to both the pilots and controllers is most important in the development of a detective wake monitoring system. The data display must provide data to the persons involved in a simple yet effective format. If the pilot is to make the decision to abort a landing or maneuver to avoid a vortex encounter, he must have sufficient data to know the most appropriate move to make. Equally important, the pilot should not be required to make an evasive maneuver if the vortex to be encountered is not of sufficient strength to constitute a hazard. To be considered along with these factors, aircraft crew members are busiest during approach and departure portions of flight and must not be over burdened with complicated display formats of vortex conditions.

An effective real time display can perhaps be incorporated into the proposed Multifunction Display (MFD) (Ref. 25), a cathode-ray tube monitor proposed to display data provided from the ground via a digital data link. The digital data link will provide computer-to-computer communication between the ground-based traffic control computers and airbourne flight computers. The display could perhaps provide an indication of vortex hazards along the projected flight path together with other pertinent navigation data already planned for the MFD.

### 3.3 CONSIDERATIONS OF MULTI-COMPONENT (MULTI-DIMENSIONAL) AND SINGLE-COMPONENT (ONE-DIMENSIONAL) SYSTEMS

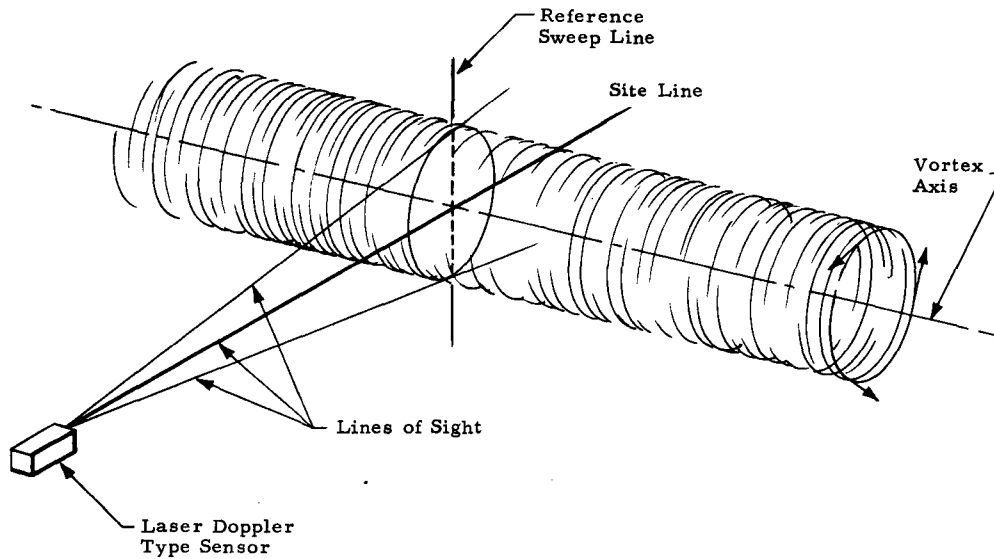
Should a detective wake vortex monitoring system be a one-, two-, or three-component detection system? This question has arisen since a laser Doppler detective wake monitoring system was first conceived. An attempt is made here to clarify the advantages and disadvantages of the single and

multicomponent systems and to indicate the preferred choice of system with today's knowledge of the vortex monitoring problem.

### 3.3.1 Single-Component (One-Dimensional) Vortex Sensor

A number of computer simulations have been made of a laser Doppler type sensor scanning through a vortex. The simulation consists of looking at the vortex flowfield with a coarse resolution instrument and attempting to recognize profiles from the resulting output. The simulated output of the sensor is plotted by an SC 4020 plotter as velocity versus locations within the vortex. Figure 3-9 defines the terms which were used in plots of the simulated sensor output. This simulation program is discussed in Section 3.4 and in Appendixes B and C.

A single-component sensor of vortex velocities can provide a realistic picture of the vortex tangential flow field of a vortex if it views the vortex at an angle perpendicular or nearly perpendicular to the axis of the vortex. Figure 3-10 illustrates this fact. The W (sensed velocity) and T, L (actual velocities) curves agree very well in this figure to indicate a good measurement of tangential velocities with a one-component sensor viewing the vortex at angles approaching 90 deg with respect to the vortex axis. However, as the viewing angle with respect to the vortex axis (angle between "site line" and "vortex axis") approaches zero degrees, the ability of a single component sensor to sense accurately the vortex tangential velocity degrades rapidly. This results from the fact that a coaxial LDV measures the along-line-of-site velocity component. Figure 3-11 shows a comparison between a simulated one-dimensional sensor's output and the actual tangential flow within the vortex as the angle between the line-of-sight of the sensor and the vortex approach zero degrees. In the upper set of curves of Fig. 3-11, this angle is approximately 2 deg, in the middle set, the angle is approximately 6 deg and in the lower set the angle is approximately 10 deg. Figures 3-10 and 3-11 show that as expected, the velocity resolution capability of a one-dimensional sensor viewing a vortex tangential flow field is greatly dependent upon the viewing angle, which improves as the angle (between sensor line-of-sight and vortex axis) approaches 90 deg.



Definitions for Simulations

<p><b>Vortex Axis:</b> runs along center of vortex core</p> <p><b>Line of Sight:</b> line of sight of the sensor as it scans across the vortex</p> <p><b>Scan Plane:</b> formed by line of sights</p> <p><b>Site Line:</b> line of sight which intersects vortex axis</p>	<p><b>Reference Sweep Line:</b> line in scan plane which passes through vortex axis and is perpendicular to site line</p> <p><b>T</b> actual tangential velocity of the vortex at the focal point of the simulated system</p> <p><b>L</b> actual line of sight velocity of the vortex at the focal point or range rate point of the simulated system</p> <p><b>W</b> Simulated velocity output of sensor resulting from logic described in Section 3.4</p> <p><b>X</b> Output from data processor which provides maximum absolute value of velocity within sensor focal volume or pulse length (X is not plotted for all figures).</p>
---	--

Fig. 3-9 - Laser Doppler Velocimeter Making Single Line Scans Through a Vortex

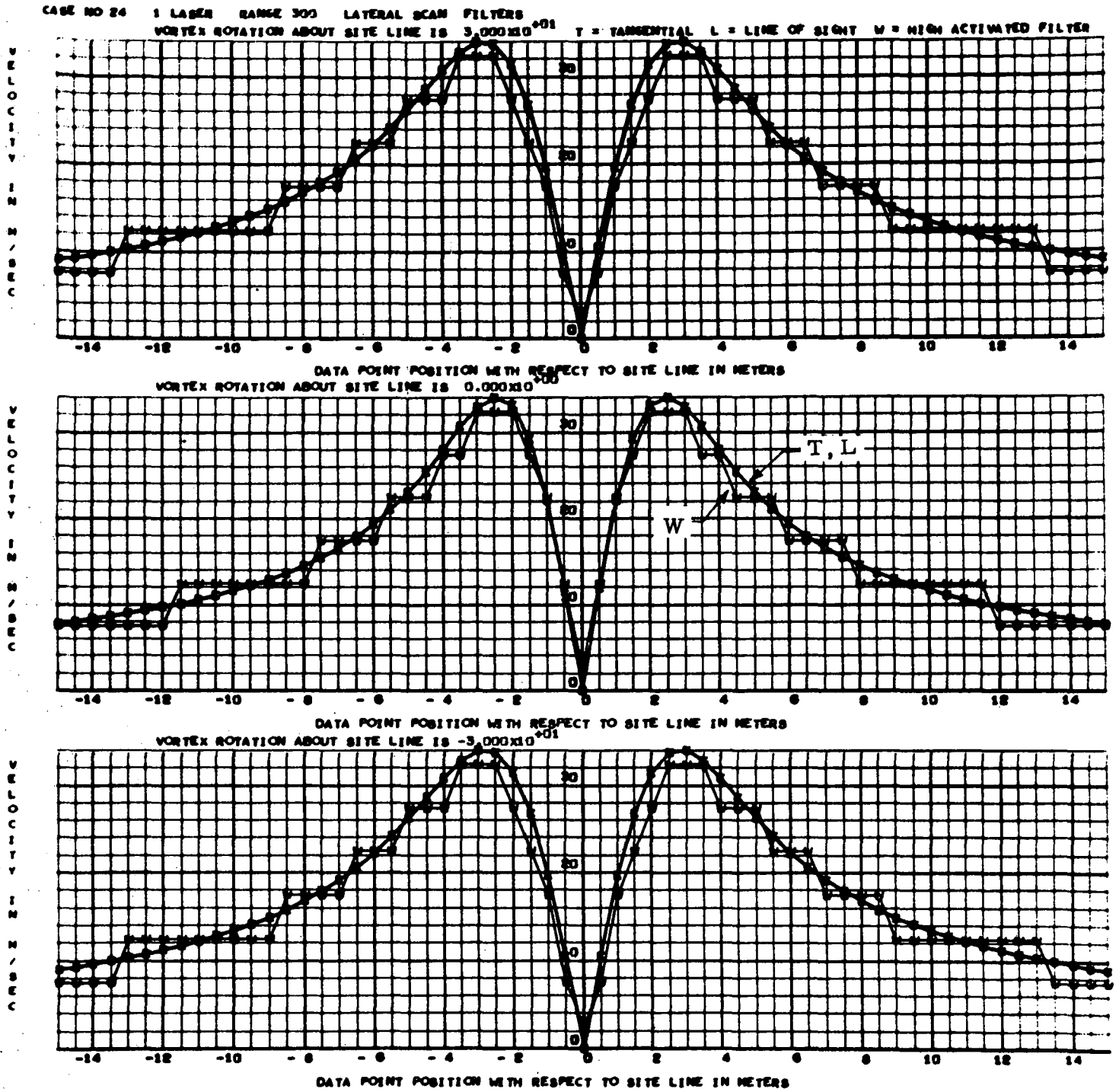


Fig. 3-10 - Viewing Vortex Tangential Flow Perpendicular to and at +60 Degrees to Vortex Axis (Range 300 m)

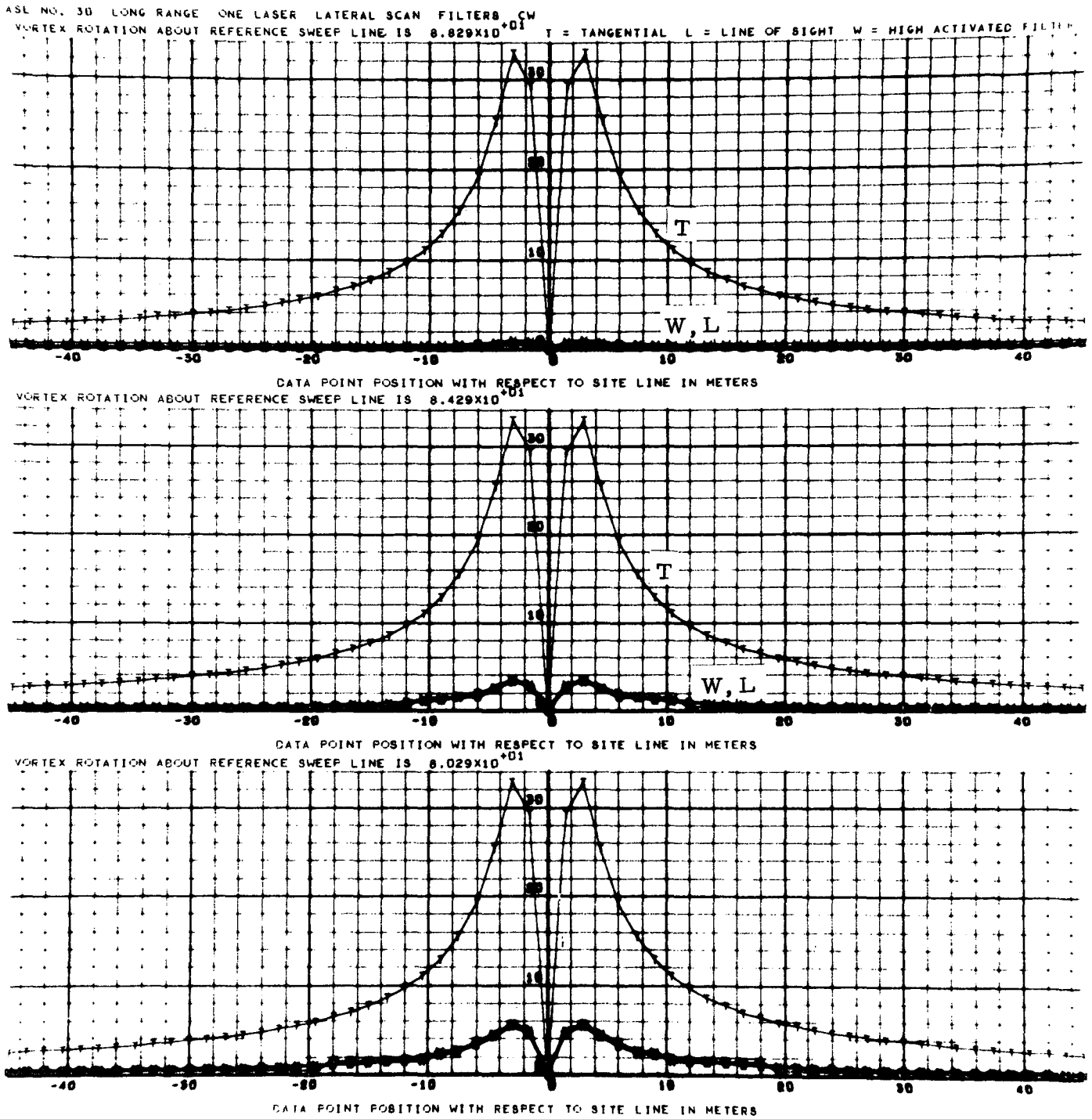


Fig. 3-11 - Viewing Vortex Tangential Flow at Angles of 1.7, 5.7 and Approximately 10 Degrees (top to bottom curves, respectively) to vortex axis (Range 300 m)

For a short range system, positioning the sensor to view the vortex with a line-of-sight nearly perpendicular to the vortex axis is a relatively simple matter. The sensor could be placed under the flight path while looking vertically (Fig. 3-12a) or to the side of the flight path to look-over to the vortex (Fig. 3-12b). In either case the sensor would view the vortex at an angle approaching perpendicular to the vortex axis.

However, for a long range sensor (the topic of Section 3), the location of the sensor such that the vortex could be viewed at a large angle (approximately 90 deg between the sensor line-of-sight and the vortex axis) becomes a most impractical task. In order to obtain this approximate 90 deg viewing angle, the sensor would necessarily be located 5 to 10 kilometers from the runway edge and scan back toward the flight path. Because of the shortage of air terminal real estate and the normal physical obstacles — terrain, buildings, etc., — in the sensor line-of-sight, locating the sensors to view the vortex perpendicularly at long ranges will probably be impractical. The vortex will normally be viewed as depicted in Fig. 3-12c with a small angle between the sensor line-of-sight and the vortex axis. The resultant measured velocities will be much smaller than actual velocities as indicated in Fig. 3-11.

#### ● Axial Flow Considerations for Single-Component Systems

The above paragraphs indicate difficulties in characterizing a vortex with a long-range, single-dimension sensor if only the tangential velocities are considered. Figure 3-13 illustrates a one-dimensional sensor's output as it scans through a vortex with simulated axial (Newman's model, Appendix A), as well as tangential flows. It is immediately evident that an axial flow component similar to the one modeled in Fig. 3-13 will greatly enhance the ability of a single component sensor to detect a vortex at small angles with respect to the vortex axis and at long ranges. However, a minimum of experimental evidence exists to verify the existence of an axial flow such as the one depicted in Fig. 3-13. There is very little theory or data to correlate either the strength or dimension of the axial flow with the generating conditions; i.e., aircraft circulation, etc. Also, tangential — not axial velocities — upset

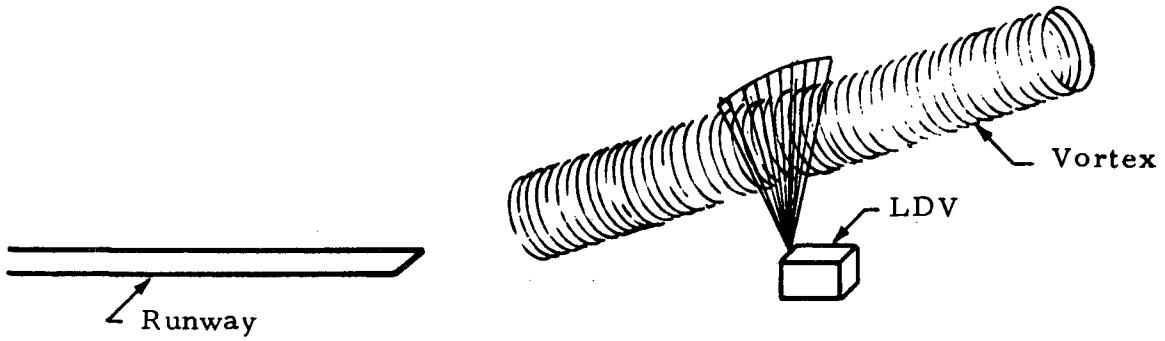


Fig. 3-12a - Sensor Located Under Flight Path Looking Up (Viewing vortex perpendicular to vortex axis)

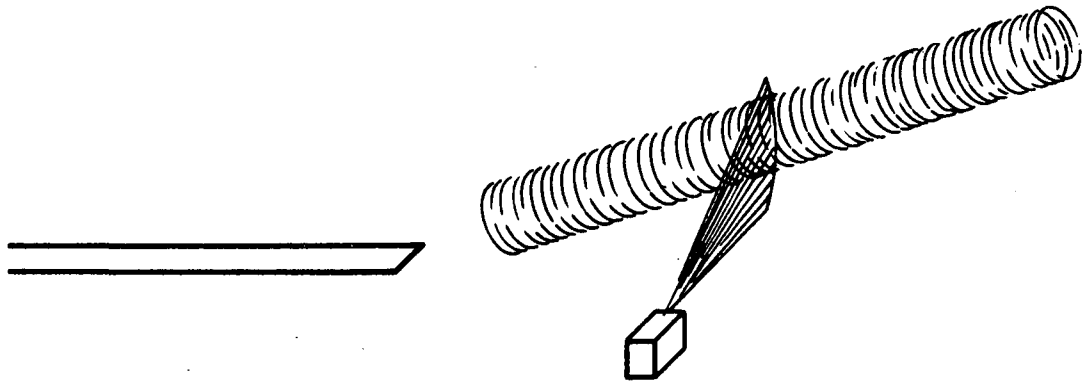


Fig. 3-12b - Sensor Located to Side of Flight Path Looking Toward Flight Path (Viewing vortex perpendicular to vortex axis)

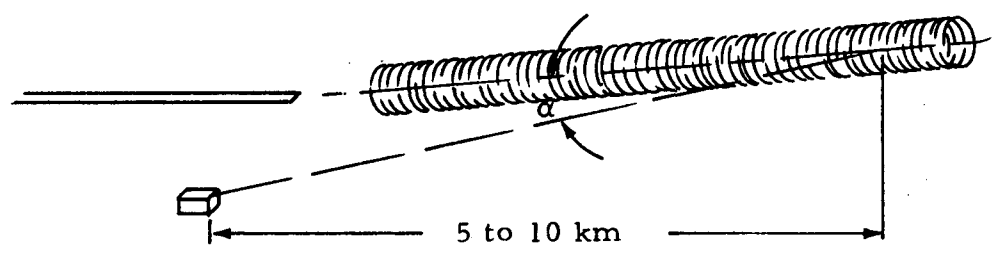


Fig. 3-12c - Long Range System - Angle Formed by Sensor Line-of-Sight and Vortex Axis ( $\alpha$ ) Necessarily Small Due to Lack of Real Estate for Locating LDV far away from Flight Path

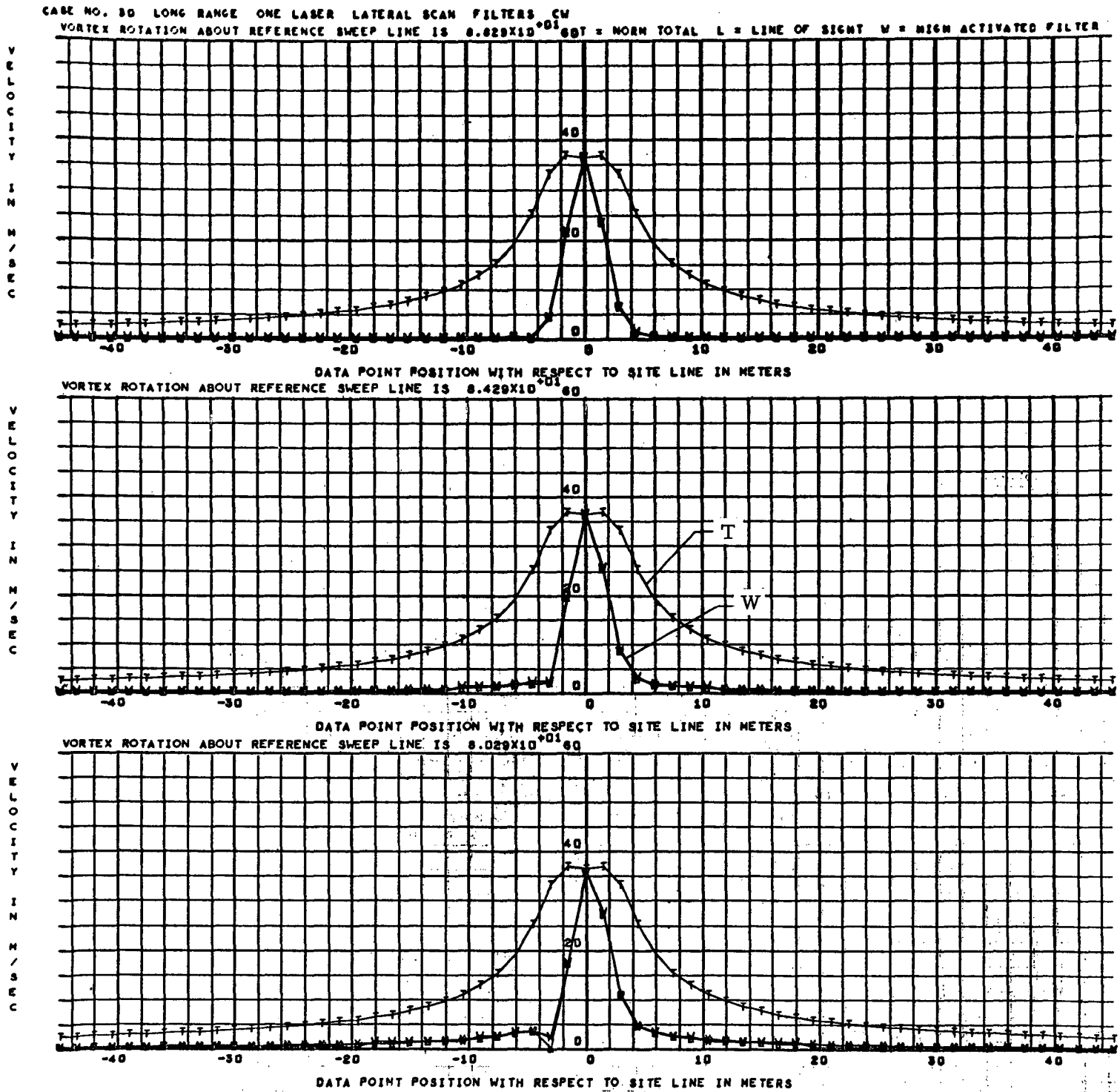


Fig. 3-13 - One-Component System with Combined Axial and Tangential Flows Viewed at Angles of 1.7, 5.7, and ~ 10 Degrees to Vortex Axis [Note: "T" represents total (axial plus tangential) simulated velocities instead of tangential velocity as in previous plots]. Maximum velocity was 38 m/sec; maximum tangential flow was 34/sec

aircraft. Therefore, it is hardly worthwhile to begin immediately to design a wake turbulence detection system based upon the existence of vortex axial flow.

● Conclusions about Utility of One-Component Long-Range Vortex Detection

If the orientation of the vortex were known, it might be possible to derive a true, long-range (2 to 10 km) picture of a vortex from one-dimensional data taken at a small angle (such as illustrated in Fig. 3-11). The vortex flow could be derived by dividing the single component velocity data by the sine of the viewing angle (with respect to the vortex axis). The drawbacks to this type system are the following:

- Difficulty in knowing exact orientation of the vortex.
- Difficulty in distinguishing between sensed vortex velocity component and wind component.
- Difficulty in resolving axial and tangential velocity contributions to measured data.

With a high spatial resolution sensor, it would be possible to determine the orientation of the vortex with some degree of accuracy. However, at small angles, a small error in angle determination would mean a large error in the resolved tangential velocity; (i.e., since  $\sin 4 \text{ deg} = 0.07$  and  $\sin 5 \text{ deg} = 0.09$ ; a 1 deg error in vortex angular orientation would result in an approximately 25% error in calculated vortex tangential velocity). Since the spatial resolution of a high resolution bistatic velocimeter (1/3 meter diameter optics, 2 meter separation) is approximately 500 meters at 5 km range and 2000 meters at 10 km range (Fig. 3-3), it would be difficult to determine the vortex orientation to within  $\pm 1$  degree at the larger ranges.

Viewing a vortex at long ranges at a small angle with the axis results in sensing a small velocity component of the tangential flow. Figure 3-11 illustrates these sensed velocities being typically below 6 meters/sec for 747 vortices 1000 meters behind the aircraft at 10 deg viewing angle and below 4 meters/

sec at 6 deg viewing angles. A 5 to 10 meter/sec wind gusting directly down the line-of-sight of the LDV sensor would not be an uncommon atmospheric phenomenon at many airports. With a one-dimensional sensor, the difficulties of unscrambling a vortex velocity component less than 5 meters/sec on top of a turbulent wind component of 10 meters/sec are obvious.

Since vortex axial velocities are presently ill defined, it is difficult to perform meaningful analysis of viewing vortices with a one-dimensional sensor from a direction such that the axial component is likely to be the predominant velocity component. Figure 3-13 presents an attempt to simulate such a case with axial flow according to Newman's model (Ref. 26 and Appendix A). The presence of the axial flow might greatly facilitate the monitoring of the vortex at long ranges with a single component velocity sensor. At present the presence of an ill defined axial flow only confuses the concept of a one-dimensional, long-range vortex sensor.

### 3.3.2 Two Component (Two-Dimensional) Vortex Sensor

A two-dimensional LDV concept would use two each of one-dimensional LDV sensors viewing the same data volume and vectorially computing a resultant vector velocity from the one-dimensional sensor outputs to provide two-dimensional data in the plane formed by the sensor line-of-sights. Since the two sensors do not necessarily give orthogonal coordinate components, the summing of their outputs is somewhat more involved than a normal vector summation. This can be illustrated graphically (Fig. 3-14a) by constructing perpendiculars from the vector tips of the velocities sensed by the individual LDVs. The intersection of the two perpendiculars defines the vortex velocity in the plane defined by the two LDV sensors and the data point.

Figures 3-15a and b compare vortex tangential flow visualizations by two-component (Fig. 3-15a) and single-component (Fig. 3-15b) sensor systems. In both figures the range is 5 km and the angle between the system sensor(s) and the vortex line-of-sight is six degrees. In Fig. 3-15b the vortex is viewed

by a single sensor with a 6 deg angle. In Fig. 3-15a each sensor views the vortex with a 6 deg angle with respect to the vortex line-of-sight; in this figure the sensors are located on opposite sides of the vortex line-of-sight. Note the improved agreement between measured (W) and actual (T) vortex velocities in Fig. 3-15a over Fig. 3-15b.

Figures 3-16a and 3-16b illustrate the effect upon the two-dimensional system by increasing and decreasing the angular separation (angle  $\beta$  of Fig. 3-14a) of the sensors. The abscissa of these curves can be expressed as the distance from the vortex axis (Fig. 3-14b) in meters. The ordinates are the resolved velocities from the mathematically combined outputs (Fig. 3-14a) of the two sensors. The curves marked T are actual tangential velocities at the data points. The curves marked L are the actual line-of-sight velocities at the data points which have been resolved by combining as depicted in Fig. 3-14a. The W curves are the sensor output velocities combined mathematically as again depicted in 3-14a. The X curves are the absolute values of the sensor outputs combined mathematically (positive and negative velocities are not distinguished from one another). Figure 3-16a indicates that the agreement between the W and L-T curves degrades as the range to the data point ("Vortex Range") increases from 1 km to 5 km and again to 10 km. This deviation between actual velocity and sensed velocity increases for the 300 meter separation between sensors (Fig. 3-16b). Both of these figures illustrate that measurement errors are magnified as the angular separation subtended by the two sensors as the data point decreases.

Figures 3-16a and 3-16b are the resolved outputs (theoretical) of the LDV sensors with capabilities of resolving the sensed velocities within plus or minus one meter per second. With a better velocity resolution for example, ( $\pm 1/3$  m/sec) for each of the LDVs, the agreement of the W and T-L curves would improve. However, it was felt that since natural atmospheric (Kolmogorov) turbulence would be added to the LDV outputs in a real system (and has not yet been added in this simulation) that  $\pm 1$  m/sec is a good conservative velocity resolution to expect from a LDV sensor operating at long range.

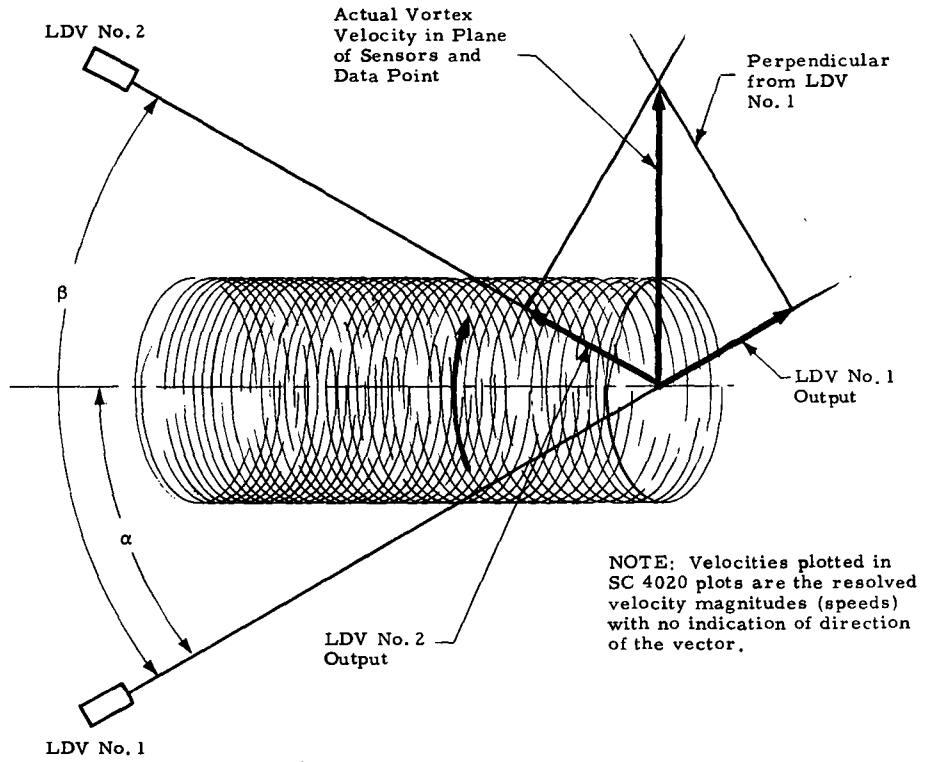


Fig. 3-14a - Derivation of Two-Dimensional Data from Two One-Dimensional Sensors in Non-Orthogonal Coordinate System

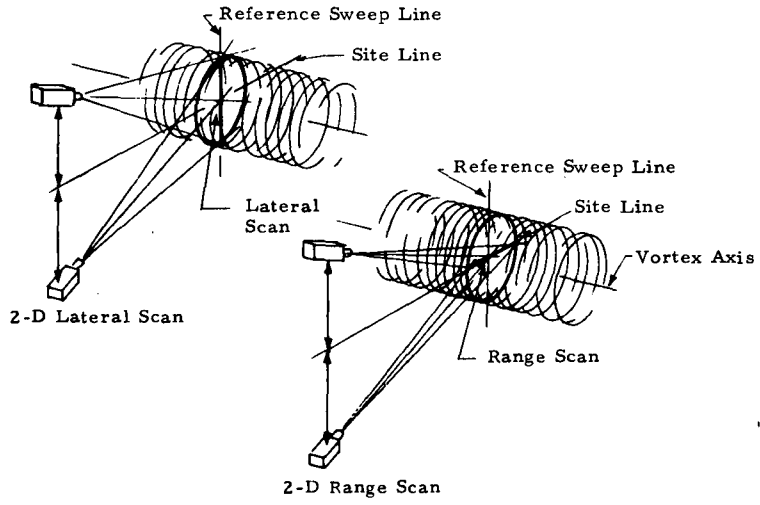


Fig. 3-14b - Plot Nomenclature for Two-Dimensional Data Presentation

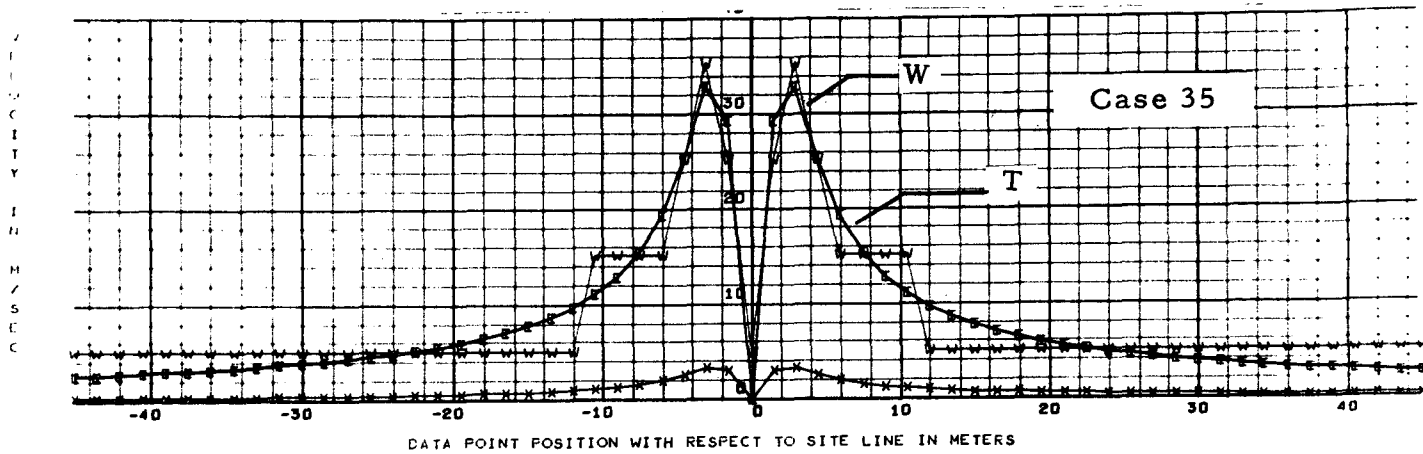


Fig. 3-15a - Two-Dimensional Visualization of Vortex Derived from Two One-Dimensional Sensors. Sensors are Located on Either Side of the Vortex Axis and View the Vortex at Angles of Six Degrees with Respect to the Vortex Axis (range is 5 km)

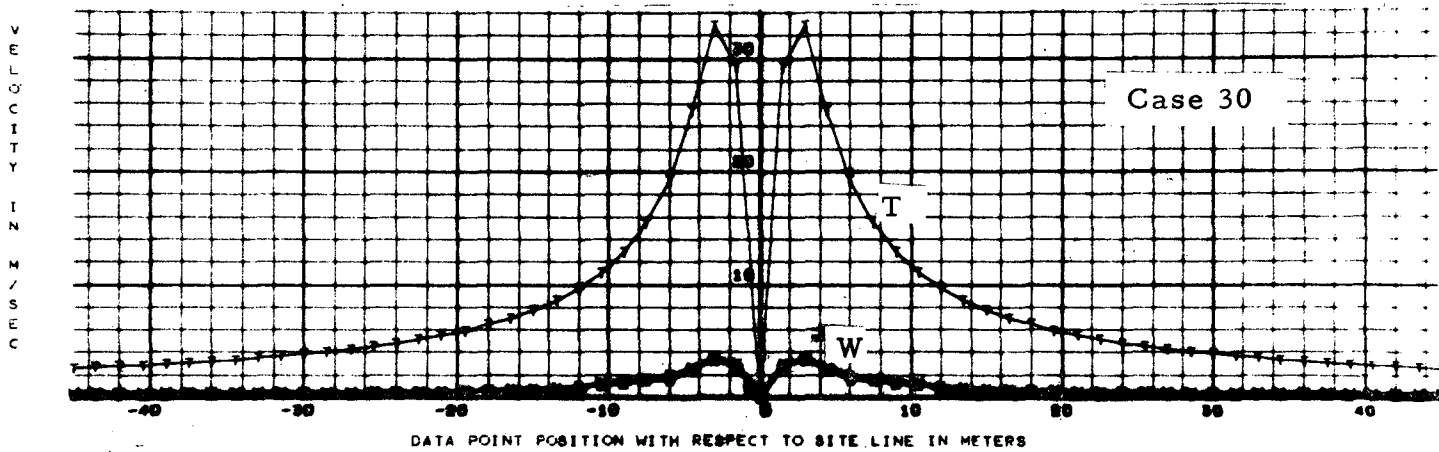


Fig. 3-15b - One-Dimensional Visualization of Vortex Derived from a One-Dimensional Sensor (range is also 5 km) Viewing Vortex at Six Degree Angle with Respect to the Vortex Axis

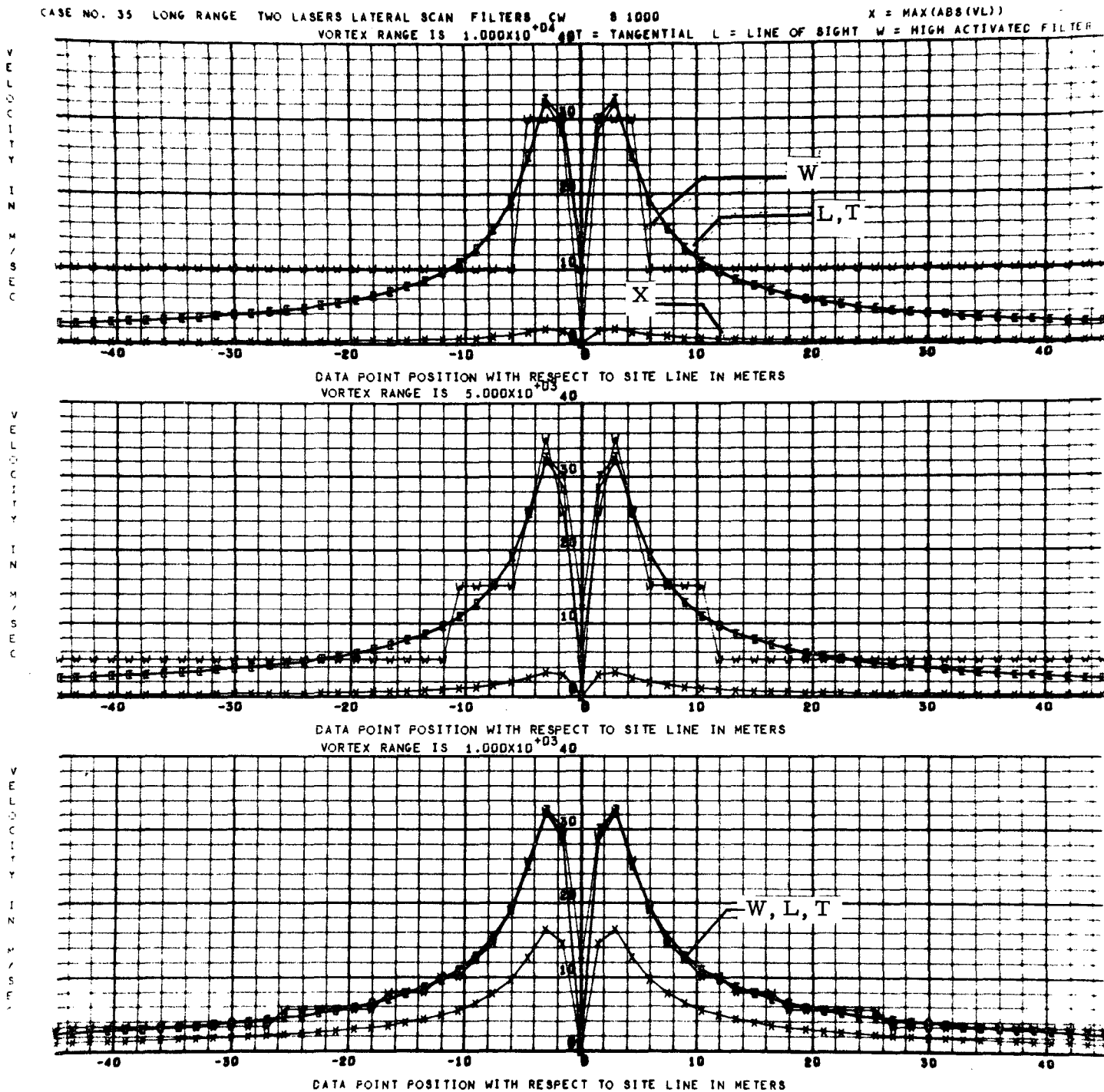


Fig. 3-16a - Two-Dimensional Data Resolved from Single Azimuth Scans Through a Vortex by Two Laser Doppler Velocimeters Separated by 1000 Meters (no axial velocity)

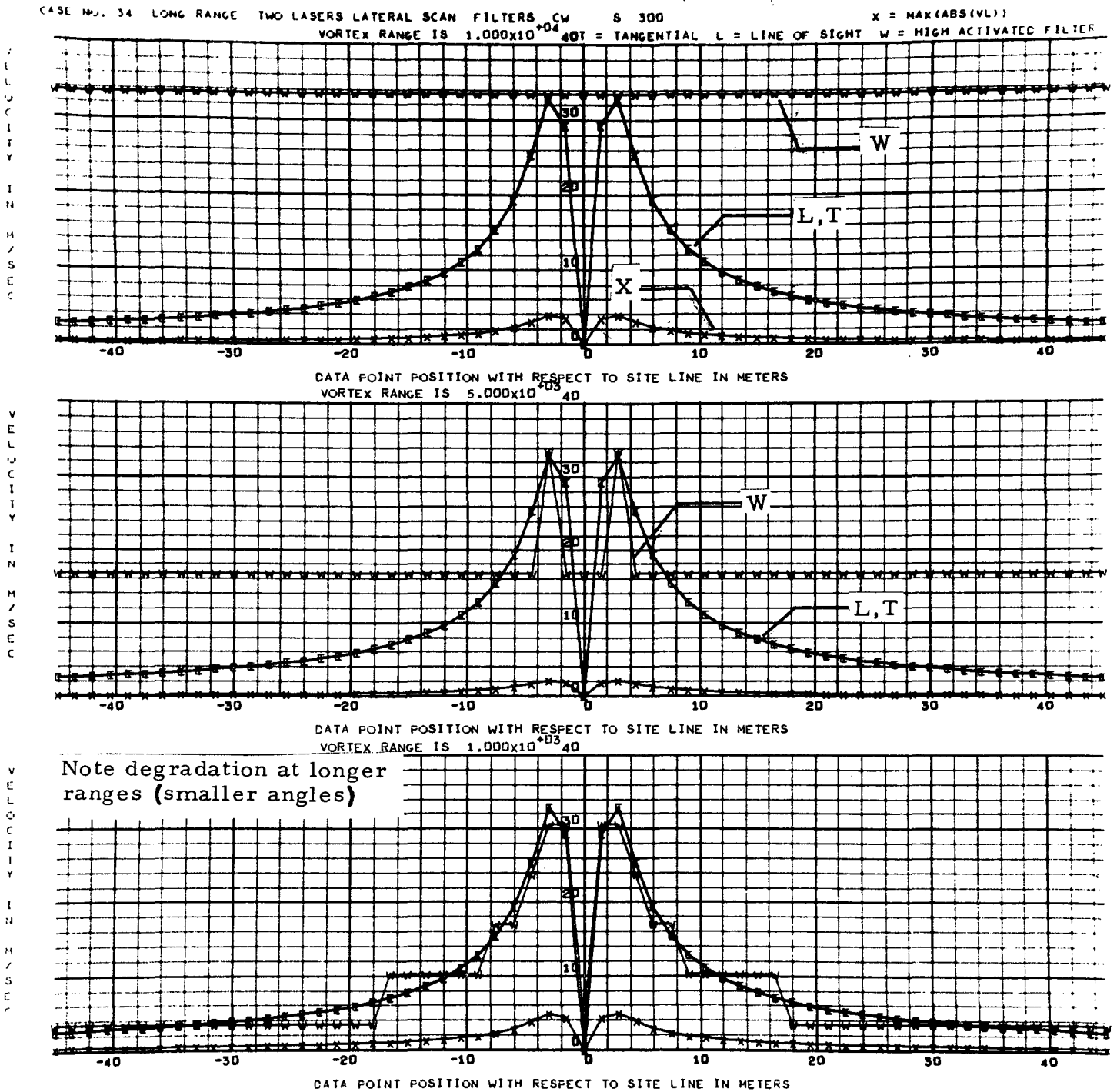


Fig. 3-16b - Two-Dimensional Data with Velocimeter Separation of 300 Meters (no axial velocity)

- Misalignment Effects on Two-Component Sensors

Requirements to maintain independent optical pointing accuracies beyond certain limits for scanning type systems greatly increase the cost and reduce the reliability of system hardware. Thus, investigation of point accuracy requirements early in the conceptual phases of system development was an important aspect of the study. Beams from sensors located on separate platforms must intersect spatially to provide data from the same points in space (Fig. 3-14a) for a true two-dimensional picture of the vortex. The beams need not pass through the same spatial point at the same instant of time. However, if they do pass through the points at different times, sensor outputs must be stored until both sensors have taken data from the spatial points of interest. The accuracy required for steering these beams is the subject of this subsection.

Figures 3-17, 3-18, and 3-19 illustrate the effects of misaligning the sensor beams in the vertical plane by 1, 3, and 5 meters respectively at the target points. With a vertical misalignment, the sensors' beams no longer intersect at the target points; but one beam is skewed above the other.

Figure 3-17 depicts a one meter misalignment. The "W" curves of this figure are practically indistinguishable from those of Fig. 3-15 (no misalignment). Thus, it can be concluded that a one-meter misalignment has little effect upon the system measurement accuracy. The vortex peak tangential velocity and core diameter are identifiable as in Fig. 3-15 where there is no alignment error.

Figure 3-18 depicts a 3-meter alignment error. In Fig. 3-18, peak tangential velocities have dropped approximately 10%, yet core diameters have remained approximately constant. The center of the core has shifted approximately one meter. A three-meter misalignment is probably permissible for a long-range, two-component, wake turbulence measurement system.

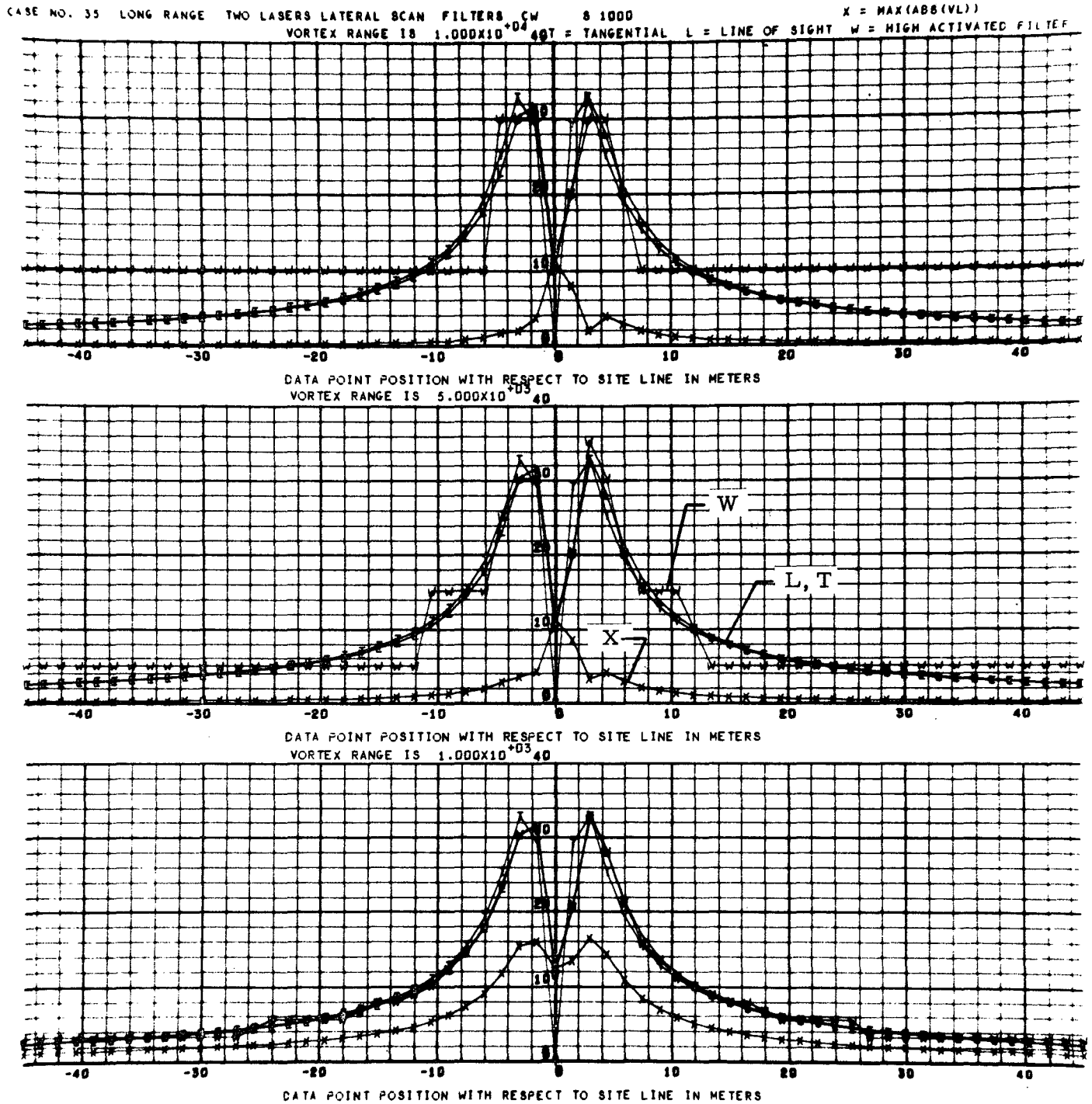


Fig. 3-17 - One-Meter Vertical Misalignment of LDVs for Ranges of 1, 5 and 10 Kilometers (1 km separation between sensors)

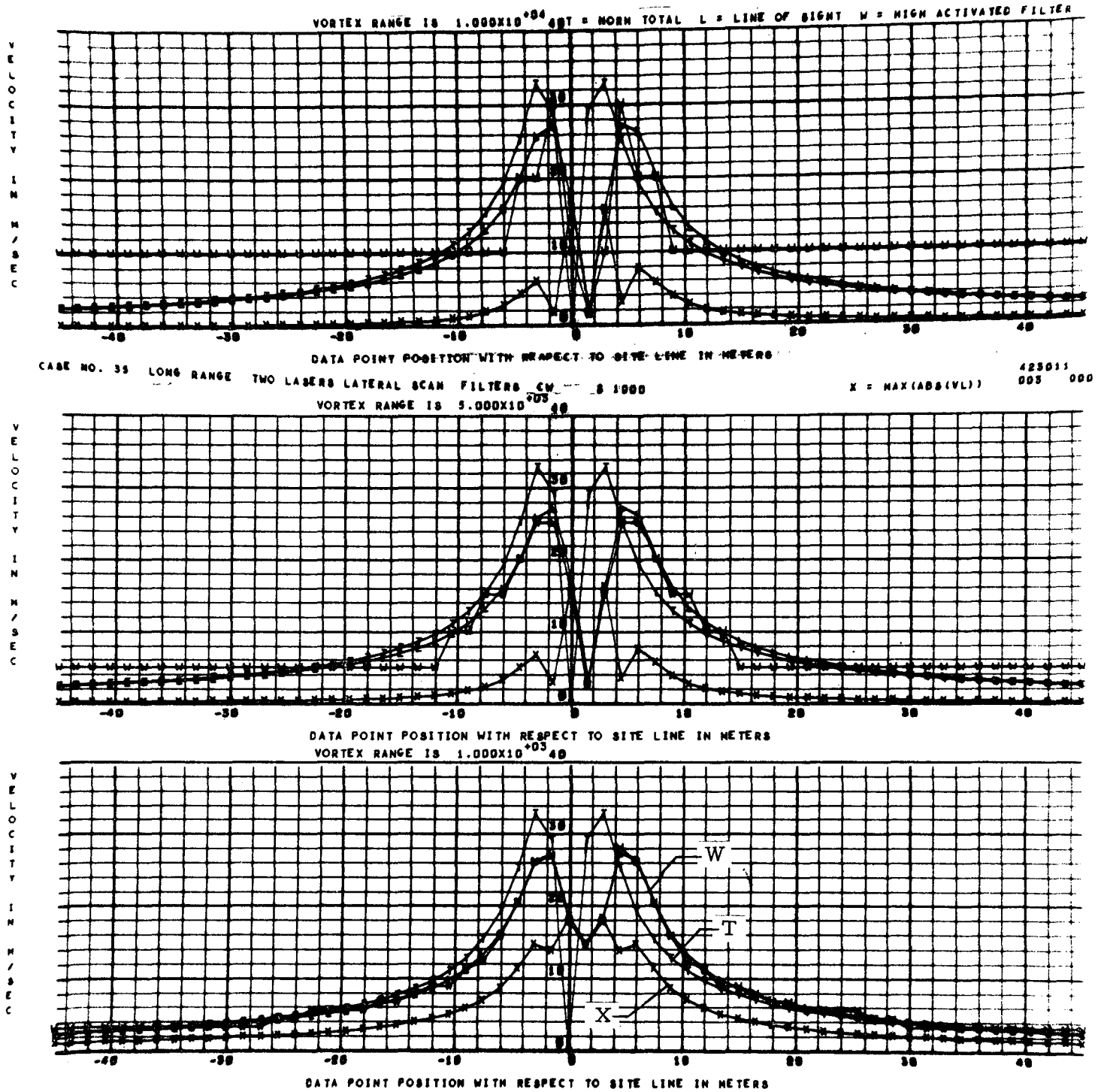


Fig. 3-18 - Three-Meter Vertical Misalignment of LDVs for Ranges of 1, 5 and 10 Kilometers

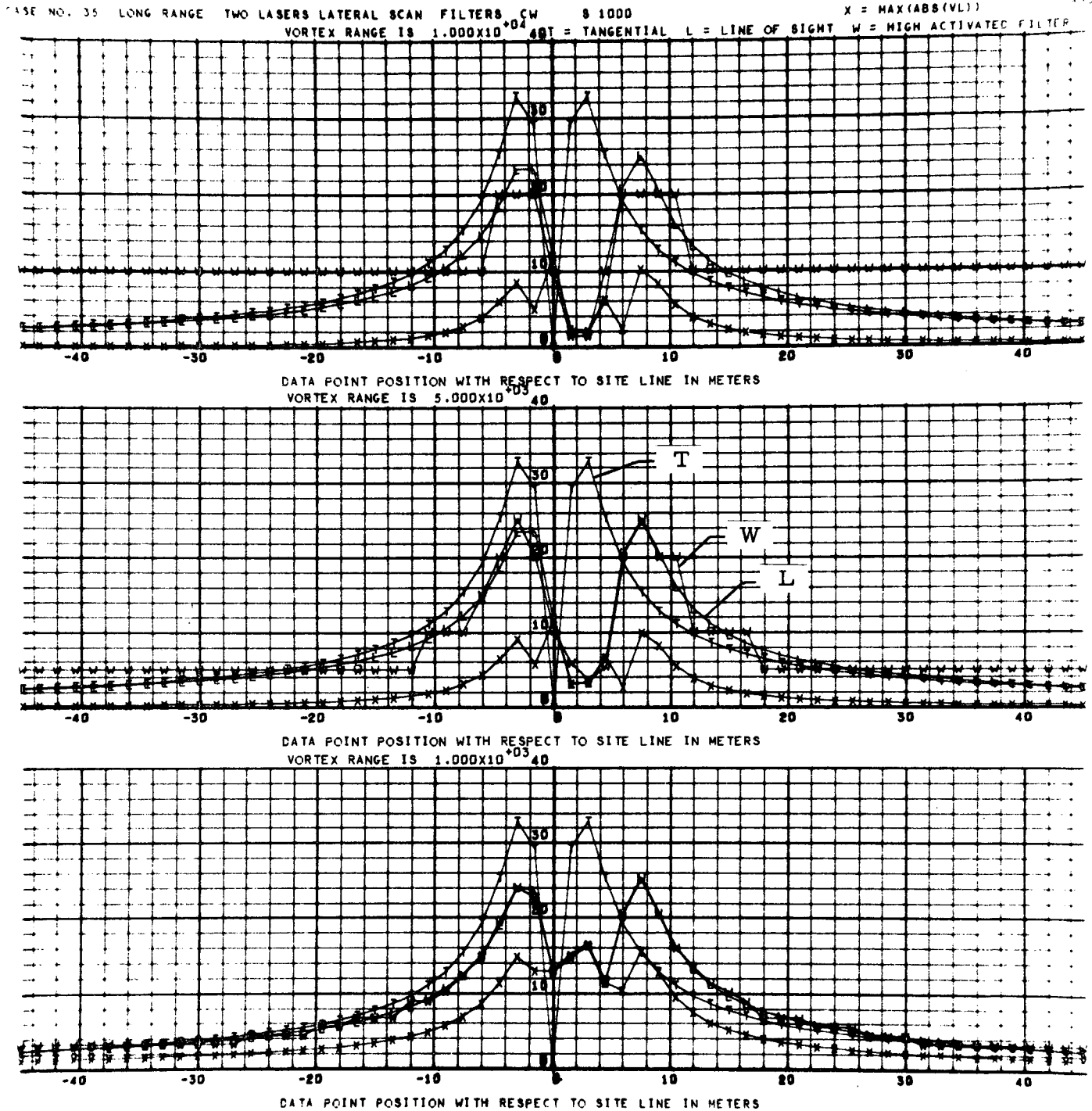


Fig. 3-19 - Five-Meter Vertical Misalignment of LDVs for Ranges of 1, 5 and 10 Kilometers

A five-meter alignment error is depicted in Fig. 3-19. At the 10 km range, the peak tangential velocity sensed by the system has dropped approximately 40%, and the core diameter has increased from 6 meters to approximately 11 meters. At shorter ranges, the peak tangential velocity error is decreased somewhat.

From these figures, it can be seen that a 3 meter pointing accuracy is adequate and possibly too stringent. This amounts to a one milliradian pointing error at a range of 3 km and a 0.3 milliradian error at a 10 km range.

Runs were also made with a horizontal misalignment rather than the vertical misalignment discussed above. The horizontal misalignment merely intersects the two beams at a point slightly in front of or behind the nominal intersection rather than causing the beams to skew as discussed above. The horizontal misalignment did not have a noticeable effect for the 1, 3, and 5 meter alignment error cases. The vertical misalignment represents a "worst" case misalignment.

● Axial Velocity Effects on Two-Component Systems

Figure 3-20a depicts a two-component scan through a vortex (with sensor outputs combined as illustrated in Fig. 3-14a with simultaneous axial and tangential flows. Figure 3-20b depicts the same sensor scanning through a vortex with the same tangential flow but no axial flow. The similarities and differences in system output can be seen. These outputs are listed below for several data point positions:

Distance from Site Line (m)	Combined Axial and Tangential		Tangential Only	
	Actual	Measured	Actual	Measured
+20	5 m/s	5 m/s	6 m/s	6 m/s
+10	12	15	12	15
+ 5	25	25	22	22
+ 2	37	37	32	32
0	37	37	0	0

CASE NO. 33 LONG RANGE TWO LASERS LATERAL SCAN FILTERS CW

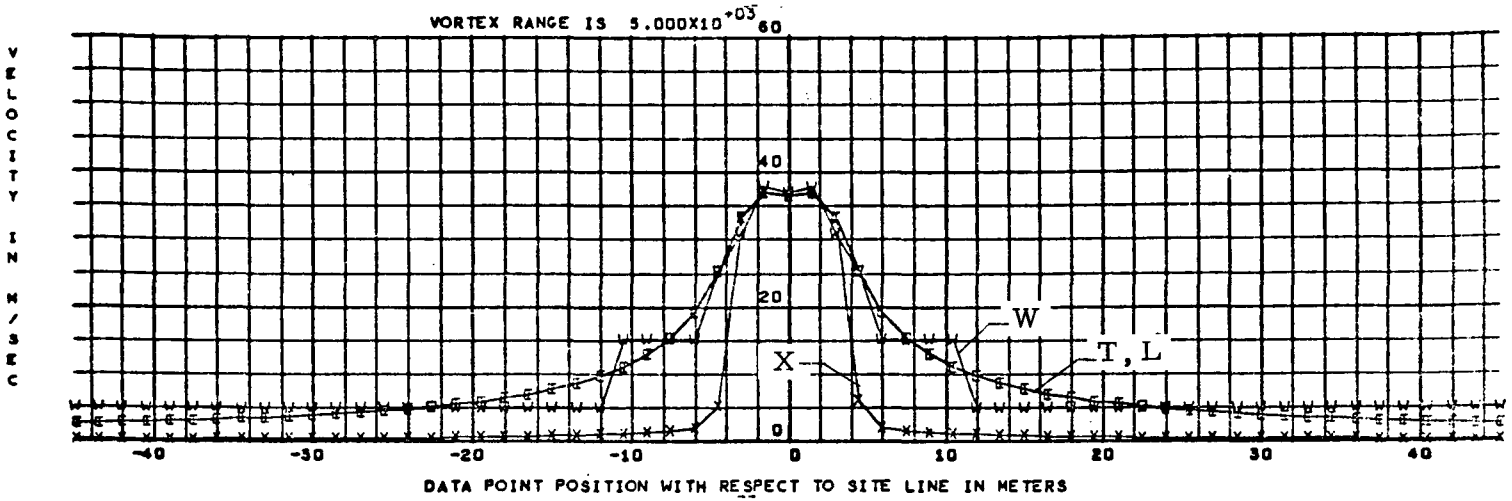


Fig. 3-20a - Two-Component Scan Through Vortex with Combined Axial and Tangential Flows

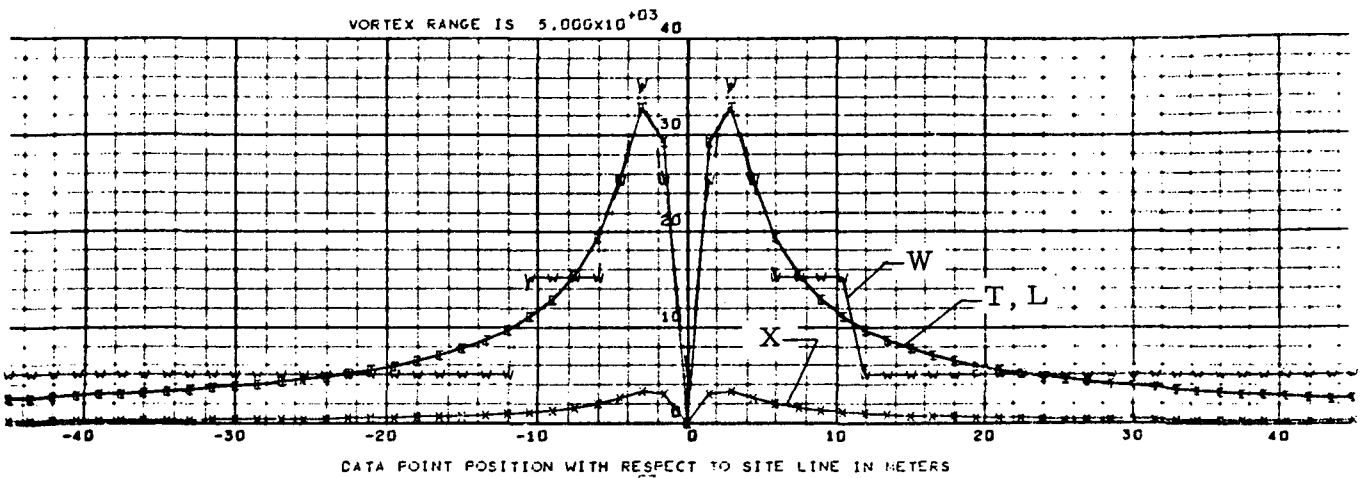


Fig. 3-20b - Two-Component Scan Through Vortex with Tangential Flow Only Simulated

The outputs of the sensors for the vortices both with and without axial flows agree quite well until the data points move into the cores. Since axial flows are confined primarily to the core in Newman's model (Ref. 26) and Appendix A) this would be expected. Once the sensors probe the core, the vortex with the axial flow displays velocities which continue to increase, while the vortex with tangential flow only displays decreasing velocities which approach zero at the core center.

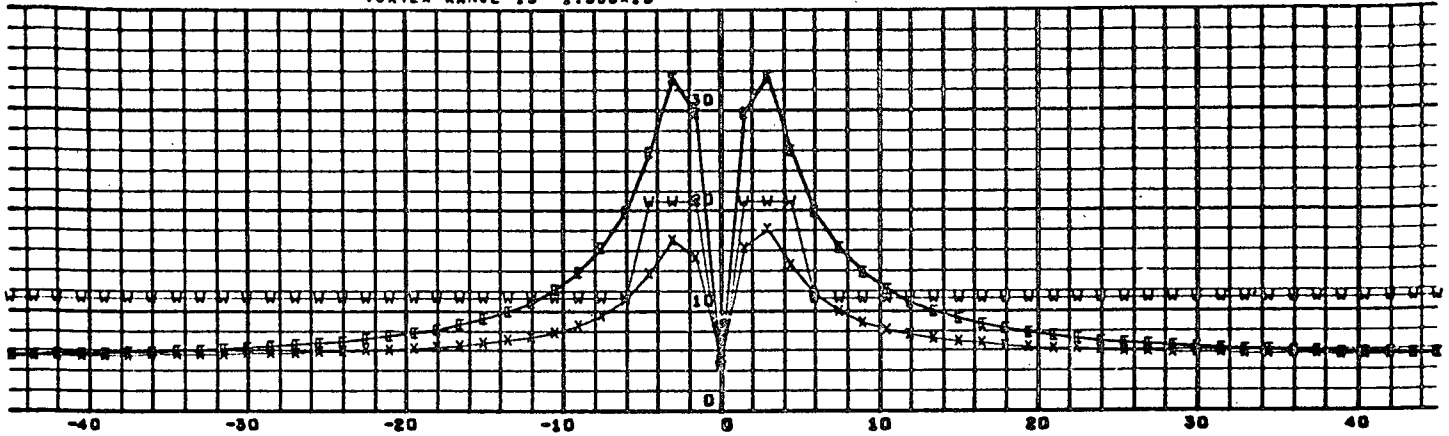
From the above data the two-component system can be seen to be capable of resolving tangential vortex velocities even in the presence of axial flow. This important property of the two-component system would allow vortex circulation to be calculated and thus vortex hazard somewhat independently of an axial flow presence within the vortex core.

● Ambient wind effects upon component systems

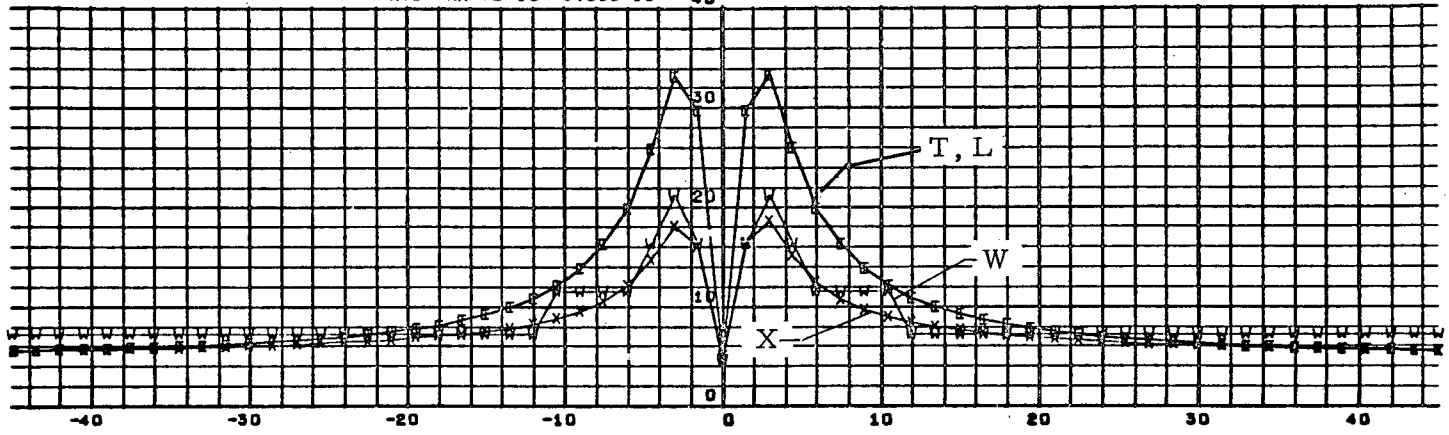
Figures 3-21 and 3-22 depict two-component scans through vortices with ambient winds superimposed on their flows. Figure 3-21 simulates vortex tangential flow without axial flow while Fig. 3-22 simulates combined axial and tangential vortex flows. These two figures are discussed in the following paragraphs. They represent a first cut at adding ambient wind effects to the simulations.

Figure 3-21 depicts two-component scans through vortices at several ranges with an ambient wind of 5 meters/second superimposed upon the tangential flow field of the vortex (no axial flow is included). The ambient wind in this case was directed along the vortex axis. This would correspond to a headwind in a real situation. A comparison of Fig. 3-21 with Fig. 3-20b – the same configuration without ambient wind – indicates that the introduction of ambient wind increases the actual flowfield velocity (T) in the wings of the vortex (at radii greater than 20m with respect to site line) but has little effect upon core velocities. Since the ambient wind simulated in this figure is normal to the vortex flow (tangential flow only simulated), the ambient wind vector (5 m/sec) – small when compared to the core max velocity (33 m/sec) – is oriented at 90 deg to the

CASE NO. 33 LONG RANGE TWO LASERS LATERAL SCAN FILTERS CW  
 VORTEX RANGE IS  $1.000 \times 10^{+04}$



DATA POINT POSITION WITH RESPECT TO SITE LINE IN METERS  
 VORTEX RANGE IS  $5.000 \times 10^{+03}$



DATA POINT POSITION WITH RESPECT TO SITE LINE IN METERS  
 VORTEX RANGE IS  $1.000 \times 10^{+03}$

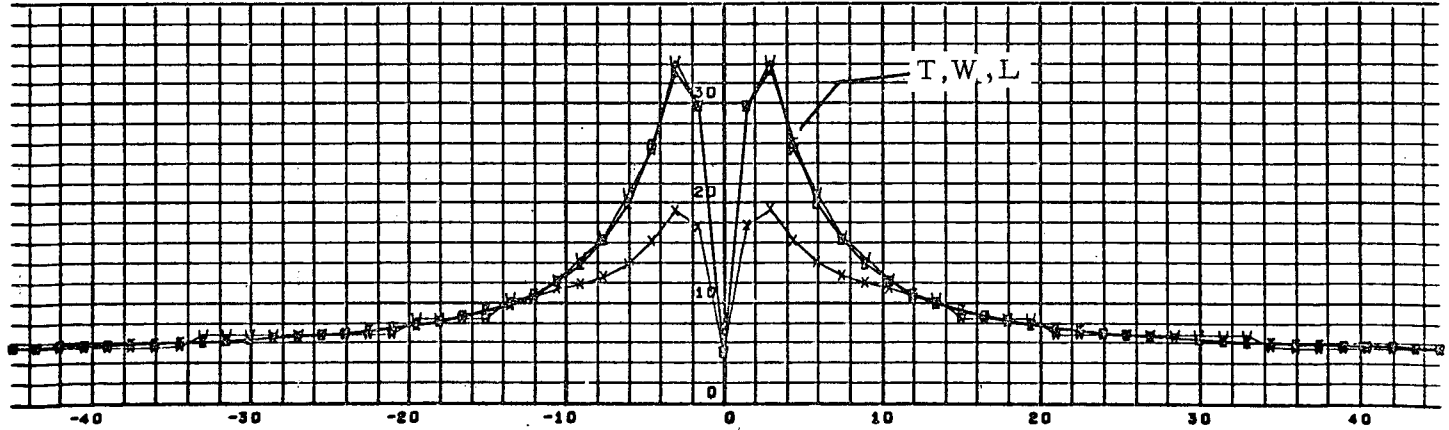
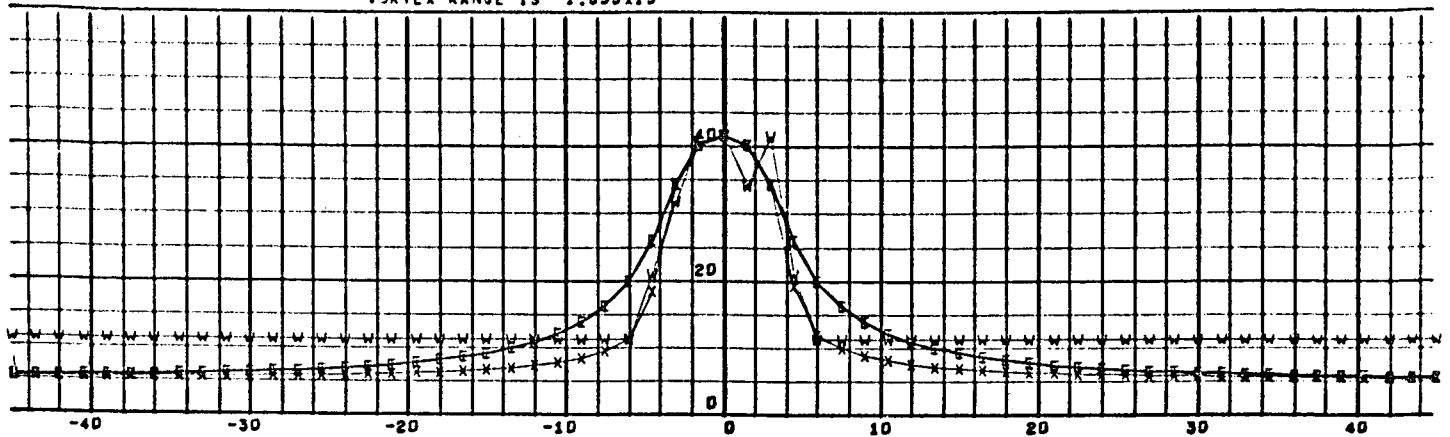
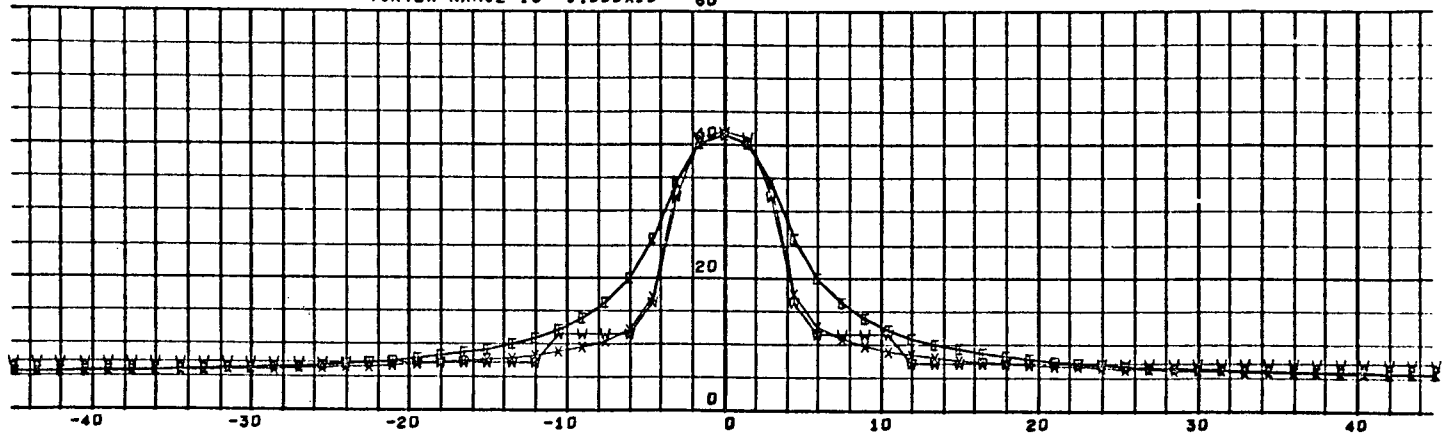


Fig. 3-21 - Two-Component Scans Through Vortex Tangential Flows at Several Ranges with Ambient Headwind of 5 m/sec (no axial flow)

CASE NO. 35 LONG RANGE TWO LASERS LATERAL SCAN FILTERS CW  
 VORTEX RANGE IS  $1.000 \times 10^{+04}$



DATA POINT POSITION WITH RESPECT TO SITE LINE IN METERS  
 VORTEX RANGE IS  $5.000 \times 10^{+03}$  60



DATA POINT POSITION WITH RESPECT TO SITE LINE IN METERS  
 VORTEX RANGE IS  $1.000 \times 10^{+03}$  60

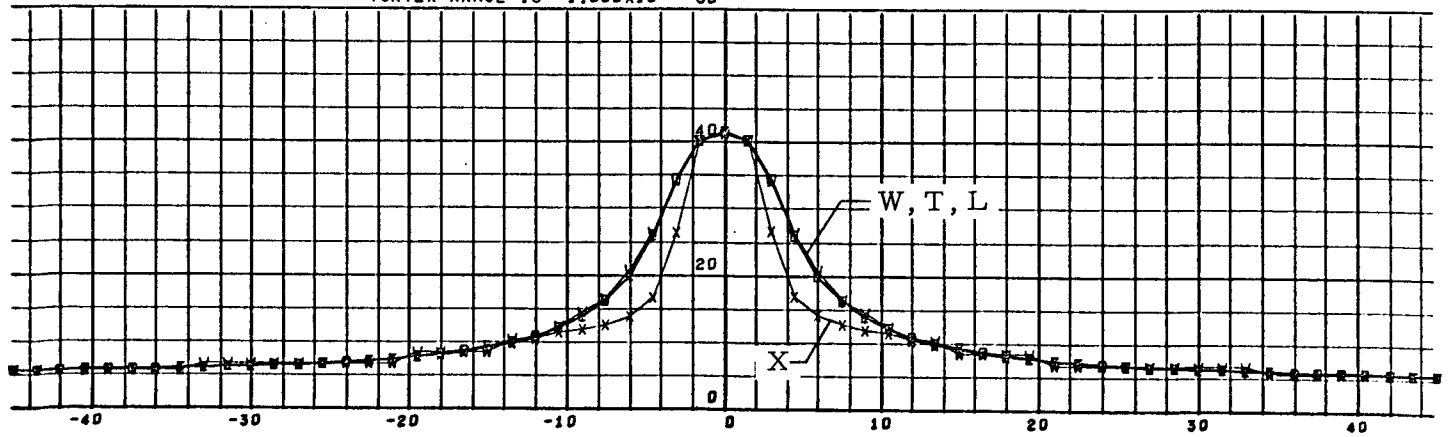


Fig. 3-22 - Two-Component Scans Through Vortex Tangential and Axial Flows at Several Ranges with Ambient Headwind of 5 m/sec

core velocity vector and has very little influence upon the combined resultant vector magnitude (34 m/sec). However, in the vortex wings, the ambient wind vector (5 m/sec) is comparable to the vortex flow vector (approximately 4 m/sec) and the two combine to form a resultant of approximately 8 m/sec.

The measured velocity (W) of Figure 3-21 closely agrees with the actual velocity (T) at close range (1 km) but falls 30% below the actual at the longer range (5 km). This can be attributed to the means of computing the two-component flow field from outputs of two one component sensors (Fig. 3-14a). The outputs of each single component sensor are extrapolated by the computer to be the highest velocity magnitude within the focal volume. If the velocity is positive a positive sign is given to the magnitude and if it is negative, the velocity magnitude is termed negative. The positive and/or negative sensor outputs are then added according to Figure 3-14a to develop a velocity magnitude for the resultant vector velocity in the plane formed by the line-of-sights of the two sensors. This mode of computing the resultant vector was not exact but provided a vector magnitude which compared very favorably with the simulated flow velocities for all vortices simulated until this particular case which included effects of ambient winds.

As can be seen from Fig. 3-21, another means should be used to improve the agreement at long ranges (narrow view angles) between actual simulated velocities (T) and measured velocities (W) where winds are involved. One means of improving this agreement would be the subtraction of ambient wind velocity components from the outputs of each of the two sensors before combining the two sensor outputs to form the two component velocity magnitude. The ambient wind velocities could be measured beyond the influence region of the vortex phenomenon.

Figure 3-22 depicts two-component scans through vortices at several ranges with an ambient wind of 5 meters/second superimposed upon the combined tangential and axial flow fields of the vortex. The ambient wind is directed along

the vortex axis as a headwind as in Fig. 3-21. The figure corresponding to 3-22 but without the ambient winds is 3-20a. In Fig. 3-22 the ambient wind translates the flowfield velocity upward in the wings (20 meters outside the vortex axis) but does not have much effect within the vortex core. The measured (W) velocities and actual (T) velocities again agree very well at the short range (approximately 1 km) but drop below the actual on the edges of the core (3 m to 10 m radii) at the longer ranges. However, since the ambient wind is in the same direction as the axial component, the measured (W) data agrees very well with the actual (T) at the vortex axis. If the ambient wind were a cross wind, this agreement may not be quite as good. Cross wind case should be simulated in the future to evaluate the effectiveness of this type of system.

### 3.3.3 Three (Three-Dimensional) or More Sensed Components

The objective of the long-range detective system is to detect the vortex and determine the hazard created by the vortex flow field. Since the hazard from a vortex is considered to be due to its tangential flow, one objective of a detective system might be to determine this tangential flow field; i.e., the vortex tangential flow versus distance from the vortex axis. The two-component sensor configuration defines the vortex flow in the plane formed by the lines of sight of the sensors as they probe the vortex. The output of the two-component configuration has been shown to be adequate in defining the vortex tangential flow field as long as scans are made through the vortex (i.e., the scan plane is moved through the vortex) in such a manner that the vortex tangential flow vectors lie in the scan plane at some time during the scan through the vortex. Since the two-component scan has been shown to be adequate to provide the desired data for the long-range detective system, the requirement for a more complex three (or more) component system is unjustified.

## 3.4 SIMULATION PROGRAM: VORTEX FLOW FIELD AND FLOWFIELD MONITORING WITH LASER DOPPLER SENSOR

Early in the contract the decision was made to emphasize mathematical modeling of laser Doppler sensors to detect simulated vortex flow fields to

develop further knowledge of sensor requirements and capabilities for a wake turbulence monitoring system. This modeling effort involved first choosing a simple but realistic vortex flow field model and, second modeling a simulated laser Doppler sensor scanning through the flow field. The vortex flow model would provide tangential flows since these were well defined and optionally axial flows (not well defined) according to Newman's model (Ref. 26). The flowfield simulation will have the capability of superimposing ambient winds. The sensor simulation is to consider optionally coaxial and bistatic optical configurations operating in both the pulsed and continuous wave laser configurations.

#### 3.4.1 Vortex Flow Field/Sensor-Detection Model

The vortex tangential flow field ( $V_T$ ) for the sensor simulation is represented by the equation (Ref. 26):

$$V_T = \frac{\Gamma_o}{2\pi D} \left[ 1 - \exp\left(-\frac{W_\infty D^2}{4\nu z}\right) \right]$$

where

$\Gamma_o$  = circulation

$W_\infty$  = freestream velocity

$\nu$  = eddy viscosity

$z$  = vortex axial coordinate

$D$  = distance from vortex centerline

and

$$\Gamma_o = \frac{4W}{\pi\rho V b}$$

$$W_\infty = V$$

$$\nu = k\mu/\rho$$

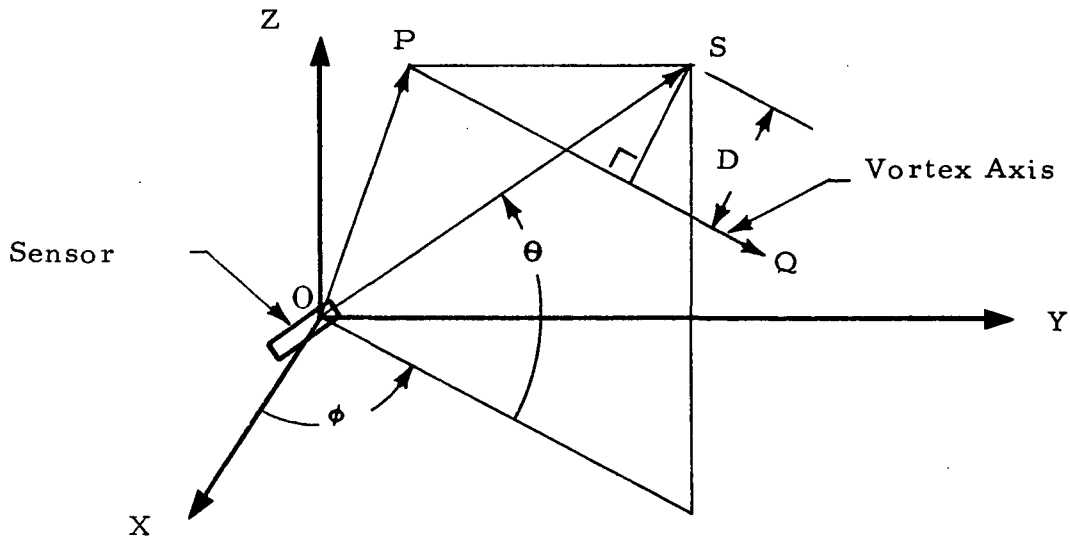
- $W$  is total aircraft weight
- $\rho$  is density of atmosphere
- $V$  is aircraft velocity
- $b$  is wing span
- $\mu$  is coefficient of viscosity
- $k$  is the coefficient that relates laminar kinematic viscosity to eddy viscosity for a particular  $\Gamma_o$

The vortex axial flow field ( $V_A$ ) is provided optionally as the following (Ref. 26):

$$V_A = \frac{D_o}{4\pi\rho\nu z} \exp\left(-\frac{W_\infty D^2}{4\nu z}\right)$$

where  $D_o$  is profile drag of the aerofoil and the other variables are those defined above.

In order to relate the tangential ( $V_T$ ) and axial ( $V_A$ ) flow fields of the vortex to some velocity sensor for a simulation of the sensor/flowfield interaction, a coordinate system was set up to describe the sensor to the flowfield. The coordinate system chosen was spherical polar with the sensor at the origin (O) and the vortex axis direction defined by the vector  $\overline{PQ}$ .



The velocity at point S is determined by D of the above equations which is the distance of S from the vortex centerline ( $\overrightarrow{PQ}$ ). The distance from S to  $\overrightarrow{PQ}$  is:

$$D = \frac{|\overrightarrow{SP} \times \overrightarrow{PQ}|}{|\overrightarrow{PQ}|}$$

where

$$\overrightarrow{SP} = \overrightarrow{OP} - \overrightarrow{OS}$$

The tangential velocity vector at S is

$$\overrightarrow{VT} = V_T \frac{(\overrightarrow{SP} \times \overrightarrow{PQ})}{|\overrightarrow{SP} \times \overrightarrow{PQ}|}$$

and the magnitude of the component of  $\overrightarrow{VT}$  in the direction of  $\overrightarrow{SO}$  (the sensor) is

$$V_{ST} = - \frac{\overrightarrow{VT} \cdot \overrightarrow{OS}}{|\overrightarrow{OS}|}$$

The magnitude of the axial component  $V_{SA}$  sensed by the sensor can be computed in a similar manner. Ambient winds can also be added vectorially to the vortex flow field.

### 3.4.2 Laser Doppler Sensor Model

The laser Doppler sensor model allows the simulated sensor to view the flow field as a typical laser Doppler sensor would, and it provides an output of velocity in terms of range and angular position of the sensor. The type of output depends upon the type of sensor (continuous wave or pulsed) and the type of processor (spectrum analyzer, filter bank, etc.) modeled.

● Coaxial Focused, Continuous Wave Laser Sensor

The focused sensor does not make a point measurement, but samples a finite volume of space along a line (the focal volume, Fig. 3-23a) and consequently observes a variety of velocities (Fig. 3-23b). The signal is the strongest at the focal point (Fig. 3-23c) and tapers off as the distance from the focal point increases. The functional dependence of the signal on range  $L$  is given by

$$I = \frac{K}{\left[ 1 + \frac{(L - f)^2}{\Delta L^2} \right] L^2} \quad (\text{Ref. 20})$$

where

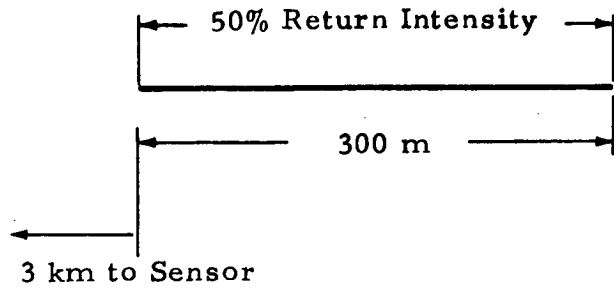
- $K$  = constant
- $f$  = distance to focus point
- $L$  = distance to point under consideration
- $\Delta L = \lambda L f / \pi R^2$
- $\lambda$  = wave length
- $R$  = radius of telescope aperture

In this program the interval  $(f - \Delta f, f + \Delta f)$  is observed along the line of sight of the laser where  $\Delta f = 2 \lambda f^2 / \pi R^2$ . Within this interval a finite number of equally spaced points are sampled. The velocity at each point ( $V_d$ ) (Fig. 3-23d) is multiplied times the weighting function ( $I_d$ ) (Fig. 3-23c) at that point; these weighted velocities ( $V_d I_d$ ) are then summed for each velocity present to determine the returned signal spectrum (Fig. 3-23e).

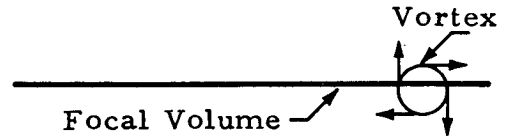
● Unfocused, Pulsed Laser Sensor

For a pulsed sensor there is a weighting analogous to the previous discussion for the focused sensor, except that the weighting function is triangular in range with the base of the triangle equal to pulsed length (see Appendix B).

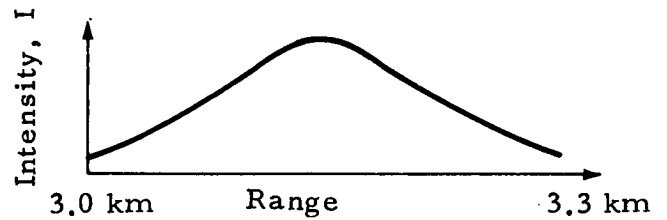
a. Focal Volume (Optic Points) of 1/3 m Diam., 1 m Separation Bistatic System at 3 km Range



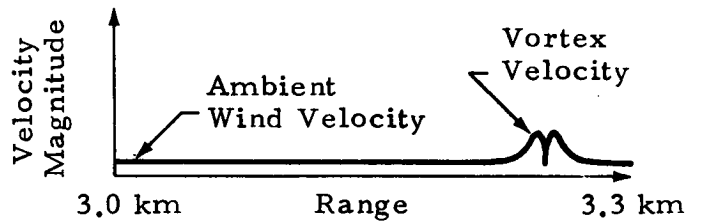
b. Typical Vortex Superimposed over Focal Volume



c. Returned Signal Intensity Weighting Function (Due to Focusing and Range Effects)



d. Flow Field Line-of-Sight Velocity Versus Range



e. Returned Signal Spectrum

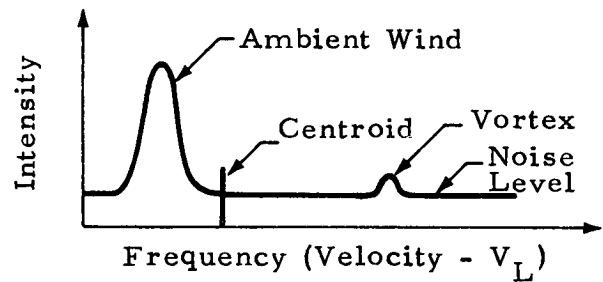


Fig. 3-23 - Example of Physical Derivation of Signal Properties for 1/3 Meter Diameter, 1 Meter Separation Bistatic Configuration Focused at 3 km Range

The sensor simulation was designed to handle either pulsed or CW-focused configurations. The simulations of both types are listed in Table 3-2.

- Preprocessing of Returned Signal

Once the returned signal is received by the detector of the laser Doppler sensor, the frequency spectrum output of the detector must be processed to provide a value which is representative of the desired data from the spatial data point. (The spatial data point is the focal volume for a focused configuration or the pulsed width volume for a pulsed configuration.) Two basic processes have been simulated to decipher a single velocity value for each spatial data point. These processes involve determining:

- Centroidal velocity, and
- Maximum velocity existing in the spatial cell

The centroidal velocity refers to the centroid of the velocity spectrum as it appears in the example of Fig. 3-23e. For short ranges where the vortex velocity signal intensity is as great as the ambient wind signal intensity, this type of processing is adequate. However, for longer ranges such that the vortex velocity signal intensity is very low in comparison to the ambient wind signal (as depicted in Fig. 3-23e), the centroidal velocity is most inadequate for representation of the vortex flow field.

Determination of maximum velocity above the noise level requires an adequate signal-to-noise ratio in order to distinguish between the portion of the velocity spectrum attributed to returned signal from the vortex and the signal attributed to noise. This type of preprocessing would provide a good representation of the vortex flow from the spectrum as illustrated in Fig. 3-23d.

Figures 3-24 and 3-25 illustrate centroidal and maximum velocity above the noise level preprocessing, respectively. Both preprocessing configurations provide adequate data at the 100-meter range. However, as the range increases

to 300 meters, note that the measured centroidal (W) velocity drops approximately 50% below the actual (T) velocity in Fig. 3-24 while the maximum velocity above the noise level (W) of Fig. 3-25 remains at the level of the actual velocity (T).

### 3.4.2 Computer Simulation Runs

Many computer simulation runs were made during the contract. A number of the runs, made during the early portion of the contract, involved multiple scans through the vortex and displayed sensor output versus sensor position and velocity contours from multiple scans. These runs are listed in Table 3.1 and discussed in Appendix B. Another larger group of runs was conducted involving single scans through vortices with results plotted as velocity versus a coordinate referenced to the vortex itself. The second group of runs is listed in Table 3-2 and discussed further in Appendix C.

### 3.5 ADDITIONAL EFFORT REQUIRED BEFORE THE LONG RANGE WAKE TURBULENCE MONITORING SYSTEM IS IMPLEMENTED

Several investigations should be performed before the long range wake turbulence monitoring system is implemented. These investigations can be grouped according to system simulations, measurement programs, and hardware development and are listed below:

- System Simulations
  - Simulate single-component sensor systems with ambient winds and turbulence.
  - Simulate two-component sensor systems with ambient (cross) winds and turbulence.
  - Simulate sensor systems with true axial velocities, after experimental axial velocity data are available.
  - Develop decision-making philosophy and simulate entire system including sensors, computer, and displays to determine system effectiveness.
  - Determine the sizes of corridors into air terminals from flight path statistics of aircraft using these corridors.

CASE NO 23 1 LASER RANGE 300 LATERAL SCAN

T = TANGENTIAL L = LINE OF SIGHT W = CENTROID

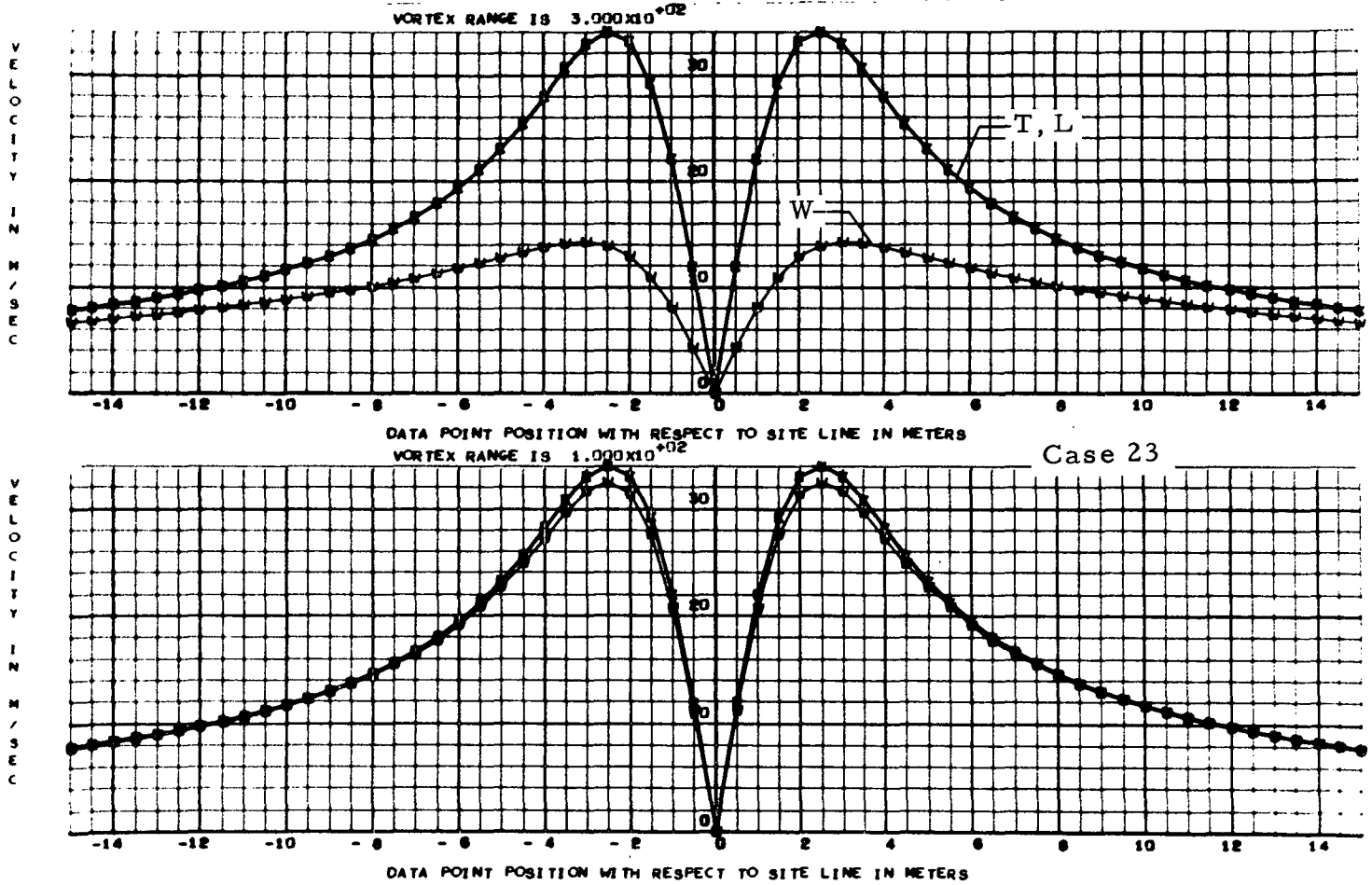


Fig. 3-24 - Data Preprocessed Using Output Centroid of Return Spectrum

CASE NO 24 1 LASER RANGE 300 LATERAL SCAN FILTERS

T = TANGENTIAL L = LINE OF SIGHT M = HIGH ACTIVATED FILTER

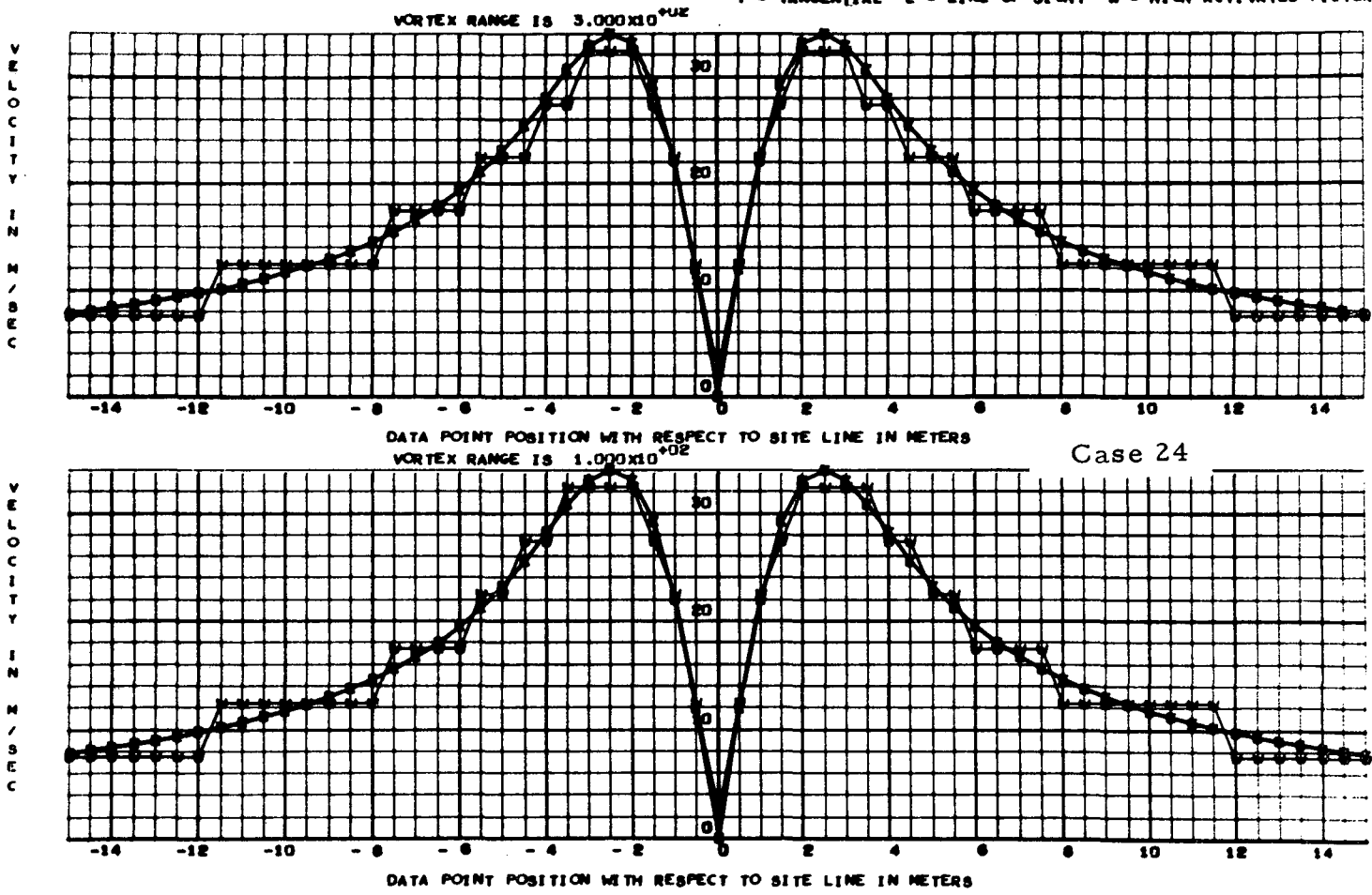


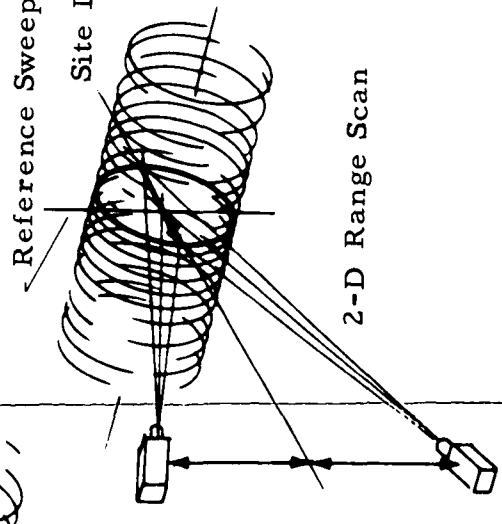
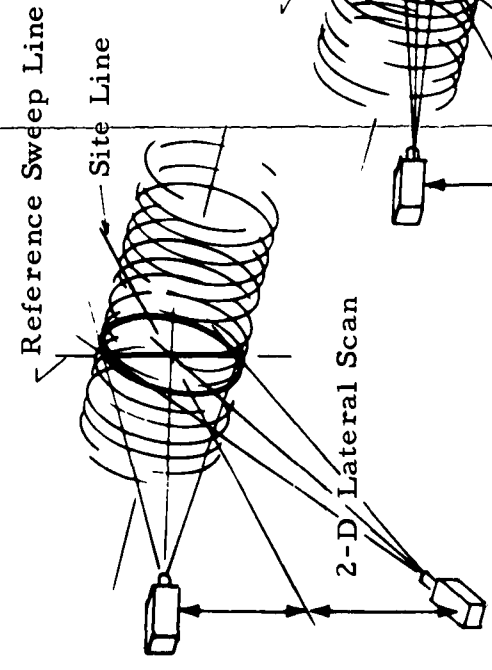
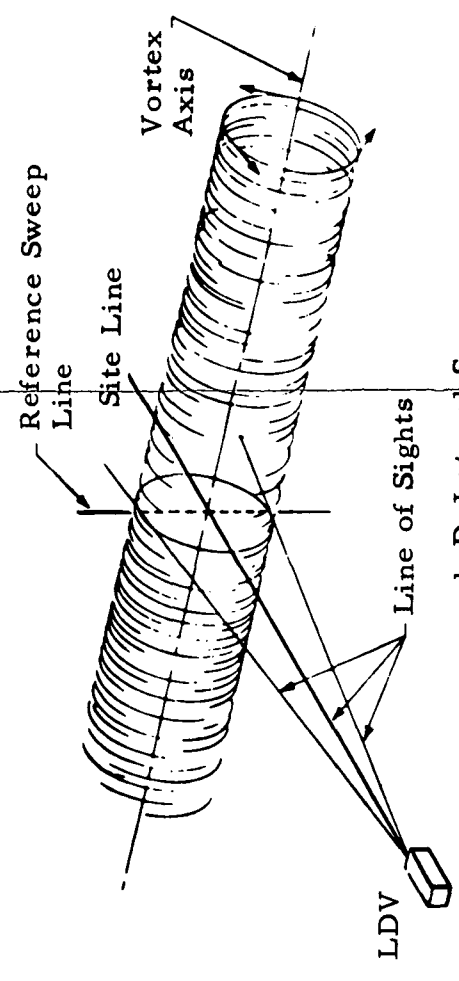
Fig. 3-25 - Data Preprocessed Using Output Maximum Velocity (above noise level) within Spectrum of Returned Signal (same scan as Fig. 3-24 but different data preprocessing)

Table 3-1  
CONTINUING DEVELOPMENT OF VORTEX SIGNATURES

System Configuration	Value Plotted	Coordinates	Range (km)	LDV Distance from Runway (m)	Vortex Distance from Runway (km)	Vortex Orientation wrt Runway	Vortex Axial Velocity	Optic Diameter (m)	Pulse Length (m)
Focused, CW	Weighted Av. Vel.	V vs $\phi$ , V vs $\theta$ , V vs R.	0.07	0	0.05	parallel	no	1/3	N/A
	Weighted Av. Vel. Contour	$\theta$ vs $\phi$ , $\phi$ vs R, $\theta$ vs R							
	Weighted Av. Vel. &  W  max	V vs $\phi$	.1, .2, .5	0	.1, .2, .5	parallel	no	.3	N/A
			.2, .5, 1		.5				
	Weighted Av. Vel. &  W  max Contours	R vs $\phi$	.1, .2, .5		.1, .2, .5			.3	
			.2, .5, 1		.5				
							.3		
							.5, 1, 5		.2
Pulsed, CW	V <sub>mx</sub> - V <sub>mn</sub> ' &  W  <sub>mx</sub> , V <sub>mn</sub> ' & Velocity Contours	V vs $\phi$ and $\theta$ vs $\phi$	2.2	1000	Inter-sects	2.5°	yes	N/A	50
	V <sub>mx</sub> - V <sub>mn</sub>	V vs $\phi$	2.2	200	Inter-sects	2.5°	yes	N/A	50
	V <sub>mx</sub> - V <sub>mn</sub>		2.2	1000		2.5°	no	N/A	50
	V <sub>mx</sub> - V <sub>mn</sub>	V vs $\phi$	.5, 1, 5, 10	200 & 1000	Inter-sects	2.5°	no	N/A	10, 50 & 300
	V  <sub>mx</sub>		.5 & 5	0		parallel	no	N/A	10, 50 & 300
	V  <sub>mx</sub> Contour	R vs $\phi$	5	0	5	parallel	no	N/A	10, 50 & 300
	Weighted ( $\Delta$ ) Av. Vel.	R vs $\phi$	.5	0	.5	parallel	no	N/A	10, 50 & 300

Case Number	Rotation About Ref. Sweep Line		Rotation About Site Line	Range to Vortex (km)	1-D, 2-D, 3-D			Multi-Dimen. Laser Coordinates			Telescope Aperture (m)	Pulse Length (m)	Vel. Sign Ambiguity (V or  V )	Range Incremental Change with Respect to Site Line and Ref. Sweep Line (m)	Centroid (C)	Max Velocity (M)	Filter Band Width (m/sec)	Filter Sensitivity (%)	Lateral or Range Scan (L or R)	Tangential Flow Only (T)	Tangential and Axial Flow (T&A)	With Ambient Headwind	Misalignment	Case Run
	Rel. Sweep Line	Site Line			S	D	E																	
1	0±10	±10	0.3	1-D	NA	NA	NA	NA	NA	0.4	NA	V	-15,-7	C	NA	NA	L	T	NA	NA	x	x		
2	0±10	±10	1.0	1-D	NA	NA	NA	NA	NA	0.4	0.4	V	-15,-7	C	NA	NA	L	T	NA	NA	x	x		
3	0±10	±10	5.0	1-D	NA	NA	NA	NA	NA	2.0	2.0	V	-15,-7	C	NA	NA	L	T	NA	NA	x	x		
7	0±10	±10	5.0	1-D	NA	NA	NA	NA	NA	2.0	2.0	V	-15,-7	C	NA	NA	L	T	NA	NA	x	x		
9	30±10	±10	5.0	1-D	NA	NA	NA	NA	NA	0.4	0.4	V	-15,-7	C	NA	NA	L	T	NA	NA	x	x		
10	0±10	±10	5.0	1-D	NA	NA	NA	NA	NA	0.4	0.4	V	-15,-7	C	NA	NA	L	T	NA	NA	x	x		
11	0±20	0±20	5.0	1-D	NA	NA	NA	NA	NA	0.4	0.4	V	-15,-7	C	NA	NA	L	T	NA	NA	x	x		
12	60±20	±20	5.0	1-D	NA	NA	NA	NA	NA	0.4	0.4	V	-15,-7	C	NA	NA	L	T	NA	NA	x	x		
13	60±20	±20	1.0	1-D	NA	NA	NA	NA	NA	0.4	0.4	V	-15,-7	C	NA	NA	L	T	NA	NA	x	x		
14	80±5	0±10	0.3	1-D	NA	NA	NA	NA	NA	0.4	0.4	V	-15,-7	C	NA	NA	L	T	NA	NA	x	x		
16	0±30	0±30	5.0	1-D	NA	NA	NA	NA	NA	0.4	0.4	V	-15,-7	C	NA	NA	L	T	NA	NA	x	x		
17	0±30	0±30	5.0	1-D	NA	NA	NA	NA	NA	0.4	0.4	V	-15,-7	C	NA	NA	L	T	NA	NA	x	x		
18	0±30	0±30	5.0	1-D	NA	NA	NA	NA	NA	0.4	0.4	V	-15,-7	C	NA	NA	L	T	NA	NA	x	x		
19	0±30	0±30	5.0	1-D	NA	NA	NA	NA	NA	0.4	0.4	V	-15,-7	C	NA	NA	L	T	NA	NA	x	x		
20	0±30	0±30	5.0	1-D	NA	NA	NA	NA	NA	0.4	0.4	V	-15,-7	C	NA	NA	L	T	NA	NA	x	x		
21	0±30	0±30	5.0	1-D	NA	NA	NA	NA	NA	0.4	0.4	V	-15,-7	C	NA	NA	L	T	NA	NA	x	x		
22	0±30	0±30	5.0	1-D	NA	NA	NA	NA	NA	0.4	0.4	V	-15,-7	C	NA	NA	L	T	NA	NA	x	x		
23	0±30	0±30	5.0	1-D	NA	NA	NA	NA	NA	0.4	0.4	V	-15,-7	C	NA	NA	L	T	NA	NA	x	x		
24	0±30	0±30	5.0	1-D	NA	NA	NA	NA	NA	0.4	0.4	V	-15,-7	C	NA	NA	L	T	NA	NA	x	x		
30	84	±10	5.0	1-D	NA	NA	NA	NA	NA	2.0	2.0	V	-7,-2	M	5	0.1	L	T&A	T&A	NA	1 mph	x		
31	84	±10	5.0	1-D	NA	NA	NA	NA	NA	2.0	2.0	V	-7,-2	M	5	0.1	L	T&A	T&A	NA	1 mph	x		
32	84	±10	5.0	1-D	NA	NA	NA	NA	NA	2.0	2.0	V	-7,-2	M	5	0.1	L	T&A	T&A	NA	1 mph	x		
33	84	±10	5.0	1-D	NA	NA	NA	NA	NA	2.0	2.0	V	-7,-2	M	5	0.1	L	T&A	T&A	NA	1 mph	x		
34	89.9	±10	5.0	1-D	NA	NA	NA	NA	NA	2.0	2.0	V	-7,-2	M	5	0.1	L	T&A	T&A	NA	1 mph	x		
35	89.9	±10	5.0	1-D	NA	NA	NA	NA	NA	2.0	2.0	V	-7,-2	M	5	0.1	L	T&A	T&A	NA	1 mph	x		
36	89.9	±10	5.0	1-D	NA	NA	NA	NA	NA	2.0	2.0	V	-7,-2	M	5	0.1	L	T&A	T&A	NA	1 mph	x		
37	89.9	±10	5.0	1-D	NA	NA	NA	NA	NA	2.0	2.0	V	-7,-2	M	5	0.1	L	T&A	T&A	NA	1 mph	x		
38	89.9	±10	5.0	1-D	NA	NA	NA	NA	NA	2.0	2.0	V	-7,-2	M	5	0.1	L	T&A	T&A	NA	1 mph	x		
39	89.9	±10	5.0	1-D	NA	NA	NA	NA	NA	2.0	2.0	V	-7,-2	M	5	0.1	L	T&A	T&A	NA	1 mph	x		
40	89.9	±10	5.0	1-D	NA	NA	NA	NA	NA	2.0	2.0	V	-7,-2	M	5	0.1	L	T&A	T&A	NA	1 mph	x		
41	89.9	±10	5.0	1-D	NA	NA	NA	NA	NA	2.0	2.0	V	-7,-2	M	5	0.1	L	T&A	T&A	NA	1 mph	x		
30-1	84	±10	5.0	1-D	NA	NA	NA	NA	NA	2.0	2.0	V	-7,-2	M	5	0.1	L	T&A	T&A	NA	1 mph	x		
35-1	89.9	±10	5.0	1-D	NA	NA	NA	NA	NA	2.0	2.0	V	-7,-2	M	5	0.1	L	T&A	T&A	NA	1 mph	x		
35-2	89.9	±10	5.0	1-D	NA	NA	NA	NA	NA	2.0	2.0	V	-7,-2	M	5	0.1	L	T&A	T&A	NA	1 mph	x		
35-3	89.9	±10	5.0	1-D	NA	NA	NA	NA	NA	2.0	2.0	V	-7,-2	M	5	0.1	L	T&A	T&A	NA	1 mph	x		
35-4	89.9	±10	5.0	1-D	NA	NA	NA	NA	NA	2.0	2.0	V	-7,-2	M	5	0.1	L	T&A	T&A	NA	1 mph	x		
35-5	89.9	±10	5.0	1-D	NA	NA	NA	NA	NA	2.0	2.0	V	-7,-2	M	5	0.1	L	T&A	T&A	NA	1 mph	x		
35-6	89.9	±10	5.0	1-D	NA	NA	NA	NA	NA	2.0	2.0	V	-7,-2	M	5	0.1	L	T&A	T&A	NA	1 mph	x		
35-7	89.9	±10	5.0	1-D	NA	NA	NA	NA	NA	2.0	2.0	V	-7,-2	M	5	0.1	L	T&A	T&A	NA	1 mph	x		

○ = nominal range for run. 3-54



Scanning Nomenclature

Table 3-2  
VARIABLES FOR SINGLE-LINE-SCAN  
COMPUTER MODELING

- Measurement Programs

- Measure axial flow velocities of full-scale aircraft vortices with remote sensors.
- Experiment with a single-component laser Doppler velocimeter detecting vortices in an air terminal environment.
- Experiment with a two-component laser Doppler velocimeter detecting vortices in an air terminal environment.

- Development Programs

- Develop MIL-Spec laser velocimeter hardware to meet high reliability standards.

## Section 4

## HYBRID WAKE VORTEX MONITORING SYSTEM

## 4.1 INTRODUCTION

The hybrid wake vortex monitoring system relies less on sensors than on the detective system and less on prediction than on the predictive system. It incorporates some features of both as a system which should provide forecasts with more accuracy than the purely predictive system without quite as much sensor sophistication as the detective system. Since the sensors of the hybrid system are not as sophisticated as those of the detective system, with maximum effort the system could become field-operational within a very few years. Although the predictive system does not provide quite the air terminal capacity increase that the detective system does, it is expected to enhance the terminal capacity over the purely predictive system because of the improved accuracy of the vortex hazard forecasting.

## 4.2 TYPICAL HYBRID WAKE TURBULENCE MONITORING SYSTEM

A typical predictive wake turbulence monitoring system is depicted in Fig. 4-1. This artist's concept of the system depicts both laser Doppler and acoustic sensors performing the measurement function. The laser velocimeter measures vortex size and movement in vertical planes normal to the runway axis and located several hundred or thousand feet beyond the end of the runway. The acoustic sensor locates the vortex position in a plane nearer the runway end where the range requirement is less. System sensory mechanisms are controlled by the system computer which also processes sensor data and performs the hazard forecasting function. The hazard status is displayed to the traffic controller who maintains spacing between aircraft according to prevailing vortex conditions. These various functions and the equipment for performing them in the hybrid system are discussed in the following paragraphs.

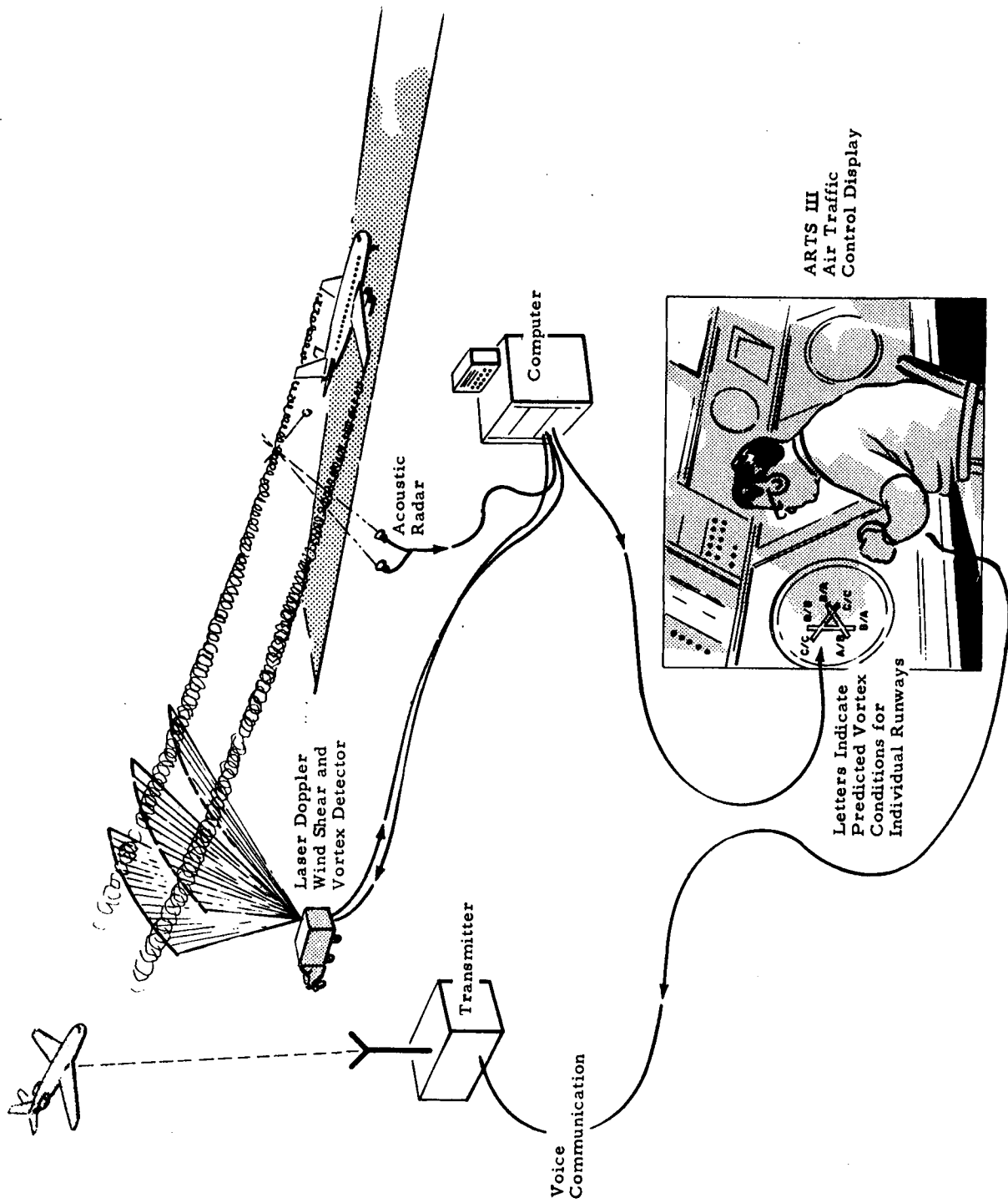


Fig. 4-1 - Hybrid System

#### 4.2.1 Detection of Current Vortex Locus

A single-component laser Doppler velocimeter should be capable of readily detecting and determining the tangential velocity distribution of a vortex if the system is configured to view the vortex perpendicularly to the vortex axis. This premise was discussed in Section 3.3.1, and is illustrated in Figs. 3-10 and 3-11. The sensor could either be under or to the side of the vortex (i.e., under or to the side of the flight corridor) and would accurately measure the tangential flow field of the vortex.

A typical air terminal layout with a hybrid laser Doppler wake turbulence sensor system is depicted in Fig. 4-2. The wind is shown in this figure blowing from left to right. Therefore, for both arrival and departure, aircraft would be traveling into the wind; i.e., from right to left. The approach corridors for this wind condition would be at the right (in the illustration) end of the field and the departure corridors at the left. The boundaries above and below ILS approach corridors are typically at 3 and 2 deg, respectively. The horizontal spread is  $2\frac{1}{2}$  deg to either side of the runway. Since planes descend onto the air terminal at widely varying vertical angles independent of the ILS corridor, the boundaries on the departure corridors include a larger vertical slice of air space (2 to 16 deg) and the same horizontal spread ( $2\frac{1}{2}$  deg to either side of the runway).

The NASA report of Ref. 27 discusses feasibility loci for vortex sensors for the hybrid wake turbulence monitoring system. A first cut at locating the sensors has indicated that the vertical scan planes at 5000 feet beyond each end of the runway would provide much useful vortex position data to feed into the wake turbulence forecasting computer. Sensors at these ranges are depicted in Fig. 4-2. By using Fig. 4-2 and simple geometry, typical maximum ranges for the sensors to scan the overhead planes adequately can be determined. The sensors located 5,000 feet from the runway end and scanning the arrival corridors should have a maximum range of approximately 1000 feet for maximum glide slope of 6 deg. Sensors located 5,000 feet from the runway end and scanning the departure corridor should have a maximum range of approximately 2500 feet. From the requirements subsection of

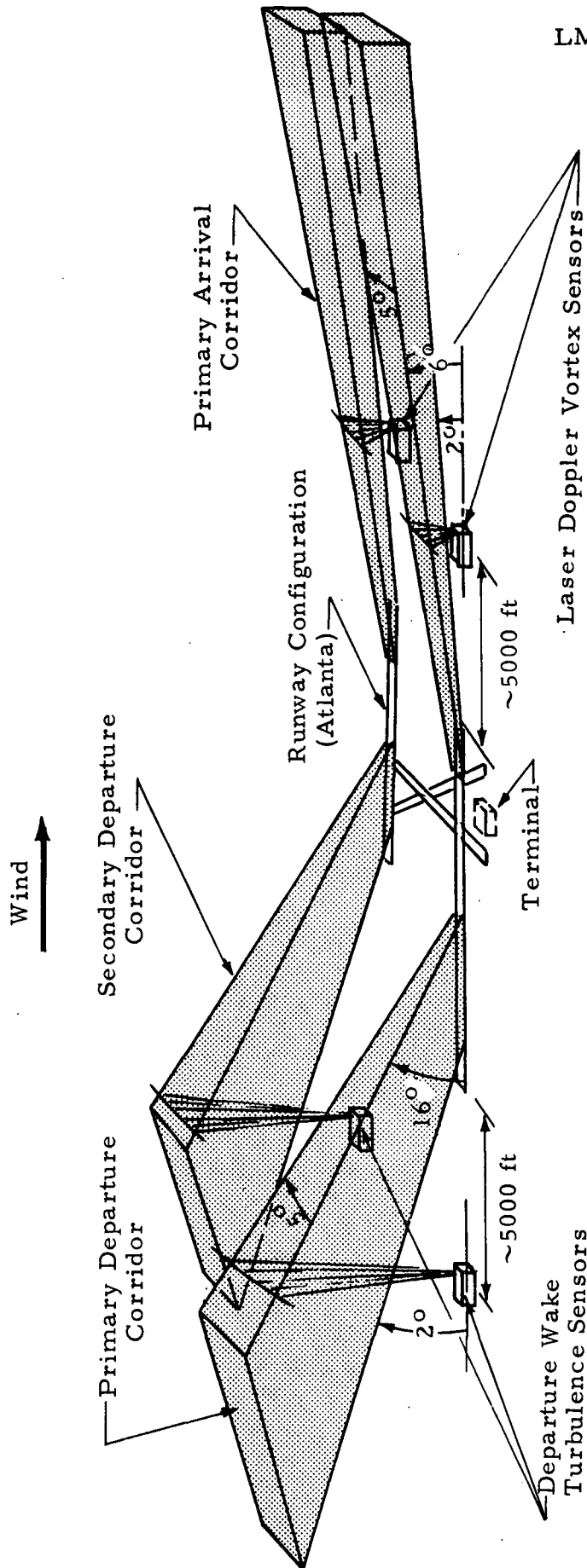


Fig. 4-2 - Typical Physical Layout of Hybrid Wake Turbulence Monitoring System

Section 1 of this document, it was indicated that the altitude of an aircraft above the ground greatly influences the controllability of the aircraft after it encounters a wake turbulence. A 2500-foot altitude above the ground could be used as a typical maximum altitude for a hybrid system monitoring capability.

Figure 4-3a illustrates a vortex scanner performing two or more near-vertical scans to determine the angular slope of the vortex axis between the two scan planes. High spatial resolution sensors would be required to perform this vortex axis slope determination unless the scan planes are widely separated.

Figure 4-3b illustrates the use of a conical scan from a single-component laser Doppler velocimeter to provide a three-component average velocity profile. The laser beam is focused at a specific range and rotated through  $\alpha$  to scan a cone of angle  $\beta$ . The average vertical wind component will appear on the returned signal as  $V_v$ , the average (dc) value of the signal. As the sensor scans into and out of the horizontal wind component, a sinusoidal output will be detected with the peak of the sine wave at the  $\alpha_h$  position indicating the direction of the horizontal wind. The average horizontal wind velocity can then be calculated by dividing the peak-to-peak amplitude of the sensor's velocity output by twice the sine of  $\beta$ , the conic angle.

At heights of up to a couple of hundred feet and at horizontal distances of 800 to 1000 feet, acoustic sensors have proven to be effective in tracking vortices (Refs. 28 and 29). The acoustic sensor vortex tracking configuration developed by the Department of Transportation's Transportation Systems Center is depicted in Fig. 4-4. The transmitter sends out an acoustical pulse of energy. The path of this pulse is altered by the flow fields of the vortices. One vortex bends the acoustic path upward; the other bends the acoustic path back toward the ground. The vortex which bends the acoustic path toward the ground is tracked by measuring the time delays of the acoustic pulses in reaching several receivers (1 and 2 of Fig. 4-4). Data of vortex tracks taken with this type system are shown in Fig. 4-5. This type sensor is designed to track vortices and not measure the velocities of their flow fields.

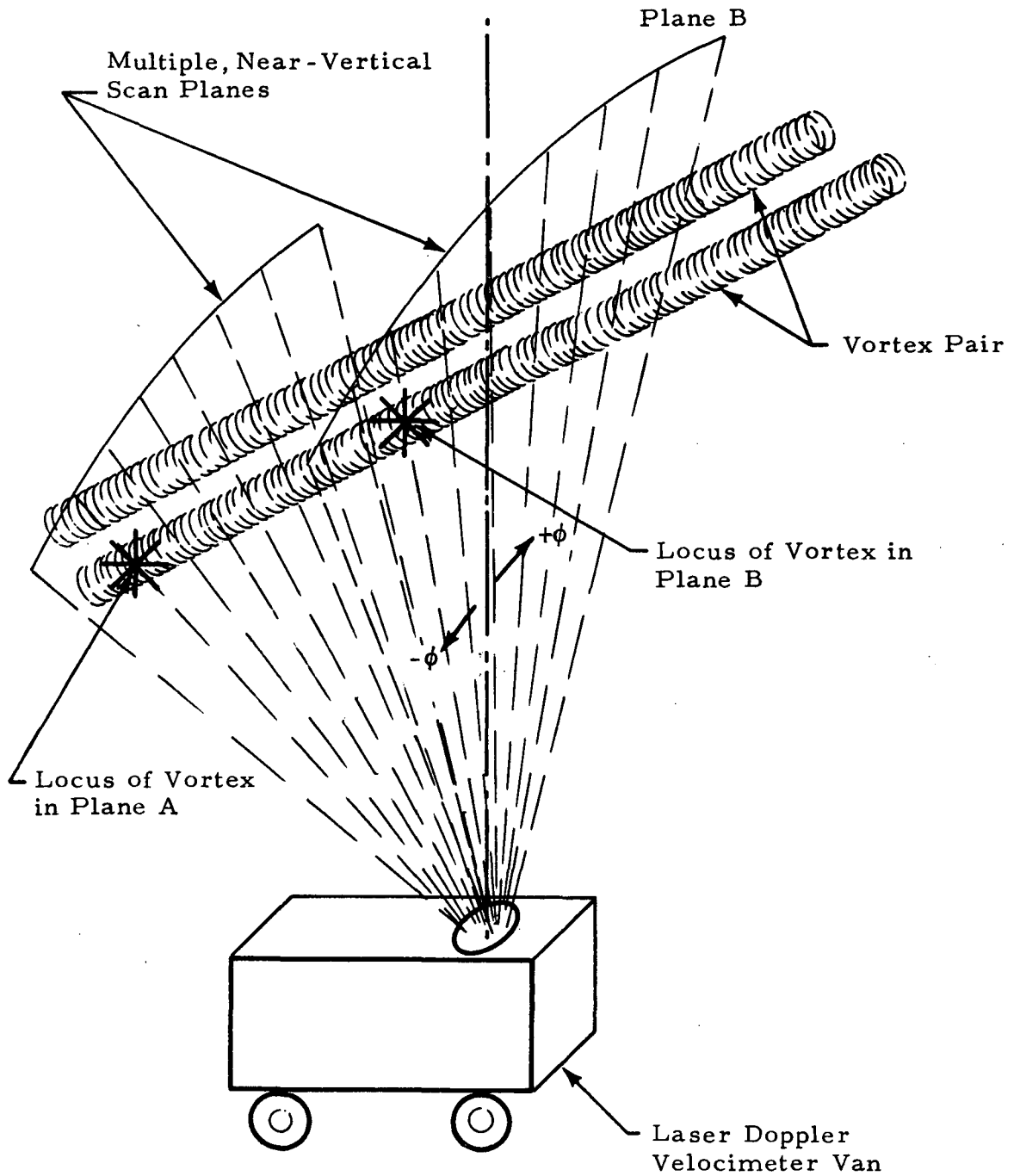


Fig. 4-3a - Determination of Vortex Loci Within Scan Planes (Multiple planes used to determine vortex trajectory)

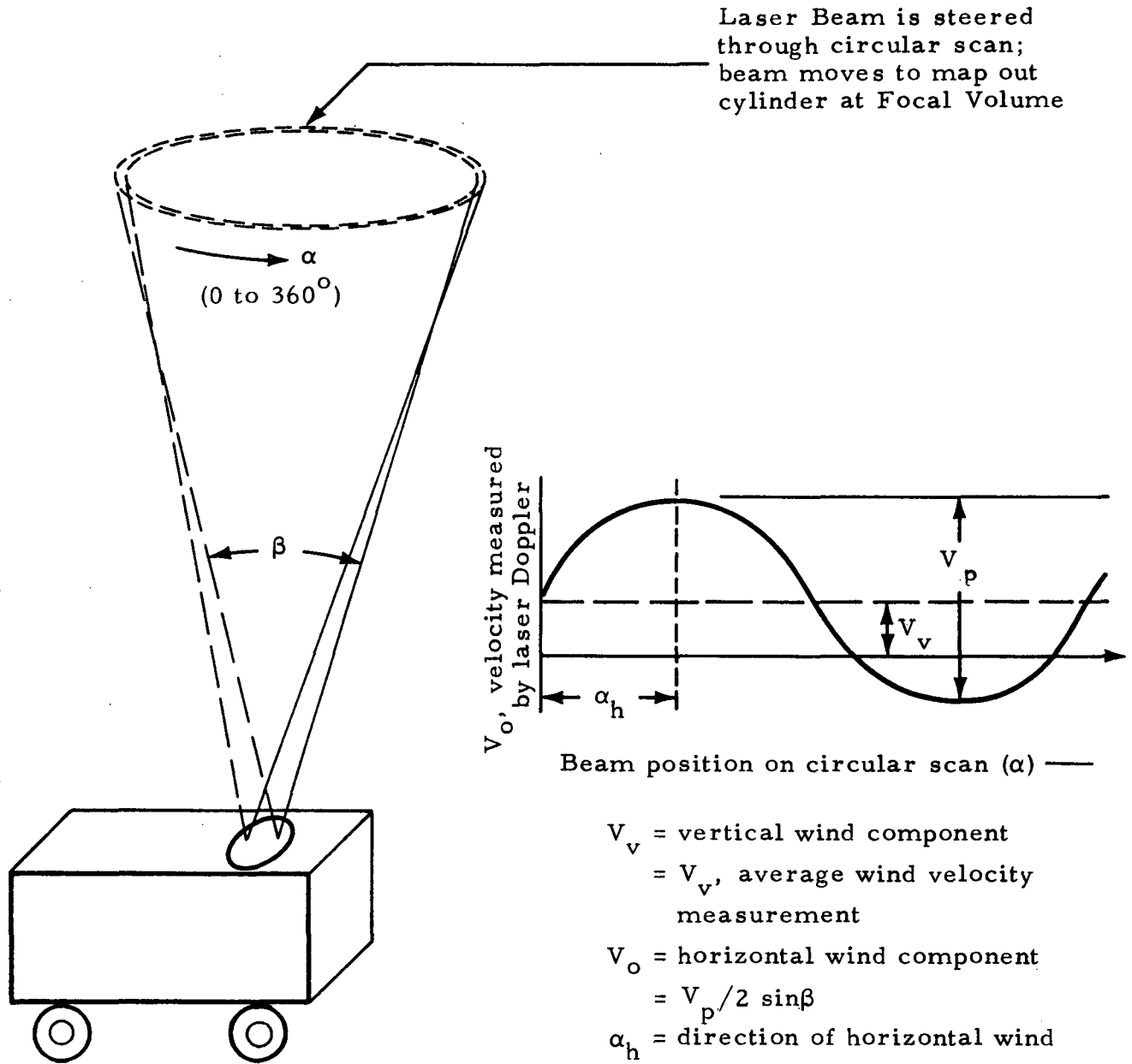
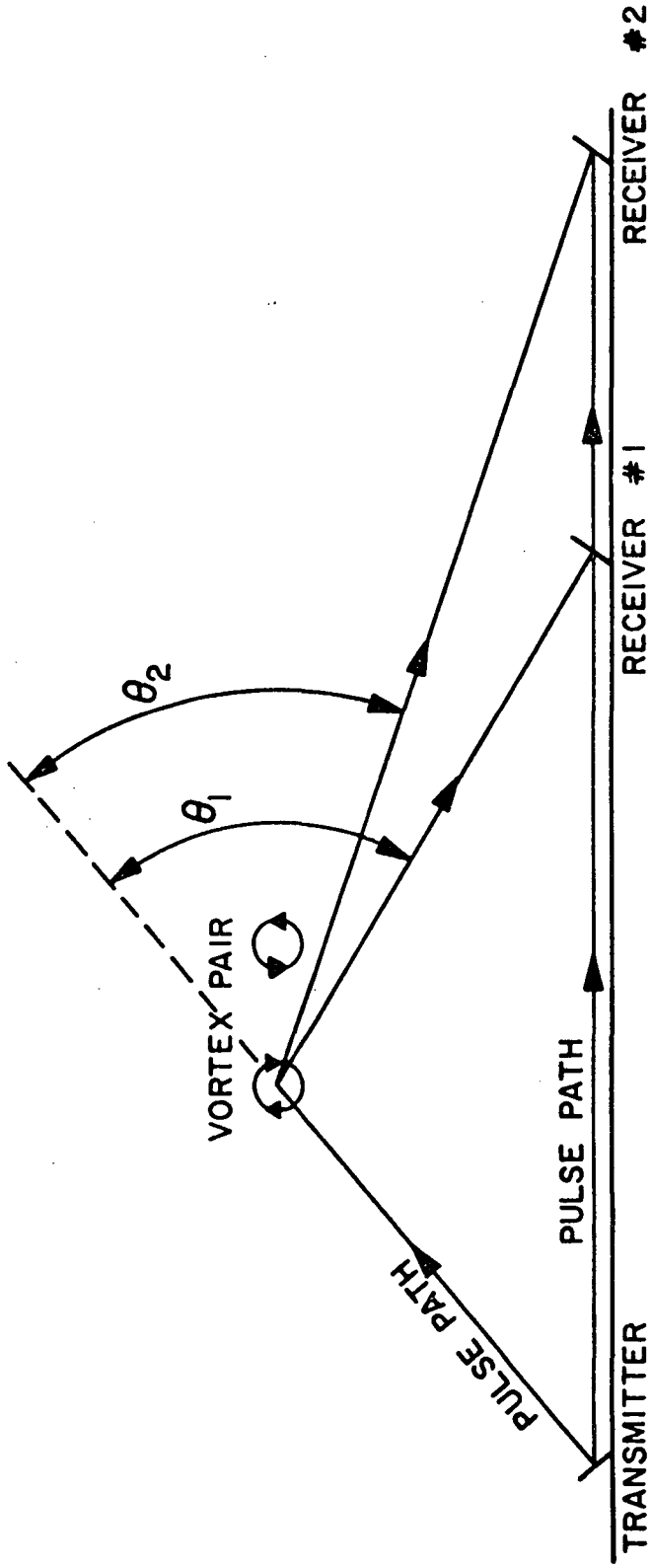


Fig. 4-3b - Determination of Average Wind Profile from Conical Scan with Single-Component Laser Doppler Velocimeter



2033

Fig. 4-4 - Pulsed Acoustic Bistatic Radar (Ref.29)

NAFEC JULY 14, 1971  
 PAN AM B-747 (C-749)  
 TAPE 32 RUN 27

LOCAL TIME 1001  
 RADAR ALTITUDE 200 FT  
 AIRSPEED 145 KTS  
 GROSS WGT 460 KLBS  
 GEAR DOWN  
 FLAP SETTING 30 DEG  
 CONFIGURATION LDG

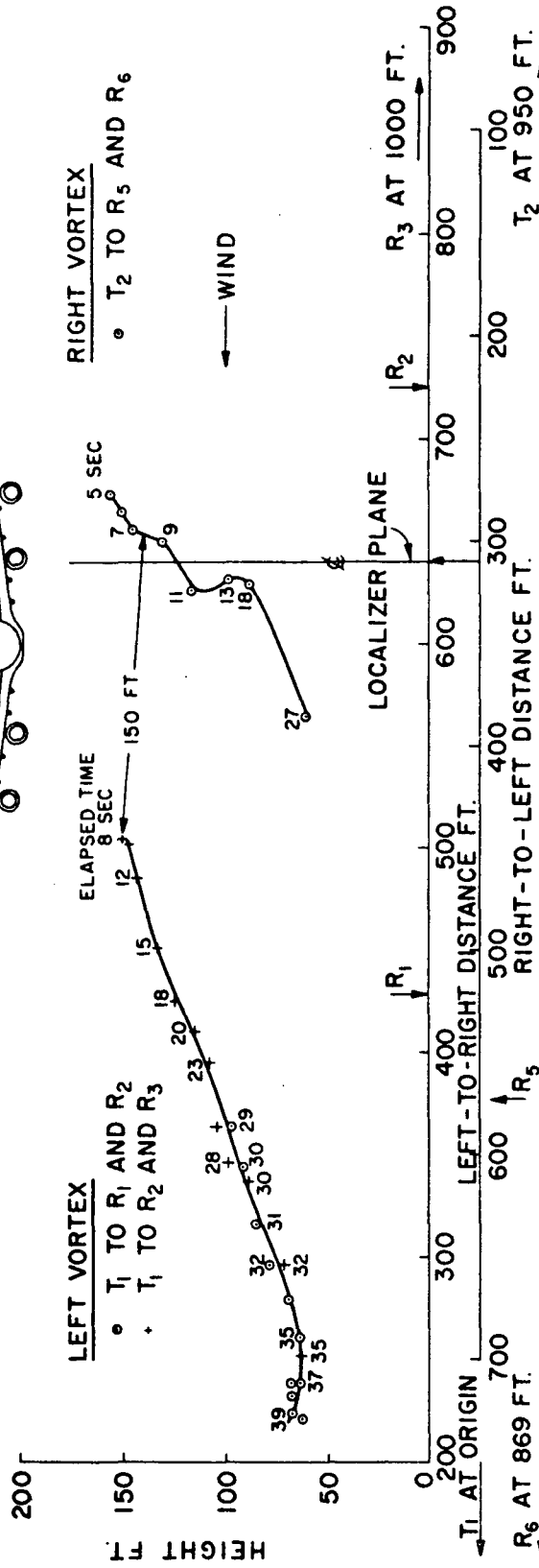
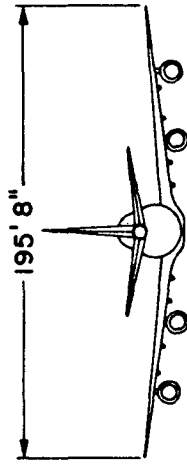


Fig. 4-5 - Vortex Tracks B-747 Nominal Vortex Spacing 155 Feet (Ref. 29)

#### 4.2.2 Forecasts of Future Hazard

The computer of Fig. 4-1 receives the inputs from the sensors discussed in Section 4.2.1 and processes these data to provide a forecast of the vortex persistence in the active air corridors of the air terminal. The forecast from the hybrid system should be more accurate than that from the purely predictive system because of the increased accuracy of the input data. The real-time wind input capability of the hybrid system (from the conical scan of the laser Doppler sensor) would alone greatly improve the system accuracy in forecasting wake turbulence persistence over the "predictive system" since the wind inputs into the predictive system are provided as a forecast by the local aviation weather forecaster. The additional sensing of the vortex locus and movement within the vertical scan planes of Fig. 4-2 should further enhance the system's forecasting capability. The computer must then predict the loci of the vortices between the scan planes and forecast their movements for several minutes. The computer then would compare the predicted vortex movement with the boundaries of the active air corridors to determine the safe separation distance required between successive aircraft about to move into the corridor. The primary improvement to be gained by going from this hybrid system to the "detective system" is that the requirement to predict vortex loci between the scan planes (the detective system would measure these directly) will be eliminated.

#### 4.2.3 Interface with Air Traffic Controllers and/or Pilots

From the computer the vortex information must be fed to the ATC and/or pilots involved in the hazard avoidance. This operation could be handled for the hybrid system in the same manner as for the predictive system (discussed in Section 2.5). The communication must be simple and precise in order not to confuse the user of the data. The computer should be used to make as many of the decisions as practical to reduce, not add to, the burden of the user.

### 4.3 HYBRID SYSTEM SIMULATION

A digital computer program was developed to simulate a single-component LDV scanning overhead searching for vortices. The simulation first performs a coarse scan overhead in  $\phi$  (Fig. 4-3a) and range to locate anomalies in the flow field. If anomalies are located, the simulation, after it makes the coarse scan, goes back for a fine scan in the regions of the anomalies. If vortices are present, the simulation maps the vortices' velocities, calculates their circulations and locates the centers of their cores.

Figure 4-6 represents the output of the simulation after the first coarse scan. The asterisks mark the loci of the high velocity points within the scan.

Figure 4-7 is a detail scan mapping of the regions of the high velocity anomalies located by the coarse scan. The mapping represents velocity in terms of the angular position ( $\phi$ ) of the sensor with scans at a number of different ranges. The ranges begin at 575 meters (bottom curve A) and are incremented in one meter increments out to 625 meters (top curve A). The velocity scales for each curve are offset by 8 meters/sec from the previous curve (starting at the bottom) so that the viewer can distinguish between the curves. High velocity activity can be depicted near the center of this figure.

Figure 4-8 represents a contour mapping of the velocities of Fig. 4-7. The contours are plotted in terms of sensor angle ( $\phi$ ) and range. The F contour is the outermost and represents velocities of approximately 5 meters/sec. The E contour represents 10 meters/sec; D represents 15 meters/sec, and so on until the innermost contour A represents 30 meters/sec sensed velocity.

Once the computer has stored the data of Fig. 4-8, computations are then made to determine peak velocity, circulation, etc. The computer picks the peak velocity at each range of Fig. 4-7 by applying a cubic least squares curve fit to the velocities measured at the specified ranges and differentiates the curve and tests for the maxima. The peak velocities at each range are

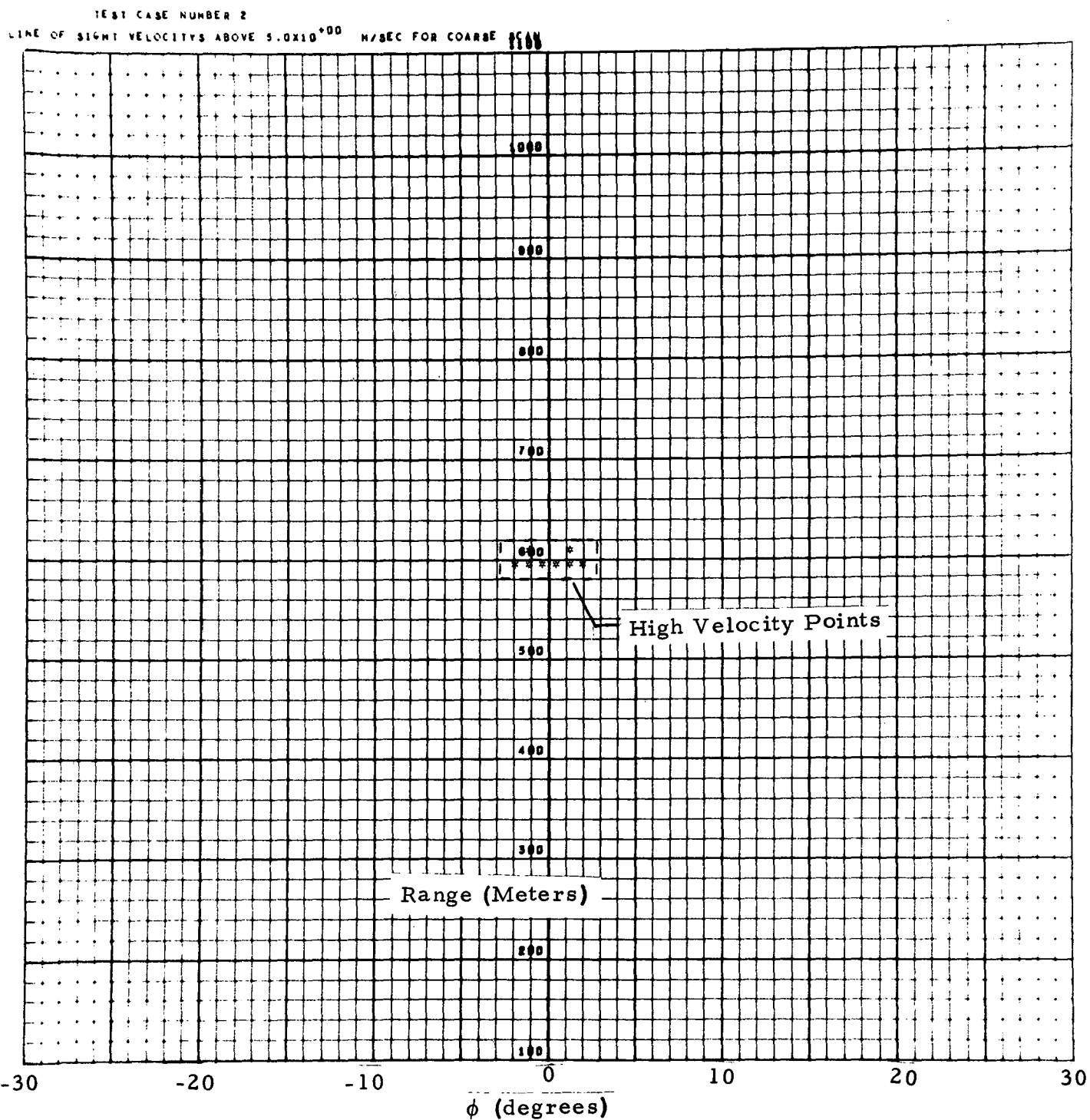


Fig. 4-6 - Hybrid System Coarse Scan; (Asterisks mark loci of high velocities)



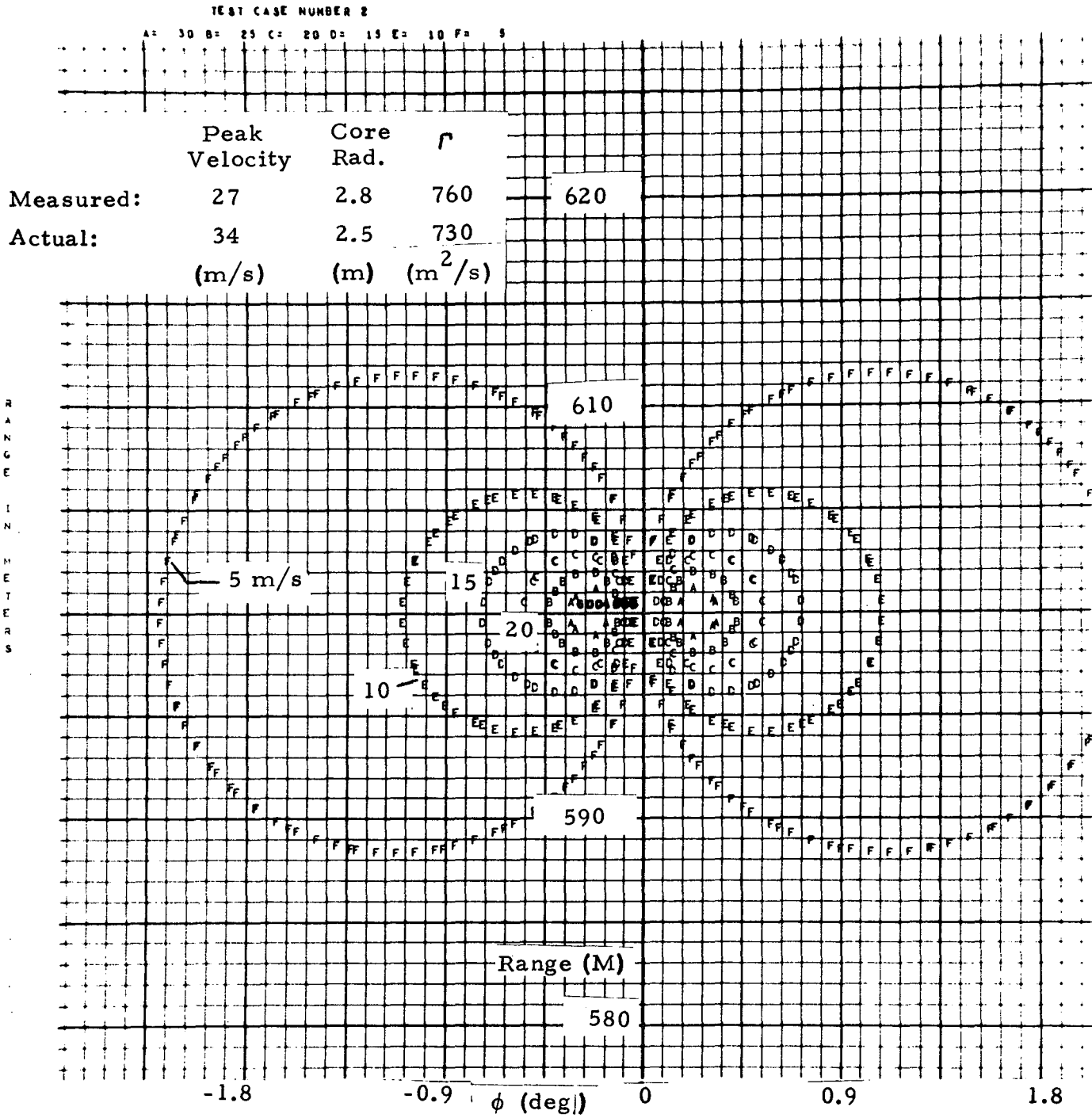


Fig. 4-8 - Contour Mapping of Velocities of Fig. 4-7

next fitted by a quadratic least squares curve to determine the peak velocity of the vortex for all ranges. This curve is differentiated as before to determine the peak.

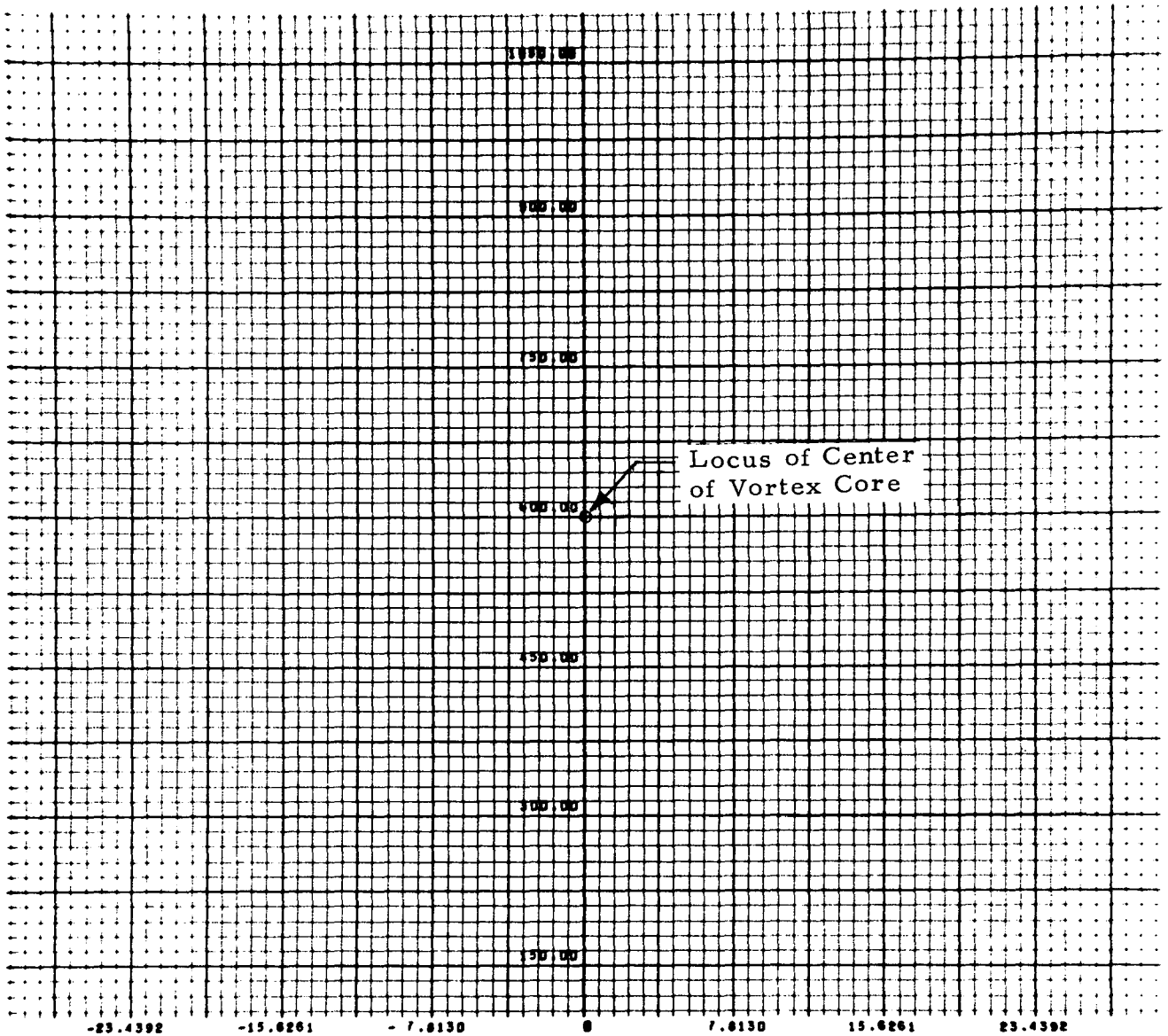
After the peak velocities within the vortex are determined (one positive peak and one negative peak), the computer determines the diameter of the vortex core (distance between these peaks) and the locus of the core center. The computer next determines the vortex velocity at a point,  $2\frac{1}{2}$  radii from the vortex center ( $2\frac{1}{2}$  radii arbitrarily chosen to provide velocity data from the region of low velocity gradients), and multiplies this value by  $2\pi r$  where  $r$  is the distance from the center of the vortex to the point. This provides the circulation. (In a real-world situation the velocities should be integrated along a line integral at some radius,  $r$ , to accurately determine the vortex circulation.)

Figure 4-9 is a map of the loci of the centers of the vortices in the example case of one vortex). The peak velocities, core radii and circulations, both actual and as detected, are displayed along the bottom of the figure.

#### 4.4 IMPLEMENTATION OF A HYBRID SYSTEM

Personnel at NASA (Ref. 27) have been statistically studying the effects of varying spatial resolution upon the probability of predicting the vortex position accurately enough for hazard avoidance. The preliminary results of these studies have indicated that a spatial resolution of approximately 40 meters is adequate. From Fig. 3-3 it can be seen that a one-half meter diameter coaxial focused optical configuration will provide a spatial resolution of 40 meters at a range of 600 meters (~2000 feet). If this spatial resolution proves to be adequate, the hybrid system could be constructed around state-of-the-art one-half meter diameter coaxial sensors with minimum of development costs. Scanning systems to perform scans similar to those required for the hybrid system are presently being fabricated by Lockheed and NASA. NASA is planning to have data processing equipment designed and fabricated in the near future which would be very similar to that required for the hybrid system.

TEST CASE NUMBER 2



Detected:

VORTEX (0) HAS A PEAK VELOCITY OF  $2.6 \times 10^{+01}$  M/SEC WITH A CORE RADIUS OF  $2.8 \times 10^{+00}$  M AND A CIRCULATION OF  $7.6 \times 10^{+02}$  MH/SEC

Actual:  $3.4 \times 10^{01}$  m/sec       $2.5 \times 10^{00}$  m       $7.3 \times 10^{02}$  m<sup>2</sup>/sec

Fig. 4-9 - Comparison of Detected and Actual Data

Because of these present NASA efforts, the development costs for the hybrid system would be primarily devoted to system integration and hardware reliability.

#### 4.5 WIND SHEAR AND TURBULENCE MONITORING AS A BY-PRODUCT OF HYBRID (AND PROBABLY DETECTIVE) SYSTEMS

Wind shear in approach corridors has become a problem of increasing interest to pilots in the past few years. An example of this problem from Ref. 30 is illustrated below.

"During a two-hour period on 4 January 1971 there were nine missed approaches to runway 4R at JFK. Included in the missed approaches were B-747s, B-727s, a B-707, a C-990, and a DH-6. During this same period an accident occurred at LaGuardia Airport where one of the probable causes was stated as 'The failure of the pilot to recognize the wind shear condition and compensate for it.'" (Ref. 30).

The conical scan configuration of Fig. 4-3b would provide wind profiles to 2000 feet. Wind shears of interest and concern to approaching pilots lie in this region. Thus, a logical by-product output of the hybrid system would be a wind shear forecast from the wind shear observation. The instrument would be readily available. The effort to develop such a by-product would be devoted to processing the LDV sensor output to provide a suitable format for display to ATC and/or approaching pilots.

## Section 5 CONCLUSIONS

When the need for a device (or system in this case) becomes recognized, a number of questions immediately arise. In the case of the wake turbulence monitoring system, some questions which arise are:

- Is a wake turbulence monitoring system feasible or within the near state of the art?
- Would a wake turbulence system be cost-effective to develop, operate, and maintain?
- What type system should be developed?
- What are the logical steps to develop the system?

These questions are considered in this conclusion. Attempts are made to answer those questions which are answerable at the conclusion of this limited study.

### 5.1 IS A WAKE TURBULENCE MONITORING SYSTEM FEASIBLE?

The studies performed by Lockheed-Huntsville have indicated that a wake turbulence monitoring system is feasible. In fact, two of the three types of systems conceived could be developed to field-operational status within two to four years, and the third, a more sophisticated system could probably be developed in three to six years. The first two types of the system would require a minimum of new technology and the third would require that concepts presently on the drawing boards be developed.

Safety is of concern in system feasibility. This is especially true when something as exotic in the public's eye as the laser is involved. Laser radiation in the wavelengths regime 0.4 to 1.4 microns is considered hazardous (Ref. 31) for ocular exposures of  $10^{-6}$  W/cm<sup>2</sup> and above. Laser radiation at 10.6

micron wavelength (far infrared) is considered hazardous (Ref. 21) for exposures of  $10^{-1}$  W/cm<sup>2</sup> and above, clearly five orders of magnitude more intense than the visible radiation hazard level. The wake turbulence monitoring system should be feasibly designed to maintain transmitted radiation levels well below the hazard level in order to assure safe operation in the air terminal environment.

## 5.2 WOULD A WAKE TURBULENCE SYSTEM BE COST EFFECTIVE ?

For a system to be cost effective, the benefits derived from the system should outweigh the costs to develop, operate and maintain the system. The benefits to be derived from such a system were outlined in the introduction to this report as well as projected dollar savings to airlines from reducing spacing behind "heavies." Increased revenues to terminals from increased capacity and thus increased landing fees were projected. An additional note was made of the approximately \$36M in litigations involving the Government in claims for wake turbulence-related accidents. The true benefits to be derived from the development and installation of wake turbulence monitoring systems is difficult to establish accurately because the capability of the system to increase terminal capacity, reduce delays and improve safety is not accurately known. Some of these values should be obtainable to a higher degree of accuracy if recommended computer simulation studies of the entire systems are performed. Some probably will not be accurately known until a prototype system is developed and operationally tested in the terminal for a reasonable period of time.

Table 5-1 presents a highly speculative picture of development prototype system costs. The dollars depicted could easily be misestimated by a factor of 50% in either direction. The costs were based upon developing one system to handle a set of parallel runways at a single air terminal. Costs for individual systems will be reduced for quantity production of the units.

A comparison of Fig. 1-2 of the report introduction with Table 5-1 indicates that over a period of several years the system should be quite cost effective. More accurate cost figures effectiveness will become available from additional development studies.

Table 5-1  
 PROJECTED DEVELOPMENT PROTOTYPE COSTS (in Thousands of Dollars)

Cost Items	Predictive	Hybrid (Medium Range)		Detective (Long ~ 10 km Range)	
		Single Sensor (1-D) Capability	Two-Runway Four Sensor (1-D) Capability	Single Sensor (1-D) Capability	Two-Runway Two-Component Capability
Development Costs	\$250	\$400	\$900	\$600	\$1,200
Equipment Costs					
CO <sub>2</sub> Lasers	\$0	\$40	\$160	\$40	\$160
Detectors	0	15	60	15	60
Preprocessors	0	15	60	30	100
Computer	75	25	75	50	125
Scanning Subsystem	0	5	20	25	55
Display	25	25	25	25	25
Misc. Hardware	<u>25</u>	<u>10</u>	<u>40</u>	<u>25</u>	<u>75</u>
Total Equipment Costs	\$125	\$125	\$440	\$210	\$600
Annual Operational Costs Including Maintenance	\$50		\$150		\$125

### 5.3 WHAT TYPE SYSTEM SHOULD BE DEVELOPED?

This report discusses three types of systems: predictive, detective and hybrid. The relative effectivenesses of the system configurations is discussed in the introduction and the relative expense and development time are listed in the table on page 1-14. The predictive and hybrid systems contain many of the same elements. The predictive system requires the least development time, but it is also least effective. A logical development path is to begin development of the predictive and hybrid systems simultaneously with the idea of installing the sensors of the hybrid system into the predictive system once they are developed. The development of the detective system could proceed at a normal rate. This approach would allow a system to be introduced — the predictive system — into field operation within the shortest possible time. The system could be updated to become a hybrid system with improved performance. The detective system could be introduced into field operation when it became available some time in the future.

Additional studies might indicate that either the hybrid or detective system should be developed, but not both. This limited study does not go into enough depth to make this determination possible.

### 5.4 WHAT ARE THE LOGICAL STEPS TO DEVELOP THE SYSTEM?

Steps to develop the system can be grouped according to the system — predictive, detective, or hybrid — to be developed. Some of these are listed below:

#### 5.4.1 Predictive System

##### ● Simulation Studies

- Develop mathematical model of predictive system.
- Determine flight path statistics of arriving and departing aircraft at specific air terminals.

- Introduce wind rose to system model to determine percentage of cases where separations could be reduced.

- Measurement Program

- Test prototype system at active air terminal.

- Equipment Development

- Develop display concept.
- Develop computer/sensors/display integration.

#### 5.4.2 Detective System

- System Simulations

- Simulate single-component sensor systems with ambient winds and turbulence.
- Simulate two-component sensor systems with ambient (cross) winds and turbulence.
- Simulate sensor systems with true axial velocities after experimental axial velocity data are available.
- Develop decision-making philosophy and simulate entire system including sensors, computer, and displays to determine system effectiveness.
- Determine the sizes of corridors into air terminals from flight path statistics of aircraft using these corridors.

- Measurement Programs

- Measure axial flow velocities of full-scale aircraft vortices with remote sensors.
- Experiment with a single-component laser Doppler velocimeter detecting vortices in an air terminal environment.
- Experiment with a two-component laser Doppler velocimeter detecting vortices in an air terminal environment.
- Determine LDV performance in inclement weather.

- Development Programs

- Develop MIL-Spec laser velocimeter hardware to meet high reliability standards.

#### 5.4.3 Hybrid System

- Simulation Studies

- Continue development of total system model including display, logic, etc.
- Continue development of model which performs overhead coarse and detail scans and calculates circulation, etc.
- Develop flight path statistics

- Measurement Program

- Setup single-component LDV system in terminal environment to perform hybrid-type scans during aircraft flybys; record and analyze data.
- Determine LDV performance in inclement weather.
- Perform conical scan with LDV to determine wind profile.

- Equipment Development

- Further develop system hardware to meet high reliability standards.

Section 6  
REFERENCES

1. Spreiter, John R., and Alvin H. Sacks, "The Rolling up of the Trailing Vortex Sheet and Its Effect on the Downwash Behind Wings," J. Aero. Sci., Vol. 18, No. 1, January 1951.
2. Luffsey, Walter S., and Nelson J. Miller, "Countering the Vortex Problem," presentation to Annual Assembly Meeting of Radio Technical Commission for Aeronautics, 19 September 1967.
3. Motion Pictures of Smoke Entrainment into Aircraft Trailing Vortices at Redstone Arsenal Airport," Aero-Astroynamics Laboratory, NASA-Marshall Space Flight Center, Huntsville, Ala., October 1969.
4. Batchelor, G.K., "Axial Flow in Trailing Line Vortices," J. Fluid Mech., Vol. 20, December 1964, pp. 645-658.
5. Garodz, Leo J., NAFEC, "Investigation of Jet Transport Aircraft System Descending into and Generated in Ground Effect," FAA Data Report, Project 504-303-03X (Special Task No. 2), November 1970.
6. Lamb, Sir Horace, Hydrodynamics, 6th ed. London; Cambridge University Press; New York, Dover Publications, Inc., 1945.
7. Squire, H.B., "The Growth of a Vortex in Turbulent Flow," Aero. Quart., Vol. 16, August 1965, p. 302 (also Brit. ARC 16,666, 1954).
8. Dee, F.W., and O.P. Nicholas, "Flight Measurements of Wingtip Vortex Motion Near the Ground," Brit. ARC CP1065, 1969.
9. Whetmore, Joseph W., and John P. Reader, "Aircraft Vortex Wakes in Relation to Terminal Operations," NASA TN D-1777, April 1963.
10. Squire, H.B., "Analysis of the Vortex Breakdown Phenomenon, Part 1," Aero Dept., Imperial College Report No. 102, Aeronautical Research Council 21977, 1960.
11. Ludwig, H., "Zur Erklarung der Instabilitat der uber angestellten Deltaflugeln auftretenden freien Wirbelkerne," z. Flugw., 1962, 10, 242. See Also: Explanation of Vortex Breakdown by the Stability Theory for Spiraling Flows," AVA-Bericht 64A14, 1964.
12. Jones, J.P., "The Breakdown of Vortices in Separated Flow," University of Southampton, USAA Report No. 140, 1960.

13. Crow, S. C., "Stability Theory for a Pair of Trailing Vortices," TR D1-82-0918, Boeing Scientific Research Laboratories, Seattle, Wash., Technical Report, September 1969.
14. Benjamin, T. Brooke, "Theory of Vortex Breakdown Phenomena," J. Fluid Mech., 1962, Vol. 14, No. 4, pp. 593-629.
15. Hall, M. G., "A New Approach to Vortex Breakdown," Proceedings of 1967 Heat Transfer and Fluid Mechanics Institute, University of California, LaJolla, 19-21 June 1967, pp. 319-340.
16. Harvey, J. K., "Some Observations of the Vortex Breakdown Phenomenon," J. Fluid Mech., 1962, Vol. 14, No. 4, pp. 585-592.
17. McGowan, William A., "Trailing Vortex Hazard," Society of Automotive Engineers, Paper No. 680220, presented at Business Aircraft Meeting, Wichita, Kans., 3-5 April 1968.
18. Hallock, J., and I. McWilliams, Transportation Systems Center, Private Communication, 1971.
19. Lawrence, T. R., et al, "A Laser Velocimeter for Remote Wind Sensing," Review of Scientific Instruments, Vol. 43, No. 3, March 1972.
20. Thomson, A., and M. C. Dorian, "Heterodyne Detector of Monochromatic Light Scattered from a Cloud of Moving Particles," CDC-ERR-AN-1090, General Dynamics/Convair, San Diego, Calif., June 1969.
21. Berkowitz, R. S., Modern Radar, John Wiley, Inc., N. Y., 1965.
22. Thomson, J. A., "Study of Conceptual and Operational Feasibility of Laser Doppler Detection Systems," Wayne State University Research Institute for Engineering Sciences, Detroit, Michigan, November 1970.
23. Wilson, D. J., et al, "Application of Laser Doppler Velocity Systems - Interim Report," LMSC-HREC D225028, Lockheed Missiles & Space Company, Huntsville, Ala., May 1971.
24. Kinnard, K. F., et al, "Development Study of a Three-Dimensional Laser Doppler System for the Measurement of Atmospheric Wind Velocity and Aircraft Trailing Vortices," LMSC-HREC D225613, Lockheed Missiles & Space Company, Inc., Huntsville, Ala., February 1972.
25. Schaffer, R. E., "Cockpit Equipment from Sperry Rand Engineering Review," Air Traffic Control, Part 2, Sperry Rand Corp., N. Y., N. Y., 1971.
26. Newman, B. G., "Flow in a Viscous Trailing Vortex," Aero. Quart., Vol. 10, 1959, pp. 149-162.

27. Jefferies, H. B., "System Requirement Matrix for an Airport Trailing Vortex Warning System," S&E AERO, MM-11-72 NASA-MSFC, Huntsville, Ala., 11 March 1972.
28. Gorstein, M., et al, "Aircraft Wake Vortex Sensing Systems," 71-FA-0, Annual Report, Systems Research and Development Service, DOT/FAA, Washington, D.C., June 1971.
29. Burnham, D., et al, "Vortex Sensing Tests at NAFEC," DOT-TSC-FAA-72-2, DOT/FAA, Washington, D.C., January 1972.
30. Kraus, K.A., "Aspects of the Influence of Low-Level Wind Shear on Aviation Operations," International Conference on Aerospace and Aeronautical Meteorology, Washington, D.C., May 1972.
31. Regulations for the Administration and Enforcement of the Radiation Control for Health and Safety Act of 1968, Public Health Service, HEW, March 1971.

Appendix A  
NUMERICAL VORTEX MODEL

A-1. (a)

Appendix A

A model was sought that would approximate the vortex flow fields generated by large transport aircraft. Consequently considerable emphasis was placed on recent flight investigations of vortex parameters using such aircraft, in particular those initiated as a result of priority action on the part of the Director, Flight Standards Services, in February 1970. Two of these investigations (Refs. 1 and 2) were concerned with aircraft response during vortex penetration while the third (Ref. 3) concerned itself with the measurement of vortex velocity profiles using tower-mounted hot wire anemometers. The latter study is the most applicable for the purposes of this investigation since the aircraft were operated in terminal-type configurations, and the vortices were monitored at altitudes of zero to several hundred feet above the ground. Such data, however, suffer from considerable scatter primarily because of the vortex not intersecting the location of the instrumentation, in most instances, through the center of the core. Consequently, considerable error exists in the estimation of core diameters and peak velocities. Figures 1 and 2 (obtained from Ref. 3) present values of peak tangential velocity versus vortex age and core diameter, respectively, for a variety of current airline transport aircraft.

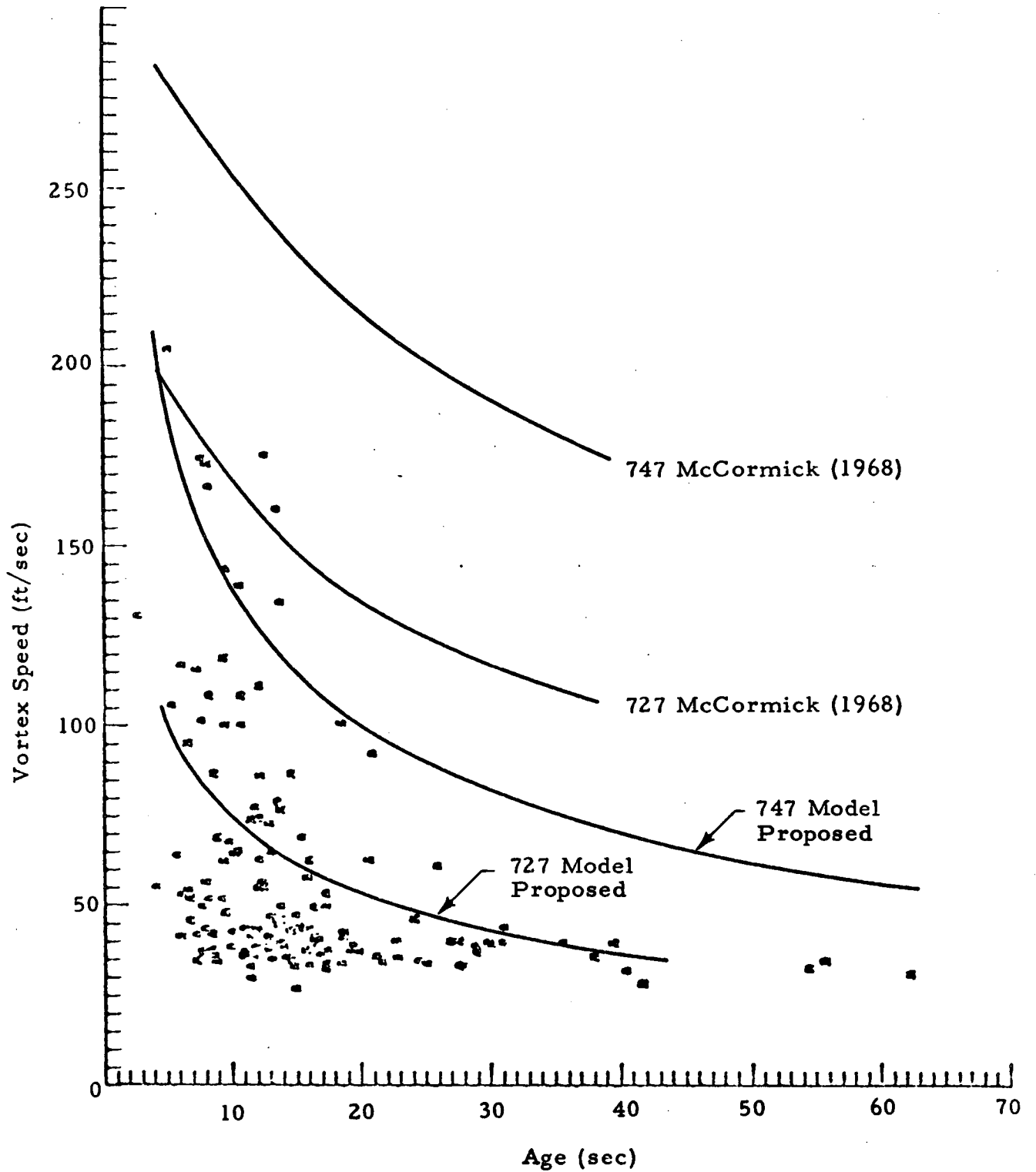


Fig. 1 - Summary of Peak Vortex Tangential Velocities vs Age for All Aircraft. Data from Various Models Superimposed (heavy lines)

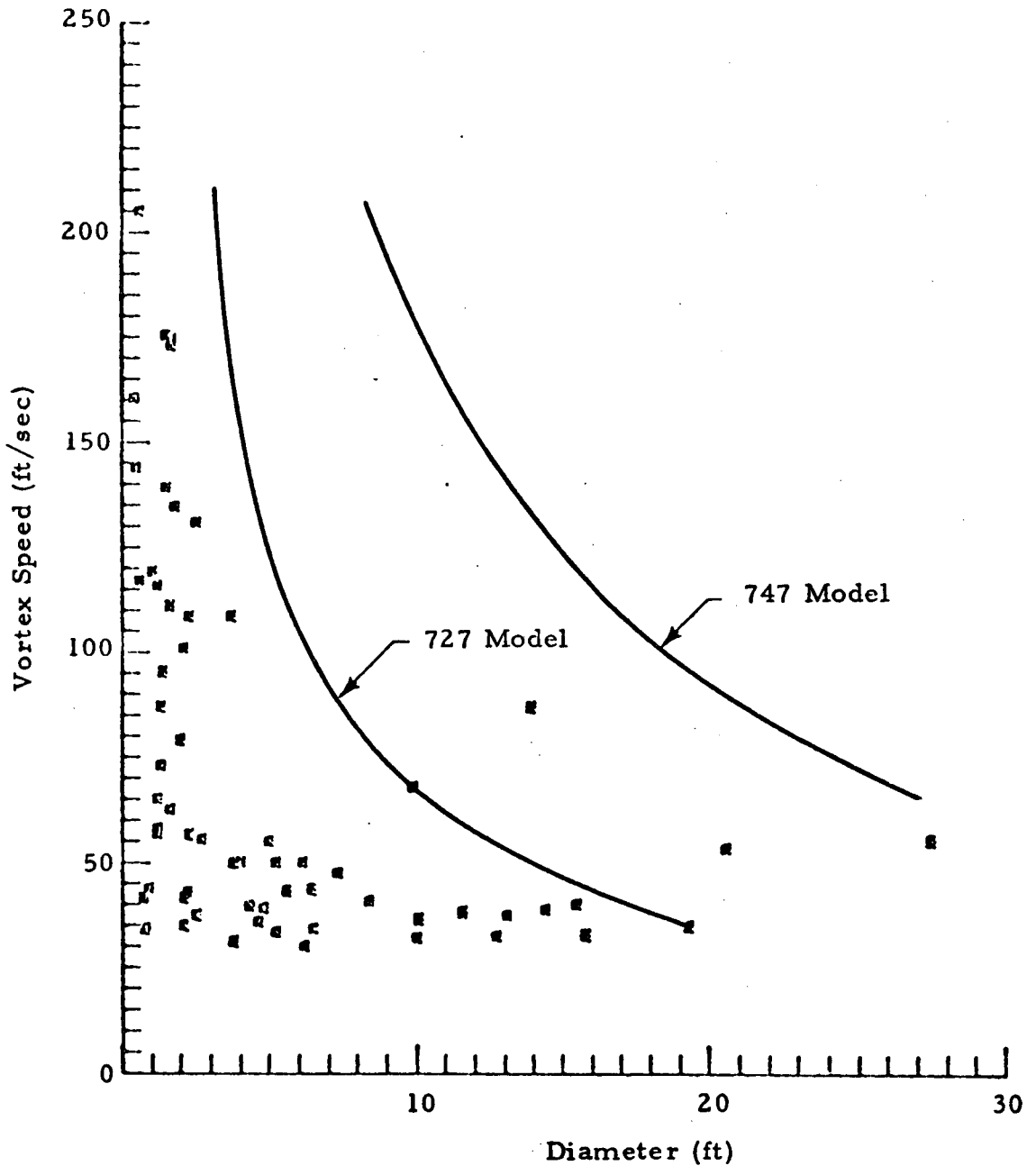


Fig. 2 - Summary of Peak Vortex Tangential Velocities vs Estimated Core Diameters for All Aircraft. Data from Proposed Model Superimposed (heavy lines)

The approach taken in the choice of a model was to choose from a comparison of the test data of Ref. 3 with various theoretical vortex models that predict both tangential and axial velocity components, that model which yields the most satisfactory agreement. Of particular interest is that of Ref. 5 which presents a numerical method for solving the equations for a vortex core. The technique solves the system of equations of motion for a steady axially symmetric spiraling motion of an incompressible fluid at large Reynolds number with the additional assumption of the boundary layer approximation. The results of an application of the technique to a trailing vortex are presented in Figs. 3 and 4, for a Boeing 727 and 747, respectively. Peak velocity magnitudes and vortex core diameters are in reasonable agreement with the data of Ref. 3 (summarized in Figs. 1 and 2).

Deficiencies in the model are the:

- Requirement of an assumption of an eddy viscosity, and
- Assumption of a set of starting conditions for the computation.

A value for the eddy viscosity is estimated from the correlation that exists between the circulation developed by the aircraft and the measured eddy viscosity coefficient deduced in Ref. 6 from various wind tunnel and flight investigations on vortex decay. Figure 5 graphically summarizes this correlation. The initial conditions for the computation were taken from the approximate theory of Newman (Ref. 7), which solves the linearized form of the set of equations used in the computational study of Ref. 5.

A comparison of the proposed model with various popular vortex models is given in Fig. 6, for a given set of conditions (a 727 at 1000 feet downstream of the aircraft).

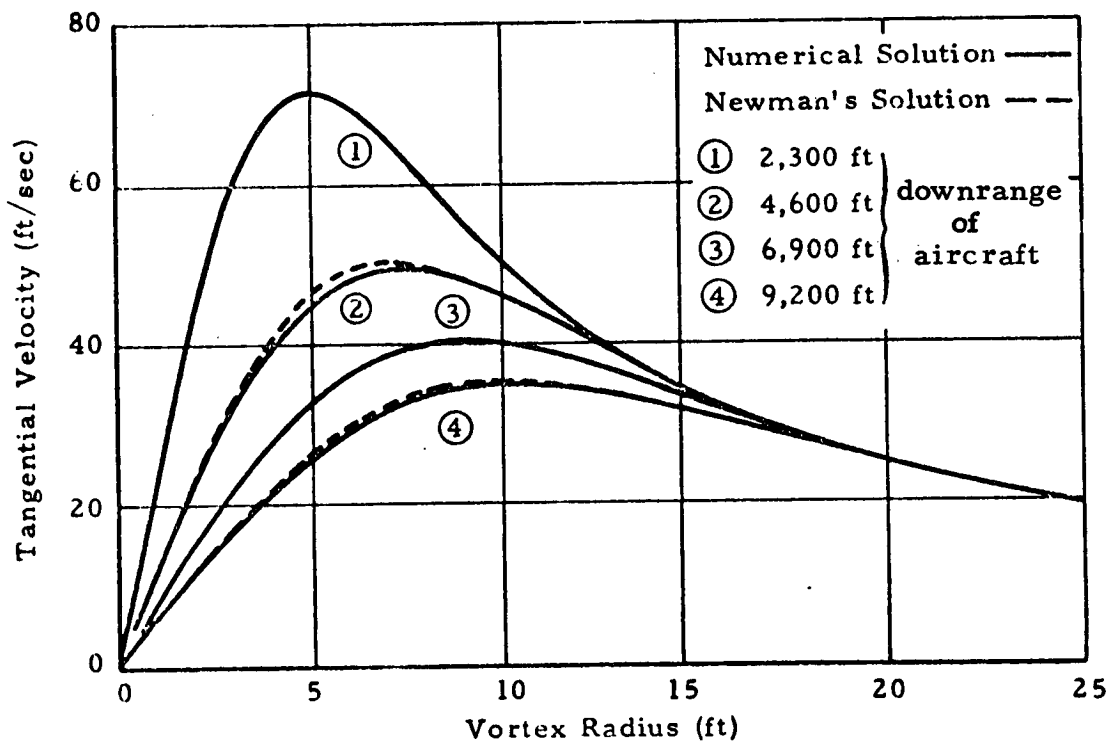
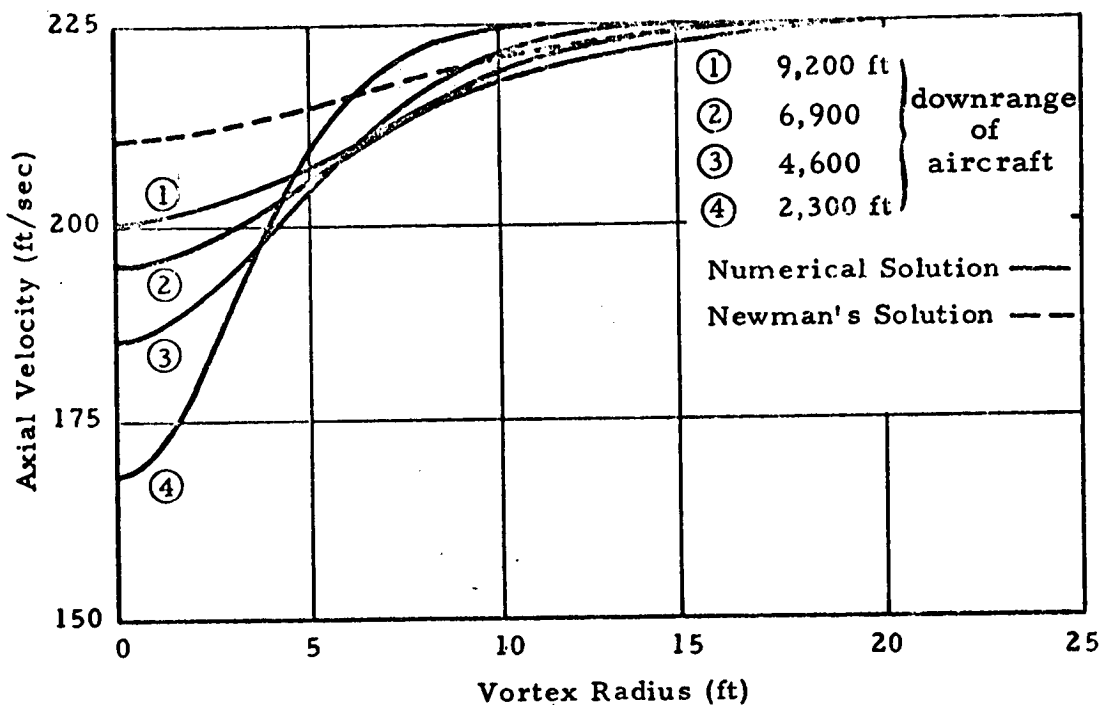
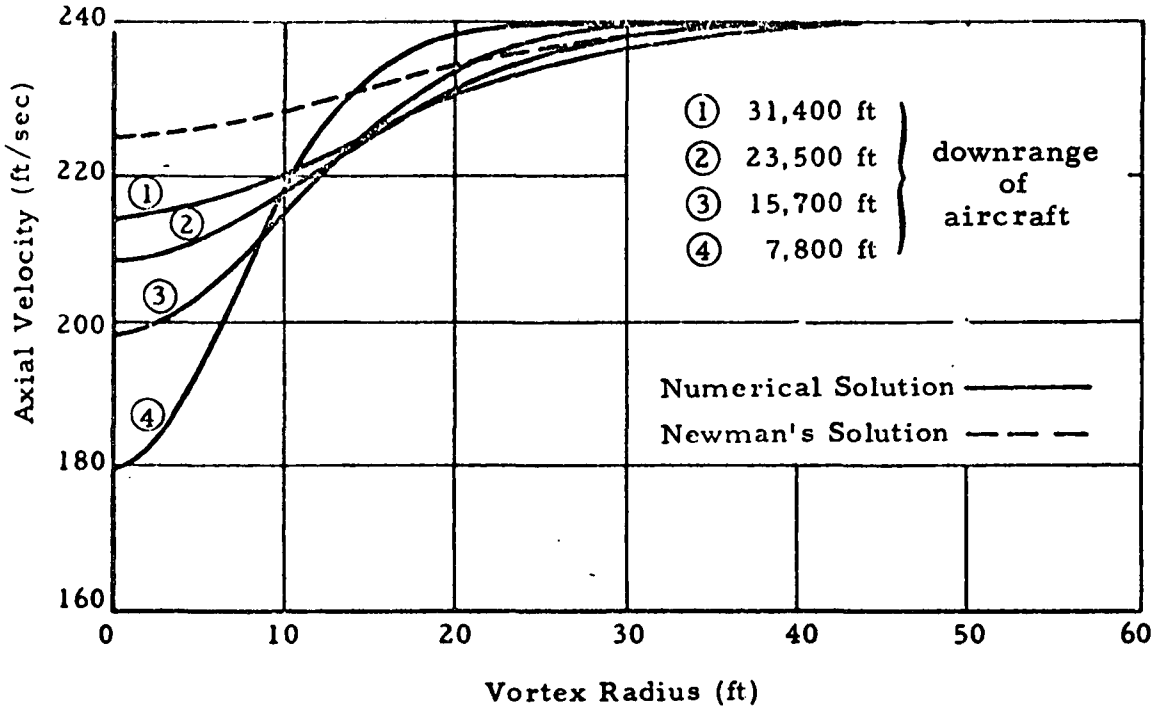
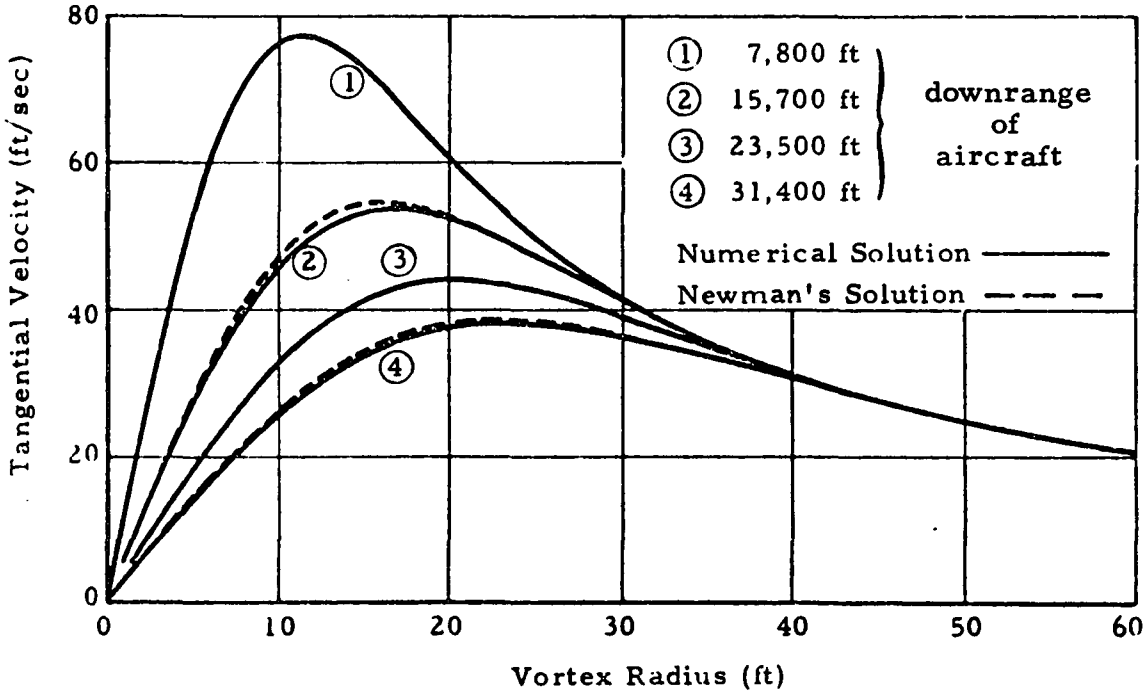


Fig. 3 - Boeing 727 Vortex Characteristics



Profiles of Axial Velocity in a Trailing Vortex



Profiles of Circumferential Velocity in a Trailing Vortex

Fig.4 - Boeing 747 Vortex Characteristics

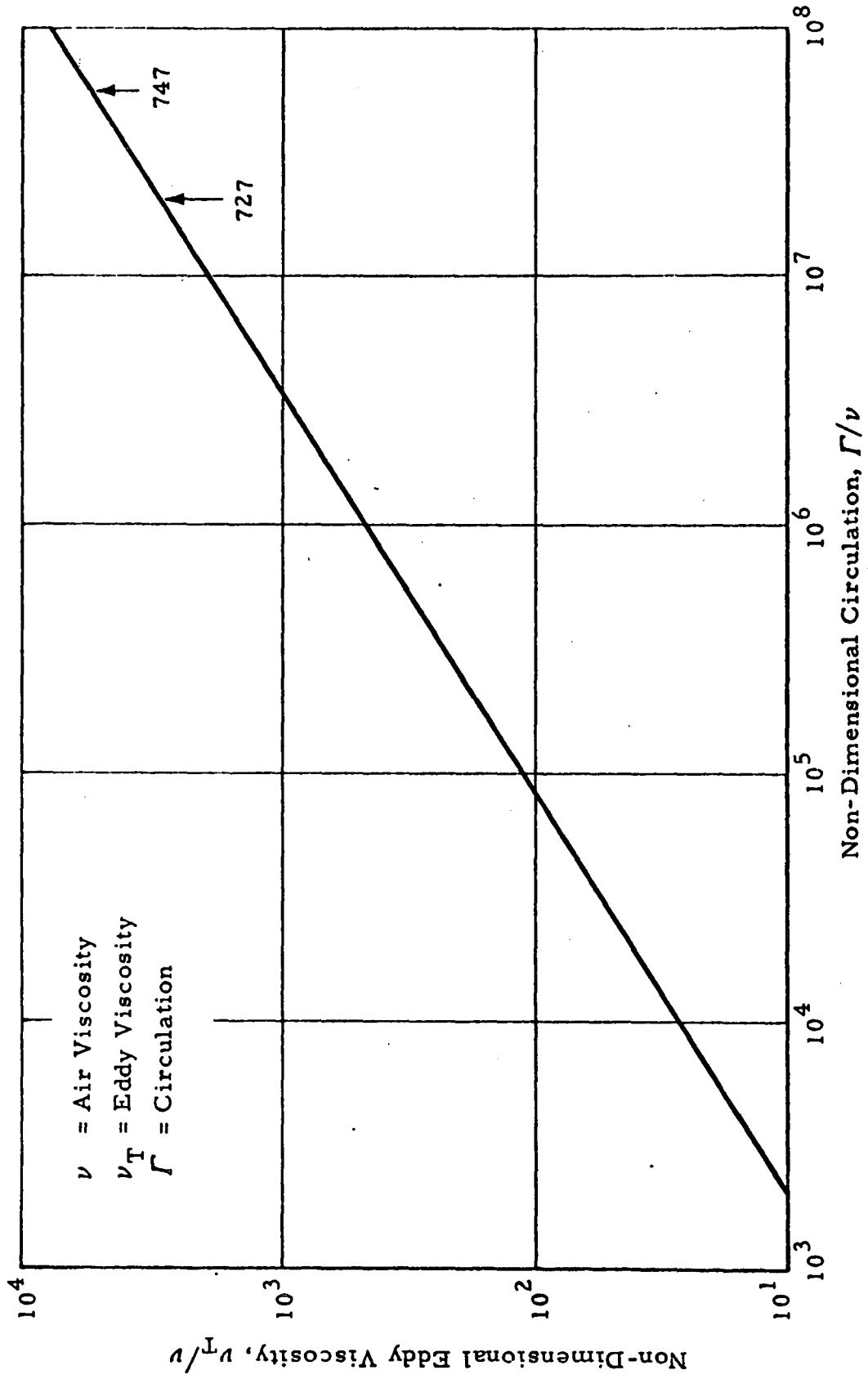


Fig.5 - Correlation Curve for Eddy Viscosity and Circulation

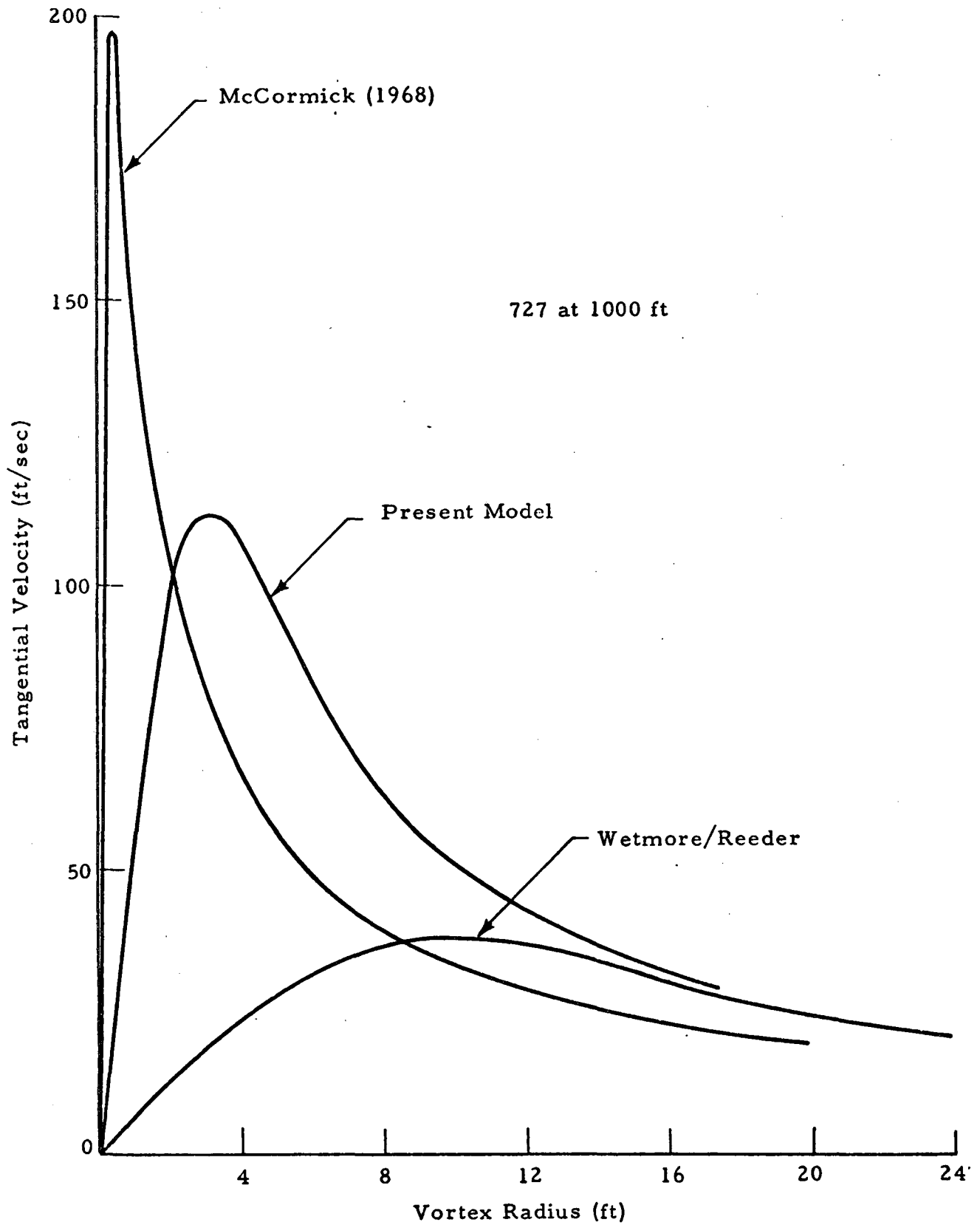


Fig. 6 - Comparison of Vortex Models

Appendix A  
REFERENCES

1. Andrews, William H., Glenn H. Robinson, Gary E. Krier, and Fred J. Drinkwater, "Flight Test Evaluation of the Wing Vortex Generated by Large, Jet Transport Aircraft," NASA FWP 18, April 1970.
2. Condit, Philip M., "Results of the Boeing Wake Turbulence Test Program," Boeing Document No. D6-30851, April 1970.
3. Garodz, Leo J., NAFEC, "Investigation of Jet Transport Aircraft Vortex System Descending into and Generated in Ground Effect," FAA Data Report, Project 504-303-03X (Special Task No. 2), November 1970.
4. McCormick, B. W., "Aircraft Wakes: A Survey of the Problem," presented at FAA Symposium on Turbulence, Washington, D. C., 22-24 March 1971.
5. Hall, M. G., "A Numerical Method for Solving the Equations for a Vortex Core," R&M No. 3467.
6. Owen, P. R., "The Decay of a Turbulent Trailing Vortex," Aero. Quart., February 1970.
7. Newman, B. G., "Flow in a Viscous Trailing Vortex," Aero. Quart. Vol. 10, 1959, pp. 149-162.

Appendix B  
LASER VELOCIMETER VOLUME SCAN  
SIMULATION PROGRAM

B-1 (a)

Appendix B

## B.1 DESCRIPTION

Program simulates one vortex and scans it with one laser velocimeter. Output is air velocity as a function of position.

## B.2 CAPABILITIES

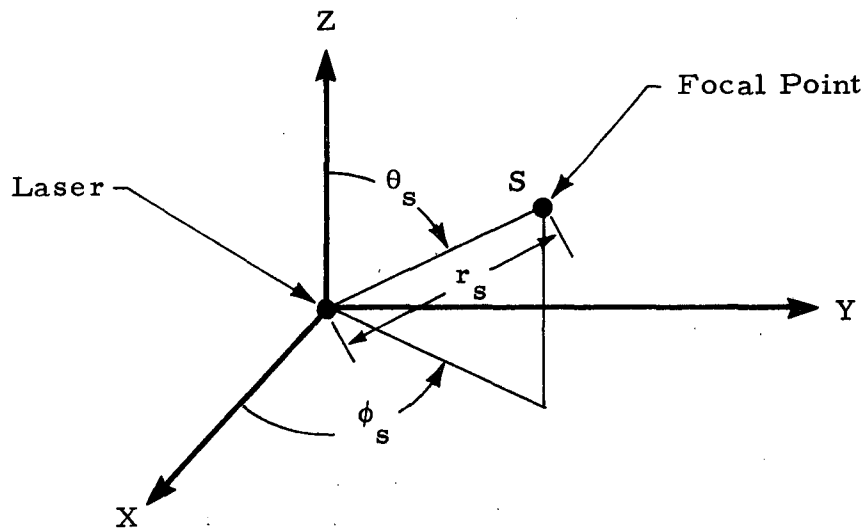
1. Vortex can be in any position.
2. Velocimeter can scan any size volume in any direction.
3. The tangential and axial velocity profile of the vortex can be input with different values.
4. For focus system aperture size can be selected; for pulse system pulse length can be selected.

## B.3 RESTRICTIONS

1. No wind exists.
2. Aerosol is assumed to be constant throughout the vortex.
3. The vortex is assumed to be uniform along its length.
4. The vortex core is assumed to be a straight line.
5. No change in vortex position or strength is allowed with change in time.
6. Infinite signal-to-noise (S/N) ratio is assumed.

## B.4 SPHERICAL COORDINATE SYSTEM OF LASER

The laser's focal point orientation is represented in a spherical coordinate system centered at the laser.



The transformation from the spherical coordinate system to the laser's rectangular coordinate system is

$$X_s = r_s \sin\theta_s \cos\phi_s$$

$$Y_s = r_s \sin\theta_s \sin\phi_s$$

$$Z_s = r_s \cos\theta_s$$

#### B.5 SCANNING OF LASER

The bounds on the scan are input

$\phi_{s1}$  lower bound of  $\phi_s$

$\phi_{s2}$  upper bound of  $\phi_s$

$\theta_{s1}$  lower bound of  $\theta_s$

$\theta_{s2}$  upper bound of  $\theta_s$

$r_{s1}$  lower bound of  $r_s$

$r_{s2}$  upper bound of  $r_s$

Also input are the number of equal divisions for each of the above intervals.

The scanning starts at the lower bound of each parameter. The simulated sensor first scans across  $\phi_s$  then moves along  $\theta_s$  while it continues to scan  $\phi_s$  and finally it moves along  $r_s$  while still scanning  $\phi_s$  and  $\theta_s$ . For each point of the scan the simulation computes the velocity component of the vortex in the direction of the laser.

#### B.6 COMPUTATION OF TANGENTIAL VELOCITY COMPONENT OF VORTEX IN DIRECTION OF LASER

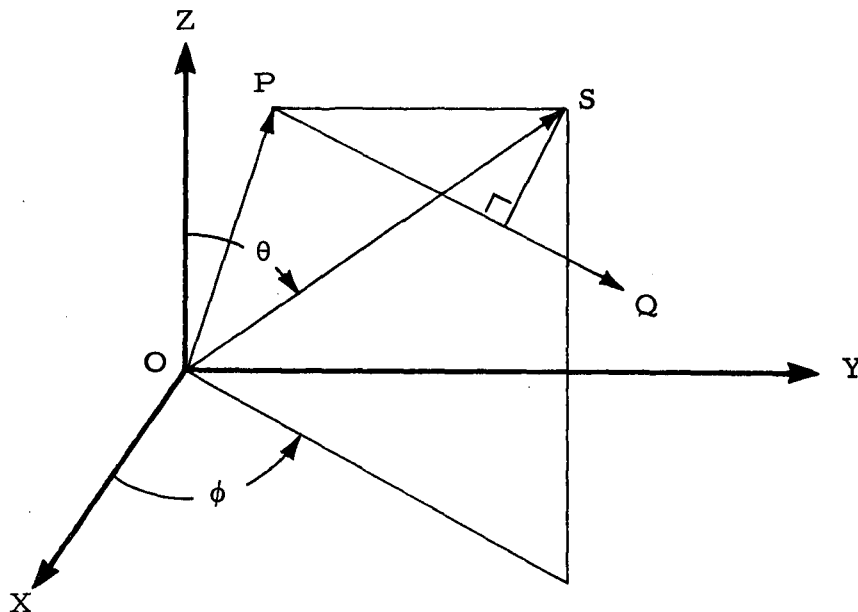
First the focal point of the laser is transformed from the spherical system to the rectangular system.

$$X_s = r_s \sin\theta_s \cos\phi_s$$

$$Y_s = r_s \sin\theta_s \sin\phi_s$$

$$Z_s = r_s \cos\theta_s$$

$$\overrightarrow{OS} = (X_s, Y_s, Z_s) \text{ focal point in laser's rectangular system}$$



$\overline{OP} = (X_1, Y_1, Z_1)$  point on vortex core axis (input)

$\overline{PQ} = (A, B, C)$  direction of vortex axis (input)

Distance from S to  $\overline{PQ}$  is  $D = \frac{|\overline{SP} \times \overline{PQ}|}{|\overline{PQ}|}$

where

$$\overline{SP} = \overline{OP} - \overline{OS}$$

Total tangential velocity magnitude of the vortex at point S, according to Newman\*

$$V_T = \frac{\Gamma_o}{2\pi D} \left[ 1 - \exp\left(-\frac{W_\infty D^2}{4\nu z}\right) \right]$$

where

$V_T$  is normal of tangential velocity

$\Gamma_o$  is circulation

$W_\infty$  is freestream velocity

$\nu$  is eddy viscosity

$z$  is vortex axial coordinate (input value is presently being used for all positions)

$$\Gamma_o = \frac{4W}{\pi \rho V b}$$

$$W_\infty = V$$

$$\nu = k\mu/\rho$$

\*Newman, B.G., "Flow in a Viscous Vortex," Aeronaut. Quart., Vol. X, May 1959, p. 149.

where

- W is total aircraft weight
- $\rho$  is density of atmosphere
- V is aircraft velocity
- b is wing span
- $\mu$  is coefficient of viscosity
- k is coefficient that relates laminar kinematic viscosity to eddy viscosity for a particular  $\Gamma_o$

The tangential velocity vector at S is

$$\vec{VT} = V_T \frac{(\vec{SP} \times \vec{PQ})}{|\vec{SP} \times \vec{PQ}|}$$

The magnitude of the component of  $\vec{VT}$  in the direction of  $\vec{SO}$  is

$$V = - \frac{\vec{VT} \cdot \vec{OS}}{|\vec{OS}|}$$

#### B.7 COMPUTATION OF AXIAL VELOCITY COMPONENT OF VORTEX IN DIRECTION OF LASER

The magnitude of the axial flow component, according to Newman, is

$$V_A = \frac{D_o}{4\pi \rho \nu z} \exp\left(-\frac{W_\infty D^2}{4 \nu z}\right)$$

where

- $V_A$  is norm of axial velocity
- $D_o$  is profile drag of the generating aerofoil

The axial velocity vector at S is

$$VA = \vec{V}_A \frac{\vec{PQ}}{|\vec{PQ}|}$$

B.8 COMPUTATION OF VELOCITY INTERPRETED BY A COAXIAL FOCUSED LASER DOPPLER SYSTEM

The laser does not make a point measurement. It effectively samples a finite volume of space along a line and consequently observes a variety of velocities. The signal is the strongest from the focal point and tapers off as the elemental volume considered increases its distance from the focus.

The power contained in the photo-detector due to N particles per cubic centimeter is proportional to the current squared, as shown in the following equation\*.

$$i^2 = \frac{1}{4} \pi \eta^2 \alpha^2 \sigma R^4 A^4 N \int_0^\infty \frac{dL}{L^2 + \frac{\pi^2 R^2}{\lambda^2 f^2} (f-L)^2}$$

where

$\eta$  is the quantum efficiency (electrons/photon)

$\alpha$  is power level of local oscillator

$\sigma$  is backscattering coefficient of particle

R is radius of transmitter lens

$A^2$  is total transmitted light flux in photons/sec

N is effective number of identical particles per (cm)<sup>3</sup>

f is nominal range of focusing

$\lambda$  is optical wavelength

L is range from transmitter lens

The current squared due to an infinitesimal unit of length dL is

$$\frac{di^2}{dL} = \left( \frac{1}{4} \pi \eta^2 \alpha^2 \sigma A^4 N \right) \frac{R^4}{L^2 + \frac{\pi^2 R^2}{\lambda^2 f^2} (f-L)^2}$$

\*This is Eq. A.8 on page A-6 of the Interim Report for Contract NAS8-25921, "Application of Laser Doppler Velocity Systems."

let  $\Delta L = \lambda L f / \pi R^2$ , then

$$\frac{di^2}{dL} = \left( \frac{1}{4} \pi \eta^2 \alpha^2 \sigma A^4 N \right) \frac{R^4}{\left( 1 + \frac{(f-L)^2}{\Delta L^2} L^2 \right)}$$

assume  $\eta, \alpha, \sigma, A, N$  are constants and let  $K_1 = 1/4 \pi \eta^2 \alpha^2 \sigma A^4 N$ , then

$$\frac{di^2}{dL} = K_1 \frac{R^4}{\left( 1 + \frac{(f-L)^2}{\Delta L^2} L^2 \right)}$$

This is proportional to the equation used in the program.

$$\frac{di^2}{dL} \approx I_n = \left( \frac{\psi_0 \pi}{\lambda} \right)^2 \frac{R^4}{\left( 1 + \frac{(f-L)^2}{\Delta L^2} L^2 \right)}$$

where  $(\psi_0 \pi / \lambda)^2$  is a constant.

Therefore, the equation in the program is proportional to the power in the detector due to a volume of space having an infinitesimal unit of length in the line of sight direction from the detector.

In this program only the interval  $(f - \Delta f, f + \Delta f)$  along the line of sight of the laser is considered.

$$\Delta f = 2\lambda f^2 / \pi R^2$$

This interval provides 50% of the signal\*. Within this interval a finite number of equally spaced points is sampled. The velocity at each point ( $V_n$ ) is multiplied times the weighting function ( $I_n$ ) at that point; these points are then summed and divided by the sum of the weighting factors.

$$V_L = \frac{\sum_{n=1}^N V_n I_n}{\sum_{n=1}^N I_n}$$

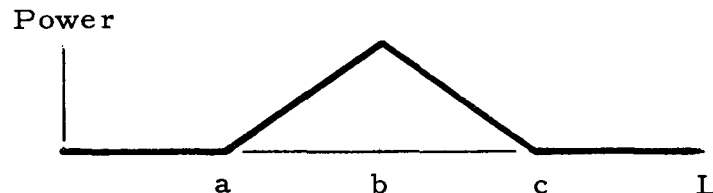
This  $V_L$  function thus provides an LDV system output which is weighted according to a calculated system spatial resolution. This type weighting function provides a data output similar to that which was recorded by using the spectrum analyzer where the one-dimensional LDV was field tested.

B.9 COMPUTATION OF VELOCITY INTERPRETED BY A COAXIAL PULSED LASER DOPPLER SYSTEM

The transmitted pulse is assumed to be a square wave. The detector is open for the same length of time as that of the transmitter; therefore, a pulse of length equal to the transmitted pulse enters the detector.

The pulse length is also assumed to be short relative to the distance to the volume being observed. Therefore, the detected power of an elemental volume is directly proportional to the length of time its illumination passes into the detector.

The power going into the detector relative to time is a square wave. But as a function of location of elemental volume, the curve looks like



\*Page 3-2 of the Interim Report.

"b" is the center of the pulse when the incoming pulse and the outgoing pulse exactly coincide. At this instant of time "a" is the back of the outgoing pulse and "c" is the front of the outgoing pulse. Figure B-1 shows the outgoing and incoming pulses passing each other. The power curve shown above is then the weighting function ( $I_n$ ) as in the focused case and  $V_L$  is computed the same way.

B.10 INPUT FOR LASER VELOCIMETER SIMULATION PROGRAM

There are two sections of input of which the first is by way of namelist. The name of the namelist is (INPUT) and it has the following variables:

<u>Name</u>	<u>Unit</u>	<u>Description</u>
GAMMAC	N-m-sec/kg	circulation of vortex from generating aircraft
W8	m/sec	freestream velocity
UNU	m <sup>2</sup> /sec	eddy viscosity
Z	m	downstream distance of vortex from generating aircraft
OP(3)	m	position vector of a point on the vortex axis
PW(3)	m	direction vector for vortex
PHI1	deg	starting PHI for sweep in PHI
PHI2	deg	final PHI for sweep in PHI
NPHI	—	number of evenly spaced PHI
THETA1	deg	starting THETA for sweep in THETA
THETA2	deg	final THETA for sweep in THETA
NTHETA	—	number of evenly spaced THETA in sweep
DIST1	m	starting range for sweep in range
DIST2	m	final range for sweep in range
NDIST	—	number of evenly spaced ranges in sweep
PSI	—	control magnitude of weighting factor. Set to one.

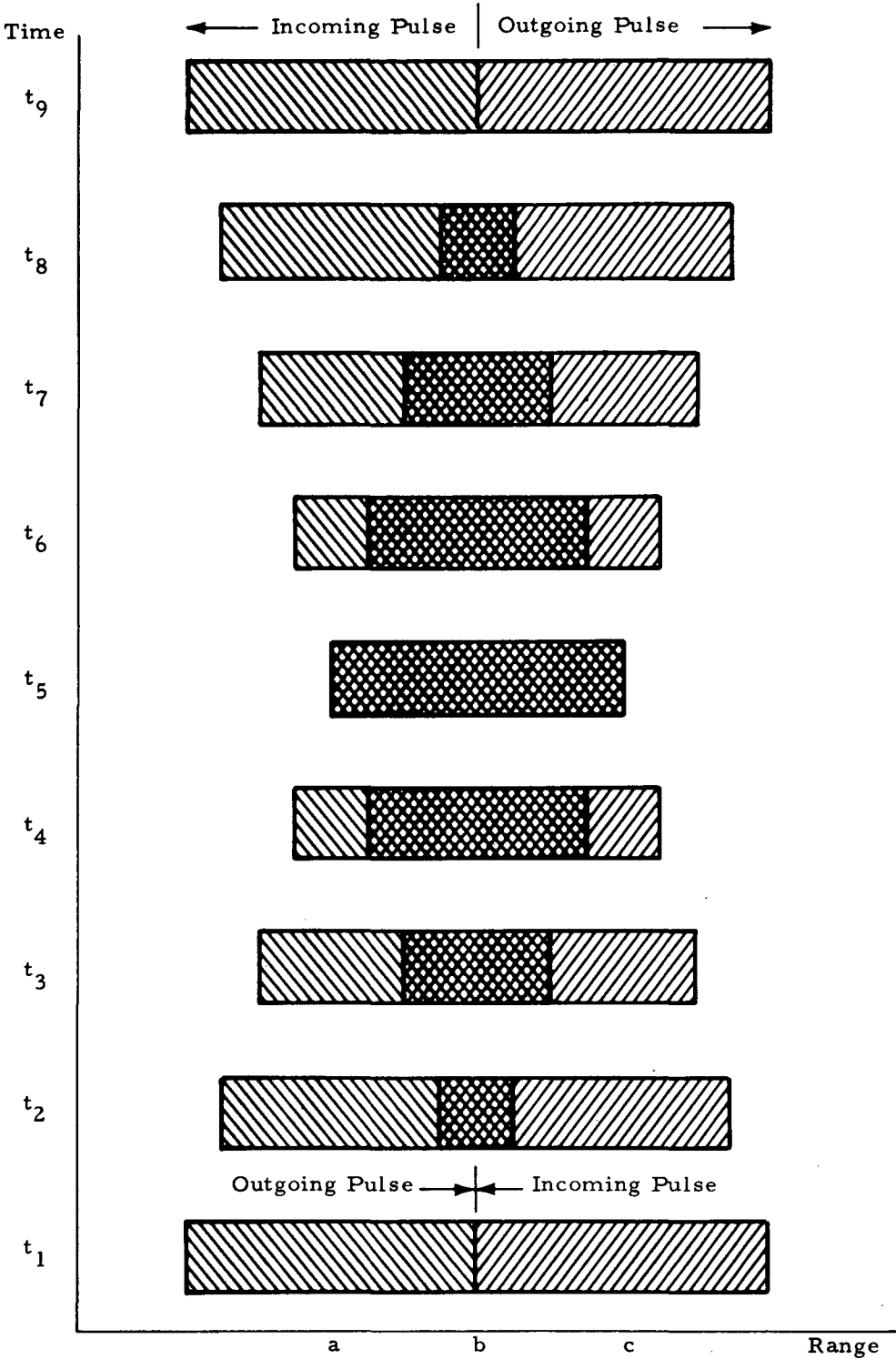


Fig. B-1 - Schematic of Outgoing and Incoming Pulses

<u>Name</u>	<u>Units</u>	<u>Description</u>
R	m	radius of telescope aperture
FLAMDA	m	wave length of laser light
PLENGT	m	pulse length
DZERO	N	profile drag of the aerofoil (Used for axial velocity. If no axial velocity wanted, set DZERO to zero.)
RHO	kg/m <sup>3</sup>	density of atmosphere
ICHOIC	—	flag for the following ICHOIC = 1 for focused continuous wave laser ICHOIC = 2 for a non-focused pulsed laser ICHOIC = 3 for perfect velocity detection
NWEIGH	—	half the number of evenly spaced points used in the illuminated volume for weighting
IOUT	—	flag for the printed output IOUT = 1 for no printed output IOUT = 2 for printing only velocity specified by IPLOT 1 IOUT = 3 for printing all velocities
IPLOT	—	flag IPLOT = 0 no SC4020 plots IPLOT = 1 SC4020 plots
IPLOT 1	—	flag indicates which velocities are to be plotted IPLOT 1 = 1 plots centroid of weighted velocity IPLOT 1 = 2 plots max-min or max (ΔBS(VL)) as specified by IVMAX IPLOT 1 = 3 plots total line of sight velocity at focus or at center of pulse volume

<u>Name</u>	<u>Units</u>	<u>Description</u>
IPLOT 1	—	IPLOT 1 = 4 plots line of sight component of tangential velocity at focus or at center of pulse volume
		IPLOT 1 = 5 plots line of sight component of axial velocity at focus or at center of pulse volume
		IPLOT 1 = 6 plots normal of vortex velocity vector at focus or at pulse center
		IPLOT 1 = 7 plots normal of tangential velocity vector at focus or at pulse center
		IPLOT 1 = 8 plots normal of axial velocity vector at focus or at pulse center
IVMAX	—	flag IVMAX = 0 program computes maximum minus minimum of line of sight velocity within the focal volume or within the pulse IVMAX = 1 program computes the absolute maximum of the line of sight velocities within the focal volume or within the pulse

The second input is for the plotting control. Each card for this input controls a group of plots. There are three variables input on each card, which are:

1. Column 10      0    for no lines between plotted points  
                      1    for lines between plotted points
2. Column 20      1    indicates PHI will be plotted on the horizontal axis  
                      2    indicates THETA will be plotted on the horizontal axis  
                      3    indicates RANGE will be plotted on the horizontal axis

- 3. Column 30      1      indicates PHI will be plotted on the vertical axis
- 2      indicates THETA will be plotted on the vertical axis
- 3      indicates RANGE will be plotted on the vertical axis

A blank card terminates the plotting and returns control to the beginning of the program for another case.

**B.11    OUTPUT FOR LASER VELOCIMETER VOLUME SCAN SIMULATION PROGRAM**

The input is printed on the printer and, in the case where plots are prouddced, the input is also printed on the plotter. This is shown in Fig. B-2.

```

                                NAMELIST (INPUT)

GAMMAC = 0.72900000E 03    W0        = 0.77300000E 02    UNV        = 0.91400000E-01    Z            = 0.10000000E 04
OP (1)  = 0.00000000E-30    OP (2)  = 0.00000000E-30    OP (3)  = 0.50000000E 02
P0 (1)  = 0.10000000E 01    P0 (2)  = 0.00000000E-30    P0 (3)  = 0.00000000E-30
PHI1    = 0.30000000E 01    PHI2    = -0.30000000E 01    NPHI     =        11
THETA1  = 0.48000000E 02    THETA2  = 0.41999995E 02    NTHETA   =        11
DIST1   = 0.69000000E 02    DIST2   = 0.71000000E 02    NDIST    =        11
PSI     = 0.10000000E 01    R        = 0.76200000E-01    FLAMDA   = 0.10600000E-04    FLENGT   = 0.00000000E-30
DZERO   = 0.50000000E 05    RHO     = 0.11920000E 01    ICHOIC   =        1            NWEIGH    =        12
IOUT    =        3            IPLOT    =        1            IPLOT1   =        1            IVMAX    =        1
    
```

Fig. B-2 - Example for Volume Scanning Program

The printer output of the velocities is controlled by the input variable IOUT. Figure B-3 is an example where IOUT = 3. In this figure

Distance = 70 represents the range of the focal point for the following measurements.

The numbers following (PHI =) represent the scan angle PHI in degrees for the measurements in the column below the angle.

	PHI =	3.0	2.4	1.8	1.2	0.6	-0.0	-0.6	-1.2	-1.8	-2.4	-3.0
THETA 48.0		-14.3	-14.6	-14.7	-13.5	-11.0	-7.1	-2.3	2.6	6.9	9.9	11.7
DVL		26.8	31.4	35.4	37.0	34.5	27.1	16.1	4.8	8.8	14.1	17.7
VL		-13.3	-12.9	-11.8	-9.9	-7.0	-3.3	0.8	4.8	8.1	10.5	12.0
VTL		-12.6	-11.7	-10.0	-7.3	-3.9	0.0	3.9	7.3	10.0	11.7	12.6
VAL		-0.7	-1.2	-1.9	-2.6	-3.1	-3.3	-3.1	-2.6	-1.9	-1.2	-0.7
V		27.1	28.9	30.5	31.6	32.3	32.6	32.3	31.6	30.5	28.9	27.1
VT		27.1	28.9	30.4	31.4	32.1	32.3	32.1	31.4	30.4	28.9	27.1
VA		0.9	1.6	2.5	3.4	4.1	4.4	4.1	3.4	2.5	1.6	0.9
RADIUS		4.2	3.8	3.6	3.3	3.2	3.2	3.2	3.3	3.6	3.8	4.2
THETA 47.4		-16.5	-17.3	-17.5	-16.5	-13.8	-9.3	-3.7	2.1	7.2	10.8	12.9
DVL		27.5	32.0	35.7	37.0	34.2	26.9	16.0	4.7	8.7	14.0	17.8
VL		-16.4	-16.5	-15.9	-14.0	-10.8	-6.3	-1.1	4.2	8.6	11.8	13.7
VTL		-15.0	-14.2	-12.2	-9.1	-4.9	0.0	4.9	9.1	12.2	14.2	15.0
VAL		-1.4	-2.4	-3.6	-4.9	-5.9	-6.3	-5.9	-4.9	-3.6	-2.4	-1.4
V		29.4	31.4	33.0	34.1	34.8	35.0	34.8	34.1	33.0	31.4	29.4
VT		29.3	31.2	32.6	33.5	33.8	33.9	33.8	33.5	32.6	31.2	29.3
VA		1.8	3.2	4.9	6.7	8.1	8.6	8.1	6.7	4.9	3.2	1.8
RADIUS		3.8	3.4	3.1	2.8	2.7	2.6	2.7	2.8	3.1	3.4	3.8
THETA 46.8		-18.6	-19.8	-20.3	-19.3	-16.4	-11.5	-5.1	1.5	7.3	11.5	13.9
DVL		28.2	32.5	35.9	36.9	33.9	26.5	15.8	4.7	8.6	13.9	17.9
VL		-19.9	-20.9	-21.0	-19.5	-16.0	-10.6	-4.0	2.7	8.6	12.8	15.2
VTL		-17.6	-16.9	-14.8	-11.1	-6.0	0.0	6.0	11.1	14.8	16.9	17.6
VAL		-2.4	-4.1	-6.2	-8.4	-10.0	-10.6	-10.0	-8.4	-6.2	-4.1	-2.4
V		31.4	33.4	34.9	35.9	36.4	36.5	36.4	35.9	34.9	33.4	31.4
VT		31.2	33.0	33.9	34.0	33.7	33.4	33.7	34.0	33.9	33.0	31.2
VA		3.2	5.6	8.5	11.5	13.8	14.6	13.8	11.5	8.5	5.6	3.2
RADIUS		3.4	3.0	2.6	2.3	2.1	2.1	2.1	2.3	2.6	3.0	3.4
THETA 46.2		-20.5	-22.0	-22.7	-21.8	-18.7	-13.4	-6.4	0.9	7.3	12.0	14.7
DVL		28.8	32.9	36.1	36.8	33.7	26.3	15.7	4.6	8.5	13.7	17.9
VL		-23.7	-25.7	-26.6	-25.6	-22.0	-15.9	-7.9	0.6	8.0	13.4	16.5
VTL		-20.1	-19.5	-17.3	-13.1	-7.1	0.0	7.1	13.1	17.3	19.5	20.1
VAL		-3.6	-6.2	-9.3	-12.5	-14.9	-15.9	-14.9	-12.5	-9.3	-6.2	-3.6
V		33.0	35.0	36.2	36.8	37.0	37.0	37.0	36.8	36.2	35.0	33.0
VT		32.7	33.9	33.8	32.5	30.7	29.8	30.7	32.5	33.8	33.9	32.7
VA		5.0	8.5	12.9	17.3	20.7	22.0	20.7	17.3	12.9	8.5	5.0
RADIUS		3.1	2.6	2.2	1.9	1.6	1.5	1.6	1.9	2.2	2.6	3.1
THETA 45.6		-22.1	-23.6	-24.7	-23.8	-20.5	-14.9	-7.5	0.3	7.2	12.3	15.3
DVL		29.4	33.5	36.4	36.8	33.5	26.1	15.7	4.6	8.5	13.6	17.9
VL		-27.2	-30.1	-31.8	-31.3	-27.7	-20.9	-11.7	-1.8	7.0	13.6	17.4
VTL		-22.3	-21.8	-19.4	-14.8	-8.0	0.0	8.0	14.8	19.4	21.8	22.3
VAL		-4.9	-8.3	-12.4	-16.6	-19.7	-20.9	-19.7	-16.6	-12.4	-8.3	-4.9
V		34.2	35.9	36.8	37.1	37.0	36.9	37.0	37.1	36.8	35.9	34.2
VT		33.5	34.0	32.5	28.9	24.6	22.5	24.6	28.9	32.5	34.0	33.5
VA		6.9	11.6	17.4	23.2	27.6	29.3	27.6	23.2	17.4	11.6	6.9
RADIUS		2.8	2.3	1.9	1.5	1.1	1.0	1.1	1.5	1.9	2.3	2.8
THETA 45.0		-23.1	-25.0	-25.9	-24.9	-21.6	-15.7	-8.1	-0.1	7.1	12.5	15.7
DVL		30.1	33.9	36.5	36.6	33.0	25.7	15.4	4.5	8.4	13.5	17.9
VL		-29.7	-33.2	-35.5	-35.3	-31.7	-24.5	-14.5	-3.7	6.1	13.5	17.8
VTL		-23.8	-23.3	-20.8	-15.8	-8.6	0.0	8.6	15.8	20.8	23.3	23.8
VAL		-5.9	-9.9	-14.7	-19.5	-23.1	-24.5	-23.1	-19.5	-14.7	-9.9	-5.9
V		34.9	36.4	37.0	37.0	36.8	36.6	36.8	37.0	37.0	36.4	34.9
VT		33.9	33.6	30.6	24.6	16.8	12.0	16.8	24.6	30.6	33.6	33.9
VA		8.4	14.0	20.8	27.6	32.7	34.6	32.7	27.6	20.8	14.0	8.4
RADIUS		2.6	2.1	1.6	1.2	0.7	0.5	0.7	1.2	1.6	2.1	2.6
THETA 44.4		-23.7	-25.5	-26.3	-25.2	-21.8	-15.9	-8.3	-0.2	7.0	12.4	15.7
DVL		30.6	34.3	36.7	36.6	32.9	25.6	15.4	4.5	8.3	13.3	17.9
VL		-30.6	-34.3	-36.7	-36.6	-32.9	-25.6	-15.4	-4.5	8.3	13.3	17.9
VTL		-24.3	-23.8	-21.2	-16.1	-8.7	0.0	8.7	16.1	21.2	23.8	24.3
VAL		-6.4	-10.5	-15.5	-20.5	-24.2	-25.6	-24.2	-20.5	-15.5	-10.5	-6.4
V		35.2	36.5	37.0	36.9	36.6	36.5	36.6	36.9	37.0	36.5	35.2
VT		34.0	33.3	29.7	22.6	12.2	0.3	12.2	22.6	29.7	33.3	34.0
VA		9.1	15.0	22.1	29.2	34.5	36.5	34.5	29.2	22.1	15.0	9.1
RADIUS		2.6	2.1	1.5	1.0	0.5	0.0	0.5	1.0	1.5	2.1	2.6

Fig. B-3 - Example Output

The first number following (THETA) is the scan angle THETA in degrees for the data until the next (THETA) is encountered. The numbers other than the first are the centroid of the weighted averages.

DVL is the maximum minus the minimum velocities observed within the focal volume. Or, if (IVMAX = 1), DVL is the maximum of the magnitude of the line-of-sight velocities.

VL is the line-of-sight velocity at the focal point.

VTL is the line-of-sight velocity at the focal point due to the tangential velocity.

VAL is the line-of-sight velocity at the focal point due to the axial velocity.

V is the norm of the total velocity vector at the focal point.

VT is the norm of the total tangential velocity vector.

VA is the norm of the total axial velocity vector.

RADIUS is the distance from the axis of the vortex and the focal point in meters.

There are two types of plots. The first plot (Fig. B-4) is velocity versus one of the scanning parameters such as PHI. In this type of plot there are a number of curves plotted with various letters. Each letter represents a different value of another scanning parameter such as THETA. In Fig. B-4, A represents THETA = 48.0 degrees, B represents THETA = 47.4 degrees and so forth.

The second type of plot is a velocity contour plot (Fig. B-5). Each letter represents a particular contour as indicated at the top of the plot. The contour lines between the points must be drawn in by hand.

#### B.12 EXAMPLE RUN FOR LASER VELOCIMETER VOLUME SCAN SIMULATION PROGRAM

For an example, take a vortex generated by a Boeing 747 while it is landing and SCAN it about 1000 meters from the generating aircraft. Approximate values for the parameters of this vortex are

$$\begin{aligned}
 \text{GAMMAC} &= 727.0 \text{ n-m-sec/kg} \\
 \text{W8} &= 77.3 \text{ m/sec} \\
 \text{UNU} &= 0.0914 \text{ m}^2/\text{sec} \\
 \text{Z} &= 1000 \text{ m} \\
 \text{DZERO} &= 50,000 \text{ n} \\
 \text{RHO} &= 1,192 \text{ kg/m}^3
 \end{aligned}$$

Let the vortex pass directly overhead and parallel to the X axis which is on the ground

$$\begin{aligned}
 \text{OP} &= (0, 0, 50) \\
 \text{PQ} &= (1, 0, 0)
 \end{aligned}$$

The following is the scanning selection

$$\begin{aligned}
 \text{PHI1} &= 3 \text{ deg} \\
 \text{PHI2} &= -3 \text{ deg} \\
 \text{NPHI} &= 11 \\
 \text{THETA1} &= 48 \text{ deg} \\
 \text{THETA2} &= 42 \text{ deg} \\
 \text{NTHETA} &= 11 \\
 \text{DIST1} &= 69 \text{ m} \\
 \text{DIST2} &= 71 \text{ m} \\
 \text{NDIST} &= 11
 \end{aligned}$$

A  $\text{CO}_2$  gas laser is used, therefore

$$\text{FLAMDA} = 0.0000106 \text{ m}$$

The value for PSI is a scale factor and, set it to one,

$$\text{PSI} = 1.$$

Let the laser Doppler system be a single, coaxial, continuous wave, focused system. Therefore

$$\text{ICHOIC} = 1$$

The lens of the telescope will be about a half foot in diameter. Therefore

$$R = 0.0762 \text{ m}$$

When the focal length is 70 meters, half the length of the focal volume is

$$\Delta f = \frac{2 \lambda f^2}{\pi R^2} = \frac{2 * .0000106 * 70^2}{\pi * (.0762)^2} = 5.7 \text{ meters}$$

To sample the velocity in the focal volume at least every half meter,

$$NWEIGH = 12.$$

To print out everything,

$$IOUT = 3.$$

To plot the centroid of the weighted velocity,

$$IPLOT = 1$$

$$IPLOT1 = 1 .$$

Let the program compute the absolute maximum of the line-of-sight velocity in the focal volume

$$IVMAX = 1$$

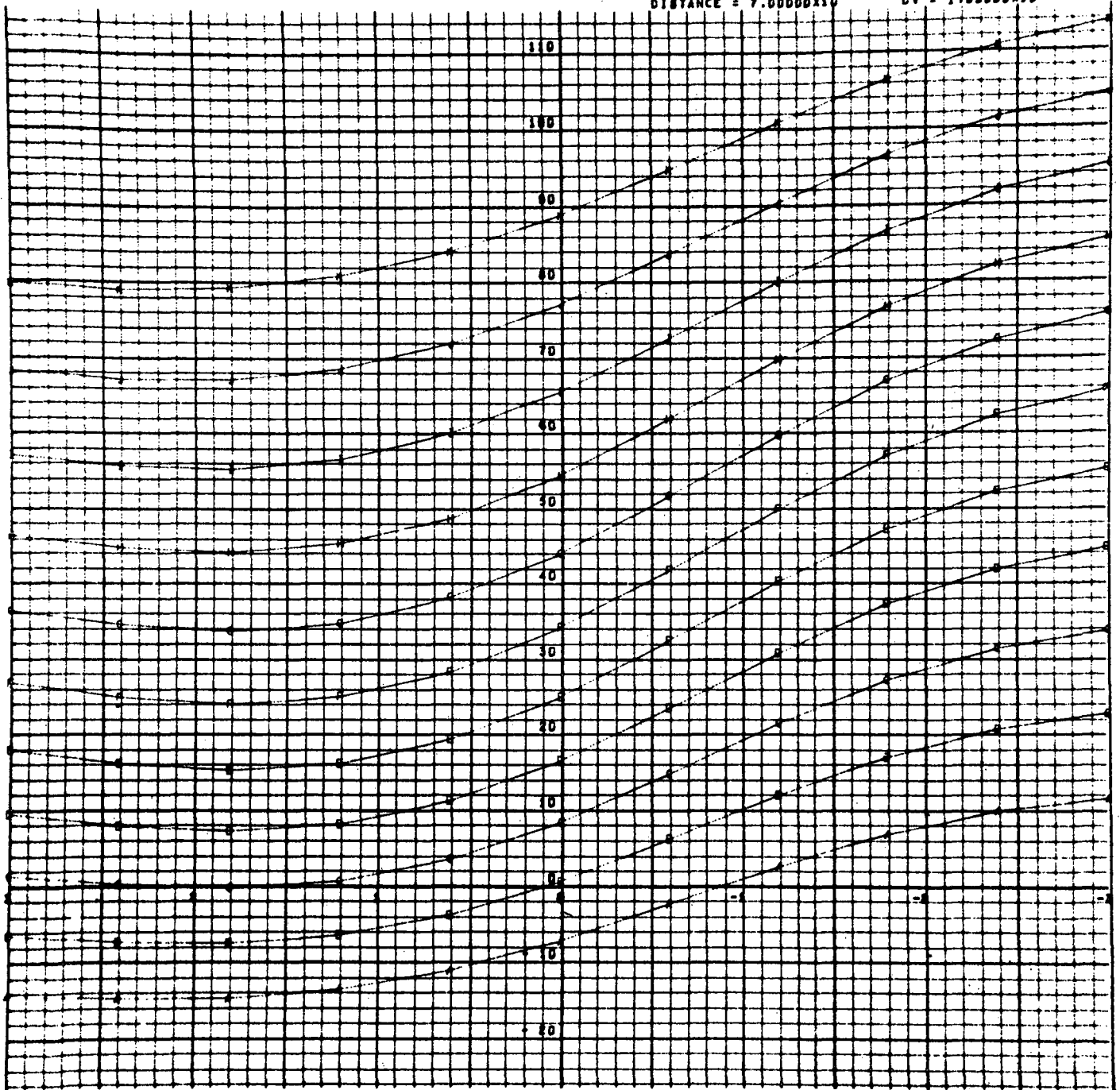
The first input is a comment on the first 72 columns of the first card. Then comes the main input which is input by way of FORTRAN namelist. The name of the namelist is INPUT and the data are the above described variables.

The final input to consider is the plotting control. Two sets of plots PHI versus THETA and RANGE versus THETA are wanted. Also, in both cases, lines will be drawn between the points.

.23012

EXAMPLE FOR VOLUME SCANNING PROGRAM

DISTANCE =  $7.00000 \times 10^{+01}$  DV =  $1.00000 \times 10^{+01}$



PMI IN DEGREES

Fig. B-4 - Example Output

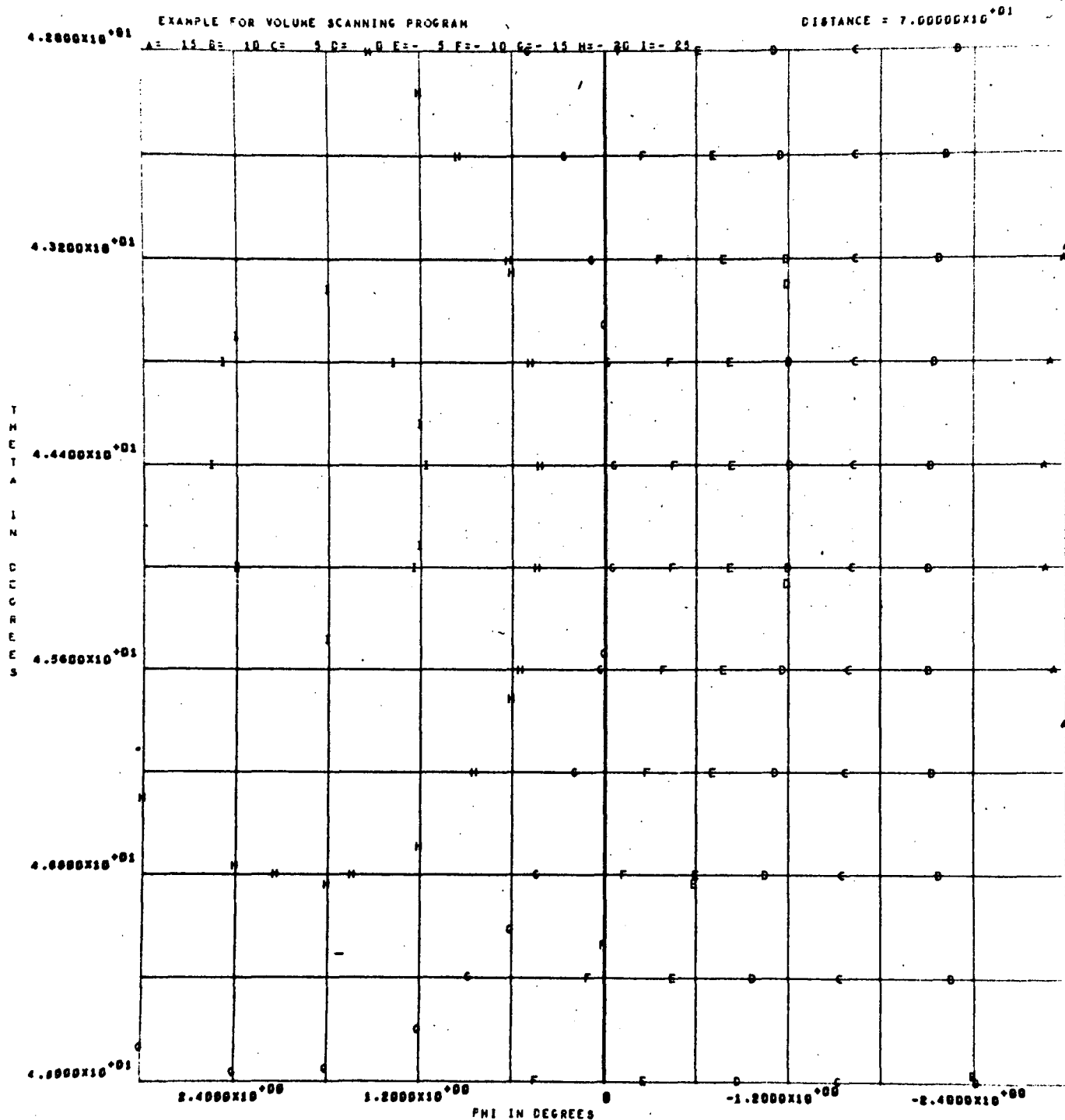


Fig. B-5 - Example Output

EXAMPLE FOR VOLUME SCANNING PROGRAM

$\rho = 2.40000 \times 10^{+00}$   $CV = 3.00000 \times 10^{+00}$

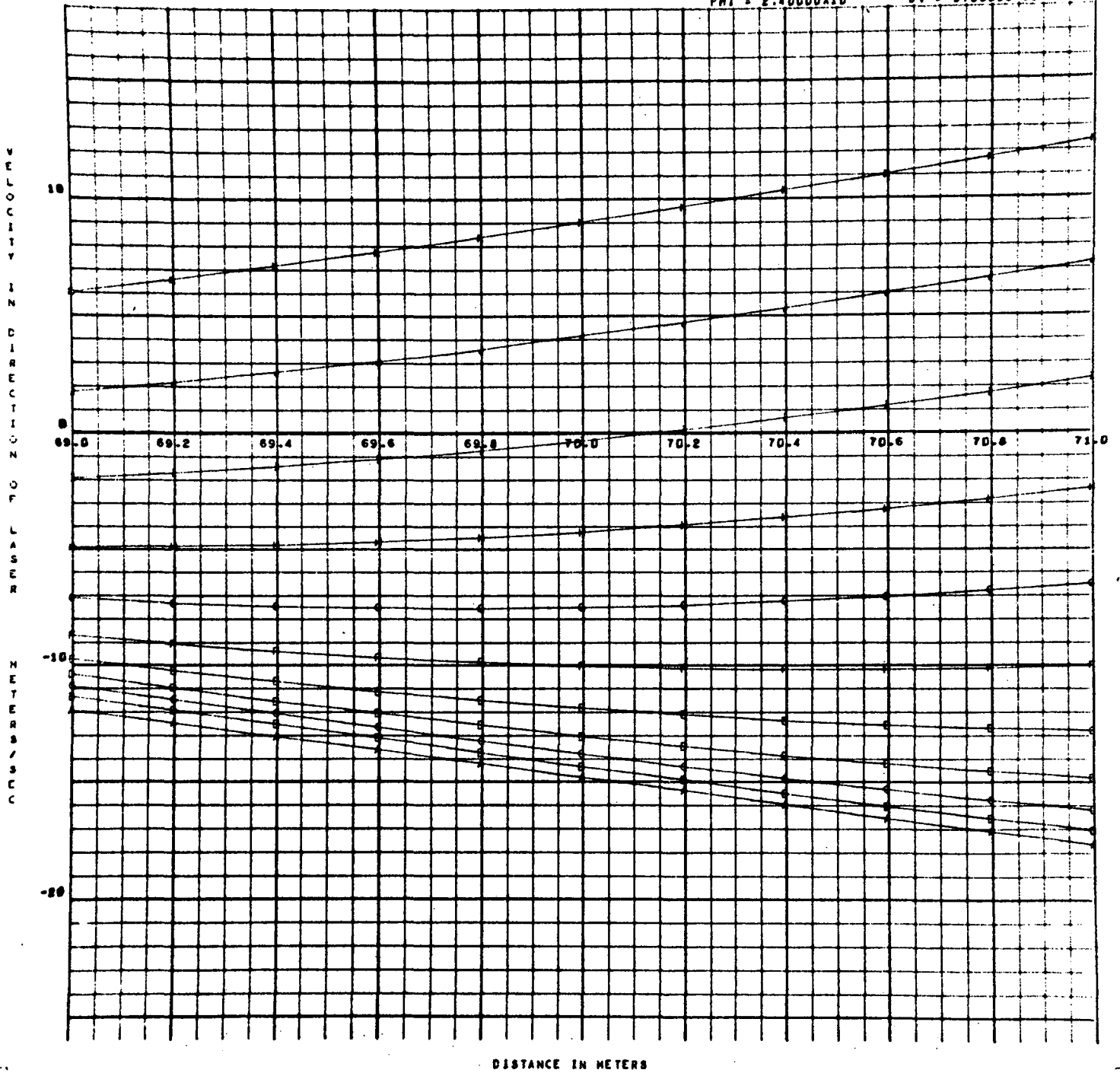


Fig. B-6 - Example Output

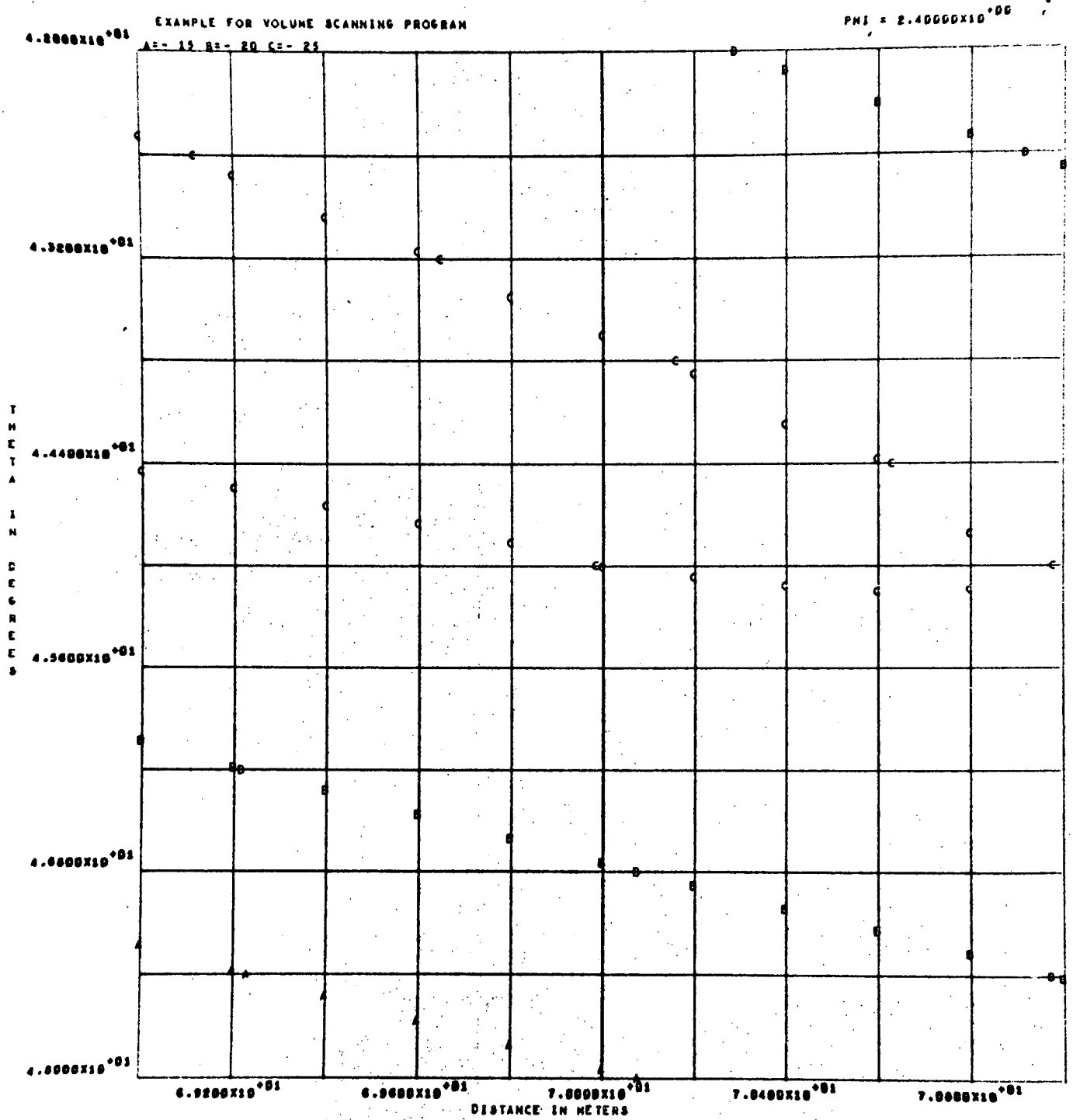


Fig. B-7 - Example Output

B-21

These input cards are

Card No.	Col. 10	Col. 20	Col. 30
1	1	1	2
2	1	3	2
3	blank	blank	blank

A sample of the printer output from this example run is shown as Figs. B-2, B-3, B-4, B-5, B-6 and B-7.

B.13 LASER VELOCIMETER VOLUME SCAN SIMULATION PROGRAM  
VARIABLES

<u>Name</u>	<u>Units</u>	<u>Location</u>	<u>Description</u>
ABC(20)	None	PSCAN	Plot label.
AVT(3)	m/sec	COMMON/A05/	Axial velocity vector at illumination point - (rectangular coordinate system).
D	m/sec	COMMON/A15/	D is the distance from illuminated point of interest to axis of vortex.
DD(20)	m	MAIN	Distance of focus point or center of pulse from axis of vortex.
DDIST	m	COMMON/A12/	Distance between points in range scan.
DDISTW	m	MAIN	Step size used in sampling the illuminated volume.
DDV	m/sec	PSCAN	Preliminary result in determining delta velocity between the curves on the graph of velocity versus a scanning parameter.
DISTL	m	MAIN	Distance from laser to focus point.

<u>Name</u>	<u>Units</u>	<u>Location</u>	<u>Description</u>
DISTW	m	MAIN	Distance from laser to point of interest in the illuminated volume.
DIST1	deg	COMMON/A09/	Starting range.
DIST2	deg	COMMON/A09/	Ending range.
DL2	-	MAIN	A preliminary result for the weighting associated with a focus system.
DPHIL	rad	MAIN	DELTA step in PHI scanning.
DPHIL1	deg	COMMON/A12/	Angle between focus points when scanning in PHI.
DPTD(3)	deg ,deg ,m	COMMON/A12/	DPTD(1) is same as DPHIL1 DPTD(2) is same as DTHEL1 DPTD(3) is same as DDIST.
DTHEL1	deg	COMMON/A12/	Angle between focus points when scanning in THETA.
DTHETA	rad	MAIN	DELTA step in THETA for scanning.
DUM	None	PSCAN	A dummy variable used in calling arguments.
DV	None	PSCAN	DELTA velocity between the curves on the graph of velocity vs a scanning parameter.
DZERO	None	COMMON/A14/	DZERO is the profile drag of airfoil from generating aircraft.
EX	-	VEL	Intermediate value for tangential velocity.
FACT1	-	MAIN	A preliminary calculation for the weighting associated with a focus system.
FACT2	-	MAIN	A preliminary calculation for the weighting associated with a focus system.
FLAMDA	m	COMMON/A20/	FLAMDA = wavelength of light.
FLDX(12, 3)	None	COMMON/A11/	Stores labels for the plots.
FLDY(12)	None	COMMON/A11/	Stores labels for the plots.
GAMMAC	(N-m-sec)/kg	COMMON/A06/	Circulation about vortex.
I	None	MAIN	The PHI do-loop parameter.

<u>Name</u>	<u>Units</u>	<u>Location</u>	<u>Description</u>
I	None	PSCAN	I is a subscript used in incrementing the parameter plotted on the horizontal scale.
IA	None	PSCAN	Used in calculation for DELTA velocity between the curves on the graph of velocity vs a scanning parameter.
IABC	None	PSCAN	X coordinate for label used on contour plot. Example (A =)
ICHOIC	None	COMMON/A20/	Flag for laser type ICHOIC = 1 indicates focused CW laser ICHOIC = 2 indicates pulsed laser ICHOIC = 3 indicates perfect velocity detection.
IERR	None	PSCAN	IERR is an error flag from a plot routine.
II	None	MAIN	The weighting do-loop parameter.
IIA	None	PSCAN	Used in calculation for DELTA velocity between the curves on the graph of velocity vs a scanning parameter.
ILINE	None	PSCAN	Determines if lines will be drawn between points of SC 4020 plots. ILINE = 0 indicates no lines. ILINE > 0 indicates lines.
IOUT	None	COMMON/A20/	Flag for printer output IOUT = 1 no velocities are printed. IOUT = 2 prints only velocity specified by flag IPLOT1. IOUT = 3 prints all available velocities

<u>Name</u>	<u>Units</u>	<u>Location</u>	<u>Description</u>
IP	None	PSCAN	Contains address of storage location to go to in order to accomplish commands of variables IX and IY. Used in "assigned go to."
IPLOT	None	COMMON/A20/	A flag indicating whether or not SC 4020 plots will be produced. IPLOT = 0 indicates no plots. IPLOT = 1 indicates plots will be made.
IPLOT1	None	COMMON/A20/	Flag indicating velocities to be plotted. IPLOT1 = 1 Plots centroid of weighted velocity. IPLOT1 = 2 Plots MAX-MIN or MAX (ABS(VL)). IPLOT1 = 3 Plots line-of-sight velocity. IPLOT1 = 4 Plots line-of-sight tangential velocity IPLOT1 = 5 Plots line-of-sight axial velocity IPLOT1 = 6 Plots velocity IPLOT1 = 7 Plots tangential velocity IPLOT1 = 8 Plots axial velocity
ISYM(20)	None	COMMON/A11/	Stores plotting symbols
IV	None	PSCAN	IV is a flag indicating if current velocity is higher or lower than contour that is being sought.
IVMAX	None	COMMON/A20/	Flag to indicate whether MAX-MIN of line of sight velocity in illuminated region is to be computed or MAX (ABS (line of sight in illuminated region)) is to be computed.

<u>Name</u>	<u>Units</u>	<u>Location</u>	<u>Description</u>
IX	None	PSCAN	Determines horizontal axis IX = 1 horizontal axis is PHI IX = 2 horizontal axis is THETA IX = 3 horizontal axis is RANGE.
IY	None	PSCAN	Determines vertical axis IY = 1 vertical axis is PHI IY = 2 vertical axis is THETA IY = 3 vertical axis is RANGE.
IZ	None	PSCAN	Indicates parameter which is constant for each plot. IZ = 1 PHI is constant IZ = 2 THETA is constant IZ = 3 RANGE is constant.
I2	None	MAIN	A do-loop parameter.
I3	None	MAIN	Indicates first velocity to be printed out when IOUT = 3. ICHOIC determines value for I3.
I4	None	MAIN	Indicates second velocity to be printed out when IOUT = 3. ICHOIC determines value for I4.
J	None	MAIN	The THETA do-loop parameter.
	None	PSCAN	J is a subscript used in incrementing the parameter plotted on the vertical scale.
JABC	None	PSCAN	X coordinate for label used on contour plot. Example (30) in label (A = 30)
JCHOIC	None	MAIN	Contains address of storage location to go to in order to accomplish command of variable ICHOIC. Used in "assigned go to."
JOUT	None	MAIN	Contains address of storage location to go to in order to accomplish command of variable IOUT. Used in "assigned go to."

<u>Name</u>	<u>Units</u>	<u>Location</u>	<u>Description</u>
JVMAX	None	MAIN	Contains address of storage location to go to in order to accomplish command of variable IVMAX. Used in "assigned go to."
K	None	MAIN	The range do-loop parameter
	None	PSCAN	Do-loop parameter for plots. Two plots are made for each value of K.
KCHOIC	None	MAIN	Contains address of storage location to go to in order to accomplish command of variable ICHOIC. Used in "assigned go to."
KK	None	PSCAN	Number of current contour program is working on while producing contour plot.
KOUT	None	MAIN	Contains address of storage location to go to in order to accomplish command of variable IOU. Used in "assigned go to."
L	None	PSCAN	Used in calculation for DELTA velocity between the curves on the graph of velocity vs a scanning parameter.
LAB(2, 3)	None	PSCAN	Plot label.
LABLE(8)	None	MAIN	Contain labeling for printer output.
LINE	None	MAIN	Line count for current page of line printer.
NDIST	None	COMMON/A09/	Number of evenly spaced ranges.
NEW	None	MAIN	Not currently used.
NNTH	None	MAIN	Number of lines of output on printer per range step. Determined by IOU.
NNX	None	PSCAN	Same as NX except NNX is negative if lines are to be drawn between points on graph.

<u>Name</u>	<u>Units</u>	<u>Location</u>	<u>Description</u>
NPHI	None	COMMON/A09/	Number of evenly spaced PHIs.
NTHETA	None	COMMON/A09/	Number of evenly spaced THETAs.
NV	None	PSCAN	NV is number of positive contours to be plotted.
NW	None	MAIN	Number of sampling points in the illuminated volume.
NWEIGH	None	COMMON/A20/	NWEIGH is half the number of evenly spaced points used in the weighting of this illuminated volume.
NX	None	PSCAN	Number of steps in parameter which are plotted along horizontal axis.
NY	None	PSCAN	Number of steps in parameter which are plotted along vertical axis.
OP(3)	m	COMMON/A01/	Position of a point on the vortex axis (rectangular coordinate system).
OS(3)	m	COMMON/A05/	Vector to indicate illumination point relative to laser (rectangular coordinate system)
PHIA	rad	MAIN	Starting PHI. Same as PHI1 except for units.
PHIB	rad	MAIN	Ending PHI. Same as PHI2 except for units.
PHIL	rad	MAIN	Current value for the angle PHI.
PHIL1(20)	deg	COMMON/A04/	PHI values to be plotted or printed.
PHIL2	deg	MAIN	Current value for the angle PHI. Same as PHI2 except for units.
PHI1	deg	COMMON/A09/	Starting PHI.
PHI2	deg	COMMON/A09/	Ending PHI.
PI	None	COMMON/A07/	PI is $\pi = 3.1415926$ .

<u>Name</u>	<u>Units</u>	<u>Location</u>	<u>Description</u>
PLENGT	m	COMMON/A20/	PLENGT is pulse length.
PQ(3)	None	COMMON/A01/	Directional vector for vortex (rectangular coordinate system).
PSI	None	COMMON/A20/	PSI is incident wave amplitude.
R	m	COMMON/A20/	R is radius of telescope aperture.
RHO	kg/m <sup>3</sup>	COMMON/A14/	RHO is the density of the atmosphere.
R2D	deg/rad	COMMON/A07/	Conversion factor for converting from radians to degrees.
SP(3)	m	COMMON/A05/	Vector from illumination point (OS) to point (OP) on vortex (rectangular coordinate system)
THETAA	rad	MAIN	Starting THETA. Same as THETA1 except for units.
THETAB	rad	MAIN	Ending THETA. Same as THETA2 except for units.
THETAL	rad	MAIN	Current value for the angle THETA.
THETA1	deg	COMMON/A09/	Starting THETA.
THETA2	deg	COMMON/A09/	Ending THETA.
THETL1(20)	deg	COMMON/A04/	THETA values to be plotted or printed.
TITLE(12)		COMMON/A02/	Contains inputted description of run.
UNU	m <sup>2</sup> /sec	COMMON/A06/	Eddy viscosity.
V(20, 20, 20)	m/sec	COMMON/A03/	Velocity values to be plotted: First index varies PHI. Second index varies THETA. Third index varies range.
VCON	m/sec	PSCAN	VCON is velocity of contour to be plotted.

<u>Name</u>	<u>Units</u>	<u>Location</u>	<u>Description</u>
VCON1	m/sec	PSCAN	Velocity of maximum contour to be plotted.
VL	m/sec	MAIN	Line-of-sight velocity at point of interest.
VLIN1	m/sec	COMMON/A15/	VLIN1 is the line-of-sight component of the tangential velocity.
VLIN2	m/sec	COMMON/A15/	VLIN2 is the line-of-sight component of the axial velocity.
VLW	None	MAIN	Sum of line-of-sight velocity multiplied by weighing factor over the illuminated volume.
VMAVT	m/sec	COMMON/A15/	VMAVT is the norm of the tangential velocity.
VMAVTD	1/sec	VEL	Scalar used to produce the axial velocity vector AVT(3) from vector PQ(3).
VMAX	m/sec	PSCAN	Maximum value for velocity of current plot being made.
VMAXX	m/sec	PSCAN	The maximum velocity on the graph of velocity vs a scanning parameter.
VMIN	m/sec	PSCAN	Minimum value for velocity of current plot being made.
VMPQ	m	VEL	Norm of vector PQ(3).
VMVT	m/sec	COMMON/A15/	VMVT is the norm of the tangential velocity.
VMVTD	1/sec	VEL	Scalar used to produce the tangential velocity vector VT(3) from vector VV(3).
VMVV	m	VEL	Norm of vector VV(3)
VP	None	PSCAN	VP is used in computing a linear interpolation between data points, for the contour.
VT(3)	m/sec	COMMON/A05/	Tangential velocity vector at illumination point (rectangular coordinate system).

<u>Name</u>	<u>Units</u>	<u>Location</u>	<u>Description</u>
VTOL	m/sec	MAIN	Norm of velocity vector at focus point.
VV(3)	None	COMMON/A05/	Vector pointing in direction of tangential flow at illumination point (rectangular coordinate system).
VV(20, 20)	m/sec	COMMON/A10/	Values of VV are obtained from V and stored in proper order for plotting.
VVMAX	m/sec	MAIN	Maximum line-of-sight velocity in the illuminated volume.
VVMIN	m/sec	MAIN	Minimum line-of-sight velocity in the illuminated volume.
VVP	deg or m	PSCAN	VVP is one coordinate on a contour.
VVV(20, 20)	m/sec	COMMON/A10/	Values of VVV computed from VV which has had a DELTA velocity added to it in order to separate the graphs on the velocity plot.
V1(20, 8)	m/sec	MAIN	Stores velocities for one sweep in PHI. V1( , 1) is centroid of weighted line of sight velocity. V1( , 2) is MAX-MIN or MAX (ABS(VL)). V1( , 3) is line of sight velocity at focus point. V1( , 4) is line of sight of tangential velocity at focus point. V1( , 5) is line of sight of axial velocity at focus point. V1( , 6) is norm of total velocity. V1( , 7) is norm of tangential velocity. V1( , 8) is norm of axial velocity.
WAT	None	MAIN	Intensity of pulse. Presently set to one.

6

<u>Name</u>	<u>Units</u>	<u>Location</u>	<u>Description</u>
WF	None	MAIN	Weighting factor for point of interest.
WFT	None	MAIN	Sum of weighting factors over the illuminated volume.
W8	m/sec	COMMON/A06/	Freestream velocity.
Z	m	COMMON/A06/	Vortex axial coordinate from source.

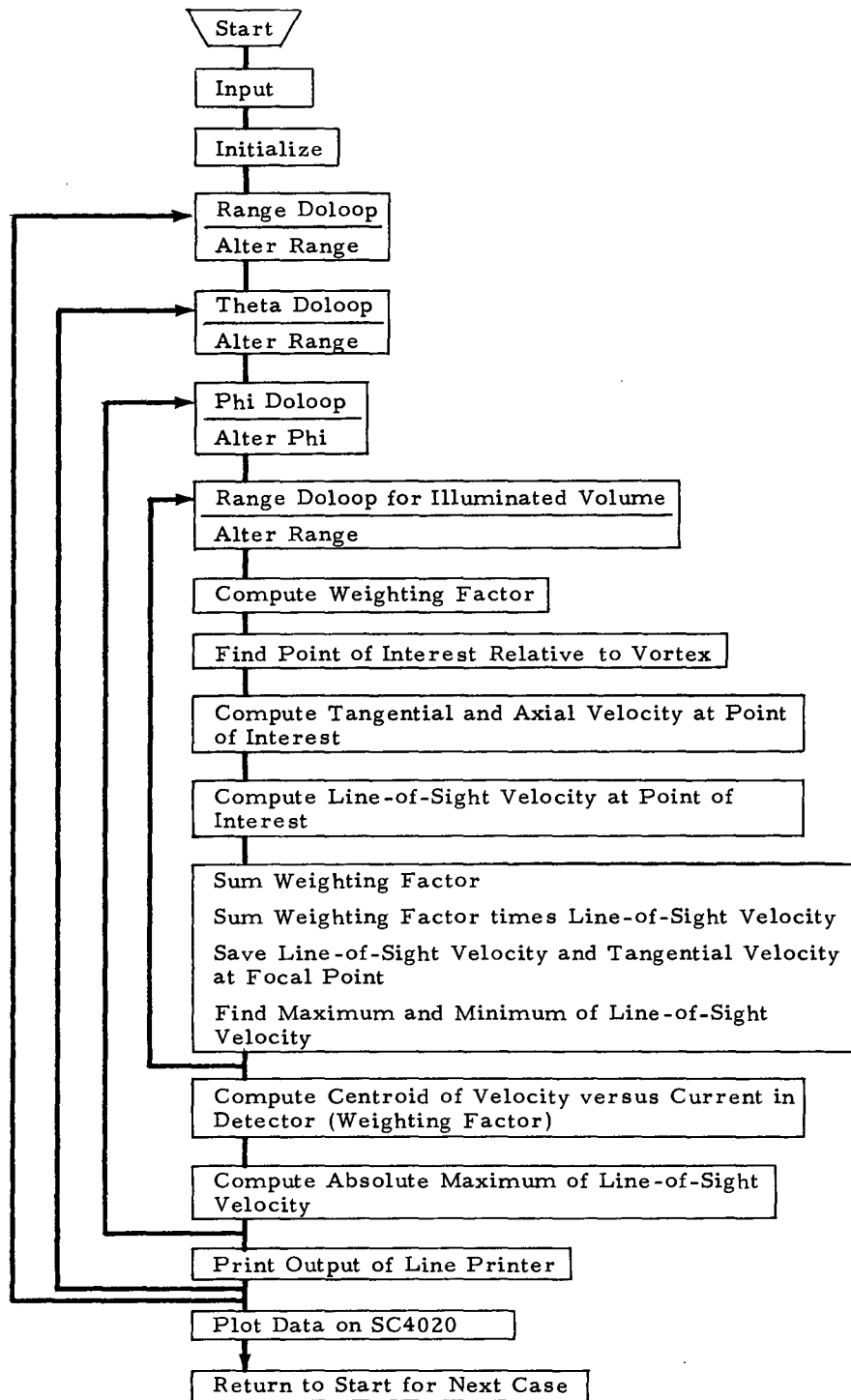


Fig. B-8 - Flow Chart of Laser Velocimeter Volume Scan Simulation Program

B.14 LASER VELOCIMETER VOLUME SCAN SIMULATION PROGRAM LISTING

```

$JOB
$SETUP LBP      TAPE,SC4020
$ASSIGN        SYSLBP
$EXECUTE       IBJOB
$IBJOB LMSC    MAP
$IFTC MAIN    DECK
C
C      LASER VELOCIMETER VOLUME SCAN SIMULATION PROGRAM
C
C      THIS PROGRAM SIMULATES ONE VORTEX AND SCANS IT WITH ONE LASER
C      VELOCIMETER. OUTPUT ON SC4020 PLOTS ARE AIR VELOCITY AS A FUNCTION
C      OF POSITION.
C
C      THIS PROGRAM COMPUTES LINE OF SIGHT VELOCITIES AND
C      WEIGHTED LINE OF SIGHT VELOCITIES.
C      SC4020 PLOTTING IS PERFORMED
C      VELOCITY CONTOURS
C
C
C      NAMELIST (INPUT)
C
C      GAMMAC      CIRCULATION
C      W8          FREESTREAM VELOCITY
C      UNU         EDDY VISCOSITY
C      Z           VORTEX AXIAL COORDINATE FROM SOURCE
C      OP          POSITION OF A POINT ON THE VORTEX AXIS
C      PO          DIRECTIONAL VECTOR FOR VORTEX
C      PHI1        STARTING PHI
C      PHI2        ENDING PHI
C      NPHI        NUMBER OF EVENLY SPACED PHIS
C      THETA1      STARTING THETA
C      THETA2      ENDING THETA
C      NTHETA      NUMBER OF EVENLY SPACED THETAS
C      DIST1       STARTING RANGE
C      DIST2       ENDING RANGE
C      NDIST       NUMBER OF EVENLY SPACED RANGES
C      PSI         INCIDENT WAVE AMPLITUDE
C      R           RADIUS OF TELESCOPE APERTURE
C      FLAMDA      WAVE LENGTH OF LIGHT
C      PLENCT      PULSE LENGTH
C      DZERO       PROFILE DRAG OF THE AFOFOIL
C      RHO         DENSITY OF ATMOSPHERE
C      ICHOIC      FLAG
C                  ICHOIC = 1      CONTINUOUS WAVE LASER
C                  ICHOIC = 2      PULSED LASER
C                  ICHOIC = 3      PERFECT VELOCITY DETECTION
C      NWEIGH      HALF THE NUMBER OF EVENLY SPACED POINTS USED IN
C                  THE WEIGHTING
C      IOUT        FLAG
C                  IOUT = 1        NO VELOCITYS ARE PRINTED
C                  IOUT = 2        PRINTS ONLY VELOCITY SPECIFIED
C                                  BY IPLOT1
C                  IOUT = 3        PRINTS ALL VELOCITYS
C      IPLOT       FLAG
C                  IPLOT = 0       NO SC4020 PLOTS
C                  IPLOT = 1       SC4020 PLOTS
C      IPLOT1      FLAG
C                  IPLOT1 = 1      PLOTS CENTROID OF WEIGHTED VELOCITY

```

```

C          I PLOT1 = 2      PLOTS MAX-MIN OR MAX(ABS(VL))
C          I PLOT1 = 3      PLOTS LINE OF SIGHT VELOCITY.
C          I PLOT1 = 4      PLOTS LINE OF SIGHT TANGENTIAL VELOCIT
C          I PLOT1 = 5      PLOTS LINE OF SIGHT AXIAL VELOCITY
C          I PLOT1 = 6      PLOTS VELOCITY
C          I PLOT1 = 7      PLOTS TANGENTIAL VELOCITY
C          I PLOT1 = 8      PLOTS AXIAL VELOCITY
C
C          I VMAX          FLAG
C          I VMAX = 0      COMPUTS MAX-MIN OF VL
C          I VMAX = 1      COMPUTS VELOCITY MAX(ABS(VL))

```

PLOTTING INPUT

```

C          COLUMN 10      0      NO LINES BETWEEN POINTS
C          COLUMN 10      1      LINES BETWEEN POINTS
C          COLUMN 20      1      PHI PLOTTED ON HORIZONTAL AXIS
C          COLUMN 20      2      THETA PLOTTED ON HORIZONTAL AXIS
C          COLUMN 20      3      DISTANCE PLOTTED ON HORIZONTAL AXIA
C          COLUMN 30      1      PHI PLOTTED ON VERTICAL AXIS
C          COLUMN 30      2      THETA PLOTTED ON VERTICAL AXIS
C          COLUMN 30      3      DISTANCE PLOTTED ON VERTICAL AXIS

```

```

COMMON / A01 / OP(3), PQ(3)
COMMON / A02 / TITLE(12)
COMMON / A03 / V(20,20,20)
COMMON / A04 / PHIL1(20), THETL1(20), DISTL1(20)
COMMON / A06 / GAMMAC, W8, UNU, Z
COMMON / A07 / PI, R2D
COMMON / A09 / PHI1, PHI2, NPHI, THETA1, THETA2, NTHETA, DIST1,
$ DIST2, NDIST
COMMON / A12 / DPHIL1, DTHFL1, DDIST
COMMON / A14 / DZERO, RHO
COMMON / A15 / VLINE1, VLINE2, VMVT, VMAVT, D
COMMON / A20 / PSI, R, FLAMDA, PLENGT, ICHOIC, NWEIGH, IOUT,
$ I PLOT, I PLOT1, I VMAX
DIMENSION V1(20,8),DD(20),LABLE(8)
DATA LABLE / 6HWEIGHT,3HDVL,3HVL ,3HVTL,3HVAL,3HV ,3HVT ,3HVA /
DATA PI,R2D / 3.1415926, 57.29578 /
DATA GAMMAC, W8, UNU, Z, OP, PQ, PHI1, PHI2, THETA1, THETA2,
$ DIST1, DIST2, NPHI, NTHETA, NDIST, NWEIGH, IOUT, I PLOT
$ / 16*0., 3*0,1,3,0 /
DATA PSI, R, FLAMDA / 3*0. /
DATA PLENGT, DZERO, RHO, ICHOIC, I PLOT1, I VMAX / 3*0.,3*1 /
NAMELIST / INPUT / GAMMAC, W8, UNU, Z, OP, PQ,
1 PHI1, PHI2, NPHI, THETA1, THETA2, NTHETA, DIST1, DIST2, NDIST,
2 PSI, R, FLAMDA,
3 PLENGT, DZERO, RHO,
4 ICHOIC, NWEIGH, IOUT, I PLOT, I PLOT1, I VMAX
10 READ (5,500) TITLE
500 FORMAT(12A6)
WRITE(6,600) TITLE
600 FORMAT (1H1,30X,12A6)

```

```

C          INPUT
C          READ (5,INPUT)
C          WRITE(6,INPUT)

```

```

C          INITIALIZE
      NFW = 1
      PHIA = PHI1/R2D
      PHIB = PHI2/R2D
      THETA A = THETA1/R2D
      THETA B = THETA2/R2D
      GO TO (11,12,13), ICHOIC
11  ASSIGN 41 TO JCHOIC
      ASSIGN 44 TO KCHOIC
      GO TO 14
12  ASSIGN 42 TO JCHOIC
      ASSIGN 45 TO KCHOIC
14  I3 = 1
      I4 = 2
      GO TO 15
13  ASSIGN 50 TO JCHOIC
      I3 = 3
      I4 = 4
15  GO TO (21,22,16), IOUT
21  ASSIGN 31 TO JOUT
      ASSIGN 110 TO KOUT
      NNTH = 0
      GO TO 17
22  ASSIGN 48 TO JOUT
      ASSIGN 85 TO KOUT
      NNTH = (10-I3)*NTHETA
      GO TO 17
16  ASSIGN 48 TO JOUT
      ASSIGN 86 TO KOUT
      NNTH = NTHETA
17  IF (IVMAX .GT. 0) GO TO 18
      ASSIGN 91 TO JVMAX
      GO TO 19
18  ASSIGN 92 TO JVMAX
19  CONTINUE
      DPIL = (PHIB - PHIA)/FLOAT(NPHI - 1)
      DTHETA = (THETA B - THETA A)/FLOAT(NTHETA - 1)
      DDIST = (DIST2 - DIST1)/FLOAT(NDIST - 1)
      DISTL = DIST1 - DDIST
      LINE = 100
      DPIL1 = DPIL*R2D
      DTHEL1 = DTHETA*R2D
      THETA L = THETA A - DTHETA
      THETA 2 = THETA L*R2D
      PHIL = PHIA - DPIL
      PHIL 2 = PHIL*R2D
      FACT1 = (PSI*PI*R**2)**2/FLAMDA**2
      FACT2 = FLAMDA/(PI*R**2)
      DO 20 I2=1,NPHI
      PHIL 2 = PHIL 2 + DPIL1
20  PHIL1(I2) = PHIL 2
      DO 25 I2=1,NTHETA
      THETA 2 = THETA 2 + DTHEL1
25  THETL1(I2) = THETA 2
C
C          RANGE DO LOOP
      DO 120 K=1,NDIST
      THETA L = THETA A - DTHETA

```

```

DISTL = DISTL + DDIST
DISTL1(K)=DISTL
GO TO JOUT,(48,31)
4A IF(LINE + NNTH .LT. 64) GO TO 30
WRITE(6,600) TITLE
LINE = 1
30 WRITE(6,620) DISTL,(PHIL1(I2),I2=1,NPHI)
620 FORMAT (/61X,10HDISTANCE =,F7.0/12H      PHI = ,20F6.1)
LINE = LINE + 4
C
C      THETA DO LOOP
31 DO 110 J=1,NTHETA
THETAL = THETAL + DTHETA
PHIL = PHIA - DPHIL
C
C      PHI DO LOOP
DO 100 I=1,NPHI
VVMAX = -1.E30
VVMIN = 1.E30
PHIL = PHIL + DPHIL
GO TO JCHOIC,(41,42,50)
41 DDISTW = 4.*FACT2*DISTL**2/FLOAT(2*NWEIGH)
GO TO 43
42 DDISTW = PLNGT/FLOAT(2*NWEIGH)
43 DISTW = DISTL - DDISTW*FLOAT(NWEIGH + 1)
NW = 2*NWEIGH + 1
VLW = 0.
WET = 0.
C
C      RANGE DO LOOP FOR ILLUMINATED VOLUME
DO 90 II=1,NW
DISTW =DISTW + DDISTW
C
C      COMPUTE WEIGHTING FACTOR
GO TO KCHOIC,(44,45)
44 DL2 = (FACT2*DISTL*DISTW)**2
WF = FACT1/(1. + (DISTL - DISTW)**2/DL2)/DISTW**2
GO TO 46
45 WAT = 1.
IF(II .GT. NWEIGH) GO TO 60
WF = WAT*FLOAT(II-1)/FLOAT(NWEIGH)
GO TO 46
60 WF = WAT*FLOAT(NW-II)/FLOAT(NWEIGH)
C
C      SUM WEIGHTING FACTOR
46 WET = WET + WF
C
C      CALL FOR VELOCITY AT POINT OF INTEREST
CALL VEL(VL,PHIL,THETAL,DISTW)
C
C      LOOK FOR FOCUS POINT AND SAVE VELOCITIES
IF(II .NE. NWEIGH + 1) GO TO 80
V1(I,3) = VL
V1(I,4) = VLINE1
V1(I,5) = VLINE2
VTOL = SQRT(VMVT**2 +VMAVT**2)
V1(I,6) = VTOL
V1(I,7) = VMVT

```

```

      V1(I,8) = VMAVT
      DD(I) = D
C
C          FIND MAXIMUM AND MINIMUM OF LINE OF SIGHT
80 IF(VL .GT. VVMAX) VVMAX = VL
   IF(VL .LT. VVMIN) VVMIN = VL
C
C          SUM WEIGHTING FACTOR TIMES LINE OF SIGHT VELOCITY
90 VLW = VLW + VL*WF
C
C          COMPUTE CENTROID OF VELOCITY CURRENT IN DETECTOR
      V1(I,1) = VLW/WFT
      GO TO JVMAX,(91,92)
C
C          COMPUTE MAXIMUM MINUS MINIMUM
91 V1(I,2) = VVMAX - VVMIN
   GO TO 100
C
C          COMPUTE ABSOLUTE MAXIMUM
92 V1(I,2) = AMAX1(VVMAX,-VVMIN)
   GO TO 100
50 CALL VFL(V1(I,3),PHIL,THETAL,DISTL)
   V1(I,4) = VLINE1
   V1(I,5) = VLINE2
   VTOL = SQRT(VMVT**2 + VMAVT**2)
   V1(I,6) = VTOL
   V1(I,7) = VMVT
   V1(I,8) = VMAVT
   DD(I) = D
100 V(I,J,K) = V1(I,IPL0T1)
C
C          PRINT OUTPUT ON LINE PRINTER
      GO TO KOUT,(85,86,110)
85 WRITE(6,610) THETL1(J),(V(I1,J,K),I1=1,NPHI)
610 FORMAT (6H THETA,F6.1,20F6.1)
   GO TO 110
86 WRITE(6,610) THETL1(J),(V1(I1,I3),I1=1,NPHI)
   DO 104 I2=I4,8
104 WRITE(6,611) LABEL(I2),(V1(I1,I2),I1=1,NPHI)
611 FORMAT (6X,A6,20F6.1)
   WRITE(6,612) (DD(I1),I1=1,NPHI)
612 FORMAT (6X,6HRADIUS,20F6.1)
110 CONTINUE
   LINE = LINE + NNTH
120 CONTINUE
C
C          CALL PLOTTING PROGRAM
      IF(IPL0T .GT. 0) CALL PSCAN(NEW)
      NEW = 0
C
C          RETURN TO START FOR NEXT CASE
      GO TO 10
      END

```

```

*IBF TO VEL      DECK
SUBROUTINE VFL(VLINE,PHIL,THETA,DISTL)
C
C      THIS ROUTINE COMPUTS TANGENTIAL AND AXIAL VELOCITYS OF A
C      VORTEX AT A POINT OF INTREST. ALSO THE LINE OF SIGHT COMPONENTS
C      FROM THE LASER ARE COMPUTED
C
COMMON / A01 / OP(3), PQ(3)
COMMON / A05 / OS(3), SP(3), VV(3), VT(3),AVT(3)
COMMON / A06 / GAMMAC, WR, UNU, Z
COMMON / A07 / PI, R2D
COMMON / A14 / DZFRQ, RHO
COMMON / A15 / VLINE1,VLINE2,VMVT,VMAVT,D
C
C      OS IS VECTOR FROM LASER TO POINT OF INTREST
OS(1) = DISTL*SIN(THETA)*COS(PHIL)
OS(2) = DISTL*SIN(THETA)*SIN(PHIL)
OS(3) = DISTL*COS(THETA)
C
C      SP IS VECTOR FROM POINT OF INTREST TO POINT ON VORTEX
SP(1) = OP(1) - OS(1)
SP(2) = OP(2) - OS(2)
SP(3) = OP(3) - OS(3)
C
C      VV IS VECTOR IN DIRECTION OF TANGENTIAL VELOCITY
CALL CROSS(SP,PQ,VV)
VMPO = VMAG(PQ)
VMVV = VMAG(VV)
C
C      D IS DISTANCE FROM VORTEX AXIS TO POINT OF INTREST
D = VMVV/VMPO
FX = EXP(-WR*D**2/(4.*UNU*7))
C
C      VMVT IS MAGNITUDE OF THE TANGENTIAL VELOCITY AT THE POINT
VMVT = GAMMAC*(1. - FX)/(2.*PI*D)
VMVTD = VMVT/VMVV
C
C      VT IS THE TANGENTIAL VELOCITY VECTOR AT POINT OF INTREST
VT(1) = VMVTD*VV(1)
VT(2) = VMVTD*VV(2)
VT(3) = VMVTD*VV(3)
C
C      VMAVT IS MAGNITUDE OF AXIAL VELOCITY AT POINT OF INTREST
VMAVT = DZFRQ*FX/(4.*PI*RHO*UNU*7)
VMAVTD = VMAVT/VMPO
AVT(1) = VMAVTD*PQ(1)
AVT(2) = VMAVTD*PQ(2)
AVT(3) = VMAVTD*PQ(3)
C
C      VLINE1 IS LINE OF SIGHT COMPONENT OF TANGENTIAL VELOCITY
VLINE1 = -DOT(VT,OS)/DISTL
C
C      VLINE2 IS LINE OF SIGHT COMPONENT OF AXIAL VELOCITY
VLINE2 = -DOT(AVT,OS)/DISTL
C
C      VLINE IS TOTAL LINE OF SIGHT VELOCITY COMPONENT
VLINE = VLINE1 + VLINE2
RETURN

```

END

```

$IRETC PSCAN  DECK
      SUBROUTINE PSCAN(NEW)
C
C           THIS ROUTINE HANDLES THE PLOTTING OF THE VELOCITIES
C
      COMMON / A02 / TITLE(12)
      COMMON / A03 / V(20,20,20)
      COMMON / A04 / PTD1(20,3)
      COMMON / A09 / PTD(3,3)
      COMMON / A10 / VV(20,20), VVV(20,20)
      COMMON / A11 / ISYM(20), FLDX(12,3), FLDY(12)
      COMMON / A12 / DPTD(3)
      DIMENSION LAB(2,3)
      DIMENSION NPTD(3,3)
      DIMENSION ABC(20)
      EQUIVALENCE (PTD,NPTD)
      DATA (LAB(I,1),I=1,2) / 6H      P,6HHI = /
      DATA (LAB(I,2),I=1,2) / 6H      THF,6HTA = /
      DATA (LAB(I,3),I=1,2) / 6HDISTAN,6HCF = /
      DATA ISYM / 17,18,19,20 ,21 ,22,23,24,25,33 ,34,35,36,37,38,39,
1 40,41,50,51/
      DATA (FLDX(I,1),I=1,12) / 6HPhi IN,6H DEGRF,6HES      ,9*1H /
      DATA (FLDX(I,2),I=1,12) / 6HTheta ,6HIN DFG,6HREES ,9*1H /
      DATA (FLDX(I,3),I=1,12) / 6HDISTAN,6HCF IN ,6HMETERS,9*1H /
      DATA FLDY / 6HVELOCI,6HTY IN ,6HDIRECT,6HION OF,6H LASER,
$ 6H      MF,6HTRS/S,6HEC      ,4*1H /
      DATA ABC /2HA=,2HB=,2HC=,2HD=,2HE=,2HF=,2HG=,2HH=,2HI=,2HJ=,2HK=,
$ 2HL=,2HM=,2HN=,2HO=,2HP=,2HQ=,2HR=,2HS=,2HT=/
      CALL CAMPAV(9 )
C
C           CALL FOR PLOTTING OF INPUT
      CALL PINPUT
C
C           READ PLOTTING INSTRUCTION
C           ILINE = 0 INDICATES NO LINES BETWEEN PLOTTED POINTS
C           ILINE = 1 INDICATES LINES BETWEEN PLOTTED POINTS
C           IX = 1 INDICATES PHI TO BE PLOTTED ON HORIZONTAL AXIS
C           IX = 2 INDICATES THETA TO BE PLOTTED ON HORIZONTAL AXIS
C           IX = 3 INDICATES RANGE TO BE PLOTTED ON HORIZONTAL AXIS
C           IY = 1 INDICATES PHI TO BE PLOTTED ON VERTICAL AXIS
C           IY = 2 INDICATES THETA TO BE PLOTTED ON VERTICAL AXIS
C           IY = 3 INDICATES RANGE TO BE PLOTTED ON VERTICAL AXIS
10 READ(5,500) ILINE, IX, IY
500 FORMAT (3I10)
      IF(IX .LE. 0 .OR. IY .LE. 0) GO TO 400
      IZ = 6 - IX - IY
      NX = NPTD(3,IX)
      NY = NPTD(3,IY)
      NZ = NPTD(3,IZ)
      NNX = NX
      IF(ILINE .GT. 0) NNX = -NX
      DO 200 K=1,NZ
      VMAX =-1.E30
      VMIN = 1.E30
      GO TO (12,13,14),IX
12 GO TO (15,16,17),IY
13 GO TO (18,15,19),IY
14 GO TO (20,21,15),IY

```

```

15 WRITE(6,610)
610 FORMAT(23H *** ERROR *** IX = IY)
GO TO 10
16 ASSIGN 26 TO IP
GO TO 40
17 ASSIGN 27 TO IP
GO TO 40
18 ASSIGN 28 TO IP
GO TO 40
19 ASSIGN 29 TO IP
GO TO 40
20 ASSIGN 30 TO IP
GO TO 40
21 ASSIGN 31 TO IP
40 DO 41 J=1,NY
DO 41 I=1,NX
GO TO IP,(26,27,28,29,30,31)
26 VV(I,J) = V(I,J,K)
GO TO 32
27 VV(I,J) = V(I,K,J)
GO TO 32
28 VV(I,J) = V(J,I,K)
GO TO 32
29 VV(I,J) = V(K,I,J)
GO TO 32
30 VV(I,J) = V(J,K,I)
GO TO 32
31 VV(I,J) = V(K,J,I)
32 IF(VV(I,J) .GT. VMAX) VMAX = VV(I,J)
41 IF(VV(I,J) .LT. VMIN) VMIN = VV(I,J)
IF(VMAX .LE. VMIN) GO TO 200
DDV=(VMAX - VMIN)*.25
L=0
IIA = DDV*10000.
IA=IIA
50 L=L+1
IA=IA/10
IF(IA.NE.0) GO TO 50
DV = (IIA/10**(L-1))*10**(L-1)
DV = DV*.0001
DO 55 J=2,NY
DO 55 I=1,NX
55 VVV(I,J) = VV(I,J) + DV*FLOAT(J-1)
VMAXV = VMAX + DV*FLOAT(NY-1)

```

Reproduced from  
best available copy.

```

C
C          PLOTS VARIABLE OF HORIZONTAL AXIS VERSUS VELOCITY
CALL QUIK3L(-1,PTD(1,IX),PTD(2,IX),VMIN,VMAXX,ISYM(1),FLOX(1,IX),
& FLOV,NNX,PTD1(1,IX),VV(1,1))
DO 100 J=2,NY
100 CALL QUIK3L(0,DUM,DUM,DUM,DUM,ISYM(J),DUM,DUM,NNX,PTD1(1,IX),
& VVV(1,J))
CALL PRINTV(72,TITLE, 32,1008)
CALL PRINTV(10,LAB(1,I7),616,988)
CALL LABLV(PTD1(K,I2),704,988,-6,1,6)
CALL PRINTV( 4, 4HDV =,840, 988)
CALL LABLV(DV,880, 988,-6,1,6)
CALL FRAMEV
CALL PRINTV(72,TITLE,124,1008)

```

```

CALL PRINTV(10,LAB(1,17),740,1008)
CALL LABLV(PTD1(K,17),828,1008,-6,1,6)
CALL PRINTV(18,FLDX(1,IX),440,16)
CALL APRNTV(0,-16,18,FLDX(1,IY),16,656)
CALL GRID1V(2,PTD(1,IX),PTD(2,IX),PTD(1,IY),PTD(2,IY),DPTD(IX),
DPTD(IY),50,50,-2,-2,-5,-5)

```

```

C
IABC = 144
JABC = 168
KK=1
NV = VMAX/5.
VCON = NV*5
IF(VMAX .LT. 0.) VCON = VCON - 5.
VCON1 = VCON
210 IF(VCON .LT. VMIN) GO TO 225
CALL PRINTV(2,ABC(KK),IABC,988 )
CALL LABLV(VCON,JABC,988,3,1,3)
DO 220 I=1,NX
IV=2
IF(VCON .GT. VV(I,1)) IV=1
DO 220 J=2,NY
GO TO (222,223),IV
222 IF(VCON .GT. VV(I,J)) GO TO 220
IV = 2
GO TO 224
223 IF(VCON .LT. VV(I,J)) GO TO 220
IV = 1
224 VP = (VCON - VV(I,J-1))/(VV(I,J)-VV(I,J-1))
VVP = VP*(PTD1(J ,IY)-PTD1(J-1,IY)) + PTD1(J-1,IY)

```



```

C
C          PLOTS VELOCITY CONTOUS
CALL APLTV(1,PTD1(I,IX),VVP,1,1,1,ISYM(KK),IFRR)
220 CONTINUE
KK= KK+1
VCON = VCON - 5.
IABC = IABC + 56
JABC = JABC + 56
GO TO 210
225 KK=1
VCON =VCON1
230 IF(VCON .LT. VMIN) GO TO 200
DO 226 J=1,NY
IV = 2
IF(VCON .GT. VV(1,J)) IV = 1
DO 226 I=2,NX
GO TO (227,228),IV
227 IF(VCON .GT. VV(I,J)) GO TO 226
IV = 2
GO TO 229
228 IF(VCON .LT. VV(I,J)) GO TO 226
IV = 1
229 VP = (VCON - VV(I-1,J))/(VV(I,J) - VV(I-1,J))
VVP = VP*(PTD1(I,IX) - PTD1(I-1,IX)) + PTD1(I-1,IX)

```

```

C
C          PLOTS VELOCITY CONTOUS
CALL APLTV(1,VVP,PTD1(J,IY),1,1,1,ISYM(KK),IFRR)
226 CONTINUE
KK = KK + 1

```

VCON = VCON -5.  
GO TO 230  
200 CONTINUE  
GO TO 10  
400 CALL CLEAN  
RETURN  
END

```

$IPETC PINPUT DECK
SUBROUTINE PINPUT
COMMON / A01 / OP(3), PO(3)
COMMON / A02 / TITLE(12)
COMMON / A06 / GAMMAC, WB, UNU, Z
COMMON / A09 / PHI1, PHI2, NPFI, THETA1, THETA2, NTHETA, DIST1,
5 DIST2, NDIST
COMMON / A14 / DZERO, RHO
COMMON / A20 / PSI, R, FLAMDA, PLENGT, ICHOIC, NWEIGH, IOUT,
8 IPLOT, IPLOT1, IVMAX
CALL SCOUTV(9 )
WRITE (16,600)
WRITE (16,600) TITLE
600 FORMAT (1H1,24X,12A6)
WRITE (16,610) GAMMAC, WB, UNU, Z, OP, PO, PHI1, PHI2, NPFI,
1 THETA1, THETA2, NTHETA, DIST1, DIST2, NDIST, PSI, R, FLAMDA,
2 PLENGT, DZERO, RHO, ICHOIC, NWEIGH, IOUT, IPLOT, IPLOT1, IVMAX
610 FORMAT(//51X,16HNAMELIST (INPUT),//
1 12H GAMMAC      =,F16.8,3X,11HWR      =,F16.8,3X,
2 11HUNU          =,E16.8,3X,11HZ       =,F16.8,/
3 12H OP(1)       =,E16.8,3X,11HOP(2)    =,F16.8,3X,
4 11HOP(3)        =,F16.8,/
5 12H PO(1)       =,F16.8,3X,11HPO(2)    =,F16.8,3X,
6 11HPO(3)        =,E16.8,/
7 12H PHI1        =,E16.8,3X,11HPHI2     =,F16.8,3X,
8 11HNPFI         =,I8,/
9 12H THETA1      =,E16.8,3X,11HTHETA2    =,F16.8,3X,
A 11HNTHETA       =,I8,/
B 12H DIST1       =,F16.8,3X,11HDIST2     =,F16.8,3X,
C 11HNDIST        =,I8,/
D 12H PSI         =,F16.8,3X,11HR        =,F16.8,3X,
E 11HFLAMDA       =,F16.8,3X,11HPLENGT    =,F16.8,/
F 12H DZERO       =,F16.8,3X,11HRHO      =,F16.8,3X,
G 11HICHOIC       =,I8,11X ,11HNWEIGH    =,I8,/
H 12H IOUT        =,I8,11X ,11HIPLLOT    =,I8,11X,
I 11HIPLLOT1      =,I8,11X ,11HIVMAX     =,I8)
RETURN
END

```

```

$IBETC CROSS    DECK
      SUBROUTINE CROSS(VA,VB,VC)                                CROSS
C      SUBROUTINE TO PERFORM CROSS PRODUCT                    CROSS
C      VECTOR VA IS CROSSED INTO VECTOR VB TO FORM VECTOR VC  CROSS
      DIMENSION VA(3),VB(3),VC(3)                             CROSS
      VC(1)=VA(2)*VB(3)-VB(2)*VA(3)                            CROSS
      VC(2)=VA(3)*VB(1)-VB(3)*VA(1)                            CROSS
      VC(3)=VA(1)*VB(2)-VB(1)*VA(2)                            CROSS
      RETURN                                                    CROSS
      END                                                        CROSS
$IBETC DOT      DECK
      FUNCTION DOT(VA,VB)                                       DOT
C      FUNCTION TO PERFORM DOT PRODUCT                         DOT
      DIMENSION VA(3), VB(3)                                   DOT
      DOT=VA(1)*VB(1)+VA(2)*VB(2)+VA(3)*VB(3)                 DOT
C      VECTOR VA IS DOTTED INTO VECTOR VB TO FORM THE SCALAR DOT PRODUCT DOT
      RETURN                                                    DOT
      END                                                        DOT
$IBETC VMAG     DECK
      FUNCTION VMAG(VA)                                         VMAG
C      FUNCTION TO DETERMINE VECTOR MAGNITUDE                 VMAG
      DIMENSION VA(3)                                          VMAG
      VMAG = SQRT(VA(1)*VA(1)+VA(2)*VA(2)+VA(3)*VA(3))        VMAG
      RETURN                                                    VMAG
      END                                                        VMAG

```

```

$DATA
  EXAMPLE FOR VOLUME SCANNING PROGRAM
$INPUT
  GAMMAC = 729.0
  WR = 77.3
  UNU = .0014
  Z = 1000.0
  DZERO = 50000.0
  RHO = 1.192
  DP = 0.0, 0.0, 50.0
  PO = 1.0, 0.0, 0.0
  PHI1 = 3.0
  PHI2 = -3.0
  NPFI = 11
  THETA1 = 48.0
  THETA2 = 42.0
  NTHETA = 11
  DIST1 = 69.0
  DIST2 = 71.0
  NDIST = 11
  FLAMDA = .0000106
  PSI = 1.0
  ICHOIC = 1
  R = .0762
  NWEIGH = 12
  IQUT = 3
  IPLOT = 1
  IPLOT1 = 1
  IVMAX = 1

```

```

$
  1      1      2
  1      3      2

```

Appendix C  
LASER VELOCIMETER LINE SCAN SIMULATION PROGRAM

C-1 (a)

Appendix C

## C.1 DESCRIPTION

Program simulates one vortex and scans it in a straight line with one or two laser velocimeters. A sequence of vortex positions, scan positions and laser parameters is automatically run for comparisons. Outputs are plots of velocity versus position.

## C.2 CAPABILITIES

1. Vortex can be in any position.
2. The tangential and axial velocity profile of the vortex can be input with different values.
3. Constant winds can be added.
4. The vortex positions, scan positions and laser parameters of the automatic sequence can be altered.
5. For two lasers the separations may be altered.

## C.3 RESTRICTIONS

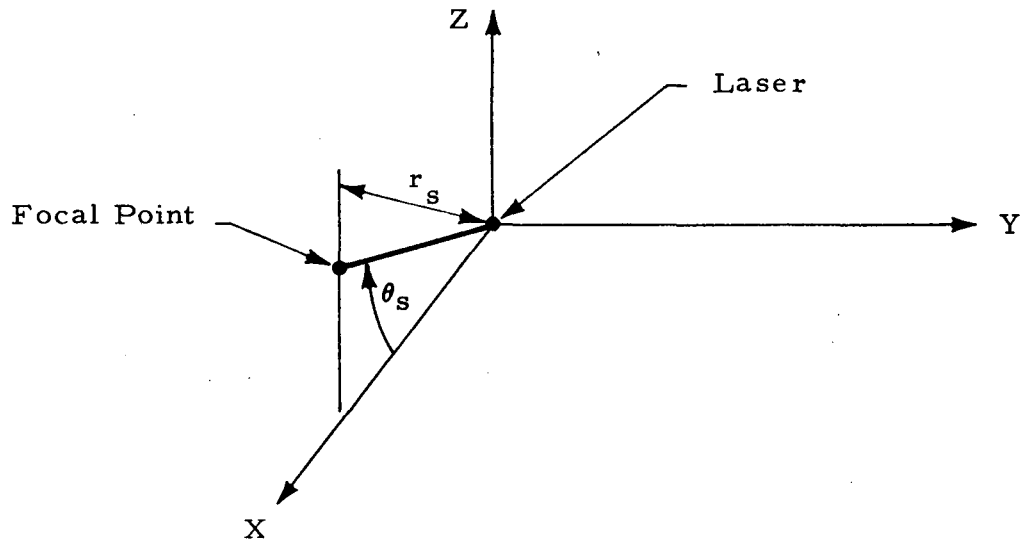
1. Infinite S/N is assumed.
2. Aerosol is assumed to be constant throughout the vortex.
3. The vortex is assumed to be uniform along its length.
4. The vortex axis is assumed to be a straight line.
5. No change in vortex position or strength is allowed with change in time.

C-1 (b)

6. Scanning is restricted, for one laser scanning is either in line with the laser (range scan) or perpendicular to that line (lateral scan). For two lasers, the scanning is the same as if there were one laser directly in between the two and the single laser controlled the scanning.

C.4 POLAR COORDINATE SYSTEM OF LASER

The laser's focal point orientation is represented in a polar coordinated system in the XZ plane of the rectangular coordinate system.



The transformation from the polar coordinate system to the laser's rectangular coordinate system is

$$X_s = r_s \cos \theta_s$$

$$Y_s = 0$$

$$Z_s = r_s \sin \theta_s$$

C.5 SCANNING OF LASER

With one laser the scanning is done with  $r_s$  constant (LATERAL SCAN) or with  $\theta_s$  constant (RANGE SCAN). With two lasers the scanning is treated as

in the one laser case but using a reference point directly between the two lasers. A sample of these is shown in Fig. C-1. In this figure the vortex is shown in its normal position with its axis parallel to the Y axis of the rectangular coordinate system.

C.6 COMPUTATION OF TANGENTIAL VELOCITY COMPONENT OF VORTEX IN DIRECTION OF LASER

This is computed the same way as shown in Appendix B.

C.7 COMPUTATION OF AXIAL VELOCITY COMPONENT OF VORTEX IN DIRECTION OF LASER

This is computed the same way as shown in Appendix B.

C.8 COMPUTATION OF VELOCITY INTERPRETED BY A COAXIAL FOCUSED LASER DOPPLER SYSTEM

This is computed the same way as shown in Appendix B.

C.9 COMPUTATION OF VELOCITY INTERPRETED BY A COAXIAL PULSED LASER DOPPLER SYSTEM

This is computed the same way as shown in Appendix B.

C.10 COMPUTATION OF VELOCITY INTERPRETED BY A COAXIAL FOCUSED CONTINUOUS WAVE LASER OR A COAXIAL PULSED LASER USING THE HIGHEST ACTIVATED FILTER TECHNIQUE

In addition to the centroid method described in Appendix B this program can use the technique of highest activated filter. The same weighting over the illuminated volume is used but in this case the weighting value for each sampled location is added to a slot representing a filter sensitive to a particular velocity range. After the illuminated volume has been sampled, the line of sight velocity representing the volume is chosen to be the mid point of the filter, representing the highest velocities, which has a predetermined fraction of the signal or more.

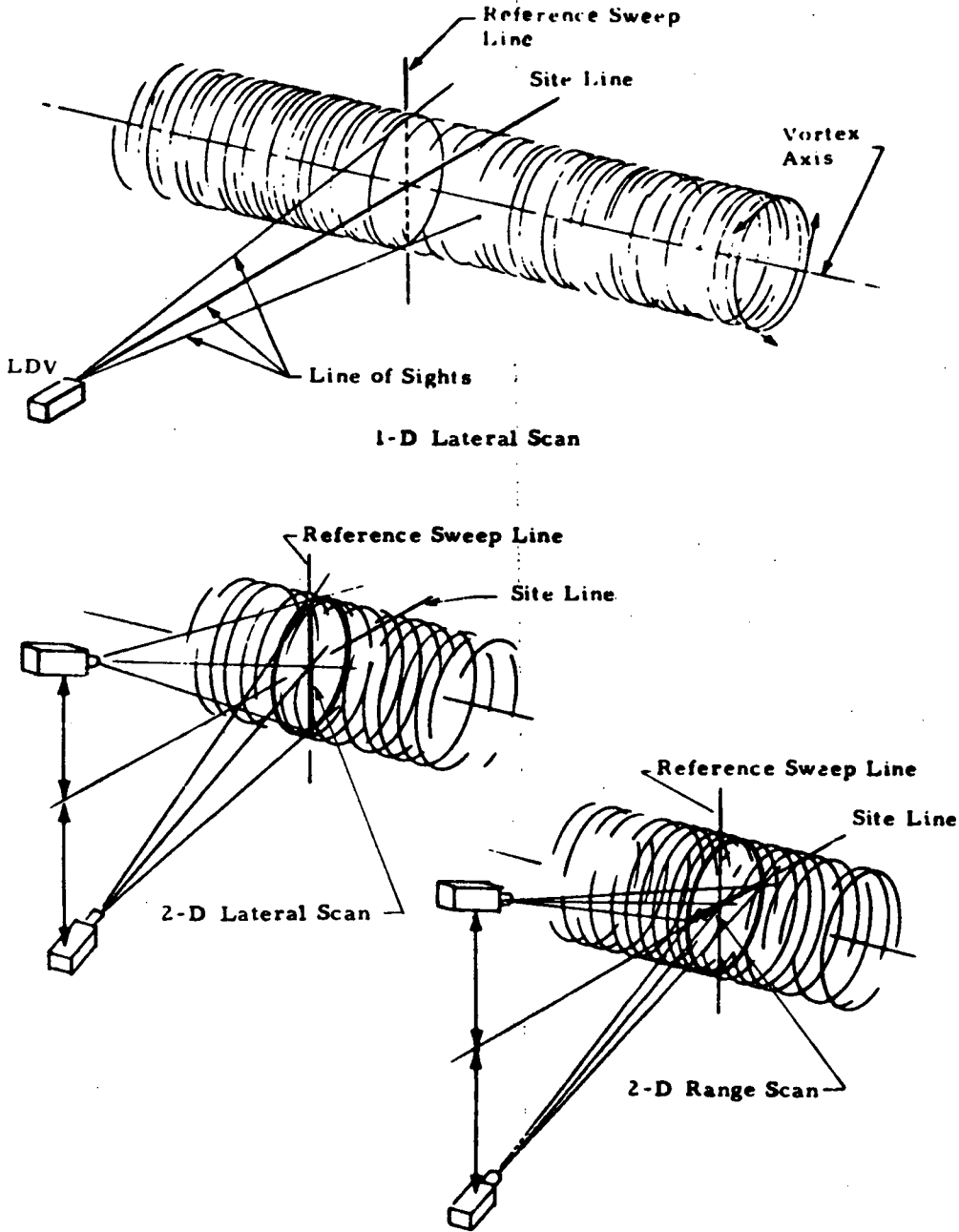


Fig. C-1 - Scanning Nomenclature

C.11 INPUT FOR LASER VELOCIMETER LINE SCAN SIMULATION PROGRAM

The first input is a title card (columns 1 through 72). Then three name-lists comprise the remainder of the input. Their names are VORTEX, SYSTEM, and SCAN. They must be input in that order. All input variables have preset values. The values describing the vortex velocity flow field are representative of that produced by a Boeing 747 while landing.

Namelist VORTEX has the following variables.

<u>Name</u>	<u>Preset Value</u>	<u>Units</u>	<u>Description</u>
GAMMAC	729.0	n-m-sec/kg	Circulation of vortex from generating aircraft.
W8	77.3	m/sec	Freestream velocity
UNU	.0914	m <sup>2</sup> /sec	Eddy viscosity
Z	1000.0	m	Down stream distance of vortex from generating aircraft.
DZERO	50000.0	N	Profile drag of the aerofoil (used for axial velocity. If no axial velocity wanted set DZERO to zero).
RHO	1.192	kg/m <sup>3</sup>	Density of atmosphere
VROTH	0.	deg	Vortex rotation about reference sweep line
VROTHC	10.	deg	Change in vortex rotation about reference sweep line.
VROTV	0.	deg	Vortex rotation about site line.
VROTV C	10.	deg	Change in vortex rotation about site line
NRANGE	2.0	none	Indicates nominal vortex range
VRANGE(8)	50.0 100.0 300.0 1000.0	m	Vortex ranges

<u>Name</u>	<u>Preset Value</u>	<u>Units</u>	<u>Description</u>
	3000.0		
	5000.0		
	-1.0		
	-1.0		
VMAX	34.0	m/sec	Upper velocity bound on plotting scale
VMIN	0	m/sec	Lower velocity bound on plotting scale

Namelist SYSTEM has the following variables.

IUNITS	1.0	none	FLAG IUNITS = 1 indicates one laser IUNITS = 2 indicates two lasers
ICHOIC	1.0	none	FLAG ICHOIC = 1 indicates continuous wave focused laser ICHOIC = 2 indicates pulsed laser
PSI	1.0	-	Controls magnitude of weighting factor. Leave set to 1.
FLAMDA	.0000106	m	Wave length of laser light
NR	2.0	none	Indicates nominal radius of telescope aperture
R(8)	0.1 0.2 0.3 0.5 1.0 2.0 4.0 6.0	m	Radius of telescope aperture
NPLENG	2.0	none	Indicates nominal pulse length

<u>Name</u>	<u>Preset Value</u>	<u>Units</u>	<u>Description</u>
PLENGT(8)	30.0	m	Pulse length
	90.0		
	150.0		
	300.0		
	900.0		
	-1.0		
	-1.0		
WEIGHL	0.5	m	Distance between sample points used in weighing
IABS	1.0	none	Flag IABS = 1 indicates no distinction between negative and positive velocities are detected IABS = 2 indicates positive and negative velocities are detected.
SLASER	0.0	m	Distance of half laser's separation along site line
DLASER	0.0	m	Distance of laser from sweep plane
ELASER	100.0	m	Distance of lasers from site line in sweep plane

Namelist SCAN has the following variables.

IDIREC	1.0	none	Flag IDIREC = 1 indicates lateral scan IDIREC = 2 indicates range scan
SCAWL	30.0	m	Scan length
SCANR	0.5	m	Scan resolution
NSWEEP	3.0	none	Indicates nominal sweep position
SWEEP(5)	-15.0	m	Sweep positions
	-7.0		
	0		
	7.0		
	15.0		

<u>Name</u>	<u>Preset Value</u>	<u>Units</u>	<u>Description</u>
IVMAX	2	none	Flag IVMAX = 1 indicates the maximum minus the minimum line-of-sight velocities observed in the illuminated volume will be plotted as X. IVMAX = 2 indicates the maximum of the absolute line-of-sight velocities observed in the illuminated volume will be plotted as X.
IWEIGH	1	none	Flag IWEIGH = 1 indicates that the highest activated filter will be plotted as W IWEIGH = 2 indicates that the centroid of the weighted velocities will be plotted as W
WFILT	0.94	megahertz	Band width of filters
DETLEV	0.1	none	Detection level in fraction of signal for filters
OFSETX(2)	0 0	m	Offset of laser focus point along site line due to misalignment
OFSETY(2)	0 0	m	Offset of laser focus point from scan plane due to misalignment
OFSETZ(2)	0 0	m	Offset of laser focus point along sweep line due to misalignment
WIND(3)	0 0 0	m/sec	Constant WIND vector

After case is completed, control returns to start of program.

## C.12 OUTPUT FOR LASER VELOCIMETER LINE SCAN SIMULATION PROGRAM

The input is outputted on both the printer and the plotter. See Fig. C-2.

The remainder of the output consists of five plots each containing three graphs with four curves. Examples of these are shown in Figs. C-3 through C-7. The four curves that appear on each graph are identified by four letters W, X, T and L. They are all velocities plotted as a function of position.

W is velocity of the highest activated filter or as indicated by the input IWEIGH, or in other cases W is the centroid of the weighted velocities.

X is the maximum of the absolute line-of-sight velocities observed in the illuminated volume, or as indicated by the input IVMAX. In other cases X is the maximum minus the minimum line-of-sight velocities observed in the illuminated volume.

T is the norm of the total velocity vector at the focal point.

L is the line of sight velocity at the focal point.

The first plot Fig. C-3 contains three graphs in which each represents a different sweep position. For the lateral scan, the sweep position represents a difference in range between the vortex axis and the sweep. For the range scan, the sweep position represents the distance that the sweep has missed the axis.

The second plot Fig. C-4 contains three graphs in which each one represents a different vortex range. The center graph is identical to the center graph of Fig. C-3. This graph is called the nominal. It appears in the center of each plot and only one parameter for each of the plots will vary with the graphs.

The third plot, Fig. C-5, contains three graphs in which the vortex is rotated in different amounts about the reference sweep line.

The fourth plot, Fig. C-6, contains three graphs in which the vortex is rotated in different amounts about the site line.

The fifth plot, Fig. C-7, contains three graphs in which the telescope aperture radius is different for each. Or in the case where a pulsed laser is used, the three graphs represent different pulse lengths.

For two lasers W, X and L are the resultants from the components seen by the two lasers. However, since X has no sign, it often badly represents the velocity. T is still the norm of the total velocity vector at the focal point. In the event of misalignment the focal point that T represents is that of the second laser.

CASE NO 24 1 LASER RANGE 300 LATERAL SCAN FILTERS

NAMelist (VORTEX)

GAMMAC	=	0.72900000E 03	WB	=	0.77300000E 02	UNU	=	0.91400000E-01	Z	=	0.10000000E 04
DZERO	=	0.00000000E-38	RHO	=	0.11920000E 01	VROTH	=	0.00000000E-38	VROTHC	=	0.30000000E 02
VROTV	=	0.00000000E-38	VROTVC	=	0.30000000E 02	NRANGE	=	3			
VRANGE (1)	=	0.30000000E 02	VRANGE (2)	=	0.10000000E 03	VRANGE (3)	=	0.30000000E 03	VRANGE (4)	=	0.10000000E 04
VRANGE (5)	=	0.30000000E 04	VRANGE (6)	=	0.50000000E 04	VRANGE (7)	=	-0.10000000E 01	VRANGE (8)	=	-0.10000000E 01
VMAX	=	0.34000000E 02	VWIN	=	0.00000000E-38						

NAMelist (SYSTEM)

IUNIT8	=	1									
ICHOIC	=	1	PSI	=	0.10000000E 01	FLANDA	=	0.10000000E-04	NR	=	2
R (1)	=	0.10000000E 00	R (2)	=	0.20000000E 00	R (3)	=	0.30000000E 00	R (4)	=	0.50000000E 00
R (5)	=	0.10000000E 01	R (6)	=	0.20000000E 01	R (7)	=	0.40000000E 01	R (8)	=	0.80000000E 01
NPLENG	=	- 2									
PLENGT (1)	=	0.30000000E 02	PLENGT (2)	=	0.90000000E 02	PLENGT (3)	=	0.15000000E 03	PLENGT (4)	=	0.30000000E 03
PLENGT (5)	=	0.90000000E 03	PLENGT (6)	=	-0.10000000E 01	PLENGT (7)	=	-0.10000000E 01	PLENGT (8)	=	-0.10000000E 01
WEIGHL	=	0.90000000E 00	IABS	=	1	SLASER	=	0.00000000E-38	DLASER	=	0.00000000E-38
ELASER	=	0.10000000E 03									

NAMelist (SCAN)

IDIREC	=	1	SCANL	=	0.30000000E 02	SCANR	=	0.50000000E 00	NSWEEP	=	3
SWEPP (1)	=	-0.70000000E 01	SWEPP (2)	=	-0.20000000E 01	SWEPP (3)	=	0.00000000E-38	SWEPP (4)	=	0.70000000E 01
SWEPP (5)	=	0.15000000E 02									
IWMX	=	2	IWEIGH	=	1	WFILT	=	0.94000000E 00	DETLEV	=	0.10000000E 00
OFSETX (1)	=	0.00000000E-38	OFSETX (2)	=	0.00000000E-38	OFSETY (1)	=	0.00000000E-38	OFSETY (2)	=	0.00000000E-38
OFSETZ (1)	=	0.00000000E-38	OFSETZ (2)	=	0.00000000E-38						
WIND (1)	=	0.00000000E-38	WIND (2)	=	0.00000000E-38	WIND (3)	=	0.00000000E-38			

Fig. C-2 - Output for Laser Velocity Line Scan Simulation Program

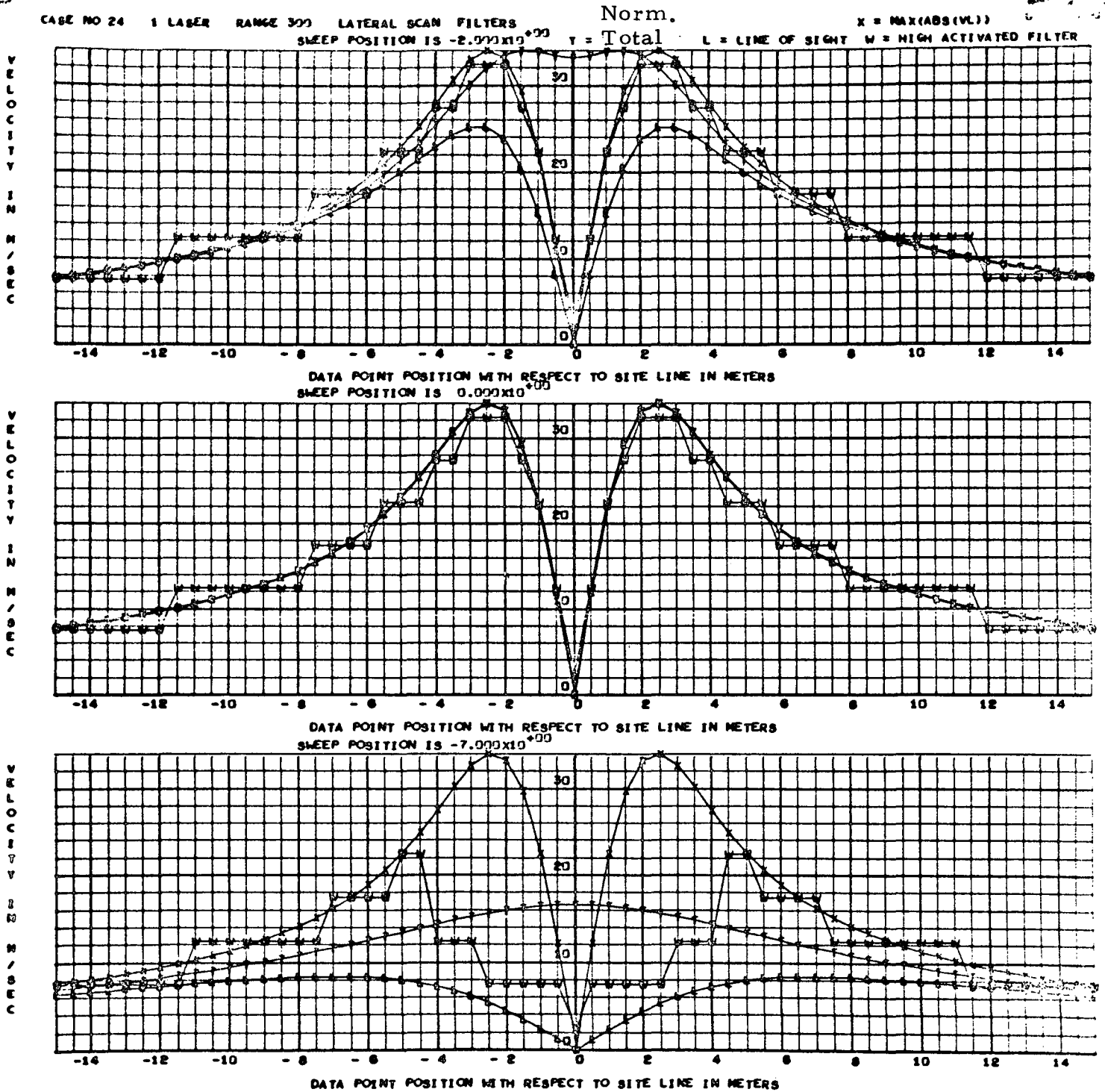


Fig. C-3 - Example Output

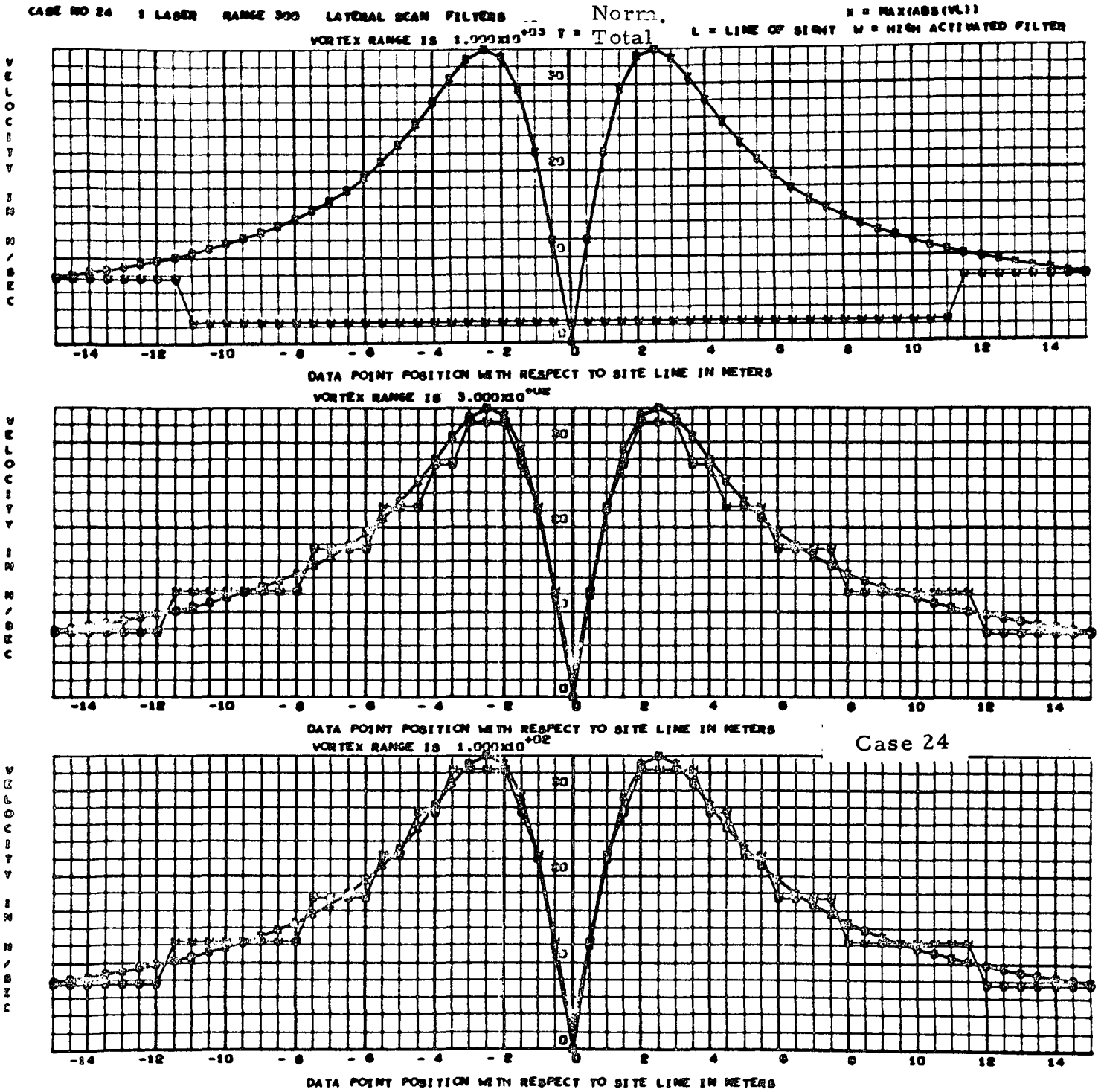


Fig. C-4 - Example Output

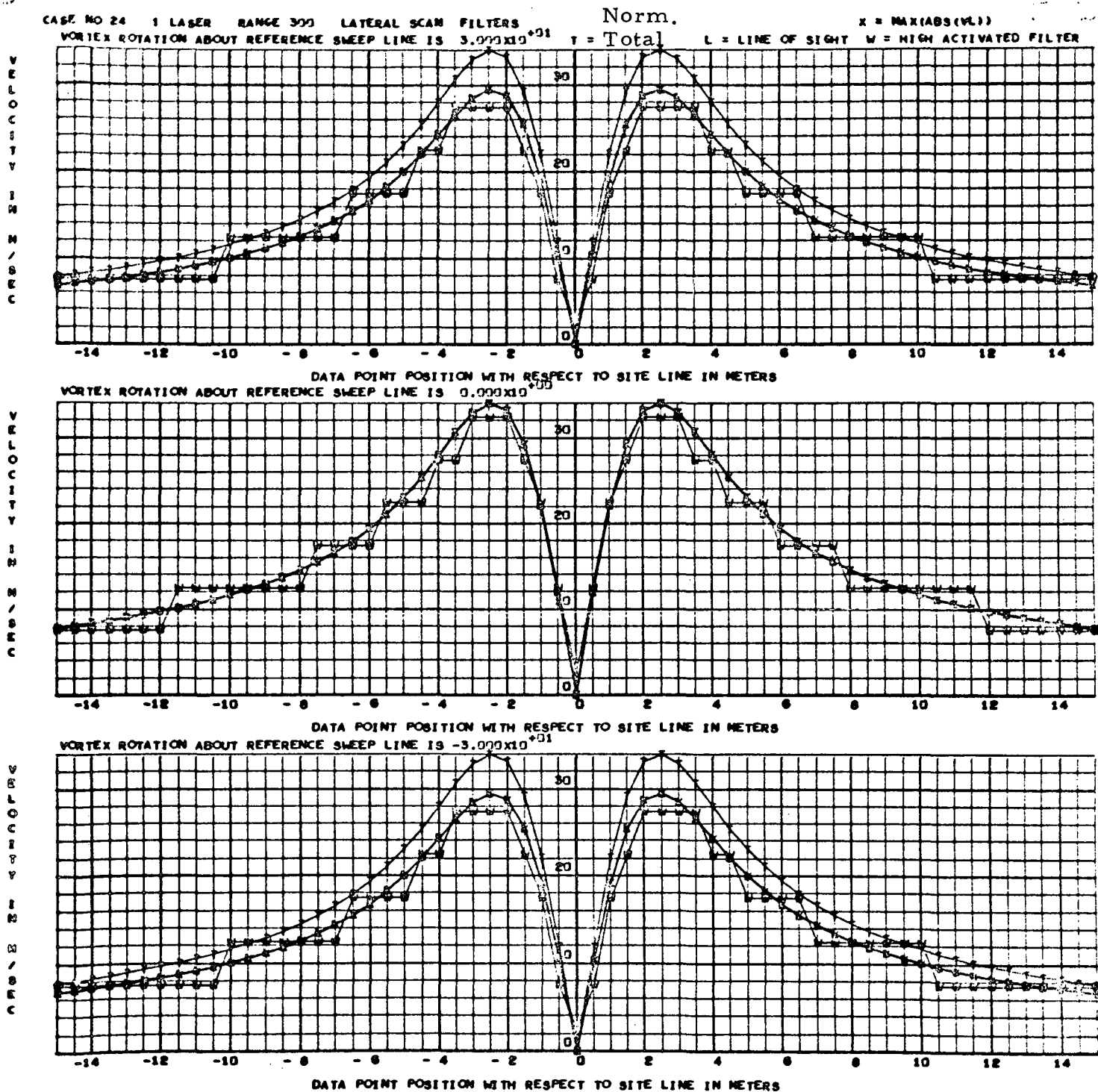


Fig. C-5 - Example Output

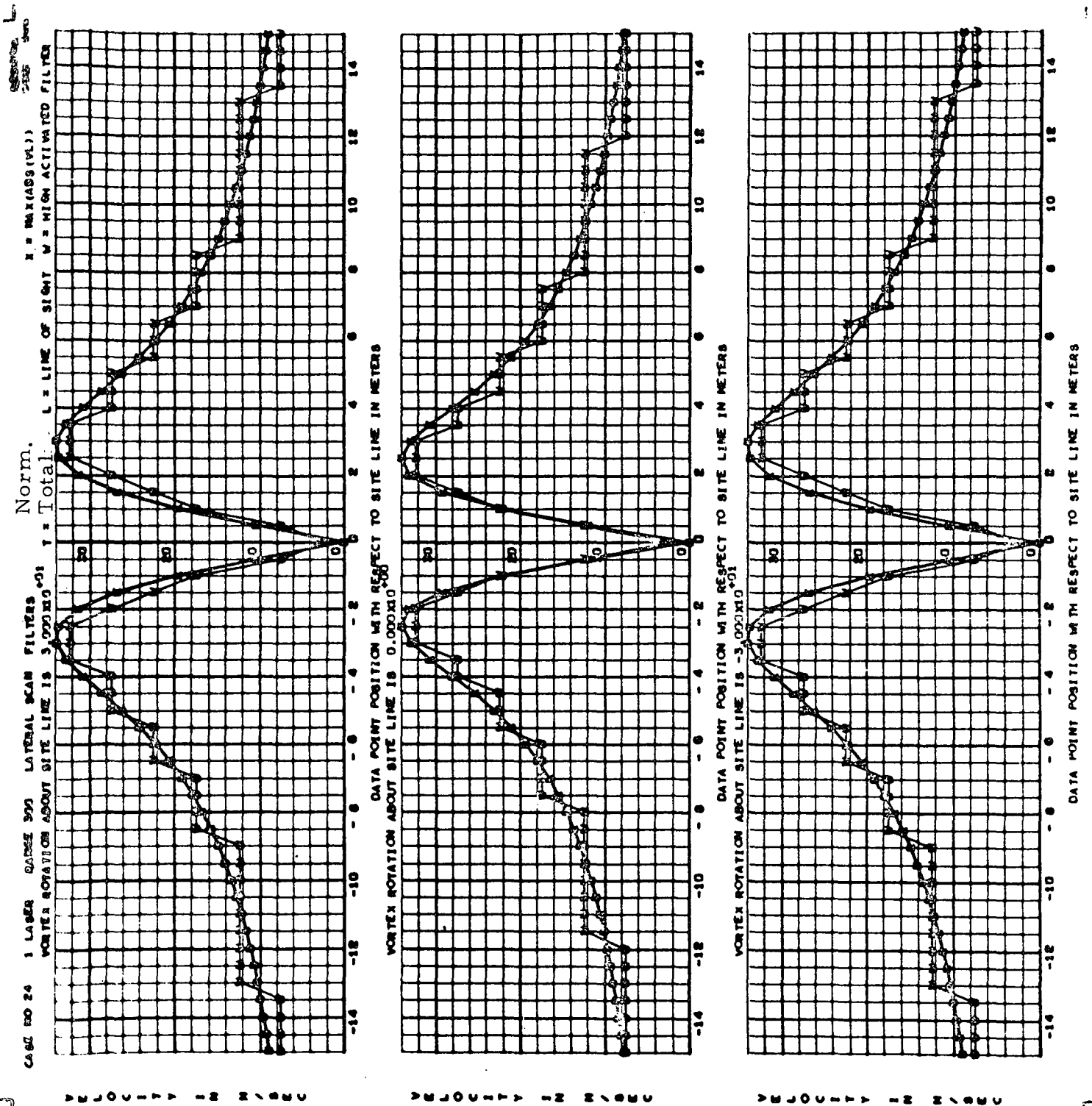


Fig. C-6 - Example Output

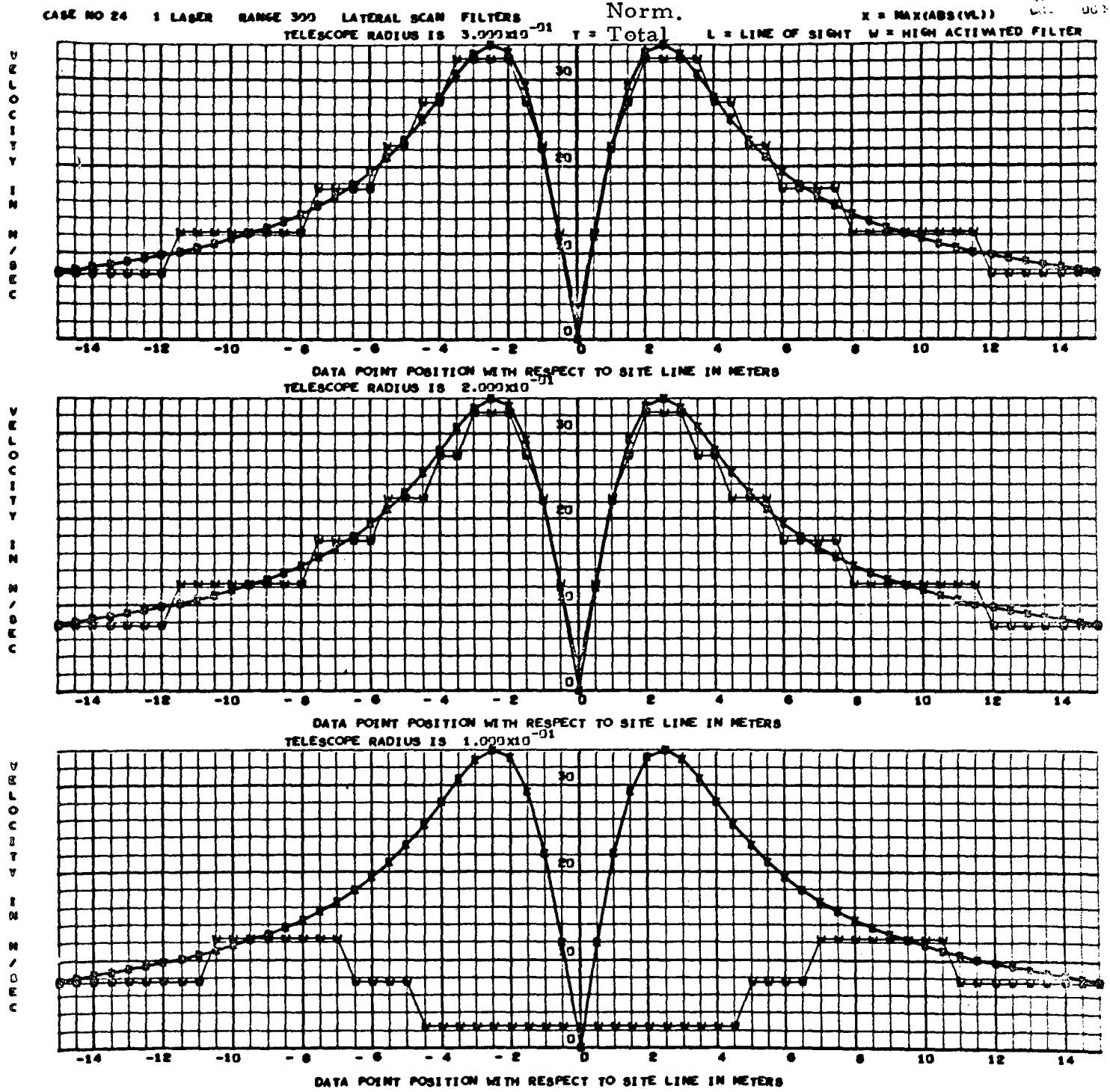


Fig. C-7 - Example Output

C.13 EXAMPLE RUN FOR LASER VELOCIMETER LINE SCAN  
SIMULATION PROGRAM

As an example, the axial component of the vortex 1000 meters downrange from a Boeing 747, will be examined. For the nominal case, let the vortex be parallel to the Y axis at a range of 300 meters. For the laser system, one continuous wave focused, CO<sub>2</sub> laser will be simulated. Assume that the velocity sign cannot be determined. Let the nominal telescope aperture radius be 0.2 meters.

A lateral scan of 30 meters with 0.5 meter increment is used. Let the nominal sweep portion go through the center of the vortex. On the W curve the filter response is observed, and on the X curve the maximum velocity in the focal volume is observed.

The first input must be the title card. CASE NO.24 1 LASER RANGE  
300 LATERAL SCAN FILTERS.

The next input is the namelist VORTEX for its variables.

GAMMAC	leave preset to 729.0	}	Set for Boeing 747
W8	leave preset to 77.3		
UNU	leave preset to 0.0914		
Z	leave preset to 1000		
DZERO	set to 0		Since no axial velocity is desired
RHO	leave preset to 1.192		Typical low altitude density
VROTH	leave preset to 0		
VROTHC	set to 30		To look at larger off- nominal vortex rotations
VROTV	leave preset to 0		
VROTV C	set to 30		To look at larger off- nominal vortex rotations
NRANGE	set to 3		300 meters is the third preset value for VRANGE
VRANGE	leave as preset		

VMAX	leave preset to 34	Good value for selected vortex
VMIN	leave preset to 0	Since all velocity will be positive, zero is a good lower limit

The next namelist to be inputted is SYSTEM. For its variables:

IUNITS	leave preset to 1	
ICHOIC	leave preset to 1	
PSI	leave preset to 1	
FLAMDA	leave preset to 0.0000106	This is the wavelength of light emitted from a CO <sub>2</sub> laser
NR	leave preset to 2	0.2 meters is the second preset value for R
R	leave as preset	
NPLENG	leave as preset	This is of no significance since pulses are not being used
PLENGT	leave as preset	
WEIGHL	leave preset to 0.5	This is a reasonable interval to sample the illuminated volume
IABS	leave preset to 1	
SLASER	leave as preset	No significance, since only one laser is needed
DLASER	leave as preset	
ELASER	leave as preset	

The last namelist to be inputted is SCAN. For its variables:

IDIREC	leave preset to 1	
SCANL	leave preset to 30.0	
SCANR	leave preset to 0.5	
NSWEEP	leave preset to 3	0 is the third preset value for SWEEP

SWEEP	set SWEEP(1) to -7 and SWEEP(2) to -2	
IVMAX	leave as preset to 2	
IWEIGH	leave as preset to 1	
WFILT	leave as preset to 0.94	Filters are to have an effective 5 m/sec velocity width
DETLEV	leave preset to 0.1	This is a reasonable signal- to-noise fraction for the filter
OFSETX	leave preset to 0., 0., )	Perfect alignment is assumed
OFSETY	leave preset to 0., 0., }	
OFSETZ	leave preset to 0., 0., }	
WIND	leave preset to 0., 0., 0.,	No wind

The output from this sample run is shown in Figs. C-2 through C-7.

C.14 LASER VELOCIMETER LINE SCAN SIMULATION PROGRAM  
COMMON VARIABLES

<u>Name</u>	<u>Units</u>	<u>Location</u>	<u>Description</u>
AVT(3)	m/sec	COMMON/A05/	Axial velocity vector at illumination point – (rectangular coordinate system).
D	m/sec	COMMON/A15/	D is the distance from illuminated point of interest to axis of vortex.
DD(100, 2)	m	COMMON/A03/	Contains distance from vortex axis to focus point. DD( , 1) is for other than nominal case. DD( , 2) is for nominal case.
DETLEV	–	COMMON/A22/	Detection level of filters in fraction of total return signal.
DISPLA(3)	m	COMMON/A01/	For use with two lasers. Is displacement vector for laser from reference point.
DLASER	m	COMMON/A21/	Determines laser separation for two lasers, DLASER is distance of lasers from sweep plane.
DZERO	n	COMMON/A14/	DZERO is the profile drag of airfoil from generating aircraft.
ELASER	m	COMMON/A21/	Determine laser separation for two lasers. ELASER is distance of lasers from site line in sweep plane.
FLAMDA	m	COMMON/A21/	FLAMDA = wavelength of light.
GAMMAC	(N-m-sec)/kg	COMMON/A06/	Initial circulation about vortex.

<u>Name</u>	<u>Units</u>	<u>Location</u>	<u>Description</u>
IABS	-	COMMON/A21/	A flag where IABS = 1 indicates that the laser cannot detect sign of line-of-sight velocity. IABS = 2 indicates that laser can detect sign of the line-of-sight velocity.
ICHOIC	-	COMMON/A21/	A flag where ICHOIC = 1 indicates a CW focused laser and ICHOIC = 2 indicates a pulsed laser.
IDIREC	-	COMMON/A22/	A flag where IDIREC = 1 indicates lateral scan and IDIREC = 2 indicates range scan.
IUNITS	-	COMMON/A21/	A flag where IUNITS = 1 indicates one laser and IUNITS = 2 indicates two lasers.
IVMAX	-	COMMON/A22/	A flag where IUMAX = 1 indicates the maximum minus the minimum line-of-sight velocity is to be plotted as X. IVMAX = 2 indicates the maximum absolute line-of-sight velocity is to be plotted as X.
IWEIGH	-	COMMON/A22/	A flag where IWEIGH = 1 indicates that the velocity for the highest activated filter will be plotted for W. IWEIGH = 2 indicates that the velocity from the centroid of the illuminated volume will be plotted for W.
JJ	-	COMMON/A08/	Indicates which plot is being made.
NOM	-	COMMON/A08/	NOM = 1 indicates non-nominal scan being made. NOM = 2 indicates nominal scan being made.

<u>Name</u>	<u>Units</u>	<u>Location</u>	<u>Description</u>
NPLENG	—	COMMON/A21/	Indicates nominal pulse length.
NR	—	COMMON/A21/	Indicates nominal radius of telescope aperture.
NRANGE	—	COMMON/A20/	Indicates nominal vortex range.
NSWEEP	—	COMMON/A22/	Indicates nominal sweep position.
NTHETA	—	COMMON/A08/	Number of points along sweep.
OFSETX(2)	m	COMMON/A30/	Offset of laser focus point along site line due to misalignment. OFSETX(1) is for first laser and OFSETX(2) is for second laser.
OFSETY(2)	m	COMMON/A30/	Offset of laser focus point from scan plane due to misalignment. OFSETY(1) is for first laser and OFSETY(2) is for second laser.
OFSETZ(2)	m	COMMON/A30/	Offset of laser focus point along sweep line due to misalignment OFSETZ(1) is for first laser and OFSETZ(2) is for second laser.
OP(3)	m	COMMON/A01/	Position of a point on the vortex axis (rectangular coordinate system).
OS(3)	m	COMMON/A05/	Vector to indicate illumination point relative to laser (rectangular coordinate system).
OSS(3)	m	COMMON/A05/	Vector position of focus point for IASEL.
PI	—	COMMON/A07/	PI is $\pi = 3.1415926$ .
PLENGTH(8)	m	COMMON/A21/	Pulse length.

<u>Name</u>	<u>Units</u>	<u>Location</u>	<u>Description</u>
PQ(3)	-	COMMON/A01/	Directional vector for vortex (rectangular coordinate system).
PSI	-	COMMON/A21/	Is incident wave amplitude.
R(8)	m	COMMON/A21/	Radius of telescope aperture.
RHO	kg/m <sup>3</sup>	COMMON/A14/	RHO is the density of the atmosphere.
R2D	deg/rad	COMMON/A07/	Conversion factor for converting from radians to degrees.
SCANL	m	COMMON/A22/	Scan length.
SCANP(100)	m	COMMON/A03/	Is distance from focus point to site line. Also is variable that runs on horizontal axis of plots.
SCANR	m	COMMON/A22/	Scan resolution.
SP(3)	m	COMMON/A05/	Vector from illumination point (OS) to point OP on vortex (rectangular coordinate system).
SLASER	m	COMMON/A21/	Determines laser separation for two lasers. SLASER is distance of lasers along site line from reference point.
SMAX	m	COMMON/A08/	Maximum position along sweep.
SMIN	m	COMMON/A08/	Minimum position along sweep.
SWEEPP(5)	m	COMMON/A22/	Sweep position.
TITLE(12)	alphanumeric data	COMMON/A02/	Contains INPUT description of run.
UNU	m <sup>2</sup> /sec	COMMON/A06	Eddy viscosity.

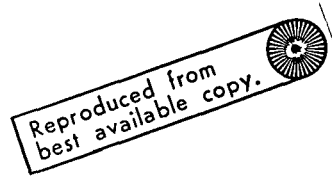
<u>Name</u>	<u>Units</u>	<u>Location</u>	<u>Description</u>
VAL	m	COMMON/A08/	Distance of sweep from reference sweep line (for lateral scan). Distance of sweep from site line (for range scan).
VLINI	m/sec	COMMON/A15/	Line-of-sight component of the tangential velocity.
VLIN2	m/sec	COMMON/A15/	Line-of-sight component of the axial velocity.
VMAVT	m/sec	COMMON/A15/	VMAVT is the norm of the tangential velocity.
VMAX	m/sec	COMMON/A08/	Upper velocity bound on plotting scale.
VMOSS	m	COMMON/A05/	Norm of vector (OSS).
VMIN	m/sec	COMMON/A08/	Lower velocity bound on plotting scale.
VMVT	m/sec	COMMON/A15/	VMVT is the norm of the tangential velocity.
VRANGE(8)	m	COMMON/A20/	Vortex ranges.
VROTH	deg	COMMON/A20/	Vortex rotation about reference sweep line.
VROTHC	deg	COMMON/A20/	Change in vortex rotation about reference sweep line.
VROTV	deg	COMMON/A20/	Vortex rotation about site line.
VROTV C	deg	COMMON/A20/	Change in vortex rotation about site line.
VT(3)	m/sec	COMMON/A05/	Tangential velocity vector at illumination point (rectangular coordinate system).
VTOL	m/sec	COMMON/A15/	Norm of velocity vector at focus point.

<u>Name</u>	<u>Units</u>	<u>Location</u>	<u>Description</u>
VV(3)	-	COMMON/A05/	Vector pointing in direction of tangential flow at illumination point (rectangular coordinate system).
VI(100, 4, 2)	m/sec	COMMON/A03/	Velocities to be plotted: VI( , 1, ) is the weighted average or filter output. VI( , 2, ) is VMAX-VMIN or MAX(ABS(VL)). VI( , 3, ) is norm of total velocity vector. VI( , 4, ) is line of sight velocity at focus point. VI( , , 1) is for other than nominal case. VI( , , 2) is for nominal case.
WEIGHL	m	COMMON/A21/	Distance between sample points in weighing.
WFILT	megahertz	COMMON/A22/	Band width of filters.
WIND(3)	m/sec	COMMON/A31/	Constant wind.
W8	m/sec	COMMON/A06/	Freestream velocity.
Z	m	COMMON/A06/	Vortex distance from generating aircraft.

C.15 LASER VELOCIMETER LINE SCAN SIMULATION PROGRAM LISTING

```

$JOB
$SETUP LB2      TAPE,SC4020
$ASSIGN        SYSLB2
$ATEND        00000,77777,1,DUMP
$EXECUTE      1BJOB
$IPJOB LMSC
$IFTC MAIN    DECK
    
```



```

C
C
C      THIS PROGRAM IS FOR DETERMINING THE USEFULNESS OF VARIOUS 2D
C      LASER DOPPLER SYSTEMS FOR USE IN SCANNING VORTICES
    
```

```

C
C      NAMELIST (VORTEX)
    
```

```

C      GAMMAC      CIRCULATION
C      WB          FREESTREAM VELOCITY
C      UNU        EDDY VISCOSITY
C      Z          VORTEX AXIAL COORDINATE FROM SOURCE
C      DZERO      PROFILE DRAG OF THE AEROFOIL
C      PHO        DENSITY OF ATMOSPHERE
C      VROTH      VORTEX ROTATION ABOUT REFERENCE SWEEP LINE
C      VROTHC     CHANGE IN VORTEX ROTATION ABOUT REFERENCE SWEEP LINE
C      VROTV      VORTEX ROTATION ABOUT SITE LINE
C      VROTVC     CHANGE IN VORTEX ROTATION ABOUT SITE LINE
C      NRANGE     INDICATES NOMINAL VORTEX RANGE
C      VRANGE(S)  VORTEX RANGE
C      VMAX       UPPER VELOCITY BOUND ON PLOTTING SCALE
C      VMIN       LOWER VELOCITY BOUND ON PLOTTING SCALE
    
```

```

C
C      NAMELIST (SYSTEM)
    
```

```

C      IUNITS     FLAG
C                IUNITS = 1      ONE LASERS
C                IUNITS = 2      TWO LASERS
C      ICHOIC     FLAG
C                ICHOIC = 1      CONTINUOUS WAVE LASER
C                ICHOIC = 2      PULSED LASER
C      PSI        INCIDENT WAVE AMPLITUDE
C      FLAMDA     WAVE LENGTH OF LIGHT
C      NR         INDICATES NOMINAL RADIUS OF TELESCOPE APERTURE
C      R(R)       RADIUS OF TELESCOPE APERTURE
C      NPLENG     INDICATES NOMINAL PULSE LENGTH
C      PLENGT(R)  PULSE LENGTH
C      WEIGHL     DISTANCE BETWEEN SAMPLE POINTS USED IN WEIGHING
C      IARS       FLAG
C                IARS = 1        ABS(VL) IS USED
C                IARS = 2        VL IS USED
C      SLASER     DISTANCE OF LASERS ALONG SITE LINE
C      PLASER     DISTANCE OF LASERS FROM SWEEP PLANE
C      FLASER     DISTANCE OF LASERS FROM SITE LINE IN SWEEP PLANE
    
```

```

C
C      NAMELIST (SCAN)
    
```

```

C      IDIREC     FLAG
    
```

LMSC-HREC D225936

```

C          IDIREC = 1      LATERAL SCAN
C          IDIREC = 2      RANGE SCAN
C  SCANL      SCAN LENGTH
C  SCANR      SCAN RESOLUTION
C  NSWEEP     INDICATES NOMINAL SWEEP POSITION
C  SWEPP(5)   SWEEP POSITION
C  IVMAX      FLAG
C             IVMAX = 1      VMAX - VMIN IS PLOTTED
C             IVMAX = 2      MAX(ABS(VL)) IS PLOTTED
C             IVMAX = 3
C  IWEIGH     FLAG
C             IWEIGH = 1     PLOT HIGHEST ACTIVATED FILTER
C             IWEIGH = 2     PLOT CENTROID
C  WFILT      BAND WIDTH OF FILTERS IN MEGAHERTZ
C  DETLEV     DETECTION LEVEL IN FILTERS
C  OFSETX(2)  OFFSET OF LASER FOCUS POINT ALONG SITE LINE DO TO
C             MISALIGNMENT
C  OFSETY(2)  OFFSET OF LASER FOCUS POINT FROM SCAN PLANE DO TO
C             MISALIGNMENT
C  OFSETZ(2)  OFFSET OF LASER FOCUS POINT ALONG SWEEP LINE DO TO
C             MISALIGNMENT
C  WIND(3)    CONSTANT WIND

```

```

COMMON / A01 / OP(3), PQ(3), DISPLA(3)
COMMON / A02 / TITLE(12)
COMMON / A03 / V1(100,4,2), SCANP(100), DD(100,2)
COMMON / A05 / OS(3), SP(3), VV(3), VT(3), AVT(3), OSS(3), VMOSS
COMMON / A06 / GAMMAC, WB, UNU, Z
COMMON / A07 / P1, P2D
COMMON / A08 / VMAX, VMIN, SMAX, SMIN, NTHETA, NOM, JJ, VAL
COMMON / A14 / DZERO, RHO
COMMON / A15 / VLIN1, VLIN2, VMVT, VMAVT, D, VTOL
COMMON / A20 / VROTH, VROTHC, VROTV, VROTV, NRANGE, VRANGE(8)
COMMON / A21 / IUNITS, ICHOIC, PSI, FLAMDA, NR, R(8), NPLENG,
* PLENGT(8), WEIGHL, IARS, SLASER, DLASER, ELASER
COMMON / A22 / IDIREC, SCANL, SCANR, NSWEEP, SWEPP(5), IVMAX,
* IWEIGH, WFILT, DETLEV
COMMON / A30 / OFSETX(2), OFSETY(2), OFSETZ(2)
COMMON / A31 / WIND(3)
DIMENSION FILTER(50), V2V(4,2), DISP(3,2)
DIMENSION FILTEN(50)
DATA FILTER / 50*0. /
DATA GAMMAC, WB, UNU, Z, DZERO, RHO, VROTH, VROTHC, VROTV, VROTV,
1 NRANGE, VRANGE, VMAX, VMIN
2 / 729., 77.3, .0914, 1000., 50000., 1.192, 0., 10., 0., 10., 2,
3 50., 100., 300., 1000., 3000., 5000., -1., -1., 34., 0. /
DATA IUNITS, ICHOIC, PSI, FLAMDA, NR, R, NPLENG, PLENGT, WEIGHL,
1 IARS, SLASER, DLASER, ELASER
2 / 1, 1, 1., .0000106, 2, .1, .2, .3, .5, 1., 2., 4., 6., 2,
3 30., 90., 150., 300., 900., 3*-1.,.5, 1, 0., 0., 100. /
DATA IDIREC, SCANL, SCANR, NSWEEP, SWEPP, IVMAX, IWEIGH, WFILT,
1 DETLEV / 1, 30., .5, 3, -15., -7., 0., 7., 15., 2, 1, .94, .1 /
DATA OP / 3*0. /
DATA (OFSETY(I),I=1,2) / 2*0. /
DATA (OFSETY(I),I=1,2) / 2*0. /
DATA (OFSETZ(I),I=1,2) / 2*0. /
DATA (WIND(I),I=1,3) / 3*0. /

```

```

DATA PI, R2D / 3.1415926, 57.29578 /
NAMELIST / VORTEX / GAMMAC, W8, UNU, Z, DZERO, RHO, VROTH, VROTHC,
* VROTV, VROTV, NPANGF, VRANGF, VMAX, VMIN
NAMELIST / SYSTEM / IUNITS, ICHOIC, PSI, FLAMDA, NR, R, NPLENG,
* PLFNGT, WFIGHL, IARS, SLASER, DLASER, FLASER
NAMELIST / SCAN / IDIREC, SCANL, SCANR, NSWEEP, SWEEPP, IVMAX,
* IWFIGH, WFILT, DETLEV, OFSETX, OFSETY, OFSETZ, WIND
10 READ (5,500) TITLE
500 FORMAT(12A6)
WRITE(6,600) TITLE
600 FORMAT(1H1,30X,12A6)
READ(5,VORTEX)
WRITE(6,VORTEX)
READ(5,SYSTEM)
WRITE(6,SYSTEM)
READ(5,SCAN)
WRITE(6,SCAN)
NEW = 1
FILT = FLAMDA*WFILT*.5F6
DO 11 I5=1,50
FILTEN(I5) = 0.
11 FILTER(I5) = 0.
IF(IARS .EQ. 1) GO TO 30
ASSIGN 67 TO JARS
GO TO 31
30 ASSIGN 65 TO JARS
31 IF(IWFIGH .EQ. 1) GO TO 32
ASSIGN 99 TO JWFIGH
ASSIGN 51 TO KWFIGH
GO TO 33
32 ASSIGN 98 TO JWFIGH
ASSIGN 50 TO KWFIGH
33 CONTINUE
IF(IUNITS .EQ. 2) GO TO 208
ASSIGN 205 TO JUNITS
ASSIGN 201 TO KUNITS
ASSIGN 111 TO LUNITS
ASSIGN 428 TO JRIGHT
ASSIGN 432 TO KRIGHT
GO TO 209
208 ASSIGN 206 TO JUNITS
ASSIGN 202 TO KUNITS
ASSIGN 110 TO LUNITS
209 IF(IDIREC .EQ. 2) GO TO 170
ASSIGN 151 TO JDIREC
ASSIGN 153 TO KDIREC
ASSIGN 157 TO LDIREC
ASSIGN 165 TO MDIREC
ASSIGN 157 TO NDIREC
GO TO 171
170 ASSIGN 152 TO JDIREC
ASSIGN 154 TO KDIREC
ASSIGN 158 TO LDIREC
ASSIGN 166 TO MDIREC
ASSIGN 155 TO NDIREC
171 IF(ICHOIC .GT. 1) GO TO 12
ASSIGN 41 TO JCHOIC
ASSIGN 44 TO KCHOIC

```

Reproduced from  
best available copy.



```

      GO TO 14
12  ASSIGN 42 TO JCHOIC
      ASSIGN 45 TO KCHOIC
14  GO TO (15,16,17),IVMAX
15  ASSIGN 91 TO JVMAX
      GO TO 18
16  ASSIGN 92 TO JVMAX
      GO TO 18
17  ASSIGN 93 TO JVMAX
18  NTHETA = SCANL/SCANP + 1.
      IF(NTHETA .LE. 100) GO TO 20
      WRITE (6,610)
610  FORMAT(/43H ** INPUT ERROR **  SCANL/SCANR IS .GT. 100)
      GO TO 10
20  CONTINUE
      IF(IUNITS .EQ. 1) GO TO 421
      DISP(1,1) = -SLASER
      DISP(2,1) = -DLASER
      DISP(3,1) = -FLASER
      DISP(1,2) =  SLASER
      DISP(2,2) =  DLASER
      DISP(3,2) =  FLASER
      IF(ABS(SLASER) + ABS(FLASER) .LT. 1.) GO TO 420
      S2 = SLASER*SLASER
      D2 = DLASER*DLASER
      F2 = FLASER*FLASER
      RB1 = 2.*S2 + E2
      RB2 = 2.*SQRT(D2 + S2 + F2)
      ASSIGN 427 TO JRIGHT
      ASSIGN 431 TO KRIGHT
      GO TO 421
420  ASSIGN 426 TO JRIGHT
      ASSIGN 430 TO KRIGHT
421  CONTINUE
      SC = -SCANL/2. - SCANR
      DO 25 I=1,NTHETA
      SC = SC + SCANR
25  SCAND(I) = SC
      SMAX = SCANP(NTHETA)
      SMIN = SCANP(1)
      DO 120 J=1,15
      GO TO (210,220,230,300,310,320,330,340,350,360,370,380,390,400,
      & 410),J
210  PHI = 0
      NOM = 1
      JJ = 1
      ISWF = 2
      IF(NSWEEP .NE. 1) ISWF = 1
      OP(1) = VRANGE(NRANGE)
      PQ(2) = 1.
      PQ(1) = TAN( VROTH/R2D)
      PQ(3) = TAN( VROTV/R2D)
      IF(ICHOIC .EQ. 2) GO TO 211
      RR = P(NR)
      GO TO 392
211  PLENG = PLENGT(NPLENG)
      GO TO 149
220  ISWF = NSWEEP

```

```

      NOM = 2
      GO TO 149
230  ISWF = 2
      NOM = 1
      IF(NSWEEP .LT. 3) ISWF = 3
      GO TO 149
300  IF(NRANGE .GT. 1) GO TO 301
      OP(1) = VRANGE(NRANGE + 2)
      GO TO 302
301  OP(1) = VRANGE(NRANGE - 1)
302  JJ = 3
      VAL = OP(1)
      GO TO 75
310  VAL = VRANGE(NRANGE)
      GO TO 130
320  IF(NRANGE .EQ. 8) GO TO 321
      OP(1) = VRANGE(NRANGE+1)
      IF(OP(1) .GT. 0.) GO TO 322
321  OP(1) = VRANGE(NRANGE-2)
322  VAL = OP(1)
      GO TO 75
330  OP(1) = VRANGE(NRANGE)
      PQ(1) = TAN((VROTH - VROTHC)/R2D)
      JJ = 4
      VAL = VROTH - VROTHC
      GO TO 75
340  VAL = VROTH
      GO TO 130
350  PQ(1) = TAN((VROTH + VROTHC)/R2D)
      VAL = VROTH + VROTHC
      GO TO 80
360  PQ(1) = TAN(VROTH/R2D)
      PQ(3) = TAN((VROTV - VROTV C)/R2D)
      JJ = 5
      VAL = VROTV - VROTV C
      GO TO 80
370  VAL = VROTV
      GO TO 130
380  PQ(3) = TAN((VROTV + VROTV C)/R2D)
      VAL = VROTV + VROTV C
      GO TO 80
390  PQ(3) = TAN(VROTV/R2D)
      IF(ICHoice .EQ. 2) GO TO 395
      IF(NP .EQ. 1) GO TO 391
      PR = P(NP-1)
      GO TO 393
391  PR = P(NP+2)
393  JJ = 6
      VAL = PR
392  FACT1 = (PSI*PI*PR**2)**2/FLAMDA**2
      FACT2 = FLAMDA/(PI*RR**2)
      IF(J .EQ. 1) GO TO 149
      GO TO 80
395  IF(NPLENG .EQ. 1) GO TO 396
      PLENG = PLENGT(NPLENG-1)
      GO TO 397
396  PLENG = PLENGT(NPLENG+2)
397  JJ = 7

```

```

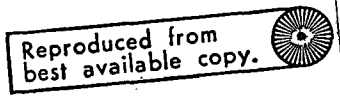
      VAL = PLFNG
      GO TO 80
400 IF(ICHOC .EQ. 2) GO TO 401
      VAL = R(NR)
      GO TO 130
401 VAL = PLFNGT(NPLFNG)
130 NOM = 2
      GO TO 120
410 NEW = 3
      IF(ICHOC .EQ. 2) GO TO 415
      IF(NR .EQ. 9) GO TO 411
      RR = R(NR+1)
      IF(RR .GT. 0.) GO TO 393
411 RR = R(NR-2)
      GO TO 393
415 IF(NPLFNG .EQ. 8) GO TO 416
      PLFNG = PLFNGT(NPLFNG+1)
      IF(PLFNG .GT. 0.) GO TO 397
416 PLFNG = PLFNGT(NPLFNG-2)
      GO TO 397
140 VAL = SWFPP(ISWF)
      GO TO JDIRC,(151,152)
151 DISTL = VRANGE(NRANGE) + SWFPP(ISWF)
      THETA1 = -ATAN(SCANL/(2.*DISTL))
      DTHETA = -2.*THETA1/FLOAT(NTHETA-1)
      GO TO 85
152 DISTC = VRANGE(NRANGE)
      THETA = SWFPP(ISWF) / DISTC
      GO TO 85
75 GO TO MDIREC,(165,166)
165 DISTL = OP(1) + SWFPP(NSWFPP)
      THETA1 = -ATAN(SCANL/(2.*DISTL))
      DTHETA = -2.*THETA1/FLOAT(NTHETA-1)
      GO TO 80
166 DISTC = OP(1)
      THETA = SWFPP(NSWFPP)/DISTC
80 NOM = 1
85 I = 0
      GO TO KDIRC,(153,154)
153 THETA = THETA1 - DTHETA
      GO TO 156
154 DISTL = DISTC - SCANL*.5 - SCANR
155 DISTL = DISTL + SCANR
      I = I + 1
156 GO TO JRIGHT,(426,427,428)
426 DELTA = 2.*ATAN(DLASER/DISTL)
      GO TO 428
427 R2 = DISTL*DISTL
      CC1 = R2 + S2 + D2 + F2
      CC2 = -R*BB2
      CC3 = R2 - S2 - D2 - F2
      CC4 = 2.*DISTL
428 CONTINUE
      GO TO LDIREC,(157,158)
157 THETA = THETA+ DTHETA
      I = I + 1
158 GO TO KRIGHT,(430,431,432)
431 DELTA1 = ARCOS(BB1/(BB2*SQRT(S2+(FLASER-SLASER*TAN(THETA))**2)))

```

```

A2 = CC1 + CC2*COS(DELTA1)
DELTA3 = ARCCOS((A2 + CC3)/(CC4*SQRT(A2)))
B2 = CC1 + CC2*COS(PI - DELTA1)
DELTA4 = ARCCOS((B2 + CC3)/(CC4*SQRT(B2)))
DELTA = DELTA3 + DELTA4
430 SDELTA = SIN(DELTA)
CDELTA = COS(DELTA)
TDELTA = SDELTA/CDELTA
DD1 = SDELTA + CDELTA/TDELTA.
432 DO 110 L2=1,2
GO TO JUNITS,(205,206)
205 DISPLA(1) = 0.
DISPLA(2) = 0.
DISPLA(3) = 0.
GO TO 207
206 DISPLA(1) = DISP(1,L2)
DISPLA(2) = DISP(2,L2)
DISPLA(3) = DISP(3,L2)
207 VVMAX = -1.E30
VVMIN = 1.E30
VLW = 0.
WFT = 0.
OSS(1)= DISTL*COS(THETA )*COS(PHI ) + DISPLA(1) + OFFSETX(L2)
OSS(2)= DISTL*COS(THETA )*SIN(PHI ) + DISPLA(2) + OFFSETY(L2)
OSS(3)= DISTL*SIN(THETA ) + DISPLA(3) + OFFSETZ(L2)
VMOSS = VMAG(OSS)
GO TO JCHOIC,(41,42)
41 DDISTW = 2.*FACT2*VMOSS**2
GO TO 43
42 DDISTW = .5*PLENG
43 NWEIGH = DDISTW/WFIGHL
NW = 2*NWEIGH + 1
DISTW = VMOSS - WFIGHL*FLOAT(NWEIGH + 1)
IVLMX = 0
IVLMN = 0
DO 90 II=1,NW
DISTW = DISTW + WFIGHL
GO TO KCHOIC,(44,45)
44 DL2 = (FACT2*VMOSS*DISTW)**2
WF = FACT1/(1. + (VMOSS - DISTW)**2/DL2)/DISTW**2
GO TO 46
45 WAT = 1.
IF(II .GT. NWEIGH) GO TO 60
WF = WAT*FLOAT(II-1)/FLOAT(NWEIGH)
GO TO 46
60 WF = WAT*FLOAT(NW-II)/FLOAT(NWEIGH)
46 CALL VFL(VL,PHI,THETA,DISTW)
IF(VL .GT. VVMAX) VVMAX = VL
IF(VL .LT. VVMIN) VVMIN = VL
GO TO JABS,(65,67)
65 VL = ABS(VL)
67 IF(II .NE. NWEIGH + 1) GO TO 87
V1(I,3,NOM) = VTOL
V2V(4,L2) = VL
DD(I,NOM) = D
87 WFT = WFT + WF
GO TO KWEIGH,(50,51)
51 VLW = VLW + VL*WF

```



```

GO TO 90
50 IF(VL .LT. 0.) GO TO 1052
   IVL = VL/FILT + 1.
   FILTER(IVL) = WF + FILTER(IVL)
   IF(IVL .GT. IVLMX) IVLMX = IVL
   GO TO 90
1052 IVL = -VL/FILT + 1.
   FILTEN(IVL) = WF + FILTEN(IVL)
   IF(IVL .GT. IVLMN) IVLMN = IVL
90 CONTINUE
   GO TO JWFIGH,(98,99)
90 V2V(1,L2) = VLW/WFT
   GO TO 89
98 I7 = 1
   I77 = 1
   IF(IVLMX .EQ. 0) GO TO 1098
   DO 94 I6=1,IVLMX
   FILTER(I6) = FILTER(I6)/WFT
94 IF(FILTER(I6) .GT. DEIFLV) I7 = I6
   IF(IWFIGH .EQ. 1) WRITE(6,630) (FILTER(I8),I8=1,IVLMX)
630 FORMAT (//(10F12.4))
1098 IF(IVLMN .EQ. 0) GO TO 95
   DO 1094 I6 = 1,IVLMN
   FILTEN(I6) = FILTEN(I6)/WFT
1094 IF(FILTEN(I6) .GT. DEIFLV) I77 = I6
   IF(IWFIGH .EQ. 1) WRITE(6,1630)(FILTEN(I8),I8=1,IVLMN)
1630 FORMAT (//(2H -,F11.4,9F12.4))
95 IF(I77 - I7) 1003,1002,1001
1002 IF(FILTER(I7) .GE. FILTEN(I77)) GO TO 1003
1001 V2V(1,L2) = -FILT*(FLOAT(I77) - .5)
   GO TO 1004
1003 V2V(1,L2) = FILT*(FLOAT(I7) - .5)
1004 CONTINUE
   DO 490 I9 =1,IVLMX
490 FILTER(I9) = 0.
   DO 1490 I9=1,IVLMN
1490 FILTEN(I9) = 0.
80 GO TO JVMAX,(91,92,93)
91 V2V(2,L2) = VVMAX - VVMIN
   GO TO 97
92 V2V(2,L2) = AMAX1(VVMAX,-VVMIN)
   GO TO 97
93 CONTINUE
97 CONTINUE
   GO TO LUNITS,(111,110)
110 CONTINUE
111 GO TO RUNITS,(201,202)
201 DO 203 K5=1,4
   IF(K5 .EQ. 3) GO TO 203
   V1(I,K5,NOM) = V2V(K5,1)
203 CONTINUE
   GO TO 204
202 DO 115 K5=1,4
   IF(K5 .EQ. 3) GO TO 115
   V1(I,K5,NOM) = SORT(V2V(K5,1)**2 + (-V2V(K5,1)/TDELTA + V2V(K5,2)
   * *DD1)**2)
115 CONTINUE
   IF(NOM .EQ. 2) WRITE(6,620) V2V(4,1),V2V(4,2),V1(I,4,NOM)

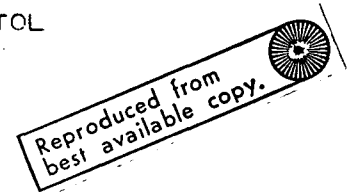
```

```
620 FORMAT (3F16.8)
204 CONTINUE
100 IF(NTHETA .GT. 1) GO TO NDIREC.(157.155)
120 CALL PV(NEW)
    GO TO 10
    END
```

```

&IPBETC VFL      DECK
SUBROUTINE VFL(VLINE,PHIL,THETA,LDISTL)
COMMON / A01 / OP(3), PQ(3), DISPLA(3)
COMMON / A05 / OS(3), SP(3), VV(3), VT(3), AVT(3), OSS(3), VMOSS
COMMON / A06 / GAMMAC, WR, UNU, Z
COMMON / A07 / PI, P2D
COMMON / A14 / DZERO, RHO
COMMON / A15 / VLIN1, VLIN2, VMVT, VMAVT, D, VTOL
COMMON / A31 / WIND(3)
DIMENSION TOT(3)
VMOSSD = DISTL/VMOSS
OS(1) = VMOSSD*OSS(1)
OS(2) = VMOSSD*OSS(2)
OS(3) = VMOSSD*OSS(3)
SP(1) = OP(1) - OS(1) + DISPLA(1)
SP(2) = OP(2) - OS(2) + DISPLA(2)
SP(3) = OP(3) - OS(3) + DISPLA(3)
CALL CROSS(SP,PQ,VV)
VMPO = VMAG(PQ)
VMVV = VMAG(VV)
D = VMVV/VMPO
EX = EXP(-WR*D**2/(4.*UNU*Z))
VMVT = GAMMAC*(1. - EX)/(2.*PI*D)
VMVTD = VMVT/VMVV
VT(1) = VMVTD*VV(1)
VT(2) = VMVTD*VV(2)
VT(3) = VMVTD*VV(3)
VMAVT = DZERO*EX/(4.*PI*RHO*UNU*Z)
VMAVTD = VMAVT/VMPO
AVT(1) = VMAVTD*PQ(1)
AVT(2) = VMAVTD*PQ(2)
AVT(3) = VMAVTD*PQ(3)
VMOS = VMAG(OS)
DO 10 I=1,3
10 TOT(I) = VT(I) + AVT(I) + WIND(I)
VTOL = SQRT(TOT(1)**2 + TOT(2)**2 + TOT(3)**2)
VLIN1 = -DOT(VT,OS)/VMOS
VLIN2 = -DOT(AVT,OS)/VMOS
VLINW = -DOT(WIND,OS)/VMOS
VLINE = VLIN1 + VLIN2 + VLINW
RETURN
END

```





```

$IRETC PV      DECK
SUBROUTINE PV(NEW)
COMMON / A02 / TITLE(12)
COMMON / A03 / V1(100,4,2), SCANP(100), DD(100,2)
COMMON / A08 / VMAX, VMIN, SMAX, SMIN, NTHETA, NOM, JJ, VAL
COMMON / A22 / IDIREC, SCANL, SCANR, NSWEEP, SWEEPP(5), IVMAX,
$ IWFIGH, WFILT, DFTLEV
DIMENSION BCDX(12,2), BCDY(12), ISYM(4), LABLF(8,7), SEMBLE(6),
$ SEM(3,3), SEMR(5,2)
DATA (BCDX(I,1),I=1,12) / 6HDATA P,6HPOINT P,6HOSITIO,6HN WITH,
$ 6H PESPE,6HCT TO ,6HSITE L,6HINE IN,6H METER,6HS ,2*1H /
DATA (BCDX(I,2),I=1,12) / 6HDATA P,6HPOINT P,6HOSITIO,6HN WITH,
$ 6H PESPE,6HCT TO ,6HREFERE,6HCE SWE,6HEP LIN,6HE IN M,6HETERS ,
$ 1H /
DATA (BCDY(I),I=1,12) / 6HVFOCI,6HTY IN ,6HM/SEC ,9*1H /
DATA (ISYM(I),I=1,4) / 54, 55, 51, 35 /
DATA (LABLF(I,1),I=1,8) / 6H ,6H ,6H ,6H ,6H ,6H ,6H ,6H
$ 6H ,6H SWEEP,6H POSIT,6HION IS /
DATA (LABLF(I,2),I=1,8) / 6H ,6H ,6H ,6H ,6H ,6H ,6H ,6H
$ 6H DISTA,6HNCE DO,6HWN VOR,6HTEF IS /
DATA (LABLF(I,3),I=1,8) / 6H ,6H ,6H ,6H ,6H ,6H ,6H ,6H
$ 6H ,6H VOR,6HTEF RA,6HNCE IS /
DATA (LABLF(I,4),I=1,8) / 6H VOR,6HTEF RO,6HTATION,6H ABOUT,
$ 6H PEFER,6HNCE S,6HWFFP L,6HINE IS /
DATA (LABLF(I,5),I=1,8) / 6H ,6H ,6H ,6H VORT,6HEX ROT,
$ 6HATION ,6HABOUT ,6HSITE L,6HINE IS /
DATA (LABLF(I,6),I=1,8) / 6H ,6H ,6H ,6H ,6H ,6H ,6H ,6H
$ 6H T,6HFLESCO,6HPE RAD,6HIUS IS /
DATA (LABLF(I,7),I=1,8) / 6H ,6H ,6H ,6H ,6H ,6H ,6H ,6H
$ 6H ,6H PUL,6HSE LEN,6HGTH IS /
DATA (SEMBLE(I),I=1,6) / 6HT = NO,6HRM TOT,6HAL L ,6H= LINE,
$ 6H OF SI,6HGHT /
DATA (SEM(I,1),I=1,3) / 6HX = VM,6HAX - V,6HMIN /
DATA (SEM(I,2),I=1,3) / 6HX = MA,6HX(ABS(.6HVL)) /
DATA (SEMR(I,1),I=1,5) / 6HW = HI,6HGH ACT,6HIVATED,6H FILTE,1HR /
DATA (SEMR(I,2),I=1,5) / 6HW = CF,6HNTROID,3*1H /
GO TO (10,20,20),NEW
10 NEW = 2
CALL CAMPAV(9)
CALL PINPUT
NL = 3
L = -3
20 IF(NL .EQ. 2) L = 3
CALL QUIK3L (L,SMIN,SMAX,VMIN,VMAX,ISYM(1),BCDX(1,IDIREC),BCDY,
$ NTHETA,SCANP,V1(1,1,NOM))
DO 100 I1=2,4
100 CALL QUIK3L (0,DUM,DUM,DUM,DUM,ISYM(I1),DUM,DUM,NTHETA,SCANP,
$ V1(1,I1,NOM))
GO TO (110,120,130),NL
130 CALL PRINTV(72,TITLE, 32,1008)
CALL PRINTV(48,LABLF(1,JJ), 24, 325)
CALL LABLV(VAL, 424, 325, -4,1,4)
GO TO 150
120 CALL PRINTV(48,LABLF(1,JJ), 24,660)
CALL LABLV(VAL, 424, 660, -4,1,4)
GO TO 150
110 CALL PRINTV(48,LABLF(1,JJ), 24, 992)
CALL LABLV(VAL, 424, 992, -4,1,4)

```

```
CALL PRINTV(33,SFMBLF,528, 992)
CALL PRINTV(25,SFMR(1,IWFIGH),808, 992)
CALL PRINTV(16,SFM(1,IVMAX),800,1008)
150 NL = NL - 1
    IF(NL .NE. 0) GO TO 155
    NL = 3
    L = 1-3
155 IF(NEW .EQ. 3) CALL CLEAN
RETURN
END
```

\$IRFETC PINPUT DECK

SUBROUTINE PINPUT

COMMON / A02 / TITLF(12)

COMMON / A06 / GAMMAC, WR, UNU, Z

COMMON / A08 / VMAX, VMIN, SMAX, SMIN, NTHETA, NOM, JJ, VAL

COMMON / A14 / DZERO, RHO

COMMON / A20 / VROTH, VROTHC, VROTV, VROTV, NRANGE, VRANGE(8)

COMMON / A21 / IUNITS, ICHOIC, PSI, FLAMDA, NR, R(8), NPLENG,

\$ PLENGT(8), WEIGHL, IABS, SLASFR, DLASER, ELASFR

COMMON / A22 / IDIREC, SCANL, SCANR, NSWEEP, SWEPP(5), IVMAX,

\* IWEIGH, WFILT, DETLEV

COMMON / A30 / OFSETX(2), OFSETY(2), OFSETZ(2)

COMMON / A31 / WIND(3)

CALL SCOUTV(9 )

WRITE (16,600)

WRITE(16,600)TITLF

600 FORMAT (1H1,24X,12A6)

WRITE(16,610)GAMMAC, WR, UNU, Z, DZERO, RHO, VROTH, VROTHC,

\$ VROTV, VROTV, NRANGE, VRANGE, VMAX, VMIN

610 FORMAT(//51X,17HNAMELIST (VORTEX),//1X,11HGAMMAC =,E16.8,3X,

1 11HW8 =,F16.8,3X,11HUNU =,E16.8,3X,11HZ =,

2 F16.8,/12H DZERO =,F16.8,3X,11HRHO =,E16.8,3X,

3 11HVROTH =,F16.8,3X,11HVROTHC =,E16.8/

4 12H VROTV =,F16.8,3X,11HVROTV =,F16.8,3X,11HNRANGE =,

5 IR, /

6 12H VRANGE(1) =,E16.8,3X,11HVRANGE(2) =,E16.8,3X,11HVRANGE(3) =,

7 F16.8,

8 3X,11HVRANGE(4) =,E16.8,/12H VRANGE(5) =,E16.8,3X,11HVRANGE(6) =,

9 F16.8,3X,11HVRANGE(7) =,E16.8,3X,11HVRANGE(8) =,F16.8,/

A 12H VMAX =,E16.8,3X,11HVMIN =,E16.8)

WRITE(16,620) IUNITS, ICHOIC, PSI, FLAMDA, NR, R, NPLENG, PLENGT,

\$ WEIGHL, IABS, SLASER, DLASER, ELASFR

620 FORMAT (//51X,17HNAMELIST (SYSTEM)//

7 12H IUNITS =,IR /

1 12H ICHOIC =,IR,11X ,11HPSI =,E16.8,3X,

2 11HFLAMDA =,F16.8,3X,11HNR =,IR /

3 12H R(1) =,E16.8,3X,11HR(2) =,F16.8,3X,

4 11HR(3) =,E16.8,3X,11HR(4) =,E16.8,/

5 12H R(5) =,E16.8,3X,11HR(6) =,F16.8,3X,

6 11HR(7) =,E16.8,3X,11HR(8) =,F16.8,/

7 12H NPLENG =,IR /

8 12H PLENGT(1) =,E16.8,3X,11HPLENGT(2) =,F16.8,3X,

9 11HPLENGT(3) =,E16.8,3X,11HPLENGT(4) =,E16.8,/

A 12H PLENGT(5) =,E16.8,3X,11HPLENGT(6) =,E16.8,3X,

B 11HPLENGT(7) =,E16.8,3X,11HPLENGT(8) =,E16.8,/

C 12H WEIGHL =,F16.8,3X,11HIABS =,IR,11X,

D 11HSLASER =,F16.8,3X,11HDLASER =,F16.8,/

E 12H FLASFR =,E16.8)

WRITE(16,630) IDIREC, SCANL, SCANR, NSWEEP, SWEPP, IVMAX,

\$ IWEIGH, WFILT, DETLEV, OFSETX, OFSETY, OFSETZ, WIND

630 FORMAT (//51X,17HNAMELIST (SCAN) //

1 12H IDIREC =,IR,11X ,11HSCANL =,E16.8,3X,

2 11HSCANR =,E16.8,3X,11HNSWEEP =,IR, /

3 12H SWEPP(1) =,E16.8,3X,11HSWEPP(2) =,F16.8,3X,

4 11HSWEPP(3) =,E16.8,3X,11HSWEPP(4) =,E16.8,/

5 12H SWEPP(5) =,E16.8 /

6 12H IVMAX =,IR,11X, 11HIWEIGH =,IR,11X ,

7 11HWFILT =,E16.8,3X,11HDETLEV =,F16.8 /

8 12H OFSETX(1) =,E16.8,3X,11HOFSETX(2) =,E16.8,3X,  
 9 11HOFSETY(1) =,E16.8,3X,11HOFSETY(2) =,E16.8 /  
 A 12H OFSETZ(1) =,E16.8,3X,11HOFSETZ(2) =,E16.8 /  
 B 12H WIND(1) =,E16.8,3X,11HWIND(2) =,E16.8,3X,  
 C 11HWIND(3) =,E16.8 )

RETURN  
 END

```

$IBFEC CROSS DECK
SUBROUTINE CROSS(VA,VR,VC)
C SUBROUTINE TO PERFORM CROSS PRODUCT
C VECTOR VA IS CROSSED INTO VECTOR VR TO FORM VECTOR VC
DIMENSION VA(3),VR(3),VC(3)
VC(1)=VA(2)*VR(3)-VR(2)*VA(3)
VC(2)=VA(3)*VR(1)-VR(3)*VA(1)
VC(3)=VA(1)*VR(2)-VR(1)*VA(2)
RETURN
END
$IBFEC DOT DECK
FUNCTION DOT(VA,VR)
C FUNCTION TO PERFORM DOT PRODUCT
DIMENSION VA(3),VR(3)
DOT=VA(1)*VR(1)+VA(2)*VR(2)+VA(3)*VR(3)
C VECTOR VA IS DOTTED INTO VECTOR VB TO FORM THE SCALAR DOT PRODUCT
RETURN
END
$IBFEC VMAG DECK
FUNCTION VMAG(VA)
C FUNCTION TO DETERMINE VECTOR MAGNITUDE
DIMENSION VA(3)
VMAG = SQRT(VA(1)*VA(1)+VA(2)*VA(2)+VA(3)*VA(3))
RETURN
END
$DATA
CASE NO 24 1 LASER RANGE 300 LATERAL SCAN FILTERS
$VORTEX NZERO = 0., VROTHC = 30., VROTVL = 30., NRANGE = 3, $
$SYSTEM $
$SCAN SWEEP = -7., -2., $

```